DIRECT ELECTRIC CURING OF MORTAR AND CONCRETE

Ian Heritage B.Eng (Hons), M.Sc

A thesis submitted in partial fulfilment of the requirements of
Napier University for the degree of Doctor of Philosophy

School of the Built Environment
Napier University
Edinburgh, UK

2001

Abstract

Direct electric curing is the method by which the hydration reactions within concrete are thermally accelerated by passing an alternating electric current through the sample. This use of electricity as a means of supplying heat to young concrete and mortar has become recognised as a more effective and energy efficient form of accelerating the curing process than traditional steam curing.

The present investigation involves studying the affects of thermally accelerated curing of cementitious materials in comparison to normally non-heated curing. Prior to mixing, tests are performed on the constituents of the cementitious mixes. Results of these tests are used in the creation of mix designs for mortar and concrete samples. A range of concrete mixes are designed with and without additives and admixtures are used to make cubes, slabs and beams.

From the testing results, the factors affecting the short and long term properties of electrically cured cementitious materials are investigated and heating regimes are presented to achieve specific properties of both strength and durability at specific ages.

A substantial section of reinforced concrete is required to gain representative results in electrically curing reinforced concrete slabs. Compressive strength is difficult to measure due to the electrical distortion affects of inserts and the damage caused by coring so that at present, basic maturity concepts are used as a compressive strength guide which limits the validity of results obtained. This research looks at refining these concepts to include early age heating effects induced by direct electric curing.

The microstructural development of concrete when subjected to accelerated curing is also considered. The affect of delay periods and maximum temperature is studied using a scanning electron microscope and the results presented.

Declaration

This thesis is submitted to Napier University, Edinburgh for the Degree of Doctor of Philosophy. The work described in this thesis was carried out under the supervision of Dr. Fouad Khalaf, Dr. John Wilson and Prof. Alan Sibbald. The work was undertaken in the School of the Built Environment, Napier University.

In accordance with Napier University regulations governing the Degree of Doctor of Philosophy, the candidate submits this thesis as original unless otherwise referenced.

During this period of research the following papers have been presented and/or published:

1. **HERITAGE, I., KHALAF, F.M. and WILSON, J.** 'Electrical curing of cement based mortar'. Presented at the 7th BCA Conference on Higher Education and the Concrete Industry, Heriot Watt University, September 1997.
2. **HERITAGE, I., KHALAF, F.M. and WILSON, J.** 'Thermal acceleration of hydration for mortars using direct electric curing'. Proc. 9th BCA Conference on Higher Education and the Concrete Industry, Cardiff University, July 1999, pp. 103-116.
3. **HERITAGE, I., KHALAF, F.M. and WILSON, J.** 'Thermal acceleration of Portland cement concretes using direct electronic curing'. ACI Materials Journal, Vol. 97, No. 1, 2000, pp. 37-40.
4. **HERITAGE, I. and KHALAF, F.M.** 'Direct electric curing of concrete'. Proc. 10th BCA Conference on Higher Education and the Concrete Industry, University of Birmingham, June 2000, pp. 69-81.

Ian Heritage

Acknowledgements

The author acknowledges the assistance and encouragement of his supervisors, Dr. Fouad Khalaf and Dr. John Wilson. Their helpful suggestions and technical advice have greatly aided the author during his research. Additionally, their recommendations and constructive discussions are much appreciated by the author.

The author wishes to thank Napier University for funding the project under an internal research grant. Additional funding was provided by Napier University through payment for the supervision and teaching of undergraduate students. The author thanks the School of the Built Environment, Napier University for making facilities available for the work. He is grateful to all School Support Staff members for their help with laboratory testing, equipment repairs and administration assistance.

The author would also like to thank his friends and colleagues of the University, especially Pauline Guo, who made his stay in Edinburgh such a unique experience.

The author dedicates this work to his parents, family and dog who have always given him great support throughout his career. For Bailey.

Contents

List of Figures

List of Tables

Chapter 1 - INTRODUCTION

1.1 History of Cementitious Materials

We may never know who made the first concrete since early attempts probably resulted in a weak material which would long since have vanished. Concrete did not immediately become the material as we know it today but rather developed over many centuries (Stanley 1999).

The oldest concrete so far discovered dates from around 7000BC from Galilee, Israel. It is a floor consisting of a lime concrete, made from burning limestone to produce quicklime, which, when mixed with water and stone sets to form an early concrete.

Evidence of the use of concrete from 5000-2500BC is scarce but it is likely that it was used in some form, but has either been destroyed, not discovered yet or degraded.

In around 1950BC the first known illustration of the various stages in the manufacture and use of mortar and concrete was produced at Thebes in Egypt. At this stage concrete was mostly used as an infill material for stone walls with only much later it being used as a structural material.

From the Egyptians, the art of making concrete spread around the eastern Mediterranean and by 500BC the Greeks used it as a lime based composition to cover walls of sun dried bricks and as a binding material between brick and stone.

It is likely the Romans developed the idea of making concrete from the Greeks and examples of early Roman concrete can be found dating to around 300BC. It is from the Romans that we get the word 'concrete'. It derives from the word 'concretus', which means grown together or compounded.

During the second century BC the Romans quarried a pink volcanic ash from near Pozzuoli and upon mixing with lime found they had a much stronger concrete than anything previously attained. During this time concrete had become readily accepted, such that by 13BC, Vitrivius had compiled a pamphlet outlining the preparation of concrete which was used throughout the Roman Empire.

Another advance by the Romans was the use of precast concrete. An example of this is at the Italian port of Puteoli where blocks were left for two months before being sunk into position to form a breakwater.

The use of concrete may have declined with the withdrawal of the Romans but examples of Saxon concrete mixers remain from around 700AD. With the advent of the Norman conquest concrete regained a measure of its former usage with it being used in such buildings as the White Tower in the Tower of London, Dover Castle and Salisbury Cathedral.

Until the 18th century there was very little use of concrete by the British with the exception of a breakwater built in 1670 at Tangier in North Africa. This was built by Henry Shere who experimented with over 30 different mixes until he selected the one with the greatest strength underwater.

In 1756 John Smeaton was commissioned to build the third lighthouse on the Eddystone Rocks, 14 miles south-west of Plymouth (Stanley 1999). To achieve the strengths required Smeaton began the first modern scientific investigations into concrete and published these findings in 'A narrative of the Eddystone Lighthouse'.

Portland cement was patented on 21st October 1824 by Joseph Aspin. He named it 'Portland' because he thought it resembled Portland stone in colour and went on to create several cement making factories.

The cement making process was improved by Isaac Johnson who raised the temperature at which the cement was fired. Johnson is often regarded as the father of modern Portland cement.

Portland cement quickly replaced 'Roman' cement in mortars and renders but was not generally mixed with aggregates to make concrete until the mid 1800s.

Although superior to the cements of the time, modern day Portland cement bares little resemblance to the original Portland cement except in name and basic ingredients and since the mid 1800s concrete has generally increased in production and quality until the present day were it is the major construction material in the World (Leung and Pheeraphan 1995) with production in the range of 10,000 million tons per year (Idorn 1990).

1.2 Accelerated Curing

Curing has been defined in many different ways. Two examples are (Cather 1994):

1. 'Curing is the creation of an environment in which hydration reactions can proceed to help fulfil the aim of producing concrete of adequately low porosity'.
2. 'Curing is adequate when the resulting concrete achieves an expected service requirement'.

Curing can be shown to have a marked effect on the rate of hydration of cement. The particular performance of the concrete to resist deterioration needs to be considered carefully in the light of the potential benefits of accelerated curing. The specification is currently based upon vague evidence and is considerably influenced by a preconception of requirements and what was previously considered adequate.

The term accelerated curing denotes a means of achieving rapid gain of compressive strength at an early age. The techniques available include the use of heat, the introduction of admixtures and, since the comparison of curing times is normally based on OPC concrete, the use of high early strength cement (Kirkbride 1971).

In the manufacture of precast concrete, accelerated curing is used to increase productivity (Kirkbride 1971). Benefits are derived not only from the more effective use of plant and labour but also from shorter storage periods and therefore from reductions in stock and stacking space. Less quantifiable benefits such as the facility to satisfy rush orders at short notice are also relevant.

1.3 Direct Electric Curing

Direct electric curing of cementitious materials is the procedure by which an alternating electric current is passed directly through a sample (acting as a resistor) to produce a heating effect, thus increasing the initial rate of hydration.

The main advantages of the DEC process are (Bredankamp et al 1993):

1. DEC is one of the most energy efficient methods for the accelerated curing of concrete.
2. The electrical power demand for this process may be during off peak hours when cheaper electricity rates are available.
3. Due to high preliminary strengths the curing process is completed before the start of the next shift.
4. After the initial capital outlay for equipment, the running costs of DEC are substantially lower than that of externally applied heat (steam, autoclave, etc.) curing.
5. DEC offers exact control of the curing cycle, which leads to minimal breakage's and improved quality control.
6. As compared to normal curing methods, the reuse of shuttering can be increased by 2-3 times. This improvement in reuse increases during winter months.

1.4 Scope of the Investigation

Prior to mixing, tests were performed on the constituents of the cementitious mixes. The results from these tests were used in the creation of mix designs for both mortar and concrete samples.

Tests were performed on the fresh and hardened concrete and the performance of Direct Electrically Cured mortar and concrete was compared to non accelerated cured samples of the same mix designs. The effects of a number of curing and mix variables was investigated.

The main objectives and scope of this study are as follows:

1. To review the current knowledge of accelerated curing and electrical aspects of cementitious materials.
2. To study the physical properties of DEC and compare to non accelerated cured cementitious materials.
3. To develop heating regimes to achieve specific properties at specific ages for DEC.
4. To study the microstructural development of electrically cured concrete.
5. To study the effect of admixtures, additives and reinforcement on DEC.
6. To achieve methods of predicting the mechanical properties of DEC samples.
7. To determine the feasibility of DEC in various circumstances and applications.

1.5 Outline of Thesis

The structure of the thesis can be summarised as follows:

Chapter 1	Introduction, scope and aim of the present investigation.
Chapter 2	Literature review of previous investigations into accelerated curing, electrical curing and electrical properties of cementitious materials.
Chapter 3	Presents the results of an experimental investigation into the physical and mechanical properties of the materials used and the testing procedures adopted.
Chapter 4	Gives the results of an experimental and theoretical investigation of electrically cured mortar samples.
Chapter 5	Gives the results of an experimental and theoretical investigation of electrically cured concrete samples.
Chapter 6	Gives the results of an experimental and theoretical investigation of electrically cured concrete samples containing admixtures and additives.
Chapter 7	Gives the results of an experimental and theoretical investigation of electrically cured concrete samples containing reinforcement.
Chapter 8	Summary of conclusions and recommendations for future research.

Chapter 2 - LITERATURE REVIEW

2.1 Introduction

This chapter provides a review of previous work covering the accelerated curing of mortar and concrete, the electrical characteristics of cement based materials, additives and admixtures.

2.2 Hydration of Cement

The chemical combination of cement and water, known as hydration, produces a strong binding medium for the aggregate particles in concrete and causes an exothermic reaction producing heat (Czernin 1980, Ramachandran, Feldman and Beaudoin 1981, Jackson and Dhir 1988, Bazant and Kaplan 1996).

The phenomena that occur during the early age of concrete curing are complex with coupling between chemical-thermal-hydration and mechanical effects. Among the main attributes that govern the non-linear behaviour of early age concrete are stiffness evolution, the development of thermal strains, creep and cracking (Niu, Tu, Liang and Zhang 1995).

The main compounds of Portland cement that react during hydration can be seen in Table 2.1. The abbreviations stated in the table denote the notation commonly used within cement hydration analysis. These compounds react at different rates and their proportions seriously affect strength development.

Table 2.1 – Main compound composition of Portland cement

Compound	Formula	Abbreviation
Tricalcium silicate	$3Cao.SiO_2$	C_3S
Dicalcium silicate	$2Cao.SiO_2$	C_2S
Tricalcium aluminate	$3Cao.Al_2O_3$	C_3A
Tetracalcium aluminoferrite	$4\ CaO.Al_2O_3.Fe_3O_3$	C_4AF

The main hydration process commences at the boundaries of particles, and the gel which is formed grows outwards from the surfaces of the particles towards the water filled capillary space as well as inwards from the boundaries of the cement particles (Bazant and Kaplan 1996). The continued formation of the hydration products result in a stiffening of the cement paste which results in 'final set' after a period of 4-6 hours after the addition of water (Neville 1988). The setting process is governed by the reaction of C_3S with sulphates which produces ettringite crystallisation creating an eventual interlocking of crystals, thus causing the set (Skalny, Jawed and Taylor 1978).

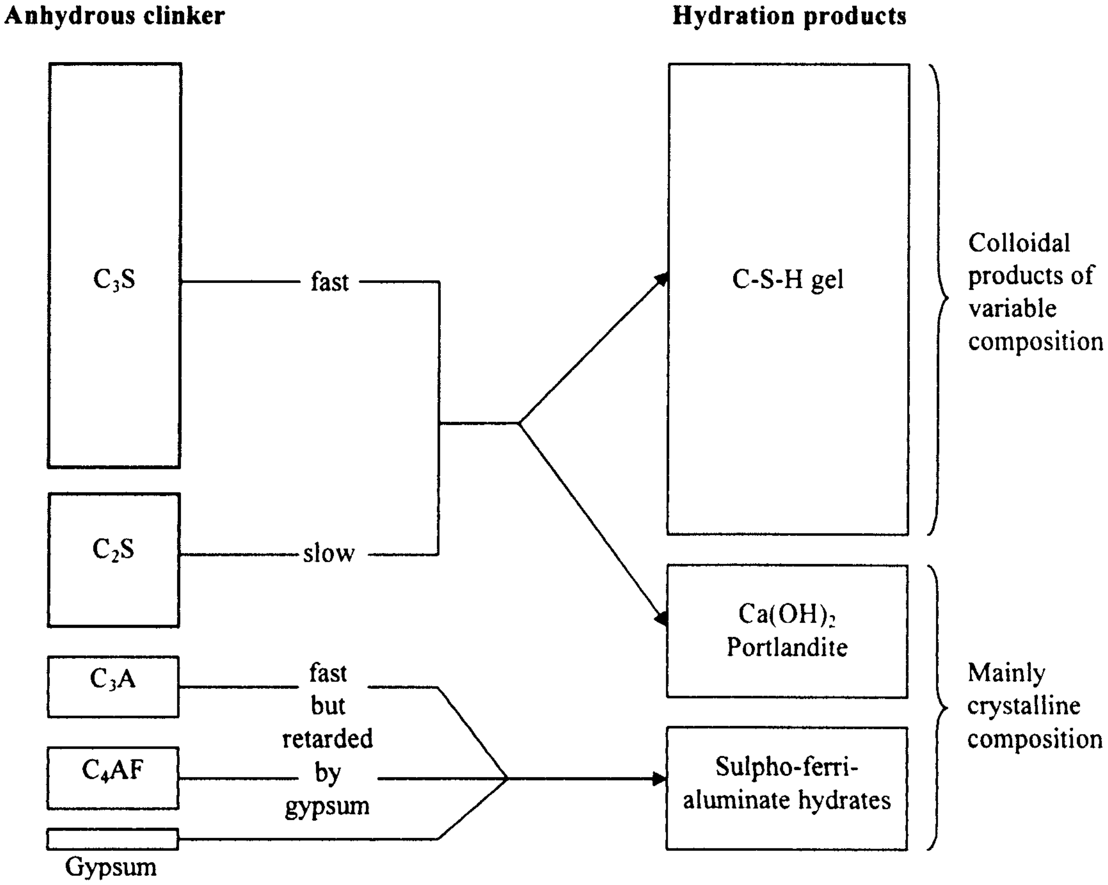

Figure 2.1 - Representation of the hydration products formed from anhydrous clinker

The Portland cement paste eventually becomes a network consisting of hydrates of the various compounds present (C-S-H gel), crystals of $Ca(OH)_2$, minor compounds, unhydrated cement and water filled voids pores. The pore fluid is strongly alkaline (pH

12-13) and originates mainly from the hydrates of calcium, sodium and potassium oxides (Jawed and Skalny 1991). The products of hydration have a low solubility in water as shown by the stability of the hardened cement paste in contact with water (Neville 1988).

A representation of the hydration products formed from the anhydrous clinker can be seen in Figure 2.1. The areas of the boxes give the approximate volume proportions of the phases (Double 1983).

2.3 Accelerated Curing of Mortar and Concrete

There is a widely held view that curing of concrete is not given the care and attention that it requires (Cather 1994).

In concrete construction, economic considerations force builders to remove formwork as soon as the concrete has gained sufficient strength to safely support its self-weight and imposed loads. As such, it is often required that the usual release time is shortened by the use of accelerated curing methods (Carino et al 1983).

The need to re-use equipment at frequent intervals, thus increasing daily production rates, makes it necessary, particularly in prefabrication, to accelerate the chemical reactions during concrete hydration.

A higher rate of strength development in concrete can greatly facilitate several important processes in the construction industry. For example, in the development of precast concrete products, it is desirable to attain sufficient strength within a short period of time so the moulds can be reused and the final products can be handled and delivered to site as soon as possible (Leung and Pheeraphan 1994).

Precasting of concrete has numerous advantages, relating to using accelerated curing techniques, over in-situ construction. These include (Richardson 1973, Levitt 1982):

1. The opportunity to speed up the on site processes of construction by delivery of already high strength members.
2. The reduction of skilled trade personnel and batching plant size on site.
3. Closer control of the quality of concrete used.
4. Greater specialisation of personnel.
5. Reduction of the need for scaffolding and other supporting services.
6. A greater degree of specialisation in products produced because of the added flexibility of the greater range of construction techniques possible.
7. The maximum reuse of moulds and other equipment.
8. The reduction of delays due to adverse weather conditions.
9. The increase of production off site thus allowing greater planning control.
10. A reduction in site overcrowding with materials.
11. The availability of specialist techniques such as accelerated curing is greatly increased, as is the possibility of humidity control.

Under normal moist curing conditions at room temperature, it can take as long as one day or longer to achieve a strength that is sufficient for handling without damage and it may take several days before significant loads may be carried.

A higher rate of strength development can greatly facilitate several important processes in construction. In the case of repairing localised damage in pavements, the traffic must be controlled until the repair material has gained sufficient strength. This is typically in the region of 14 N/mm^2 (Parker and Shoemaker 1987). To minimise the effect of repair on traffic flow, the repair material should develop strength that is sufficient within five hours so that any repair work can be carried out during off peak times of the day.

Several non-chloride admixture accelerators have been developed but their long term performance is not generally well understood. Also many accelerators require precise control of dosage which can make their application difficult or expensive to adjust.

The strength gain in Portland cement concrete can also be accelerated by the application of thermal energy and during the past several decades, economic and technological changes have greatly enhanced the attractiveness of accelerated curing, especially in the precast concrete industry (Wadhwa, Srivastava, Gautum and Chandra 1987).

Steam curing is the most popular form of accelerated curing, but others, such as vacuum, accelerating agents, hot water, microwave, infra red and electrical heating are available.

Steam curing involves hot water installations carrying low grade heat and is therefore relatively uneconomical. The use of hot air and infra red emissions need special care to avoid significant loss of moisture (Wadhwa et al 1987). Other forms of accelerated curing have different advantages and disadvantages and are discussed in greater detail in Section 2.5.

2.4 Requirements for Accelerated Curing

2.4.1 Economical considerations

The selection of a suitable method of accelerated curing (Federation Internationale De La Precontrainte 1982) depends on the product to be cured, the performance expected and on the manufacturing conditions (rate of production, floor space, staff skill and equipment available), but the cost of the process is often the influencing factor. The cost can be assessed by examining the following factors:

1. *Cost of the energy brought into the mould*
    - The cost of the electricity, gas or other fuel delivered to site on the basis of a five year period.
    - The cost of the transformation of this energy into usable energy for the type of thermal curing selected.
    - The cost of equipment necessary for the transformation of the electrical energy into usable energy (boilers, pipes, insulation, transformers etc.)

- The cost of maintenance of the transformation system and the cost of transfer of the energy within the plant.
- The cost of transfer of this usable energy from the transformation place to the mould

2. *Minimising the losses of energy*
    - The optimisation of the energy distribution circuits (reduction of paths)
    - The thermal insulation of circuits and moulds
    - Temperature regulation
3. *Concrete preparation for thermal curing*
    - Reducing the quantity of water
    - Using the heat of hydration to aid the accelerated curing
    - Replacing the precuring phase at ambient temperatures by a precuring phase with a slightly increased temperature in the case of a lower than required ambient temperature

A main concern in any accelerated curing process is the energy required to cure a given mass of concrete. The approximate values of energy consumption can be seen in Table 2.2 (Wadhwa et al 1987).

Table 2.2 - Energy requirements of various accelerated curing methods

Type of accelerated curing	Energy (kW.h) consumed per m^3 of concrete	Initial cost of equipment	Maintenance cost of equipment
Steam	160-180	High	High
Infra red	120-160	Moderate	Moderate
Hot water	140-160	Moderate	Moderate
Electrical curing (Semi-direct)	40-50	Low	Negligible
Electrical curing (DEC)	30-60	Very low	Negligible

The table clearly shows that the initial cost of equipment and maintenance for DEC is very low compared to the other types of accelerated curing.

2.4.2 Parameters relating to materials

(a) Cement

For Portland cements without additives, the tricalcium aluminate (C_3A) content appears to be important for the suitability of a cement in accelerated curing. An optimum value for C_3A lies between 9-10% (Federation Internationale De La Precontrainte 1982). A high tricalcium silicate (C_3S) content is advantageous, especially when C_3S:C_2S is greater than 3. Also, a relatively high C_3A content must be accompanied by a high SO_3 content, but this must not exceed 3-4%.

(b) Aggregates

As aggregates do not take a significant part in the chemical reactions during hydration, the suitability for accelerated curing must be examined only as due to their thermal properties. Such properties that must be considered are thermal expansion, thermal conductivity, specific heat and diffusion.

Also, care must be taken when using lightweight aggregates due the extra percentage of voids which requires a reduction in heating rate and maximum temperature.

(c) Water

Care must be taken to avoid excessive evaporation by the use of suitable heating regimes and enclosures to allow adequate humidity in the environment of the concrete.

(d) Admixtures

The use of admixtures must be considered very carefully when in association with accelerated curing as some admixtures alter properties at higher temperatures and as such preliminary mixes should be carried out.

2.4.3 Summary of requirements

Studies (Hanson 1963 and Higginson 1961) have previously shown that high early age compressive strengths can be achieved when expenditure of the energy used was not a concern.

The specific factors that could influence the development of an energy efficient, high early and long-term strength, curing technique are:

1. The cement should have a C_3S content of 55 to 65 percent.
2. The cement should have a C_3A content of 8 to 14 percent.
3. The fineness of the cement should be as high as practicable.
4. The loss on ignition should be as low as possible.
5. The water cement ratio should be between 0.30 and 0.40.
6. The water reducing admixture dose and the time when added require consideration.
7. The initial temperature of the fresh concrete should be between 22 and 38°C and should be kept between these limits during the initial delay period.
8. Concrete slump should be as low as possible.
9. The delay period should be set as close to the initial setting time as possible.
10. The rate of temperature rise should be between 22 and 44°C/hr.
11. The maximum temperature should be between 71 and 82°C.
12. Appropriate and efficient thermal insulating barriers should be used to minimise heat losses.
13. The applied heat can be turned off after several hours so long as efficient insulators are used.

It has been stated (Pfeifer and Landgren 1982) that a difference in the maximum temperature attained does not greatly effect the level of strength development at both early and long term ages. It has also been shown that increases in concrete strength was not dependent upon the length of the heating period with 3 hours heating showing only an 8 percent loss when compared to a heating period of 10 hours.

2.5 Methods of Accelerated Curing

2.5.1 Steam curing

The reduction of the curing period in the precast concrete process is an important factor for the productivity, capital saving and the reduction of workshop area. The traditional thermal curing technique has long been used in the concrete industry. Steam at 90-100°C is introduced into a chamber to heat up the precast concrete pieces. It can take more than 10 hours to complete a curing cycle before demoulding. Research shows that the quality of concrete is generally lower as the compressive strength after 28 days is on average 10-15% lower than for concretes under normal curing conditions (Xuenquan, Jianbgo and Mingshu 1987).

Conventional heating techniques, such as steam curing, rely on the conduction of heat from the exterior to the interior (Leung and Pheeraphan 1994). The heating is therefore non uniform and a long heating period is required to attain the required temperature.

Steam curing and autoclaving are widely used in the precast concrete industry. However, these require the use of expensive equipment and long processing time. Also, the long term strength is adversely affected. This loss is attributed to the non uniform formation of hydration products when reaction rates are high such as when temperature is increased.

2.5.2 Autoclave

With the use of autoclaving (high pressure steam curing), specimens treated at 75°C and 90°C exhibit, even after only 8 hours curing, strengths higher than those attained at 25°C and by comparison, for the specimens treated at 60°C, 15 to 36 hours are required to achieve analogous results (Marcialis, Massidda and Sanna 1983).

If autoclaving is used in a mix containing PFA with prolonged hydration a gradual combination of the calcium hydroxide with fly ash takes place.

The increase in temperature by autoclaving from 60°C to 75°C results in a reduction in porosity whilst that from 75°C to 90°C gives rise to an increase in total porosity and a shift of the pore sizes towards the coarser class sizes (Marcialis et al 1983).

2.5.3 Microwave

Microwave energy can heat materials that have a high dielectric constant, such as concrete, both rapidly and uniformly.

Microwave energy generates heat in cementitious materials due to the dielectric nature of the water contained within the mix (Sohn and Johnson 1999).

Microwave energy can heat a specimen uniformly and volumetrically, being independent of the thermal conductivity of the specimen. It can also more easily enhance the evaporation rate and allows better control of the energy absorption, thus optimising the heating process.

Excessive microwave energy can lead to a long term decrease in strength due to over evaporation and overheating.

Conventional thermal energy accelerates curing and reduces the induction period of OPC mortars. Using steam, the samples must be cured in water in order to avoid reducing the ultimate strength of the concrete at later ages. With steaming, heating occurs at the edge of the sample causing thermal gradients which can lead to cracking (Hutchinson, Chang, Jennings and Brodwin 1991).

With microwave curing the amount of energy must be carefully calculated: too much energy and the water boils while too little has no effect (Hutchinson et al 1991).

Compared with conventional thermal curing, the most distinct features of microwave curing are that the curing period is only 15-30 minutes, much shorter than for steam curing and the strength of concrete, especially in the case of early ages, is improved (Xuenquan et al 1987).

The permeability of microwave treated mortar is much lower than for untreated ones, indicating that the former is denser in microstructure. Part of the free water could be removed prior to setting during the short term microwave treatment, resulting in plastic shrinkage of the mortar slurry and reducing the porosity (Xuenquan et al 1987).

When the starting time of the microwave treatment is delayed, the effect of the microwave curing is reduced. For example, if the starting time is delayed to 45 and 120 minutes after mixing, the compressive strength after three days decrease to 90% and 83% by comparison to that of the specimen treated just after mixing. It is believed that the network structure of cement is formed in this period, so that the effect of plastic shrinkage is next to impossible under microwave treatment and the porosity of concrete can not be reduced (Xuenquan et al 1987).

There are no distinct differences of the morphology between a specimen treated with or without microwave energy as found by scanning electron microscope observation.

Unlike steam cured specimens, the 28 day compressive strength of microwave cured specimens is also increased. The increase in later age strength can be attributed to the removal of water from the fresh concrete when energy is applied, causing the collapse of the capillary pores and subsequent density increase of the concrete (Leung and Pheeraphan 1994).

The strength of microwave cured specimens have been found to be slightly higher than that of conventionally cured control specimens. Microwave application can significantly increase the degree of hydration during the first day, after which the microwave cured specimens and the control specimen attain similar degrees of hydration (Leung and Pheeraphan 1994).

For concrete specimens treated at lower microwave energy levels, accelerated cured specimens and conventionally cured specimens exhibit almost identical strength at 7 days. Also, for all microwave energy levels, the 4.5 hour strength of concrete specimens are higher than that for corresponding mortar specimens (Leung and Pheeraphan 1994).

It has been found (Leung and Pheeraphan 1994) that the most important parameter to control was specimen temperature during the curing process using a feedback temperature controller.

Previous studies (Leung and Pheeraphan 1994) have been uncertain of the thermal history of the specimen during the accelerated phase of the curing as power, rather than temperature, was usually used as a control.

Sohn and Johnson (1999) used a 30 minute delay with a 7°C/min rate of temperature rise with a 2 hour isothermal period to heat their specimens. They found that with the procedures used, overheating did not occur and as such, an isothermal curing phase could be achieved using microwave curing. They also found that at 40°C maximum temperature the strength values achieved were similar to normally cured mortars. Compressive strength at 28 days reduced to 80% of the normally cured samples for a maximum temperature of 60°C and at a maximum of 80°C the 28 day strength was found to be only 50% of the normally cured specimens.

A reduced isothermal period was attempted and it was found that the 28 day strength of the accelerated cured specimens could be maintained if the isothermal period of the 60°C maximum specimen was reduced to 48 minutes. The 80°C specimen always had a reduced 28 day strength when compared to normally cured samples and the 40°C maximum had a comparable strength with 120 minutes isothermal period.

Microwave curing allows a more uniform distribution of heat within the sample and as such much less process time (less than one hour) is sufficient to provide high early strength. When the process is applied before the concrete has set, the removal of water causes the capillary pores to collapse which consequently densifies the concrete.

The effect of microwaving concrete on microcracking and pore structure has also been investigated (Leung and Pheeraphan 1995). This was achieved by painting sections with black paint and applying white zinc oxide which reveals pores and microcracks. From this it was revealed that microwave cured samples generates many more pores and microcracks. This is likely to be due to localised boiling of water leading to bubble formation. However, in concrete, this effect seems to reduced when compared with an equivalent mortar. This may be due to the presence of large aggregate particles in concrete which restrain the expansion of the mortar which reduces the amount of microcracks and number of pores thus improving strength.

It is clear (Leung and Pheeraphan 1994) that microwave heating generates many more pores and microcracks in mortar specimens. One possible explanation for the improved performance of microwave cured concrete over mortar specimens can then be given as follows. During microwave heating, differential expansion of the aggregate and cement gel and air bubble expansion due to localised boiling causes thermal stresses and can lead to the formation of microcracks and pores. In concrete, where the presence of aggregates restrains the expansion of the mortar, the amount of microcracks and pores is reduced and the strength is comparatively improved.

It has been concluded (Hutchinson et al 1991) that microwave energy acts as an accelerator only during the first 24 hours and that the induction period of the treated specimens is significantly shorter. Also, it has been concluded that microwave heating does not significantly influence compressive strength at 7 or 28 days.

2.5.4 Hot water

Hot water curing involves the input of heated water directly into the dry mix or immersion directly after mixing to increase hydration reactions. No further heating is generally used. This immersion method is covered by BS 1881: Part 112 where it is used as an accelerated method of determining ultimate compressive strength. This procedure uses water at temperatures of 35, 55 and 82°C.

It has been shown (Jonasson 1985) that when the mixing water is heated, this increases the relative rate of hardening within concrete.

2.5.5 Hot air heating

Heating of concrete contained within shelters in Canada since the 1950s typically uses two methods (Turenne 1985). These are circulation of hot air around the specimen at the same pressure as the outside air and the pressurisation of the shelter by forcing hot air from outside. Both methods can easily cause large differences in heating distribution.

2.5.6 Infra-red heating

Competition in the construction industry and the rise of energy costs have forced the need to perfect concrete casting methods. This has lead to shorter casting times and more effective methods of heating concrete.

Infra-red heating developed at the end of the 1950s and this method has the advantages of speed, directability and favourable heating costs.

It has been shown that for heating concrete, radiators with a radiation temperature of 800-900°C should be used (Penttala 1985).

It has also been shown (Penttala 1985), that for infra-red heat curing, the maximum temperature of the concrete should be between 40°C and 60°C. At 60°C the long term strength loss was shown to be between 25 and 30%.

2.5.7 Heated mix components

The heating of concrete has traditionally been carried out after the addition of water but it is possible to heat components of the mix, or the mix itself during mixing. This procedure has been used in Finland since the early 1980s (Kukko 1985).

The temperatures used in this method range from 40°C to 60°C because temperatures in excess of 60°C cause a rapid loss of strength and workability difficulties.

It has been shown that with the use of preheated constituents the effectiveness of a plasticiser is severely reduced.

It has been shown that the shrinkage of preheated concrete is approximately the same as for ordinarily cured concrete of the same proportions. Important with respect to shrinkage is the need to increase the water requirement of the mix for a given workability. The risk of cracking is mainly dependent on the temperature difference between the concrete and ambient air at the demoulding age. In many cases, the difference between concrete temperature and ambient air is smaller than when concrete is heated on site.

When using this method, it has been recommended (Kukko 1985) that the most important tasks are to:

1. Ascertain rapid concreting and rapid heat insulation
2. Plan additional heating of the edges of members
3. Plan a temperature monitoring program

4. Plan for changes in ambient conditions

Heat insulation of 3-5cm of mineral wool has been recommended (Kukko 1985) for wooden forms and 5cm for steel forms. However, special attention must be made to the tightness of any insulation used and extra insulation should be used to protect exposed corners of the heated sample.

2.5.8 Additives and admixtures

Accelerating admixtures increase the rate of strength gain in young concrete. They are generally either calcium chloride (where no reinforcement is used) or calcium formate (Neville 1988). Accelerating admixtures are covered in greater depth in Section 2.10.

2.5.9 Special cements (RHPC)

Rapid hardening Portland cement causes accelerated strength gain in concrete made with it in place of ordinary Portland cement. This is due to both the increased fineness of RHPC and the high C_3S content which rapidly reacts with water during early hydration (Neville 1988).

2.5.10 Mass concrete

Temperature rises in mass concrete can be up to 80°C. This can lead to maturity differentials and corresponding strength variances.

For Portland cement mortars (Owens 1985) at 20°C the amount of $Ca(OH)_2$ will increase with time, indicating further hydration and strength gain but with an increase in internal heat, the amount of $Ca(OH)_2$ increases, but the strength falls. At 11 days there can be as much $Ca(OH)_2$ present as there is at one year at 20°C.

This reduction in strength would also imply a possible increase in permeability and an abandoning of the usual relationship between permeability and water/cement ratio.

2.5.11 Climate heating

The strength of concrete in hot climates has been proved to adversely affected (Jalali and Abyaneh 1995). The final strength is known to decrease with increased initial curing temperatures even when other factors such as desiccation are precluded.

Physical causes for this effect are believed to be due to the large differences in volumetric expansion of the different concrete constituents. The large increases in volume of air and water with high temperatures creates internal stresses in the concrete. If the tensile strength of the concrete is not sufficient to withstand these forces then porosity increases and microcracking may occur which results in a lower long term strength. The physical effect seems to be related to relatively high temperatures with microcracks being observed at 85°C but not at 60°C (Jalali and Abyaneh 1995).

Possible chemical causes for the loss of strength could be that the chemical composition of the hydrates is affected by the curing temperature, the microstructure of the hydrates is partially changed or the degree of hydration is altered (Jalali and Abyaneh 1995).

Problems associated with hot weather concreting can include increased water demand, increased rate of slump loss and setting, difficulty in pumping concrete, lower long term strength and increased shrinkage due to an increase in the water content of concrete (Gaynor, Meininger and Khan 1985).

It has been shown (Gaynor et al 1985) that were curing after placement was favourable and prolonged mixing was not involved, the ultimate strength disadvantages in increasing the concrete temperature from 23 to 38°C was less than 10%.

It has also been concluded that higher mixing temperatures (35°C) have little effect on the drying shrinkage and that for an increase in mixing temperature from 18 to 35°C an increase of 4.7kg/m^3 of cement is required to maintain strength levels. Also the water required to achieve a target slump has to be increased by around 2-6% and that strength loss at 28 days is around 10%.

Hydration at low temperatures provides sufficient time for the hydration products to diffuse in the interstitial space among the cement grains in a relatively uniform manner. When accelerated climate curing occurs the hydration products tend to be diffused in a non uniform way. This non uniformity results in a reduction in strength due to weak zones in the matrix. Further to this, the high concentration of hydrated products in the zone surrounding the cement grains retards subsequent hydration. This non uniformity might be expected to decline as time passes with gradual diffusion of the hydration products but the effect of increased initial curing temperature on C_3S has been shown to not be dissipated after 5 years of curing at 21°C. The effect of temperature on final strength is probably a combination of its effects on a variety of physical and chemical parameters (Jalali and Abyaneh 1995).

Some possible adverse effects of hot weather concreting include (Berhane 1992):

1. A reduction in setting time which creates difficulty in handling and finishing fresh concrete.
2. Thermal and plastic shrinkage which may initiate and accelerate other deterioration processes.
3. Reduced ultimate strength
4. Enhanced permeability and reduced durability due to macro and microcracking.
5. Formation of cold joints.

The ACI Manual of Concrete Practice (1992) refers to a maximum ambient temperature of 32°C for the production of good quality concrete.

When concreting is carried out in hot weather, the strength of the concrete is adversely effected by the early age heat increasing the rate of hydration of the cement which causes a thicker than usual coating around the cement grains and also by the non uniform distribution of hydration products within the cement matrix. Reduction in strength also occurs due to the reduction of water available for hydration due to rapid evaporation (Al-Gahtani, Abbasi and Al-Amoudi 1998).

It has been shown (Idorn 1990) that in the Middle East the temperature of the interior of a concrete mix can be as high as 87°C after twelve hours were as at the corner of the same mix the temperature is only 38°C. This is with an initial fresh concrete temperature of 37°C. This led to early cracking of the structure even though laboratory tested cubes from the same batch matched required specifications.

2.5.12 Electrical curing

Several methods of electrical curing have been tried (Kirkbride 1996). Internal methods using either the reinforcement or special coils of wire as the heating element do not appear to have enjoyed commercial success in the United Kingdom. The most successful form of electrical curing element is the heating panel incorporating concrete bonded to a steel plate. Electric heating cables have also been incorporated in concrete beds. In general, with electrical curing, enclosures are necessary to retain moisture.

Electrical curing can be of an internal method (Wadhwa et al 1987). In the semi direct method, either comparatively cheap electrical elements are embedded in the mass of the concrete, or the ends of the reinforcement is connected to an electrical power source and reinforcement is used as a direct heating element. Limitations of these methods include:

1. Loss of electrical heating elements in the mass of the concrete.
2. Difficulties in achieving a uniform temperature gradient in thick products.

Electrical curing is now being put to use in larger scales in the precast concrete industry but has little usage in situ.

2.5.13 Direct Electric Curing

Direct electric curing is the process through which electricity is passed through concrete or mortar in order to raise the temperature. DEC is covered in more depth in Section 2.7.

2.6 Electrical Properties of Concrete

2.6.1 Introduction

The electrical conduction through concrete can be divided into three parts:

1. Macroscopic being made up of conduction through the partially saturated aggregate particles.
2. Microscopic involving the conduction through the hydrating cement phase.
3. Submicroscopic involving the electrolytic aspects of the aqueous phase of the concrete.

(a) Macroscopic

The resistance of normal aggregates when compared to the cement paste is approximately 100 times greater (Monfore 1968). The majority of current flow is carried by the aqueous phase of the cement paste.

(b) Microscopic

Ohmic resistance is caused by the restriction of current flow through the hydrated microstructure of the hydrating cement paste. Previous (Monfore 1968) conductivity tests have shown that the conductivity of wet samples is approximately 10,000 more than the equivalent oven dried samples which means that the solid phase of concrete can be considered to be an insulator when dry.

2.6.2 Conduction paths

The paths of conduction stems from the principle that ionisation of water will conduct electricity. A concrete mix will provide such a medium because of its heterogeneous nature. There are three possible electrical paths through a fresh mix. Firstly, the electrical current may pass through the cement paste only. The second path is the converse, where the current passes through the aggregate only, this occurs where there is physical contact between the aggregate particles. The third possible path is through both the aggregate and the cement paste. These paths (McCarter and Curran 1984) are shown in Figure 2.2.

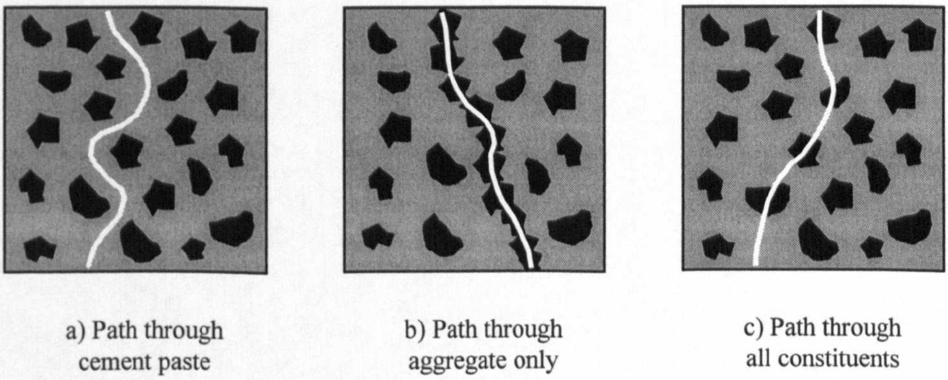

a) Path through cement paste

b) Path through aggregate only

c) Path through all constituents

Figure 2.2 - Conduction paths through concrete

2.6.3 Electrochemical structure of cement paste

In general (Farrar 1978, Sriravindrarajah and Swamy 1982) it has assumed that purely resistive effects are present in concrete. The cement paste has a controlling influence upon the overall electrical properties of concrete. Other work (McCarter and Afshar 1985) has used a combination of capacitance and resistance effects to model the electrical properties of concrete. Previous models have assumed that conduction in a cement paste is purely ionic through evaporable water in the continuous water filled capillaries within the paste.

In most fine grained materials (such as cement) there are free unbound charges in the aqueous phase and electrostatically held charges adjacent to the surfaces of the individual particles. The amount of charges and the strength by which they are held depends on:

1. The net electrical charge in the particle itself
2. The particle surface texture
3. The number of unsatisfied surface bonding sites

When an alternating current is applied, the free unbound charges within the aqueous phase give rise to ionic conduction and bound particles oscillate with varying amplitudes. The amplitude at which these oscillate is dependent on:

1. Type of charge
2. Degree of association with the surface of the particle
3. Temperature
4. Strength of the applied electric field
5. Frequency of the applied electric field

The electrochemical properties of cement pastes are time dependent and can be divided into unhydrated cement grains, hydration by-products and the aqueous phase. A summary of this can be seen in Figure 2.3.

Unhydrated cement particles and the solid products of hydration can be said to be non conductive and as such, the only means of conduction of electricity through the hydrating cement paste is through the aqueous phase which acts as an electrolyte due to the presence of ionic compounds. This is shown by the fact that when concrete is oven dried it can be classed as an insulator with a resistance of around 2-3x$10^3\Omega$m (Farrar 1978).

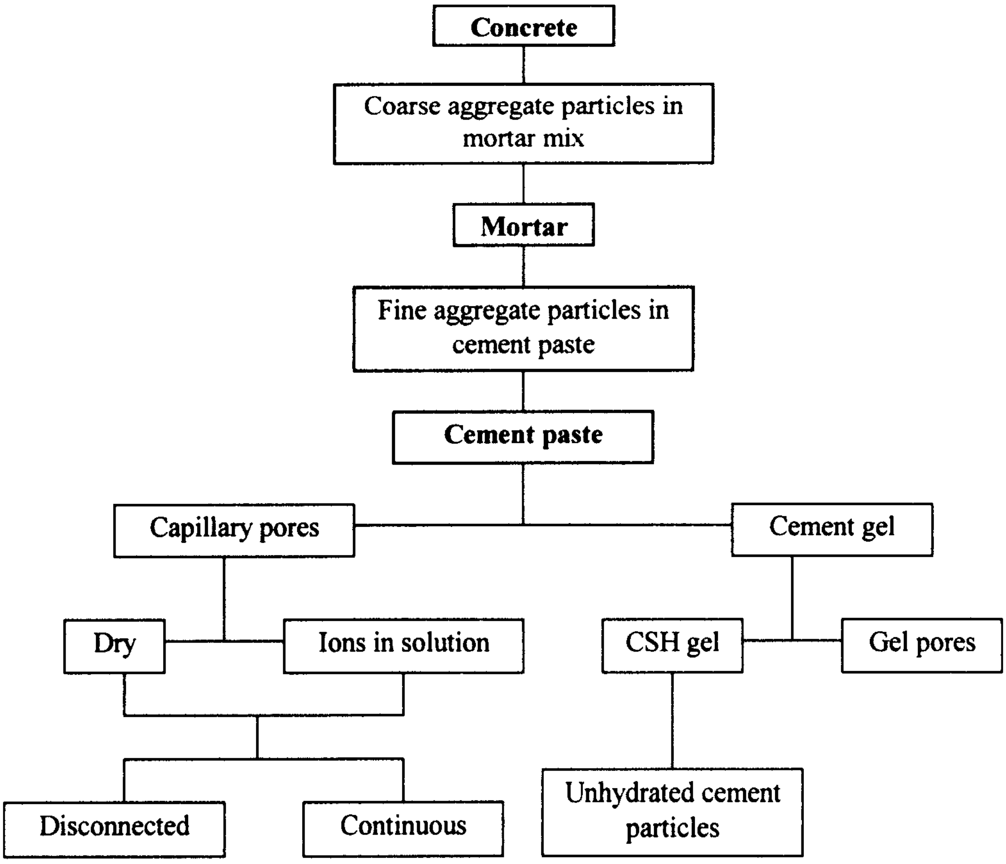

Figure 2.3 - Schematic breakdown of concrete composition as relating to conduction

Because the aqueous phase acts as an electrolyte, concrete exhibits a negative temperature coefficient of resistivity which is particular to electrolytic materials and as such the resistance must be corrected for by a temperature coefficient of resistivity (Wilson and Gupta 1996).

Electrical conduction through a damp cement paste is achieved by the mobility of ions in the evaporable water content. The aqueous phase is initially saturated with Hydroxyl and Calcium ions which mainly contribute to the conduction process. Ions such as Sodium, Potassium, Aluminium, Silicates and other oxides (though highly soluble) occur, but exist only at low levels of concentration, thus not significantly affecting conduction (Neville 1988). Also, during the initial 24 hours after gauging with water, Sulphates are present, but these precipitate into Sulphoaluminate hydrate and as such can be disregarded.

2.6.4 Electrolytic conductance

Electrolysis can be defined as the changes in the chemistry of a liquid medium caused by the passage of an electric current. Conduction is only possible in electrolytes where at least some of the liquid contains oppositely charged ions. The electrodes through which current enters and leaves the electrolyte are known as the anode and cathode, with positive ions (cations) flowing towards the negatively charged cathode and negative ions (anions) flowing towards the positively charged anode.

At the surface of both of the electrodes the methods of conduction change. Ions discharge causing the substance concerned to come out of solution and are either deposited on the electrode or liberated as bubbles of gas. Also fresh ions are formed from the material of the electrode and passed into the electrolyte. This reaction causes interference in the measuring of conductance and as such necessitates the use of high frequency alternating current so as to reverse the minimal electrolysis taking place every half cycle.

2.6.5 Ionic concentration and speed

As an ionic compound dissolves it splits into ions with the more dilute the electrolyte, the more complete the ionic dissociation. As the solution becomes more concentrated less ions split from the compound. Charge may be transferred at a greater rate at higher levels of ionic concentration.

The transfer of charge is greater the faster the ionic speed. The ionic speed is dependent on:

1. Electric field density. An ion experiences a force attracting it to the appropriate electrode in proportion to the electric field density.

2. Viscosity of the solvent. With increasing viscosity the terminal velocity of the ion is decreased.
3. The effect of asymmetry. A charged ion will tend to attract the ions of an opposite charge and repel ions of a like charge. This reduces the speed of the ion as its corresponding cloud of oppositely charged ions move in the opposite direction but still attract the original ion causing a net reduction in velocity.
4. Electrophoretic effect. Momentum is transferred from the moving ions to the solvent and is also exchanged between ions of opposite charges as they travel in opposite directions. This causes a greater loss of momentum than the solvent by itself would otherwise exert.

2.6.6 Electrode/electrolyte interface

The charge of the electrode attracts the oppositely charged ions within the liquid resulting in a layer of ions predominantly composed of either positive or negative charges. This layer adjacent to the electrode in turn attracts ions of a specific type. Thus, on either side of the interface layer are charges of the opposite charge. Within the bulk of the sample ions are randomly distributed.

2.6.7 Polarisation

(a) Electrode polarisation

The polarisation of the electrodes is a result of the process by which charged particles are transferred from the solution to the electrodes. These charged particles delay the conduction process causing an increase in resistance and thus a rise in the potential difference occurs. Hence the cathode becomes more negative and the anode more positive.

The greatest problem to the application of direct current to a fresh cement paste is the activation polarisation caused by the formation and liberation of hydrogen gas at the electrodes which obstructs the flow of charges to the electrode surface. This is in the form of:

$$2H^{-}+2e\text{---->}H_2$$

In an electrolyte, polarisation effects known as back e.m.f. occur at the electrode interface, resulting in an increased resistance. This can be minimised through the use of alternating current which causes a capacitance to occur in parallel with the resistance of the specimen. As such, concrete can be considered to be a network of capacitors and resistors in parallel through the liquid and solid phases.

(b) Bulk electrolyte polarisation

A secondary polarisation effect occurs away from the electrodes in the bulk of the electrolyte. This involves the alignment of dipoles and other charged particles in the direction of the current flow (McCarter and Afshar 1985). If direct current is applied this realignment is stable.

The magnitude of the stored charge is defined as the dielectric constant and is independent of sample size:

$$\varepsilon = \frac{C}{C_0} \qquad \text{Eqn. 2.1}$$

where:

ε = Dielectric constant

C = Capacitance of specimen

C_0 = Capacitance of equivalent sample size in a vacuum

2.6.8 Temperature dependence

Electrolytes are affected by temperature in two ways. These are:

1. A rise in the temperature of the solvent reduces viscosity causing the mobility of the ions to increase thus reducing resistance.
2. Ionic concentration increases with higher temperatures. This is due to increased dissociation of ions within the electrolyte.

From the above, it can be seen that electrolytes have a negative temperature coefficient of resistivity with an increase in temperature reducing resistance (Rait 1992).

Because of the high temperature coefficient of resistivity for ionic solutions, resistance values corrected to a particular temperature must be used. These values are calculated using the formula (Wilson and Gupta 1996):

$$R_c = R(1 + \alpha[T - T_0]) \qquad \text{Eqn. 2.2}$$

where:

R_c = Corrected resistance (Ω)

R = Measured resistance (Ω)

α = Temperature coefficient (per °C) = 0.022 per °C

T = Temperature (°C)

T_0 = Reference temperature (°C) = 20°C

This shows a considerable increase in resistance at higher temperatures. After an initial period of constant resistance corresponding to the setting time, it can be seen that the relationship becomes linear. In view of the published data (Wilson and Gupta 1996) relating log (maturity) to strength, this suggests that corrected resistance is also closely related to strength.

The electrical resistance of a material depends on its temperature. It is known that the resistance of a metal (Figure 2.4a) increases as its temperature increases and conversely the resistance of an insulator decreases with temperature as shown in Figure 2.4b.

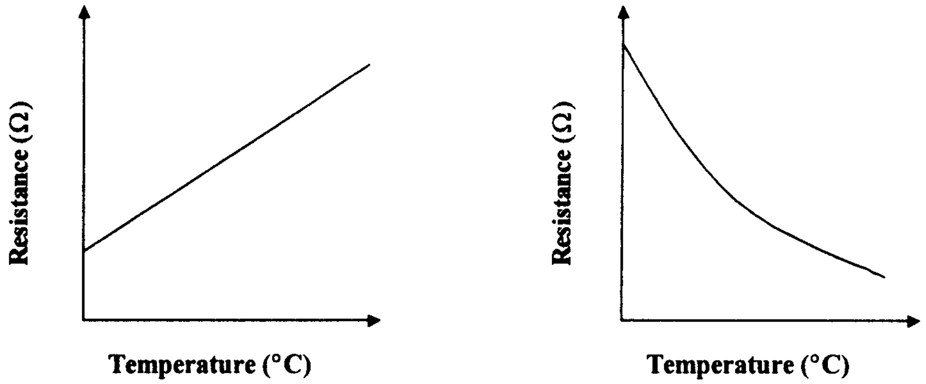

a) Metal or alloy

b) Insulator or dielectric

Figure 2.4 - Resistance versus temperature for metals and insulators

The temperature coefficient, α, is used to indicate how the resistance of a conductor will change with temperature (Rait 1992) and is found using the expression:

$$\alpha = \frac{R_2 - R_1}{R_1} \times \frac{1}{\theta_2 - \theta_1} \qquad \text{Eqn. 2.3}$$

where:

R_1, R_2 = Values of resistance (Ω)

θ_1, θ_2 = Temperatures at which R_1 and R_2 are respectively measured (°C)

This is generally of more importance in the production of electrical components which employs almost pure metals as opposed to mortar and concrete which are a combination of numerous compounds.

2.6.9 Resistivity

The resistivity (Ωm) of a certain conductor is dependent on:

1. The temperature
2. The specific conductor material

The resistivity of a sample of concrete of a specific composition is dependent on the amount of free water present and the density of the sample. Increases in density are caused by the continuing hydration of the cement paste which in turn causes an increase in resistivity. Resistivity also increases due to the dehydration of the saturated pores by evaporation.

Resistivity is a fundamental property of any material which depends on the chemical composition and the physical treatment which the material has received (Rait 1992). It can be determined by using the following equation:

$$R = \frac{\rho L}{A} \qquad \text{Eqn. 2.4}$$

where:

R = Resistance (Ω)
ρ = Resistivity (Ωm)
L = Length (m)
A = Area (m^2)

Also conductivity (Sm^{-1}) is defined as the reciprocal of resistivity. Hence:

$$\sigma = \frac{1}{\rho} \qquad \text{Eqn. 2.5}$$

The conduction of electricity through concrete is dependent upon both the ohmic resistivity and ionic conductivity with the ohmic conductivity being dependent on the fractional volume of aggregate and the proportional volume of the non conducting cement compounds.

2.6.10 Impedance

The alternating current impedance of concrete is almost identical to its direct current resistance (Neville 1988). This is due to the fact that the capacitive reactance is significantly larger than its resistance and as such only the resistance contributes significantly to its impedance.

2.6.11 Capacitance

The capacitance of concrete is small when using an alternating electric current (0.020 microfarads at 50Hz at 7 days) and decreases with age (0.003 microfarads at 50Hz at 113 days) (Neville 1988).

2.6.12 Electrical properties as an indication of concrete properties

It has been found (Zhao, Zhou, Zhu and Feng 1998) that concrete permeability is one of the intrinsic properties of concrete and is directly related to its durability.

Table 2.3 - Comparison of concrete resistance, permeability and ASTM C1202

ASTM C1202		**Alternating Current**	
Charge (Coulombs)	**Permeability of chloride**	**Conductance (10^{-5} Siemens)**	**Resistance (Ohms)**
>4000	High	>287	<348
2000-4000	Moderate	154-287	649-348
1000-2000	Low	87-154	1149-649
100-1000	Very Low	27-87	3704-1149
<100	Negligible	<27	>3704

The resistance of the specimen measured by alternating current (1V at 1kHz) was converted into conductance and then compared to the conductance from ASTM C1202. The correlation with this was found to be 0.9867 with conductance = 0.0666026xcharge +20.446 (Zhao et al 1998) and can be seen in Table 2.3.

The conductivity of pastes of ordinary Portland cements containing a variety of admixtures at a frequency of 3kHz has been measured (Tamas 1982). The results showed that:

1. In the case of cements, the conductivity of the paste increased during the initial period, reached a first maximum after 1-3 hours and then decreased again until around 6-10 hours whereupon a second maximum occurred.
2. This second maximum did not occur when pastes were made of clinker or pure clinker materials.
3. The effect of several accelerating admixtures (NH_4HCO_3 and $CaCl_2$) was to slightly delay the appearance of the second maximum but in the use of formate accelerators the second maximum occurs after a shorter time and was less intensive.
4. The effect of retarders such as citric acid was to greatly delay the appearance of the second maximum.
5. With an increase in temperature of the paste, the second maximum occurred after a shorter period of time.

Electrical conductivity is a consequence of the movement of charge carriers and in the case of cements this is achieved by ions. Electrophoretic charge transport can be excluded in view of the relatively large size of cement particles (Tamas 1982). Thus an increase in the conductance of paste can be attributed solely to an increase in the mobility or number of ions. The mobility of ions can be affected by the formation of electrically insulating layers during hydration. However, the previous results can be explained by changes in ion numbers.

The first conductivity maximum, which takes place shortly after gauging with water is a consequence of hydrolysis, which yields Ca^{++}, OH^- and in the case of gypsum also SO_4^- ions. These are readily absorbed by the formation of CSH and ettringite which decreases the conductance again. β-C_2S reacts slowly with water and showed a flat maximum approximately 6-7 hours after mixing with an overall conductivity much lower than with C_3S. At approximately 5 hours the conductance of each sample crossed being due to the higher reactivity of C_3S.

The second maximum was considered to be due to ettringite being converted into monosulfate creating 2 mols of Ca^{++} and SO_4^- ions per mol of ettringite. Also, the effect of admixtures was attributed to the formation of monosulphate phases from ettringite.

It has also been found (McCarter, Chrisp and Starrs 1999) that electrical testing can also be used to find a number of distinct regions of alkali-activated slag which rate the chemical reactivity and rigidity of the mixture.

2.7 Direct Electric Curing

DEC was first introduced in the railway sleeper industry, utilising single cell moulds. These techniques have now been largely superseded by multicell moulds on highly automated production lines (Bredankamp et al 1993). Casting operations are normally performed within normal working hours, with the accelerated curing taking place after working hours.

In colder climates it has been the standard practice to stop most concrete construction work during the winter months. However, with limited time and economical considerations, this has lead to the implementation of direct electric curing (DEC).

It has been found (Bredankamp et al 1993) that at constant times and differing voltages for DEC as compared to normal curing:

1. At approximately 80 hours after the concrete had been cast, the strength of the naturally cured samples exceeded that of the DEC samples.
2. The DEC cycle causes no subsequent loss of strength at 28 days. This ultimate strength depends on the initial temperature rise.

It has been stated (Wadhwa et al 1987) that direct electric curing is based on the fact that concrete is a resistor of approximately 500-1500Ω/cm and as such can be heated when an electric current is passed through it. Concrete has also a negative temperature coefficient and behaves like an electrolyte and as such only alternating current can be used.

It has also been noted (Bredankamp et al 1993) that DEC should have the following guidelines when used in situ:

1. Before heating is started, a period of 3-5 hours after adding water is required to allow the concrete to gain sufficient strength to withstand the thermal forces applied.
2. It is essential that the concrete must be adequately vibrated upon placing and that the minimum water/cement ratio is used.
3. All efforts must be made to stop the evaporation of water from the surface of the sample by the use of a suitable covering.

2.7.1 Practical application of DEC

The design criteria for heating of electrically cured concrete in a practical environment require the following data (Kafry 1993):

1. Quantity of concrete to be cured in an 8 hour shift.
2. Number of shifts per day.
3. Demoulding strength required.
4. Mix proportions.

5. Reinforcement data.
6. Geometry of specimens.
7. Ambient temperature and moisture conditions.
8. Availability of electric power supply.

The actual design procedure consists of (Kafry 1993):

1. Calculating the power.
2. Calculating the working voltages and currents.
3. Designing the curing scheme.
4. Designing the control scheme.
5. Specifying the equipment.

This design procedure can be calculated by comparing maturity values of normally and accelerated cured concrete with an emphasis on the analysis of electric field density when reinforcement is used. The equipment specification is also relatively simple as electrical curing equipment has already been implemented in numerous places. This equipment has been shown to have adequate safeguards for worker safety and quality control (Kafry 1993).

2.8 Heating Cycles

Due to the heterogeneous nature of concrete, being composed of a number of different materials including water and air, the values of each materials coefficient of thermal expansion differ considerably. Therefore, once heating has begun, the differential expansion of the materials causes voids to form within the mix resulting in a reduction of final strength.

Heat can be applied to fresh concrete using DEC, to drive off trapped air and allow residual water to be drawn to the surface during this fluid-plastic stage, without any detrimental effect on the concrete. However, with dry mixes, this should be avoided due to the fact that the initial setting time for a relatively dry mix is considerably shorter than that of a wet mix.

2.8.1 Heating period

This period, as the name suggests, is where heat is added to the system to accelerate the curing process. Unlike other methods, DEC has the advantage that the heat is spread evenly throughout the mix, therefore internal temperature differences are minimal.

Consideration should be given to the geometry and construction of the mould in that stiff, deep moulds with small casting openings can withstand higher heating rates more than weak, shallow and open moulds.

2.8.2 Isothermal period

The maximum temperature is held constant during this period by either reducing the amount of energy being supplied or shutting of the power completely when the maximum temperature is reached but supplying short bursts of energy to the system when required to maintain the maximum temperature (Kirkbride 1971).

The energy required to maintain the maximum temperature at this stage is largely dependent on the surface area of the unit being cured. Units with very large surface areas (i.e. long thin units) will loose heat more readily than those with small surface areas which can store large amounts of heat energy within them (Kafry 1993).

The temperature may continue to rise for a period of time due to the heat of hydration and it is this which necessitates the use of a predetermined maximum temperature to avoid boiling of surplus water.

In Denmark (Danish Ministry of Transport 1985), the maximum curing temperature in concrete can be no higher than 60°C because it is supposed that temperatures higher than this value cause damage due to the formation of the microstructural cracks which cannot later be remedied.

2.8.3 Cooling period

The time taken for this stage to complete is again dependent on the geometry of the unit in that large surface areas tend to cool more quickly than small areas. However care should be taken to ensure that the rate of cooling is not too rapid thus avoiding thermal over-stressing.

2.8.4 Curing cycle curve

From the descriptions given previously, the general curve used in most forms of accelerated curing is that shown in Figure 2.5.

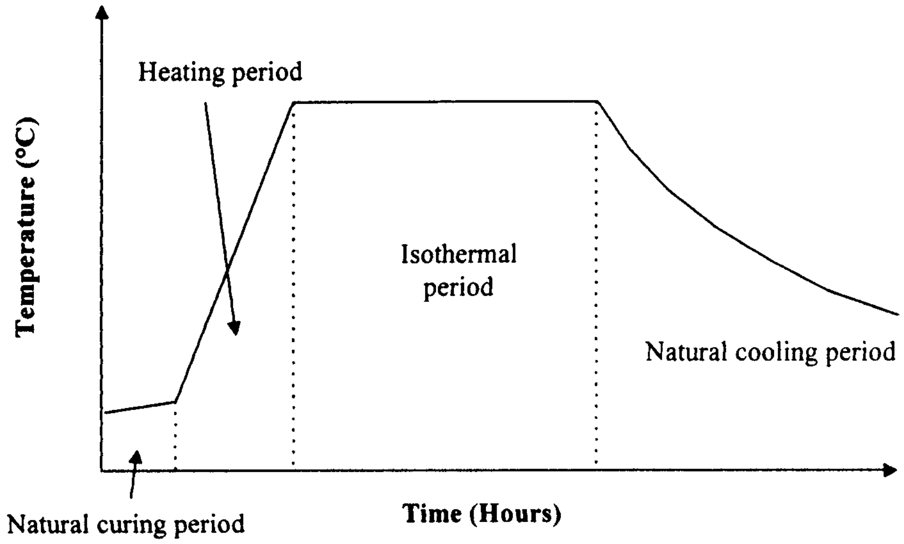

Figure 2.5 - General temperature curve used for accelerated curing methods

A number of guidelines concerning various heating cycles have been proposed by several authors (Kirkbride 1971, Orchard and Barnett 1971, Wilson and Gupta 1996). These include:

1. The temperature should not be raised during the setting period and that even after this period the rise in temperature should be limited to 22-33°C/hr rise with a maximum of 66-82°C.
2. The rate of temperature rise should not exceed 25°C/hr.
3. To get the highest long term strength from a given mix there should be a delay of 3-5 hours from the mixing of the concrete to the commencement of the temperature rise, the rate of temperature rise should not exceed 20°C/hr and the maximum curing temperature should not exceed 80°C.
4. After approximately 6 hours the temperature may be raised to 100°C without serious loss of long term strength.
5. Cracks are also liable to occur if the difference between the temperature at the core of the unit and that at the surface is greater than 15°C.

It has also been stated that the increase in strength per hour reaches a constant low value at an age of 24 hours for a maximum curing temperature of 90°C and the same low value at increasing ages up to 42 hours as the maximum curing temperature is reduced to 20°C. Hence, there is no advantage in accelerated curing after 42 hours and very little advantage after 24 hours.

2.8.5 Maturity

Saul's maturity law (Saul 1951) (where compressive strength relates to increases in time and temperature of curing) is generally accepted as a way to correlate a relationship between time and temperature of curing and compressive strength (Kirkbride 1971). The concept is that the strength of any concrete can be related to its maturity expressed as a product of time and temperature of curing. In fact, the maturity is usually calculated from a base of –10 or -11°C. Although there is a conflict of opinion as to its reliability, where in some cases it underestimates the actual strength achieved by high temperature curing. The law provides a useful design aid in the calculation of a high temperature curing cycle.

It has been presented (Neville 1988, Wilson and Gupta 1996) that graphs of log (maturity) against strength will show a linear relationship except at low values of maturity. Maturity is defined as:

$$M = \int_0^t (T - T_m)dt \qquad \text{Eqn. 2.6}$$

where:

M = Maturity (°C.hr)

t = Time (hr)

T = Temperature (°C)

T_m = Maturity reference temperature (°C) = -11°C

Experiments have been carried out to relate the electrical resistance to log (maturity), and to demonstrate how measurement of electrical resistance could be used to measure the reduction in the time required using accelerated curing.

The maturity concept has been recommended by organisations such as the ACI as an alternative to testing field cured cubes or cylinders. From the maturity values, the strength of hardening concrete can be estimated. However, maturity implies that with increasing age, concrete will continue to gain strength for an infinite amount of time.

It has also been shown (Jonasson 1985) that the maturity concept works well for permanently high temperature concretes up to around 14 days but then over estimates strength at later ages.

Alternatives have been suggested (Carino et al 1983) such as using a semi-logarithmic function as an appropriate strength maturity relation.

$$S = a + b \log(M) \qquad \text{Eqn. 2.7}$$

where:

S = Strength (N/mm^2)

M = Maturity (°C.hr)

a, b = Regression coefficients

However, this equation is only a good approximation at intermediate maturity values.

It has also been suggested (Carino et al 1983) that the strength maturity relation should be in the form of a hyperbola with the following equation:

$$S = \frac{M}{\left(\frac{1}{A} + \frac{M}{S_u}\right)} \qquad \text{Eqn. 2.8}$$

where:

S = Strength (N/mm^2)

M = Maturity (°C.hr)

S_u = Limiting strength as maturity tends to infinity (N/mm^2)

A = Initial slope of the strength-maturity curve (N/°C.hr.mm^2)

Parameters A and S_u have a physical significance and are determined by a computerised least squares fit of the data.

The temperature at early ages has been shown to have a disproportionate effect on the early strength development compared with time. In addition, early age temperature affects strength at later ages, with high early temperatures reducing long term strength development.

Above a certain maturity value, when the C_2S is the principal contributor to strength gain, a rise in the initial maximum temperature does cause a comparative strength increase at a given maturity. The conclusion to be drawn is that for a given constant maturity a higher strength can be achieved if that maturity is reached rapidly (Orchard and Barnett 1971).

Despite the mild atmosphere present in the UK, there are around 30 days during a typical winter that the temperature falls below freezing. This can double when in the north of Wales or Scotland or if above 350m.

It has been recommended (Pink 1985) that concrete should attain at least 5N/mm^2 compressive strength before being exposed to the damaging effects of frost.

In the temperature range of 0°C to 20°C and during the first 72 hours Weaver and Sadgrove (1971) have proposed the concept of 'equivalent age' based on a factor F from which an equivalent maturity at 20°C can be calculated.

$$F = \frac{(t+16)^2}{36} \qquad \text{Eqn. 2.9}$$

where:

t = Temperature of concrete during curing (°C)

F = Equivalent age

The Arrhenius equation can be defined as (Naik 1985):

$$f(T) = k_1 \exp\left(-\frac{E}{RT_k}\right) \qquad \text{Eqn. 2.10}$$

where:

k_1 = Proportionality constant

T_k = Temperature of concrete in degrees Kelvin

E = Activation energy in kilo joules per mole

R = Universal gas constant

The Arrhenius equation takes into account the activation energy for the hydration process. Since this reaction is exothermic, for each temperature there is a slightly different activation energy (E). Also, different cements have different compositions and as such have different activation energies.

It has been reported (Naik 1985) that E could be predicted by the following relationship:

at $T_c \geq 20°C$, $E(T_c) = 33.3$ kJ/mol

and at $T_c \leq 20°C$, $E(T_c) = 33.3+1.47(20-T_c)$ kJ/mol

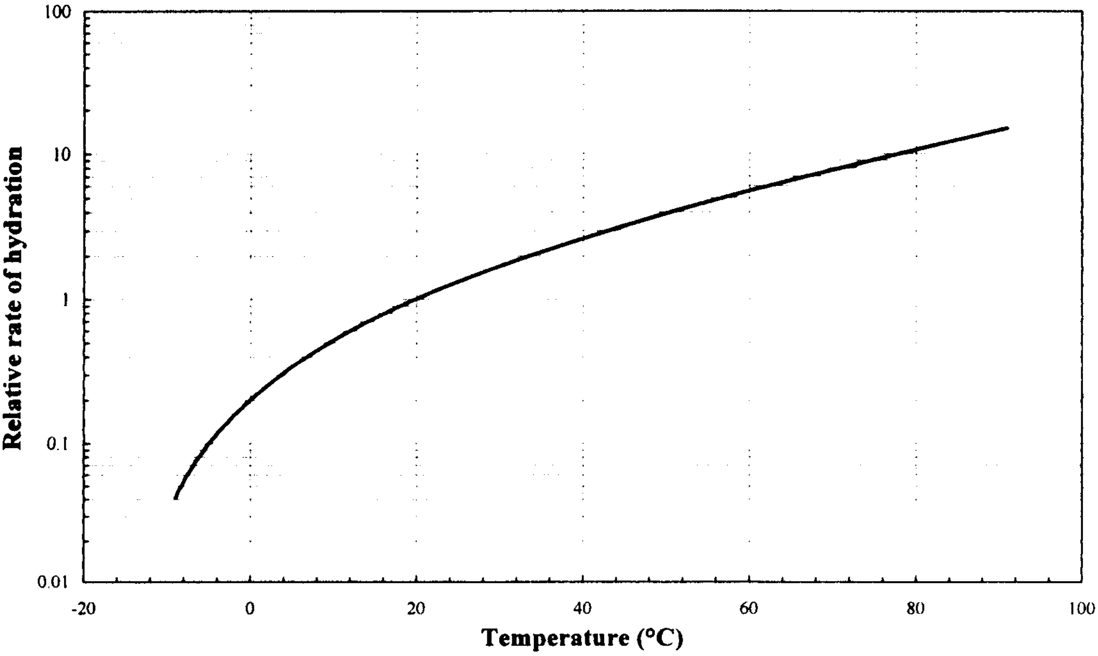

Figure 2.6 - Dependence of rate of hydration of a cement paste on temperature

Figure 2.6 shows the temperature function, illustrating the dependence of the rate of hydration of the cement upon the temperature. In the 1950s, formulae by Nurse, Saul-

Bergstrom, Verbeck and Rastrup served well for classical concrete curing as long as extreme temperatures were not attained. It can be seen from Figure 2.7 that for high hydration temperatures the Rastrup formula does not apply, while the Nurse and Saul-Bergstrom formulae lead to an underestimation of the hydration rate.

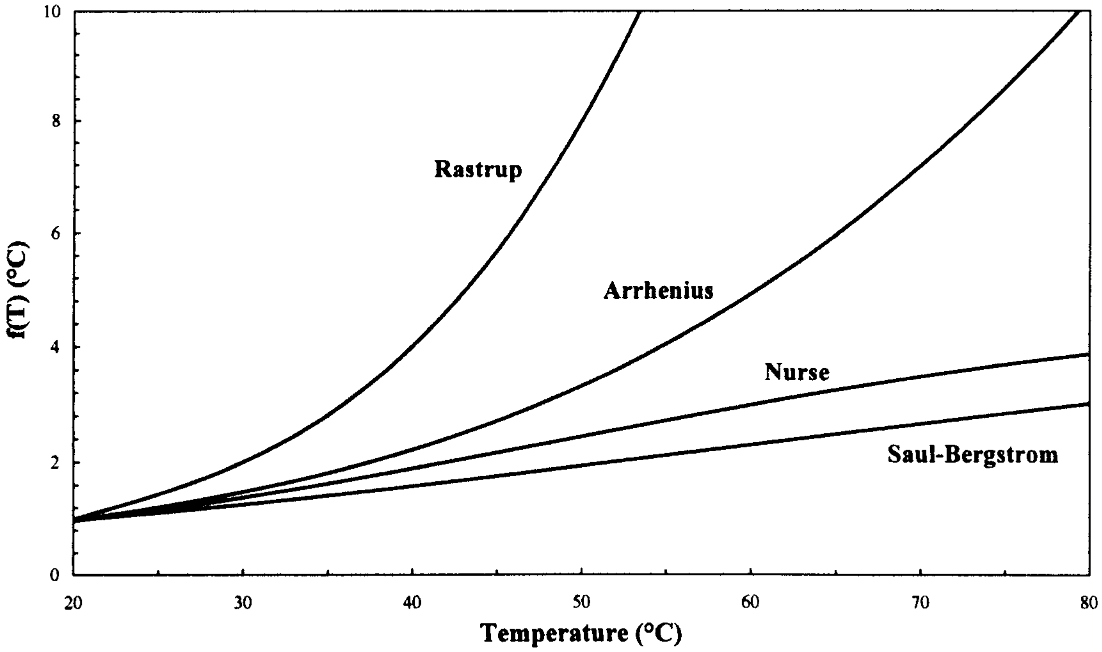

Figure 2.7 - Temperature functions of various formulae to predict cement hydration rates

2.8.6 Thermal conductivity of concrete

A knowledge of the thermal conductivity of concrete during the early hydration period is essential to obtain an accurate estimate of the thermal stresses that will develop in a concrete structure as a result of the heat produced by the binder during hydration (Gibbon and Ballam 1998).

Traditionally, the values for the thermal conductivity used for heat models of concrete structures have been based on the properties of the aggregate or the hardened concrete, with a single value being assumed for all stages of hydration. This does not represent the actual conditions of the concrete during hydration (Gibbon and Ballam 1998). It has been shown that the thermal conductivity of concretes and mortars decrease in the first 2 days by 10-20%, depending on mix constituents, whereupon small decreases continue to occur during the following 7 days. Typical values of thermal conductivity are in the range of 0.6-2.6 W/m.°C for a time after mixing of 0-4 days.

2.8.7 Thermomechanical affects

Fresh concrete consists of a mixture of materials with different coefficients of thermal expansion; hardened cement paste and aggregates have relatively similar coefficients; water and air are about 20 and 300 times higher respectively (Kirkbride 1996). Cold fresh concrete placed in a mould and subsequently heated after 1 hour, undergoes a series of differential expansions within its composition as the cement, aggregates, water and air expand at vastly different rates. In these circumstances it may be postulated that internal stresses within the concrete could occur. However, if heating is delayed for 3 to 5 hours the concrete at this time has achieved a degree of homogeneity and strength which, if the rate of temperature rise is kept within limits, is sufficient to sustain the disruptive forces.

Heat contours have been obtained (Orchard and Barnett 1971). The shapes of temperature contours were very similar irrespective of temperature or time once thermodynamic equilibrium had been established. A temperature differential of as high as 16°C was obtained between the centre and the outside of the specimen when the central temperature was 88°C and the ambient was 20°C. These temperature contours could be reduced by insulating the specimens or by placing the specimens in a preheated area to follow the heating regime.

It was also noticed (Orchard and Barnett 1971) that the failure pattern of electrocured samples during compressive failure was consistently a near perfect cone fracture. This was considered to be due to the variances in maturity across the sample which set up regular patterns of internal stresses and differing strengths.

2.9 Effects of Accelerated Curing on Mortar and Concrete

2.9.1 Fresh properties

It has long been known (Abbasi and Al-Tayyib 1985) that when concrete ingredients are mixed in hot weather rapid evaporation of water occurs. This results in a lower effective water content and hence lower effective water/cement ratio. From this, workability is reduced and also lower slump values are obtained.

2.9.2 Microstructure

A comparison of hot air cured samples (Bajza and Rousekova 1983) shows that increasing curing temperatures lead to changes in the structure of the matrix; with the more intensive the heat treatment, the coarser the structure.

2.9.3 C-S-H formation

Within the high volume production of precast concrete the use of elevated temperature curing techniques to accelerate early strength development has become widespread (Patel, Bland and Poole 1995). However, research has shown that such curing leads to the development of a modified microstructure leading to the formation of secondary ettringite. Mature pastes cured at temperatures of between 50 and 70°C have been reported to exhibit a coarser C-S-H morphology and pore structure than that of pastes cured under ambient conditions. The width of the C-S-H shell around the hydrating grains has been observed to increase with increasing cure temperature, while the inner C-S-H in a paste cured at 80°C has been reported to be denser than the outer hydrate. At elevated temperatures a greater proportion of portlandite has been found to form dense clusters as opposed to the more lamellar type morphology observed under ambient conditions (Patel et al 1995).

Samples manufactured at curing temperatures up to 46°C show a similar microstructure to that seen at 20°C with only a limited coarsening of the cement matrix at 42 and 46°C. Concretes cured at higher temperatures exhibited a coarser microstructure than that of concrete cured at 20°C, particularly with respect to portlandite (Patel et al 1995).

It is clear that concrete is a poor conductor of heat (Xuenquan et al 1987). It takes time to raise the temperature of a specimen and as such differential temperature gradients will be formed. Meanwhile, the early hydration of cement, especially for C_3S, can be too fast under such a high temperature, resulting in the formation of a large amount of very fine C-S-H gel, which may surround the unhydrates, causing hindrance of diffusion and further development of strength.

Concrete outside the laboratory cures at temperatures other than 20°C and often under less than ideal moisture conditions. High curing temperatures may result from hot weather, accumulated heat of hydration or applied heat. Heat curing is generally used in the production of precast concrete products in order to increase the early age strength, primarily to allow rapid production. The long-term properties are often observed to be negatively influenced by elevated curing temperatures. Strength and other mechanical properties are often reduced and permeability increased. It has been shown (Kjellsen 1995) that curing at elevated temperatures influences microstructure considerably.

It has also been shown (Kjellsen 1995) that curing at elevated temperatures leads to reduced surface areas of the hydrates formed and a coarser pore structure. Also that a coarser pore structure of the outer product phase prevails at mature ages as a result of isothermal curing at elevated temperatures. It has been shown (Kjellsen 1995) that the distribution of reaction products is much more uniform in pastes cured at relatively low temperatures. In pastes cured at high temperatures, relatively dense shells of reaction products form around the hydrating cement grains, while the outer product phase remains relatively porous as relatively little reaction product is formed in this phase.

Curing at temperatures above 70°C at early ages may influence the formation of ettringite decisively as this phase may not form at higher temperatures. At even higher temperatures monosulphate also becomes unstable and hydrogarnet may appear. Ettringite may also reform at later ages, resulting in destructive cracking. Another effect of heat curing is caused by a too rapid temperature rise at early ages, which may lead to microcracking and increased porosity due to differences in the thermal properties of the concrete constituents.

Although reaction products with less chemically bound water have been reported to form at elevated temperatures (Kjellsen 1995), no indications have been found that the reaction products formed at 50°C contained less overall non-evaporable water than the reaction products formed at 20 or 5°C. Assuming a constant water chemically bound in the C-S-H gel, the greater total oxides in the inner product of a sample cured at 50°C suggest that this phase has a somewhat lower fine porosity than the outer product or hydrated phases of a specimen cured at 5°C.

Oxide totals have indicated (Kjellsen 1995) that the local finer porosity of the outer C-S-H gel is largely independent of curing temperature. At higher curing temperatures the C-S-H in the inner product apparently becomes denser primarily due to lower fine porosity and the outer product contains relatively coarse pores.

Microanalytical and microscopic examination have supported the idea that the early curing temperature has relatively little influence on the final distribution of C-S-H. The inner product of heat cured concrete does not appear denser than that of concrete cured at 20°C, and the outer product does not appear to have a higher porosity. With a 0.50 W/C ratio paste non-isothermally cured, the specimen reached considerably less maturity at the end of its heat curing period and showed, in contrast to a heat cured concrete, some influence of heat curing as regards C-S-H distribution (Kjellsen 1995).

For many precast applications concrete undergoes a period of curing at elevated temperatures to accelerate strength development. It has been found (Scrivener 1992) that in virtually every case, concrete continues to hydrate after the heat treatment has ceased.

As an example of microstructural development for a concrete sample cured at room temperature, placed in a bath at 20°C for 4 hours, heated to 80°C over 4 hours and maintained at this temperature for 16 hours, then cured normally until tests at 35 and 135 days, it has been reported (Scrivener 1992) that immediately after heating the microstructure of the paste reveals rims of product 1-2μm thick around the cement grains. After 35 days a region of darker inner product C-S-H develops inside the bright rim and at 135 days this dark region had grown thicker as the cement grains continue to react. The outer part was said to have formed at 80°C while the inner part formed at 20°C in a much greater period of time. It was also reported that there were no significant differences in composition at either 35 or 135 days.

2.9.4 Delayed ettringite formation

The observed expansion of some laboratory and field Portland cement mortars and concretes exposed to elevated temperatures has been attributed to delayed ettringite formation (DEF) (Yang, Lawrence, Linsdale and Sharp 1999).

Others have stated (Shayan and Ivanusec 1996, Shayan and Quick 1992) that DEF alone cannot cause deterioration by itself and other factors such as Alkali Silica Reaction (ASR), freeze-thaw cracks or microstructural damage are the major factors.

Expansions have been reported (Odler and Chen 1995) in cement pastes cured to a maximum of 80-90°C.

According to investigations by optical microscopy and scanning electron microscopy (SEM), many ettringite bands can be observed in concretes and mortars particularly in the transition zone between paste and aggregate.

There are two principle hypotheses concerning ettringite formation. These are the ettringite crystal growth pressure theory and the uniform paste expansion theory (Yang et al 1996).

The former hypothesis suggests that pressure from ettringite crystals growing in preformed microcracks in the transition zone between the paste and the aggregate widens these cracks and causes the observed expansion. It has been suggested that the degree of supersaturation of ettringite in the pore solution of the cementitious material was insufficient to cause sufficient crystal growth pressure to achieve this expansion. However, it has also been suggested (Diamond 1996) that on the basis of basic concepts of fracture mechanics that a relatively small degree of ettringite supersaturation is enough for ettringite growth to expand the preformed cracks as the stress concentration at the tip of a long crack in concrete is large due to the brittle nature of concrete in tension.

The uniform paste expansion theory suggests that expansion of the cement paste matrix occurs, leaving gaps around the cement grains. Subsequently, newly crystallising ettringite rapidly fills the cracks produced by this expansion to result in ettringite band formation. Ettringite formation does not contribute directly to the observed expansion. It has been found (Yang et al 1996) that the widths of the ettringite bands around the aggregate were proportional to the width of the aggregate. This has been attributed to the effect of uniform expansion of the cement paste. Microscopic investigations (Diamond 1996) showed that many ettringite and rim cracks form as portions of a continuous crack network distributed throughout the concrete, which develops partially around the aggregate grains. The results of X-ray microanalysis (Yang et al 1996) suggests that portions of sulphate and aluminate species may be mixed with C-S-H gel immediately after the heat cure due to dissolution and decomposition of ettringite. The sulphate content of the C-S-H gel was found to decrease, while ettringite recrystallised during the period of expansion. At the end of the expansion, the gel was seen to have only mixed with monosulfate. It has also been suggested that recrystallisation of ettringite initially occurs in C-S-H gel and then in the cracks and voids which may then cause the uniform expansion of the paste.

Most of the ettringite in the mortars normally cured formed within seven days of hydration commencing. Ettringite could not be detected in the heat cured samples immediately after curing (Yang et al 1999). However, the overall amount of ettringite in the heat cured samples was seen to increase after seven days of water storage. It was generally shown to have a lower ettringite content than the normally cured specimens at all ages.

For mortars cured at 100°C hydrogarnet was detected but monosulfate could not be detected. In contrast, monosulfate was found in the normally cured specimens but hydrogarnet was not found to be present even after hydration for one year.

The microstructure at one year for normally cured specimens showed only empty cracks which may have been caused by the drying process necessary for SEM. Several regions of high monosulfate concentrations appeared in the mortar but only a few concentrations of ettringite could be observed.

For heat cured (100°C) specimens no concentrations of ettringite could be found immediately after heating and there were found to be no significant differences in the frequency or width of cracks between the cement matrix and aggregate when compared to normally cured specimens (Yang et al 1999).

Indications of an initial ettringite band formation and areas of ettringite concentration could be identified in the heat cured mortar after 90 days. These bands were seen to develop both in the transition zone between the cement matrix and the aggregate and in the cement paste matrix itself. Most of the bands seemed to form directly from the gel hydration products rather than having been deposited in preformed empty cracks as an inert filling. Also, the cracks linking the ettringite bands were observed to be of a lesser diameter than the ettringite bands.

In heat cured mortars after 155 days of water storage at room temperature, ettringite bands were shown to have developed (Yang et al 1999) both in the aggregate-paste transition zone and in the cement-paste matrix, in the region near and parallel to the surface of the prisms. More ettringite bands were observed in the transition zone than in the paste matrix. These bands passed through the transition zones along one or two sides of the aggregate rather than completely around the aggregate.

At later stages of the prism expansion, ettringite bands were seen to develop from the surface region to the central area of the prism. Many large grains were seen (Yang et al 1999) to be covered with ettringite bands from one, two, or occasionally three sides. Some ettringite bands were seen to have developed in the paste matrix and formed bridges between the aggregate grains.

From the above results it was concluded that there was little evidence to support the paste expansion hypothesis. It has also been found (Lawrence 1993) that DEF is dependent on the cement composition, with certain cements showing expansions, while others show none.

2.9.5 Microcracking

The phenomena that occur during the early age of concrete curing are complex with coupling between chemical-thermal-hydration and mechanical effects. Among the main attributes that govern the non-linear behaviour of early age concrete are stiffness evolution, the development of thermal strains, creep and cracking (De Borst, Van Den Boogard, Van Den Bogert and Sluys 1993).

Recent work indicates a growing concern that concrete cured at elevated temperatures may show abnormal expansion and associated microcracking (Patel et al 1995). In most of these studies delayed ettringite formation was identified as the probable cause of the expansion.

The chemical processes that occur during cement hydration in the first days after casting are accompanied by an increase in temperature and volume change. However, because the stiffness of the concrete at this stage is relatively low, a change in volume results in only moderate, mainly compressive, stresses. As the hydration of the cement continues, the stiffness of the concrete increases significantly. During the hardening phase, if concrete temperature drops, significant tensile stresses may develop which lead to the formation of cracks (Niu et al 1995).

Microcracking has been observed in many concretes, forming a prominent network in concretes cured at 85°C, and also in eighteen year old precast concrete.

The fissures within the most extensively microcracked concretes are characterised by hydrate infill, notably ettringite with some associated portlandite. Where microcracks occur at the paste/aggregate interface, the ettringite occurs as a crust like layer on the surface of coarse aggregate particles.

The presence of microcracks increases moisture mobility within the concrete which may produce density gradients within the matrix leading to further microcracking. The domination of the matrix by a network of microcracks is conductive to the formation of secondary ettringite (Patel et al 1995).

Table 2.4 - Coefficient of linear thermal expansion

Component	Coefficient of linear thermal expansion (per°C)
Gravel	4-5x10^{-6}
Limestone	2-3x10^{-6}
Sand	2x10^{-6}
Cement	11-20x10^{-6}

Owing to the considerable differences in the coefficient of thermal expansion of aggregate and cement matrix that can be seen in Table 2.4 (El Hussein and Abd El Halim 1993, Neville 1988), the aggregate will attempt to expand at a different rate than the cement matrix during temperature changes. This can be seen for the cooling case in Figure 2.8.

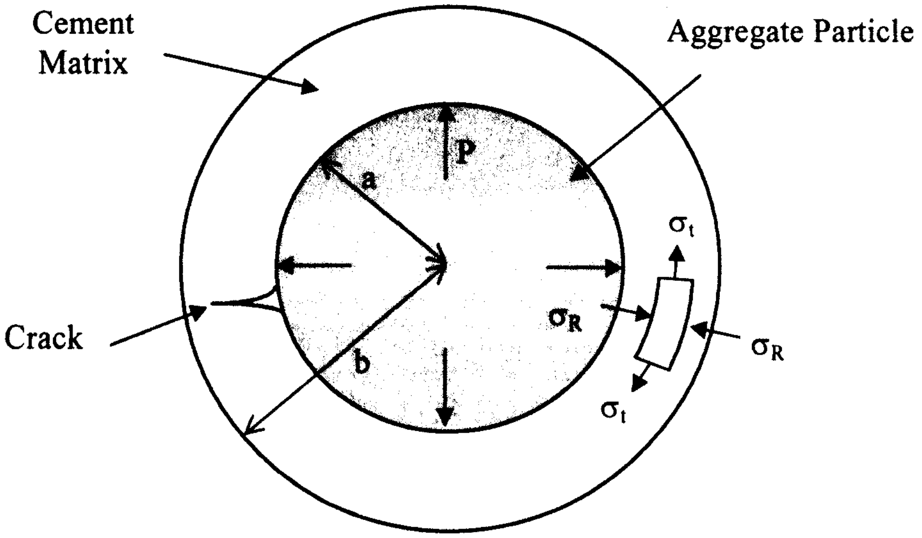

Figure 2.8 - Localised damage caused by thermally induced stresses

The cement matrix/aggregate interaction with temperature changes and the development of thermally induced stresses at high temperatures has been described (El Hussein and Abd El Halim 1993). Since expansion of the aggregate during thermal heating is limited by the cement matrix, a contact pressure will develop at the aggregate/cement matrix interface. Therefore, the contact pressure produced by differential expansion will result in radial and tangential stresses in the cement matrix surrounding the individual aggregate particle. As a result, the cement matrix around the aggregate will be under tension.

A number of assumptions have been made concerning Figure 2.8. These include:

1. No stress relaxation through creep occurs.
2. Uniform temperature throughout is assumed.
3. Coefficient of thermal expansion and Poisson's ratio are assumed constant throughout the temperature range.

Once these assumptions have been made, Figure 2.8 can be modelled as:

$$P = \Delta T(\alpha_2 - \alpha_1) \Big/ \left[\frac{K(1-\upsilon_2)+\upsilon_2}{E_2} + \frac{1-2\upsilon_1}{E_1} \right] \qquad \text{Eqn. 2.11}$$

where:

P = Contact pressure

ΔT = Change in temperature (°C)

α_1, α_2 = Coefficients of thermal expansion for aggregate and cement ($°C^{-1}$)

ν_1, ν_2 = Poisson's ratio for aggregate and cement

E_1, E_2 = Young's modulus for aggregate and cement

In Equation 2.11, K can be calculated by:

$$K = \frac{(2a^3 + b^3)}{2(b^3 - a^3)} \qquad \text{Eqn. 2.12}$$

where:

a = Radius of aggregate (mm)

b = Radius of cement matrix coating (mm)

From this the tangential stress (σ_t) and radial stress (σ_R) can be calculated by:

$$\sigma_t=KP \qquad \text{Eqn. 2.13}$$

and

$$\sigma_R=-P \qquad \text{Eqn. 2.14}$$

Localised damage in the form of microcracks resulting from high tensile stresses may result in reducing the mix resistance to externally applied loads.

2.9.6 Pore structure

In general cement porosity is composed of a well interconnected porosity, composed of tubular pores, and a disconnected porosity of rounded pores. Also cement total porosity decreases due to the hydration process but at the same time chemical shrinkage generates new pores which increase total porosity at the time of cement setting. Pores generated by shrinkage are only free pores well interconnected between each other. Curing under pressure can delay the appearance of these pores due to shrinkage (Parcevaux 1984).

Up to cement setting, trapped porosity is solely determined by the original dispersion of cement grains in water and increases sharply during cement hardening due to the formation of hydrated species in the intergranular porosity or because of the plugging of some pores through microporous hydration products.

Curing temperature was found to have little influence on cement pore size distribution except when it exceeds 80°C. Above 80°C, cement hydration proceeds at a higher rate and gives rise to larger pores through production of steam.

The total pore size distribution of hardened cement pastes has been described (Parcevaux 1984) as being composed of a threshold diameter and several families of pores, macro or capillary porosity, micro or C-S-H gel porosity and mesoporosity (porosity between particulate hydration products). Macroporosity has been found to be composed of pores wider than a few thousand Angstroms (Å) and gel porosity narrower than a few hundred Angstroms. The effect of curing conditions on the pore size distribution of hardened cement can be categorised as the width of the pores increasing with a reduction in curing temperature. It has been found (Parcevaux 1984) that as curing temperature increases from 25 to 65°C, the macroporosity increases while the micro and mesoporosity decreases without any change in overall porosity. The relationship between pore size and mechanical properties has been found to be controversial.

Samples cured at higher temperatures have been shown (Goto and Roy 1981) to have lower porosities. This is reasonable because the percentage hydration for samples cured at higher temperatures is larger than for those cured at lower temperatures, for early age samples and the porosity decreases with increased percentage hydration. However, there is evidence that the degree of hydration for samples cured at higher temperatures will eventually be smaller to those cured at lower temperatures for longer times.

With samples cured at 27°C, a peak occurs in the pore size distribution at 75-140Å, revealing no pores larger than 4300Å in radius, while samples cured at 60°C had two peaks, at 75-140Å and at 1400-2300Å. It was also noted that the total pore volume measured by mercury intrusion porosimetry was 19% and 13.5%, instead of 33.9% and 37.9% for samples cured at 60°C and at 27°C, respectively. The differences reflected the volumes of the larger pores, greater than 7.5μm in radius.

With additional water curing the values of total pore volume were seen (Bajza and Rousekova 1983) to decrease. Analysis of pore size distribution data shows that the amount of small pores increases with time of heat treatment as well as by additional water curing.

Specifications dealing with curing of concrete have been limited to specifying the desirable properties of the constituents without reference to the quality of the end product.

It is widely accepted that proper curing of concrete is essential if the concrete is to achieve its full potential. It is also true that the curing phase of concrete construction is neglected. This is because at present it is difficult to have any verifiable control over how well the concrete is being cured.

The capillary pores represent space not filled by gel or other solids such as calcium hydroxide and the gel pores are characteristic features of the structure of the gel formed by the hydration products.

Poor curing affects only the exposed surface for a depth of approximately 3cm (Senbetta and Scholer 1984).

It has been found (Bajza and Rousekova 1983) that after 1 day, specimens cured at 80°C have a lower pore volume of pores of radius 3.75-7.50nm than specimens normally cured at 20°C.

The proportion of small pores in the pore size distribution was shown to increase with the time of heat treatment as well by additional water curing. It has also been found (Bajza and Rousekova 1983) that with an increase in the temperature of curing, coarser structure of the cement paste was apparent.

2.9.7 Compressive strength

The primary benefit of heat curing is early compressive strength (Kirkbride 1971). Approximately 60% of the 28 day strength can be achieved in 24 hours. In many types of precast manufacture a much lower percentage strength is required for the purposes of demoulding and to facilitate mechanical handling, and two production cycles a day can be achieved.

It has been shown (Hutchinson et al 1991) that the adverse effect on long-term strength of a high initial temperature increases as the water/cement ratio increases. It has also been stated (Hutchinson et al 1991) that the adverse effect on strength at later ages after initially high temperature curing could be reduced considerably by the addition of gypsum to the mix. A likely cause of this is that the gypsum interferes with the phases of hydration that readily form in the presence of heat (C_3A and C_4AF). As such these phases are not disturbed by the later hydration of slower acting phases (C_2S and C_3S) which reduces microstructural damage and increases long-term strength.

It has also previously been stated (Hutchinson et al 1991) that little difference is produced in the 24 hours compressive strength if the delay before commencement of accelerated curing was 1 hour or 4 hours. Similarly there is little difference in the rates of temperature rise of 8.75 and 35°C/hr. This is contradictory to the expected changes in maturity. However, there is some evidence that a delay of 4 hours before accelerated curing produces a higher long term strength than a 1 hour delay period. It has also been stated that the varying types of cement gained strength at approximately the same rates.

The 28 days strength of microwave cured concrete is seemingly unaffected by temperatures up to 80°C whilst a small loss was noticed at 90°C. This is a substantial improvement over steam curing were it has been reported that large ultimate strength losses for temperatures of 95°C occur unless a delaying period of up to 7 hours is achieved (Hutchinson et al 1991).

2.9.8 Durability

Durability of accelerated cured concrete has been a major concern. The following states the primary durability characteristics of accelerated concrete (Kirkbride 1971):

1. Permeability: Permeability is one of the most important properties of concrete relating to its durability (Goto and Roy 1981). The permeability is influenced not only by the total pore volume, but also by the pore size distribution. The permeability values decrease exponentially with decreasing W/C ratio, at a constant curing temperature. Samples, which are cured at higher temperatures, have higher permeabilities and therefore have a coarser, more connected, pore structure. Steam cured specimens kept moist after heating show similar permeabilities as water cured samples.
2. Freeze/thaw resistance: Approximately the same for both accelerated and normally cured after 7 days.
3. Sulphate attack: Steam cured concrete appear to have greater resistance to sulphate attack.

2.9.9 Setting times

The setting of ordinary Portland cement paste occurs primarily by the hydration of C_3S with the initial set being identified by the rapid rise in heat of hydration and the final set being identified by the approximate peak temperature. (Neville 1988).

The setting times can be estimated by the use of Vicat apparatus (BS 4550: Part 3). When a proportion of the cement is replaced by PFA or GGBS, the setting times are generally increased when compared to ordinary Portland cement only. This is due to the hydration of the cement is retarded until calcium hydroxide is liberated from the hydrating cement. It has been reported (Gebler and Klieger 1986) that increases in the initial and final sets can be as high as 25 and 45 minutes respectively for a replacement level of 25% PFA. Setting times can also be further increased by the alteration of PFA class, grading or composition as well as increasing the setting times when a greater degree of replacement is used.

For a ordinary Portland cement with or without PFA inclusion (Mailvaganam, Bhagrath and Shaw 1983) reported that the initial set can double when curing temperature changes from 20 to 5°C. It has also been found (Kanazawa, Yamada and Sogo 1992) that reductions in setting times of concrete occur up to a temperature of 80°C where the cement was 50% replace by GGBS.

Results have shown that (Eren, Brooks and Celik 1995):

1. For the same temperature, increasing the level of replacement of PFA or GGBS increases the setting times.
2. For the same temperature and replacement level, the setting times of GGBS cements are less than for PFA concrete.
3. For the same temperature between 6 and 20°C, increasing the level of replacement of ordinary Portland cement by GGBS increases the setting times and for higher temperatures the setting times are reduced with no consistent trend of replacement level.
4. The general effect of an increase in temperature is to decrease the setting times, but the reductions are different for the initial set, final set and type of concrete.

2.9.10 Tensile, flexural strengths and modulus of rupture

Tensile and flexural strengths are accelerated in the same manner as compressive strength. However, it has been noted that microcracking normally associated with accelerated curing affects tensile and flexural strength to a slightly greater degree than compressive strength due to the nature of the applied load.

It has been found (Abbasi and Al-Tayyib 1985) that the modulus of rupture and the tensile splitting strength of concrete prepared and cured in hot weather conditions are reduced with the increase in the maximum temperature of concrete at preparation. This is the case even when all necessary precautions have been taken to achieve the required compressive strength and shows that tensile strength is more affected by increased temperatures.

2.9.11 Other properties

A number of other properties are important when evaluating the desirability of accelerating curing. These include:

1. Shrinkage. A significant reduction of drying shrinkage has been found for steam cured specimens when compared to water cured specimens (Kirkbride 1971).
2. Creep. Reductions of up to 50% have been reported for steam cured specimens (possibly due to the rapid drying out of samples) (Kirkbride 1971).
3. Loss on ignition. At 90°C, the LOI values are found (Bajza and Rousekova 1983) to be lower than those for samples hydrated at 80°C; this being possibly caused by premature evaporation of water at the low relative humidity of the hot curing air, and the subsequent lack of water for hydration. Additional water curing, at room temperature, increases the water content but its relative increase diminishes with an increase in temperature of hot air curing.

2.9.12 Effects of incorporating reinforcement

Incorporating reinforcement to a mix that is to be subject to most forms of accelerated curing can be said to be similar to varying the aggregate. This is because any accelerated curing technique acts solely on the cement hydration characteristics of the mix and leaves both aggregate and reinforcement unaffected. However, due to differentials in the coefficient of heat expansion, thermal stresses will occur at the boundary between reinforcement and cement matrix. However, it has been shown (Wilson and Gupta 1996) that even with incorporated reinforcement, structural gain is still readily achievable and for a range of heating regimes up to maximum of 80°C with no adverse effect due to using reinforcement being noted.

In the case where heating is intended to be due to current passing through the reinforcement, one end was connected to the live voltage and the other end to neutral. Assuming that the neutral and the mould are at earth potential, there will be leakage currents along the length of the reinforcement into the concrete which will generate heat by direct electric conduction.

In the case where direct electric conduction is intended, current must be passed through the reinforcing bars, which will heat up due to their inherent resistance (Wilson and Gupta 1996). The heating of the concrete is thought to take place due to both the ohmic heating of the concrete itself and the direct conductive heating caused by the ohmic heating of the reinforcement.

2.10 Additives and Admixtures

2.10.1 General

Additives and admixtures are materials that are added to a mix to alter either the short term or long term properties of concrete. Admixtures are generally added during the mix and additives are normally used as a partial replacement for cement. A classification of admixtures can be seen in Figure 2.9 (Rixom 1977).

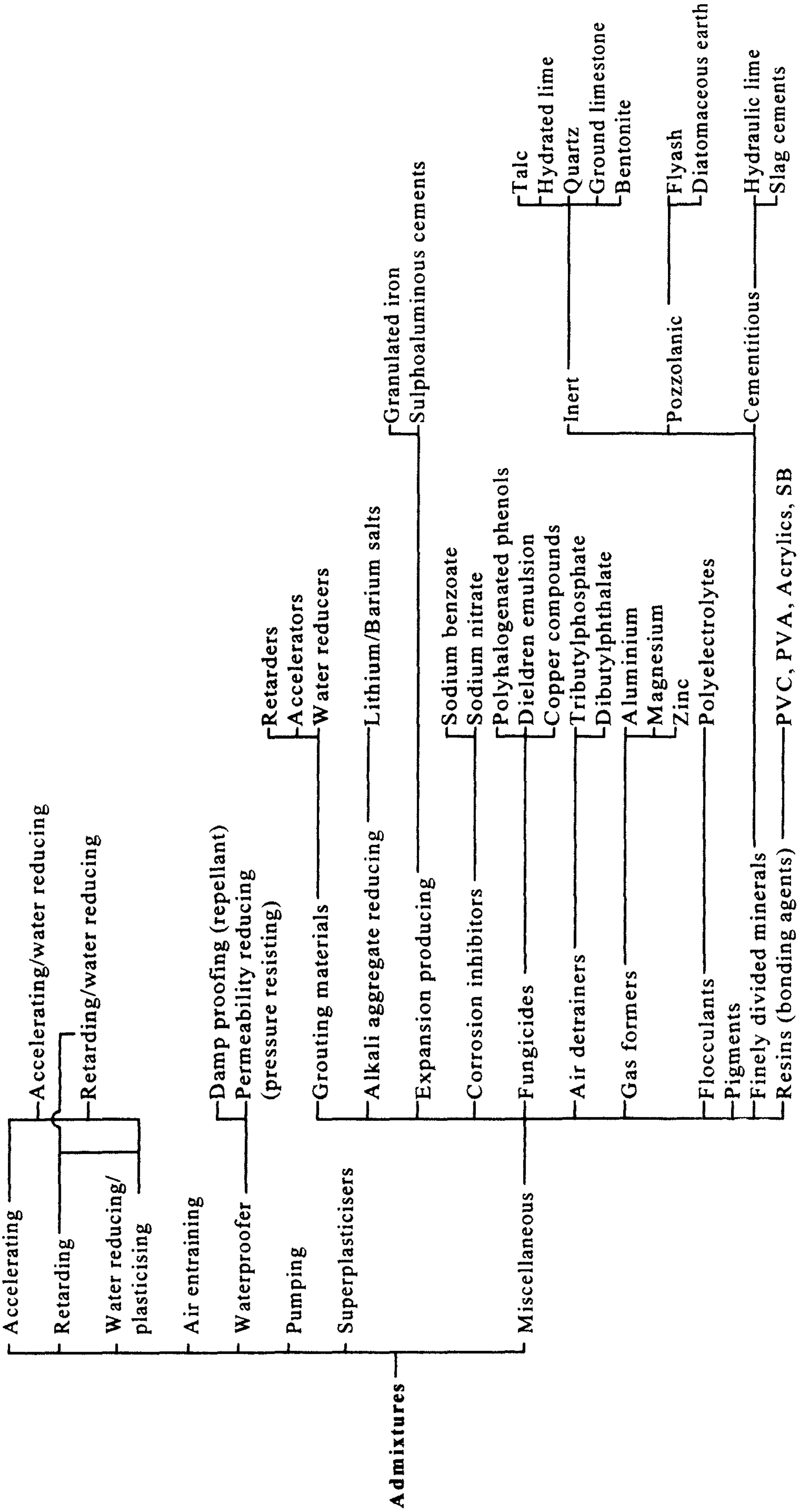

Figure 2.9 - Admixtures by type

2.10.2 Accelerating admixtures

These materials shorten the setting time of cement based mixes and/or increase the rate of strength gain. The most popular accelerator was calcium chloride (Neville 1988) but due to problems with reinforcement corrosion, other compounds were used. All accelerators increase the rate of hydration of the different chemical constituents in the cement powder.

2.10.3 Retarding admixtures

Retarding admixtures slow down the rate of setting of cement based materials. They are usually used to offset heat build up in large mass concrete structures or for retaining workability for extended periods of time. They are generally in the form of sugars or hydroxycarboxylic acids (Rixom 1977). It is thought that retarding admixtures form a film on the C_3A compound and as such interfere with hydration through the barrier to water. This film then breaks down which allows hydration to continue. Also, retarders interact with the C_3S compound, which allows retardation of up to several days.

Compared to normally mixed concrete, hot-mixed concrete requires more water for a given consistency. Any elevation of the mix temperature accelerates the changes in consistency and as such there is a more limited time from mixing to compaction.

It has been concluded that the use of retarding admixtures delay the chemical reactions in hot-mixed concrete, and stabilise the mobility of the fresh mixes for at least 20 minutes. It has also been found that the use of a retarder accelerates strength development, and the 28 day compressive strength of hot-mixed concrete is similar to that of normally cured concrete of the same mix (Berge 1976).

2.10.4 Air entraining admixtures

Air entraining admixtures do exactly as their name implies and creates numerous air bubbles (0.05-1.25mm diameter) within the concrete mix. This improves resistance to freezing conditions due to the presence of large chambers for the freezing water to expand into and can also improve workability. However, such a large amount of voids inevitably causes both short and long term compressive strength loss. Examples of materials commonly used as air entrainers are; natural wood resins, certain fats and oils and lignosulphates (Rixom 1977).

2.10.5 Superplasticising admixtures

The addition of a plasticiser to a mix allows a number of properties of both plastic and hardened concrete to be altered. These include (Rixom 1977): greater workability to be achieved for any given water/cement ratio, consistent workability for a reduction in water content and a slight increase in air content.

2.10.6 Pulverised fuel ash (PFA)

Pulverised fuel ash is created in electricity generating power stations when pulverised coal (passing 75μm sieve) is combusted. Generally, more than 85% of the ash produced in this manner is composed of amorphous glass and compounds formed from silicon, aluminium, iron, calcium and magnesium.

Physically, PFA consists of hollow, spherical particles generally between 1 and 150μm although, especially in the largest particles, both shape and surface texture can change significantly.

It has long been known (Davis, Carlson, Kelly and Davis 1937) that the addition of PFA to a concrete mix will increase its workability for a given water content. This is generally considered to be due to the spherical form of PFA which gives rise to a ball-bearing effect.

Portland cement grains tend to coagulate in the fresh concrete producing a non uniform hydrate structure. The reason that PFA inclusion results in improvement of the workability is that the fine sized spherical particles physically disperse the cement coagulations which frees more paste to lubricate the aggregates. This in turn produces a more homogenous matrix as hydration proceeds (Dhir 1986). It follows that finer ashes increase workability more than coarse ashes (Ivanov and Zacharieva 1982).

For a concrete mix incorporating PFA designed for equivalent properties of workability, 28 day strength and 20°C water curing as an OPC mix, it has been shown (Berry and Malhotra 1980) that there is very little difference in strength values of the concretes up to 28 days, but thereafter, the PFA concrete goes on to develop significantly higher strength values. Initially the concrete containing PFA will not be as strong as the equivalent OPC mix but at later ages and depending on PFA quality the mix containing PFA is significantly stronger.

The addition of PFA to OPC concrete significantly changes the permeability characteristics of the concrete. It has been suggested (Bakker 1983) that PFA inclusion decreases permeability due to the size and number of pores. This occurs because of increased precipitation of gel products in the paste as a result of the pozzolanic reaction of PFA. This has the effect of reducing leaching of $Ca(OH)_2$ in later life which would further increase the concrete permeability.

The rate at which carbonation occurs is dependent on a number of factors. These include the permeability of the concrete, its degree of saturation and the mass of $Ca(OH)_2$ available for reaction.

As has been stated previously the inclusion of PFA decreases the long term permeability and reduces the amount of $Ca(OH)_2$ available for reaction. Due to this restriction of the amount of $Ca(OH)_2$ available for reaction, carbonation in concretes containing PFA has been seen to be reduced slightly (Ho and Lewis 1983).

PFA has been widely accepted as a method of combating alkali aggregate reaction (AAR). However, it has also been stated (Mehta 1983) that PFAs vary in effectiveness and that some PFAs (mostly high calcium PFAs containing large amounts of soluble alkali sulphates) increase AAR.

The reduction in AAR has been said to be (Hobbs 1982) because PFA acts like a cement with an alkali content of 0.2 % by weight thus diluting the total alkali content.

Table 2.5 summarises the effects of PFA on the properties of fresh and hardened concrete (Bamforth 1992).

Table 2.5 - Summary of the effects of PFA on the properties of concrete

Property	**Effect of PFA**
Water demand	Reduced with increasing proportion of PFA
Workability	At constant W/C ratio, slump of PFA concrete is increased
Bleed	Reduced bleed for PFA concretes
Setting time	Increased by PFA use
Standard cured strength	Early strength gain is reduced, but long term strength increased
Heat cycled strength	For equivalent grade mixes, PFA concrete will have higher heat cycled strength at 28 days
Air cured strength	Air curing affects OPC and PFA concretes equally
Drying shrinkage	Reduced with PFA inclusion
Sulphate resistance	Increased compared with OPC concrete
Acid resistance	Increased due to lower permeability
Water and gas permeability	Comparable with OPC at 28 days, but reduced to a greater extent with age
Carbonation	Small increase
Chloride ingress	Chloride diffusion is decreased as is deterioration under cyclic salt exposure

If 30% of the cement is replaced by a class F fly ash (LOI = 3%, amount passing 45μm sieve = 5.8%) then it has been shown that:

1. At 20°C and at 11 days, the amount of $Ca(OH)_2$ present is proportional to the reduced amount of cement present, indicating no reaction, but at 1 year about 30% of the $Ca(OH)_2$ has been removed, indicating considerable reaction.

2. At 11 days and as the internal heat increased, the strength increases as the $Ca(OH)_2$ content is reduced.
3. At 1 year, the strengths are significantly greater than those of the 100% OPC mixtures, and further hydration has been shown to have taken place over the full range of heated mixes. This indicates that at temperatures over 50°C, the pozzolannic reaction is retarded by the increase in $Ca(OH)_2$.

Permeability tests carried out show that with OPC mixes, as internal heat increases, so does permeability, but with OPC/PFA mixes the opposite is true.

Chapter 3 - MATERIAL PROPERTIES AND TESTING PROCEDURES

3.1 Introduction

This chapter provides results of the properties of the constituent materials used, test set-up and the experimental procedure used for the preparation and testing of samples.

All electrically and normally cured mortar samples consisted of 150x150x150mm cubes unless otherwise stated.

3.2 Constituent Materials Testing Procedures

3.2.1 Sieve analysis

The sieve analysis (BS 812: Part 103) was used to determine the particle size distribution for both fine and coarse aggregate.

Table 3.1 – Grading limits for coarse aggregates (BS 882)

	Percentage by mass passing BS sieve						
	Graded aggregate			**Single-sized aggregate**			
Sieve size (mm)	**40-5mm**	**20-5mm**	**14-5mm**	**40mm**	**20mm**	**14mm**	**10mm**
50.00	100	-	-	100	-	-	-
37.50	90-100	100	-	85-100	100	-	-
20.00	35-70	90-100	100	0-25	85-100	100	-
14.00	-	-	90-100	-	-	85-100	100
10.00	10-40	30-60	50-85	0-5	0-25	0-50	85-100
5.00	0-5	0-10	0-10	-	0-5	0-10	0-25
2.36	-	-	-	-	-	-	0-5

It entails the sieving of a random dry sample of material through successively smaller sieves and recording the amount retained on each. This is converted into a percentage passing and is then compared to tables specifying the grading limits (BS 882) for various classes of aggregates (Tables 3.1-3.2).

Table 3.2 – Grading limits for fine aggregates (BS 882)

Sieve size (mm)	Percentage by mass passing BS sieve			
		Additional limits for grading		
	Overall limits	C	M	F
10.00	100	100	100	100
5.00	89-100	89-100	89-100	89-100
2.36	60-100	60-100	65-100	80-100
1.18	30-100	30-90	45-100	70-100
0.60	15-100	15-54	25-80	55-100
0.30	5-70	5-40	5-48	5-70
0.15	0-15	0-15	0-15	0-15

3.2.2 Impact test

The impact test apparatus (BS 812: Part 112) gives a relative measure of the resistance of an aggregate to sudden shock or impact. The impact value was determined by dropping a standard hammer mass onto an aggregate and measuring the weight of fines caused by the impact. The sample for the test was obtained by sieving the aggregate through 14 and 10mm sieves and retaining the mass retained on the 10mm sieve. The fines were calculated by sieving the impacted sample through a 2.36mm sieve and a percentage passing value was then calculated.

The maximum allowable impact values for concrete aggregates are stated in BS 882 as:

- 25% when the aggregate is to used for heavy duty concrete flooring.
- 30% when the aggregate is to be used for pavement wearing surfaces.
- 45% when to be used for other concretes.

3.2.3 Density bottle

The density bottle test in accordance with BS 1377: Part 2 was used to determine the density of the fine aggregate used in all of the mixes.

This was achieved by weighing a sample of fine aggregate within a 50ml density bottle, then adding distilled water until the bottle is full. The bottle was then placed in a vacuum air stirred to remove trapped air. This was then repeated until all air was removed. The bottle was then transferred to a temperature bath at 25°C and subsequently weighed in air when containing the water and fine aggregate and the water alone. From this the density (ρ_s) was calculated by:

$$\rho_S = \frac{(m_2 - m_1)}{(m_4 - m_1) - (m_3 - m_2)} \qquad \text{Eqn. 3.1}$$

where:

m_1 = Mass of bottle (g)

m_2 = Mass of bottle + sample (g)

m_3 = Mass of bottle + sample + water (g)

m_4 = Mass of bottle full of water only (g)

m_3-m_2 = Mass of water used (g)

m_2-m_1 = Mass of sample used (g)

(m_4-m_1) - (m_3-m_2) = Volume of soil (ml)

3.2.4 Speedy test

The 'Speedy' test was carried out to determine the moisture content of the fine aggregate used. The test involved the mixing of a standard amount of fine aggregate with calcium carbide in a sealed pressure vessel. The calcium carbide reacted with water present in the fine aggregate to produce a gas which pressurised the vessel. This excess pressure was then measured and a direct reading of the percentage of water present in the surface of the fine aggregate was then found.

This test was carried out for every mix to allow the free water content to be accurately determined and altered were necessary.

3.2.5 Vicat test

The Vicat test determines the initial and final setting times of the cement in accordance with BS 4550: Part 3. The test involved measuring the penetration of a needle into a standard cement paste mix. When this paste stiffened sufficiently for the needle to penetrate to a point 5 ± 1mm from the bottom of the mould, initial set was said to have taken place. BS 12 specifies a minimum time of 45 minutes for ordinary and rapid hardening Portland cements.

The final set was determined using a similar needle with a 5mm circular cutting edge set 5mm behind the leading edge of the needle. Final set was said to have taken place when this needle made an impression on the surface of the paste, but the circular cutting edge failed to do so. BS 12 states that the final set should be no more than 10 hours for ordinary Portland cements.

3.2.6 Loss on ignition (LOI)

The loss on ignition (LOI) test was carried out on the cement and PFA to ascertain the level of carbon present. This involved the heating of pre-weighed samples in a kiln to a temperature of 975°C ± 25°C for 1 hour to burn off any carbon. Samples were then weighed again to establish the percentage carbon present (BS EN 196: Part 2).

3.2.7 Fineness

The most commonly method of determining fineness of PFA is by calculating the percentage retained on a 45μm sieve (BS 451: Part 2). This is because it is quick to perform, easily repeatable and uses cheap equipment (Malhotra 1987). However, this only considers the particle size at one cut off, thus enabling two differently size distributed PFAs to be considered equal fineness. Even so, it has been shown that the residue retained on a 45μm sieve is roughly proportional to the pozzolanic activity index and water requirement (Dhir 1986).

3.3 Constituent Material Properties

3.3.1 Coarse aggregate

A coarse aggregate of 20mm single sized crushed granite was used subject to BS 812: Part 103. The aggregate impact value was found to be approximately 8.5% in accordance with BS 812: Part 112. The relative density was found to be 2.7 according to BS 812: Part 2.

Results for the coarse aggregate properties can be seen in Tables 3.3-3.4 and Figure 3.1.

Table 3.3 - Sieve analysis of coarse aggregate

BS sieve size (mm)	Mass retained (g)	Mass passing (g)	Percentage retained	Percentage passing	Cumulative % retained
20	240	2121	10.2	89.8	10.2
14	1629	492	69.0	20.8	79.2
10	464	28	19.7	1.2	98.8
5	24	4	1.0	0.1	99.9
2.36	0	4	0.0	0.1	99.9
Tray	4	0			

Table 3.4 - Impact values of coarse aggregate

Sample	Test 1	Test 2
Mass of aggregate pre-test (g)	539	465
Fractions passing 2.36mm sieve (g)	38	47
Impact value	7%	10%
Average impact value	8.5%	

3.3.2 Fine aggregate

The fine aggregate used was found to be class M grading according to BS 812: Part 103 with a relative density of 2.7 in accordance with BS 1377.

Results for the fine aggregate sieve analysis can be seen in Table 3.5 and Figure 3.1.

Table 3.5 - Sieve analysis of fine aggregate

BS sieve size (mm)	Mass retained (g)	Mass passing (g)	Percentage retained	Percentage passing	Cumulative % retained
10	0.4	117.9	0.3	99.7	0.3
5	0.6	117.3	0.5	99.2	0.8
2.36	19.0	98.3	16.1	83.1	16.9
1.18	19.7	78.6	16.7	66.4	33.6
0.60	25.4	53.2	21.4	45.0	55.0
0.30	23.9	29.3	20.2	24.8	75.2
0.15	13.6	15.7	11.5	13.3	86.7
Tray	15.7	0			

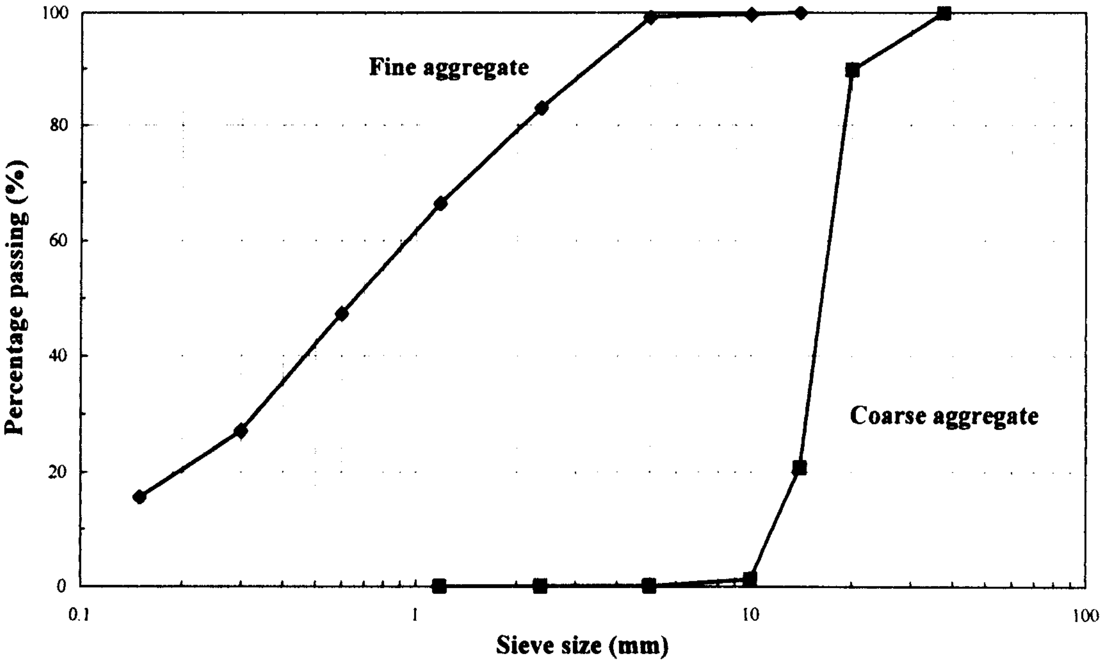

Figure 3.1 – Coarse and fine aggregate sieve results

3.3.3 Cement

The cement used was ordinary Portland cement in accordance with BS 12 and of class 42.5N. Referral was made to the manufacturers literature and a summary of results can be seen in Table 3.6.

Table 3.6- Properties of cement used

Cement property	Value
Initial setting time	270 min
Final setting time	360 min
Fineness (45μm residue)	345m^2/kg
LOI	0.85%

3.3.4 Lime

The lime used being derived from calcium carbonate limestones and chalks being subject to the tests and requirements of BS 890.

3.3.5 Admixtures

(a) Superplasticiser

The superplasticiser used was the FOSROC Conplast M1. Reference was made to the manufacturers literature and a summary of properties can be seen in Table 3.7.

Table 3.7 – Properties of superplasticiser

Chemical basis	Sulphonated melamine polymers
Appearance	Clear liquid
Specific gravity	1.10 at 20°C
Chloride content	Nil
Air entrainment	<1%
Alkali content	40.0g Na_2O equivalent/litre of admixture
Typical dosage	2l/100kg of cement

(b) Air entrainer

The air entrainer used was the FOSROC Conplast AE 316. Reference was made to the manufacturers literature and a summary of properties can be seen in Table 3.8.

Table 3.8 – Properties of air entrainer

Chemical basis	Blend of synthetic and natural occurring surfactants
Appearance	Brown liquid
Specific gravity	1.02 at 20°C
Chloride content	Nil
Alkali content	<15.0g Na_2O equivalent/litre of admixture
Typical dosage	0.03l/100kg of cement for a 5% air entrainment

(c) Retarder

The retarder used was the FOSROC Conplast R. Reference was made to the manufacturers literature and a summary of properties can be seen in Table 3.9.

Table 3.9 – Properties of retarder

Chemical basis	Hydroxycarboxylic materials
Appearance	Brown liquid
Specific gravity	1.13 at 20°C
Chloride content	Nil
Air entrainment	Slightly less than normal equivalent mix
Alkali content	<55.0g Na_2O equivalent/litre of admixture
Typical dosage	0.4l/100kg of cement

(d) Accelerator

The accelerator used was the FOSROC Conplast A650. Reference was made to the manufacturers literature and a summary of properties can be seen in Table 3.10.

Table 3.10 – Properties of accelerator

Chemical basis	Selected inorganic materials
Appearance	Clear liquid
Specific gravity	1.49 at 20°C
Chloride content	Nil
Air entrainment	<1%
Alkali content	5.0g Na_2O equivalent/litre of admixture
Typical dosage	0.4l/100kg of cement

3.3.6 Pulverised fuel ash

The pulverised fuel ash was found to have a fineness of 18% passing a 45μm sieve and a loss on ignition of 3.8%.

3.3.7 Water

Ordinary tap water was used in accordance with BS 3148.

3.4 Mix Design and Casting

3.4.1 Mortar

Having found the values of specific gravity for each material, mix proportions with respect to mass was calculated. Table 3.12 shows the mix proportions by volume (cement:lime:sand of 1:¼:3) used to produce the mortar samples. The mix is proportioned to the required mass of cement and the required masses for 1m^3 of mortar can also be seen in Table 3.12. These values were calculated from Eqn. 3.2:

$$\text{Proportions compared with cement} = \left(\frac{3.15}{3.15}\right) : \left(\frac{0.25 \text{ x } 2.3}{3.15}\right) : \left(\frac{3 \text{ x } 2.68}{3.15}\right) \qquad \text{Eqn. 3.2}$$

Therefore (by mass): cement:lime:sand = 1:0.183:2.55

Table 3.12 - Mix proportions of mortar

	Proportion by volume	Mass (kg/m^3)
Cement	1	741
Lime	¼	136
Sand	3	1890

The water content was calculated directly from the cement content as required by the W/C ratio.

3.4.2 Concrete

All concrete mixes were designed with reference to Department of the Environment guidelines (1992). A summary of the mix proportions for 1m^3 can be seen in Table 3.13. The full mix design sheets can be seen in Appendix A.

Table 3.13 - Summary of mix proportions for 1m^3 of concrete for various mix designs

Mix type	Cement content (kg/m^3)	Water (kg/m^3)	Fine aggregate (kg/m^3)	Coarse aggregate (kg/m^3)
C30 (Slump 10-30)	345	190	743	1162
C50 (Slump 10-30)	475	190	568	1207
C30 (Slump 60-180)	409	225	751	995
C30 (Slump 10-30) 2% air entrained	442	190	684	1070
C30 (Slump 10-30) 5% air entrained	442	190	652	1021

PFA addition was based solely on a percentage of the cement values with no alteration to the overall mix design.

The addition of a superplasticiser, retarder and accelerator replaced an equivalent mass of water within the mix.

3.4.3 Casting

All electrically and normally cured samples (cubes, beams and slabs) were cast in accordance with BS 1881: Parts 108 and 125. Samples were demoulded after a period of 1 or 3 days and placed in a water tank at a temperature of 20°C ± 1°C in accordance with BS 1881: Part 111.

3.5 Fresh Concrete Testing Procedures

3.5.1 Slump

The slump test indicates the workability of fresh concrete and is extensively used throughout the world. This was achieved by filling and compacting (3 layers each tamped 25 times) a standard sized cone with concrete and then the cone was removed cleanly and vertically. The concrete then 'slumped' to a reduced height and this reduction was measured and compared to qualitative tables relating to workability. The slump test was used in accordance with BS 1881: Part 102.

A slump test was carried out for every mix to ensure compliance with the original mix design.

3.5.2 Vebe consistometer

The Vebe consistometer test was also used to indicate the workability of fresh concrete. This was achieved by placing a sample of concrete formed in a similar manner to the slump test in a bowl of standard dimensions. A standard plate (free to move vertically) was then placed onto the sample and the apparatus was vibrated. The time taken for the sample to completely cover the lower surface of the plate as the concrete collapses and fills the bowl was then recorded and compared to workability charts and the mix design. The Vebe test was used in accordance with BS 1881: Part 104.

A Vebe test was carried out for every mix to ensure compliance with the original mix design.

3.5.3 Air entrainment test

The amount of air entrained in a concrete sample can be assessed by the use of the air entrained test in accordance with BS 1881: Part 106.

This test involved placing a standard compacted sample of concrete within an airtight vessel. The vessel was then filled with water to a datum and a standard calibration air pressure of $125kN/mm^2$ was pumped into the vessel. This resulted in a reduction of water level as the air contained within the concrete compressed and from this a direct percentage value of air entrained was found.

The air entrained test was carried out for every mix containing air entraining admixture.

3.6 Hardened Concrete Testing Procedures

3.6.1 Compressive strength test

The crushing machine used for the compressive strength tests was a 2MN Avery-Denison machine, which complied with BS 1881: Part 115. All compressive strength tests were carried out on 150x150x150mm cubes in accordance with BS 1881: Part 116.

3.6.2 Splitting tensile test

The splitting tensile test in accordance with BS 1881: Part 117 is a method for determining the indirect splitting tensile strength of a cubic sample.

The test involves the placing of the sample in the arrangement shown in Figure 3.2 whereupon an increase in load of 0.02-0.04 $(N/mm^2)/s$ is imposed on the sample. The tensile splitting strength (σ_{ct}) can then be calculated by:

$$\sigma_{ct} = \frac{2F}{\pi l d} \qquad \text{Eqn. 3.3}$$

where:

F = Failure load (N)
l = Length of specimen (mm)
d = Cross sectional dimension of the specimen (mm)

Tensile tests were carried out solely on concrete beams at varying ages and were carried out at least a distance d from the end surface of the beams and other tensile testing sites in such a way that the fracture plane crossed the trowelled surface. A diagrammatic representation of this can be seen in Figure 3.3.

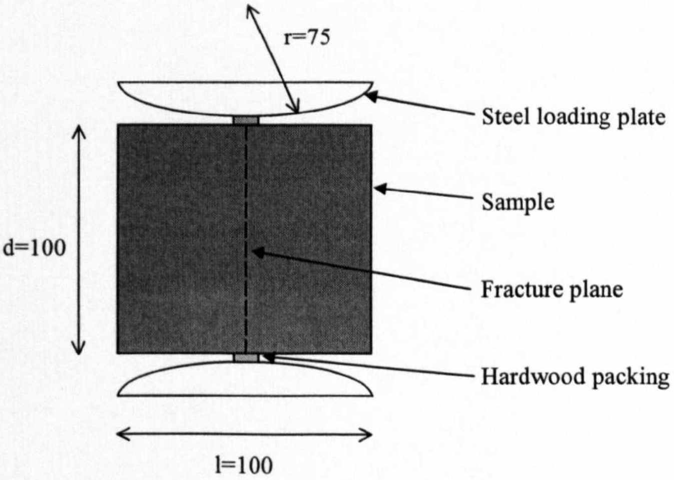

Figure 3.2 – Arrangement of splitting tensile test

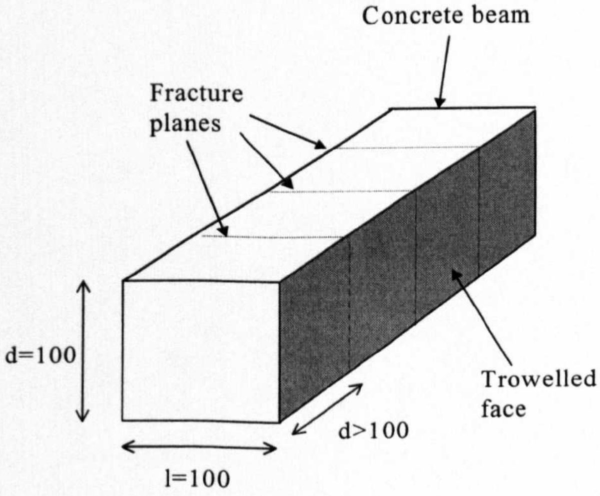

Figure 3.3 – Fracture planes of splitting tensile test

3.6.3 Flexural tensile strength

The flexural tensile strength of concrete is determined by means of a constant moment in the central part of a beam using a two-point loading system (Figure 3.4). A load is applied without shocking at a rate of 0.06 ± 0.04 (N/mm^2)/s until failure occurs. The flexural tensile strength (f_{cf}) is then calculated by:

$$f_{cf} = \frac{Fl}{d_1 d_2^2} \qquad \text{Eqn. 3.4}$$

where:

F = Failure load (N)

d_1 = Depth of beam (mm)

d_2 = Width of beam (mm) = 100mm

l = Maximum distance between rollers (mm)

Beams were tested after 28 days in accordance with BS 1881: Part 118 on both normally and electrically cured specimens. The test set-up was in a similar manner to the splitting tensile test with the crack face running perpendicular to the unloaded trowelled surface.

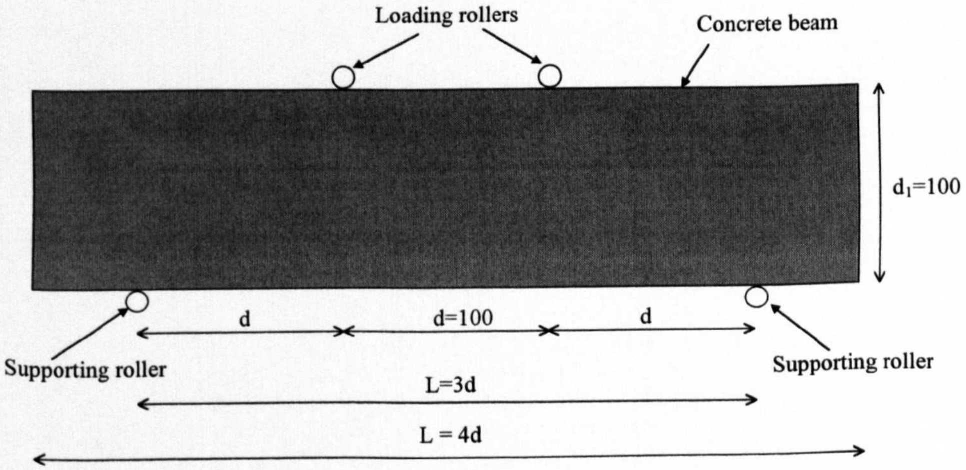

Figure 3.4 – Arrangement of flexural tensile test

3.6.4 Core samples

The examination and compression testing of cores cut from hardened concrete is a well established method, enabling visual inspection of the interior regions of a member as well as an estimation of strength by testing (Bungey 1982).

Cores were taken vertically from the cast slabs at various locations between the reinforcement on the underneath side. The cores were cut by means of a rotary cutting tool with a diamond bit and were of 50mm diameter. This diameter was chosen to allow a sufficient number of cores to be taken for the analysis of compressive strength distribution throughout the slab. Core length was also 50mm and each core was cut in such a manner that the section 50mm below the surface was removed and discarded. The cores were then ground at each end to allow a parallel surface normal to the vertical axis of the core at either end of the sample.

Initially a visual inspection of the cores was carried out and following this a compressive strength test was performed on each sample at a rate of 12-24(N/mm^2)/min. The visual inspection allowed a qualitative analysis of crack location and size.

The compressive strength of the cores was correlated by initially coring a normally cured slab which was based upon a mix design of known compressive strength at various ages. The electrically cured cores were then correlated to this curve to estimate the equivalent 150mm cube compressive strength.

Density, porosity and water absorption determination was carried out at various ages on the core samples taken from the slabs.

3.6.5 Initial surface absorption test (ISAT)

The ISA test measures the water absorption into the concrete specimen. This is dependent on capillary suction which in turn is dependent on the pore radius, temperature, connections within the pore network, water concentration gradient and degree of saturation. The water absorption in turn affects the durability characteristics of concrete.

The ISAT (Levitt 1969) was initially used as a quality control test for the manufacturing of precast concrete curbs. The test was later adopted for general concrete testing as part of BS 1881: Part 5. The test apparatus can be seen in Figure 3.5. The cap void covers a surface area of the sample of 5000mm^2.

The ISAT theory is based upon viscous flow through a fine capillary which is modelled by Poiseulles empirical equation for the rate of flow for straight, parallel cylindrical capillaries (Levitt 1969) as shown below:

$$\frac{dv}{dt} = \frac{Hr^4}{8L\mu} \qquad \text{Eqn. 3.5}$$

where:

dv/dt = Rate of flow (m^3/s)

H = Head pressure (m)

r = Radius of capillary (m)

L = Length of water filled capillary (m)

μ = Viscosity of water (m^2/s)

This is different to the actual case for the convoluted pore network that exists in concrete but does serve as a useful approximation.

In Eqn. 3.2 the average pore radius (r), pressure head (H = 200mm) and viscosity (μ) are assumed to be constant. The capillary length (L) is assumed to be proportional to the volume of pores filled by water (v), hence:

$$\frac{dv}{dt} = \frac{a}{v} \qquad \text{Eqn. 3.6}$$

where:

a = Constant

This can then be integrated to give:

$$v^2 = 2at + C \qquad \text{Eqn. 3.7}$$

where:

C = Constant

This can then be substituted into Eqn. 3.6 to give:

$$\frac{dv}{dt} = at^{-0.5} + C \qquad \text{Eqn. 3.8}$$

For a more applicable approach to concrete testing, it has been shown that the equation is in the form:

$$\frac{dv}{dt} = at^{-n} + C \qquad \text{Eqn. 3.9}$$

where:

n = Material constant

The value of n is constant for a given material but has been shown to vary (Dhir and Byars 1991) from approximately 0.3 to 0.7 depending on the quality of the concrete tested. The value of n can be taken from the graph of Log (t) against Log (dv/dt). This produces a straight line from which the value of n is equal to the gradient of the line.

The value of n is proportional to the rate of decrease in absorption. Hence a high value of n is equivalent to a relatively rapid decrease in absorption rates which has been shown (Dhir and Byars 1991) to be caused by silting of the pores, decreasing capillary pressure caused by moisture within the concrete or depth related changes of microstructure. A lower value of n is equivalent to a reduced rate of decrease in the rate of absorption which has been similarly shown to be caused by lateral spread of the test area, micro cracking or increases in the effective pore radius due to capillary flushing.

All ISA testing was carried on two 150x150x150mm specimens in accordance to BS 1881: Part 5.

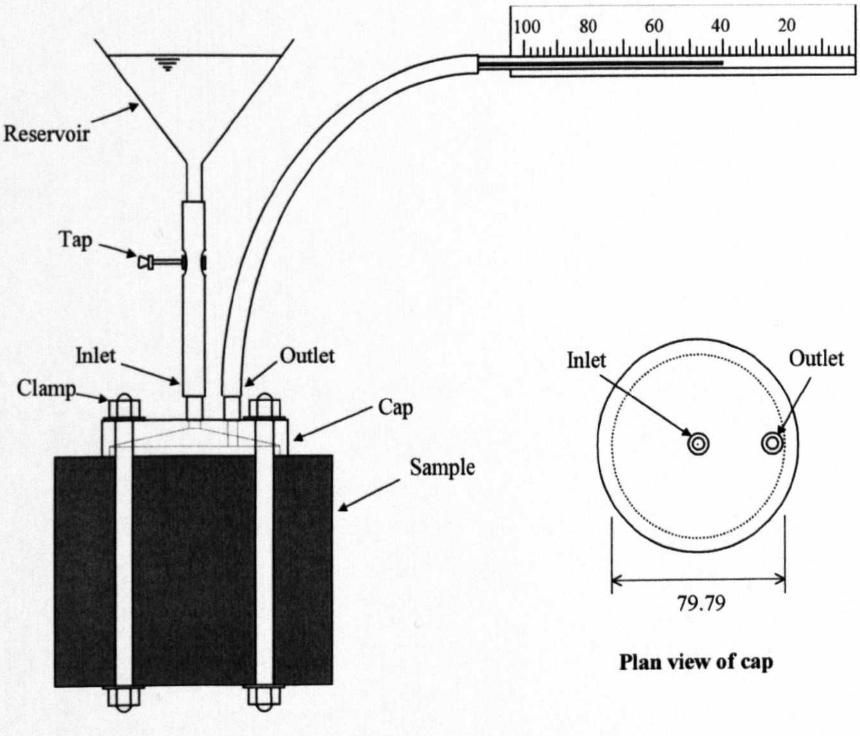

Figure 3.5 - ISAT assembly

3.6.6 Porosity

Porosity measurements were taken of various samples of normally and electrically cured specimens at various ages (DeVenny and Khalaf 1998).

The test was achieved by drying the samples (min 100g) in an oven at 105°C ± 5°C for a period of 24 hours. The samples were then weighed and placed in a vacuum at 600mm below atmospheric pressure for a period of 0.5 hours. The vacuum chamber was then filled with distilled water and allowed to soak for a period of 24 hours. The samples were then weighed in air and water and from this the porosity was calculated by:

$$P = \frac{(m_{wa} - m_{da})}{(m_{wa} - m_{w})} x100 \qquad \text{Eqn. 3.10}$$

where:

P = Porosity (%)

m_{da} = Mass of dry sample in air (g)

m_{wa} = Mass of saturated sample in air (g)

m_{w} = Mass of saturated sample suspended in water (g)

3.6.7 Water absorption

Water absorption was calculated for various samples of normally and electrically cured specimens at various ages (DeVenny and Khalaf 1998).

Water absorption was achieved by drying the samples (min 100g) in an oven at 105°C ± 5°C for a period of 24 hours. The samples were then weighed and placed in a vacuum at 600mm below atmospheric pressure for a period of 0.5 hours. The vacuum chamber was then filled with distilled water and allowed to soak for a period of 24 hours. The samples were then weighed in air and water and from this the water absorption was calculated by:

$$W = \frac{m_{wa} - m_{da}}{m_{da}} x100 \qquad \text{Eqn. 3.11}$$

where:

W = Water absorption (%)

m_{da} = Mass of dry aggregate in air (g)

m_{wa} = Mass of saturated aggregate in air (g)

3.6.8 Density

Density measurements in accordance with BS 1881: Part 114 were taken of various samples of normally and electrically cured specimens at various ages.

The volume of the samples (cube or core) was calculated by:

$$V = \frac{m_a - m_w}{1000} \qquad \text{Eqn. 3.12}$$

where:

V = Volume of sample (m^3)

m_a = Mass of sample in air (kg)

m_w = Mass of sample suspended in water (kg)

The samples (minimum of 100g) were then dried in an oven at 105°C ±5°C for a period of 24 hours. The samples were then weighed in air and from this the density was calculated by:

$$\rho = \frac{m_a}{V} \qquad \text{Eqn. 3.13}$$

where:

ρ = Density (kg/m^3)

The specific gravity could then be found by dividing the density by the density of water ($1000kg/m^3$).

3.6.9 Ultrasonic pulse velocity

This test involves a pulse of sound at various frequencies (depending on transducer selection) being passed through a sample of known length. This pulse will travel faster in a dense medium and as such can give a relative indication of compressive strength. However, again this indication can only be assumed if the sample being tested is of type that mirrors the specimen in-situ. Many factors greatly influence the readings achieved from this piece of apparatus. These include temperature, stress history, path length, moisture content, aggregate type and the presence of reinforcement.

From these variations it can be assumed that for a comparison with compressive strength, variations of around 20% can be expected. However, concrete can be qualitatively classified according to Table 3.11. The ultrasonic pulse velocity test conforms to BS 1881: Part 203. A diagrammatical layout of the test can be seen in Figure 3.6.

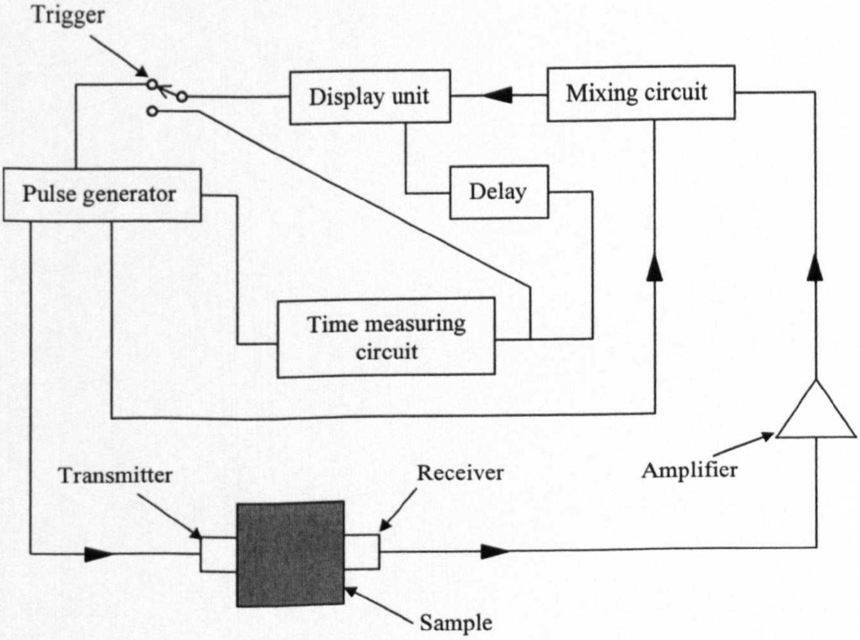

Figure 3.6 – Set-up of ultrasonic pulse velocity meter

Ultrasonic tests were carried out on 150x150x150mm cubes at various ages.

Table 3.11 – Classification of concrete quality on the basis of pulse velocity

Longitudinal pulse velocity (km/s)	Quality of concrete
>4.5	Excellent
3.5-4.5	Good
3.0-3.5	Doubtful
2.0-3.0	Poor
<2.0	Very poor

3.6.10 Schmidt hammer

This test is based on the principal that the rebound of an elastic mass will depend on the surface hardness of the test subject in question. From this test, information can be gathered on surface characteristics up to 30mm deep in concrete. The results give only a measure of the relative hardness of the cover zone and as such, a direct comparison with other properties, such as compressive strength, is difficult unless a good degree of calibration can be achieved. This calibration must be based on the particular mix under consideration, and the concrete surface, curing history and age of specimens should correspond as closely as possible to the in-situ concrete. The results from a Schmidt hammer are significantly influenced by: coarse aggregate type, moisture condition, curing history, cement type, cement content, member mass, degree of compaction, surface type, surface carbonation, stress state and temperature (Nasser and Al-Manaseer 1987).

The range of correspondence between Schmidt hammer and compressive strength results are not better than 15% and in most cases a value of 25% is more likely.

Schmidt hammer tests, in accordance with BS 1881: Part 202, were carried out on both the electrically cured and normally cured concrete slabs over the lower surface at regular spacing intervals at various ages.

3.6.11 Scanning electron microscope (SEM)

The scanning electron microscope was used to determine the microscopic structure of both electrically and normally cured concrete samples at various ages. Specimens were first coated in platinum to present a suitably reflective surface to the electrons.

A representation of the SEM can be seen in Figure 3.7. The electron gun produces a stream of electrons, which travel through condenser lenses and condenser apertures to form a tight, coherent beam which then interact with the sample and are detected by various instruments to produce a visual image.

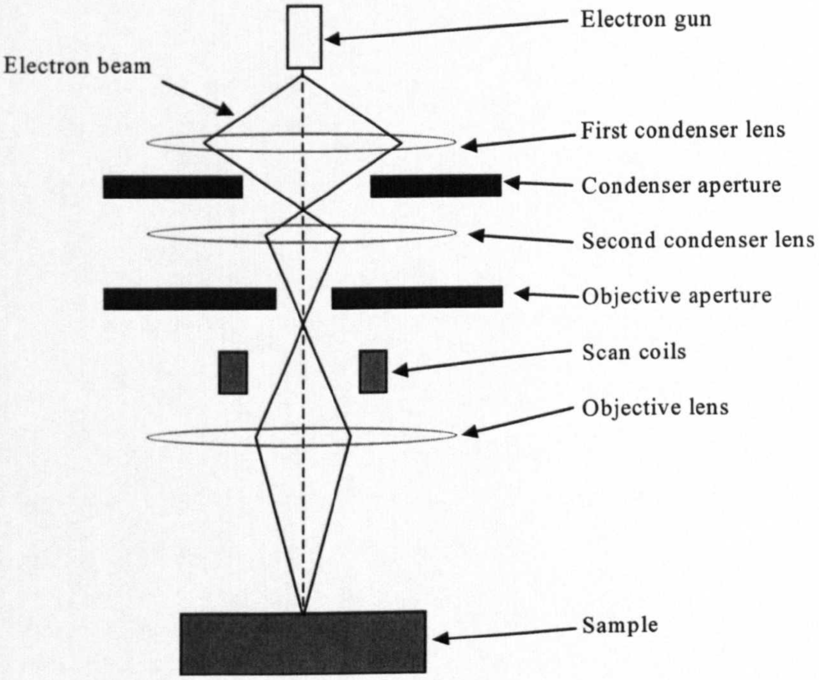

Figure 3.7 – Scanning electron microscope set-up

3.7 DEC Set-up

3.7.1 Equipment used

An alternating power supply which consisted of a Regavolt Variac (step-down) transformer was used to supply current through the cubes.

A Hydra 2625A data logger was configured to take temperature readings from a series of thermistor wires placed within the electrically cured samples.

Two Thurlby 1504 r.m.s. multimeters and a Feedback EW604 electronic wattmeter were used in the electrical circuit.

A diagrammatic representation of the connection of the power supply and the specimens to be electrically cured can be seen in Figure 3.8. The circuit consists of the electrically cured specimens connected to the alternating current power supply with a voltmeter across the supply and an ammeter in series.

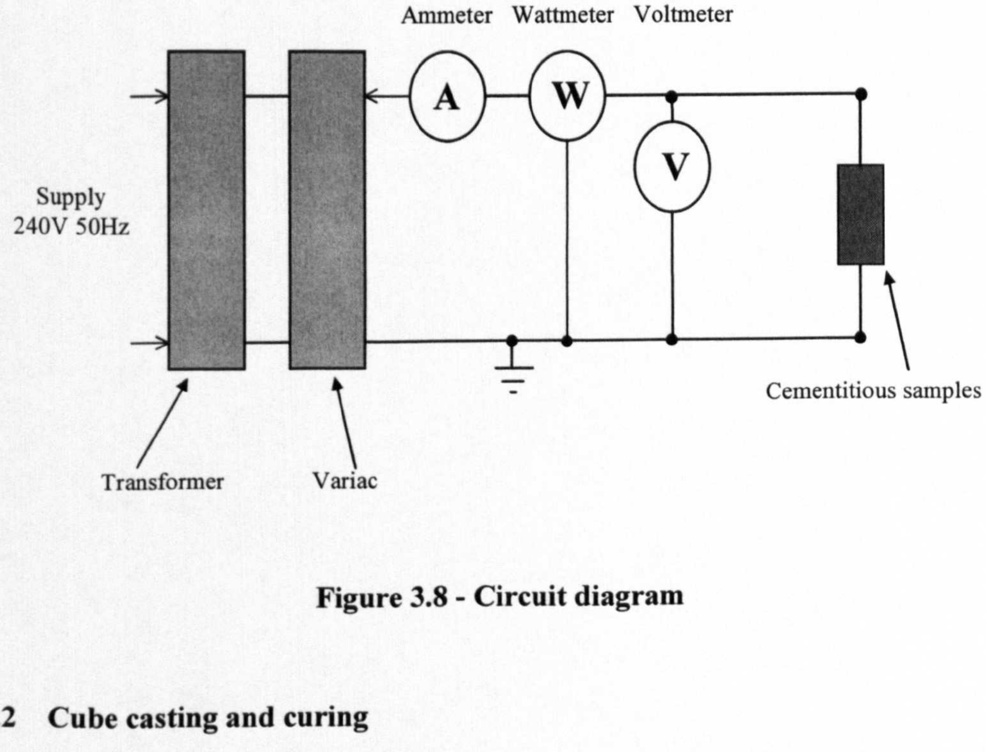

Figure 3.8 - Circuit diagram

3.7.2 Cube casting and curing

150x150x150mm plastic moulds were used for casting the electrically cured specimens. These moulds were externally reinforced to reduce deformation at the higher temperatures used as shown in Figure 3.9.

Two stainless steel plates of dimensions 150x250x2.5mm were used as electrodes during the electrical curing. These were placed at opposite faces of the cube prior to the placement of the material in the cube as shown in Figure 3.10 and were not coated in demoulding agent due to the possibility that this procedure may seriously affect the contact properties between the plate and the mix.

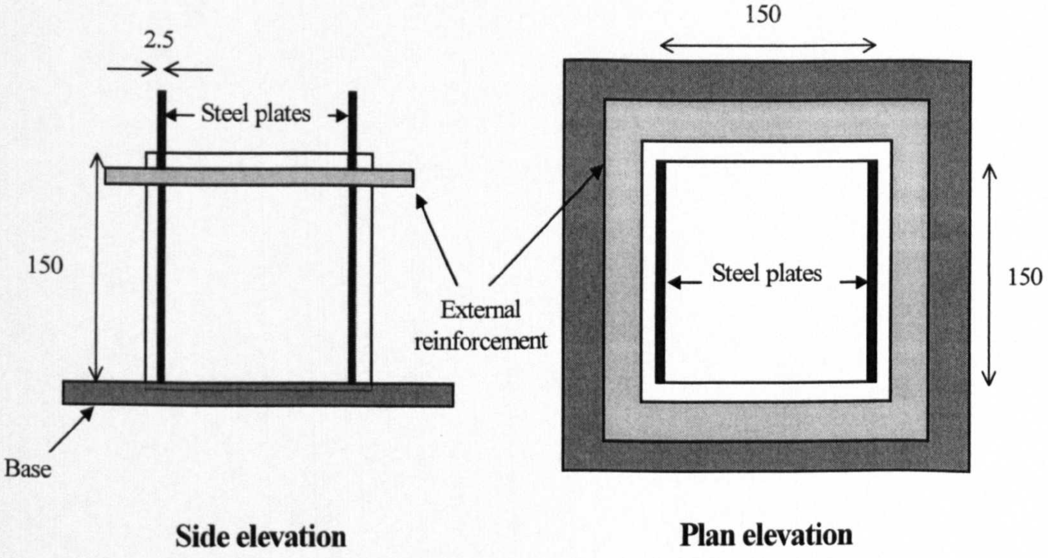

Figure 3.9 - Plastic cube moulds

A thermocouple temperature sensor was embedded in the centre of each sample immediately after vibration at a depth of approximately 20mm unless otherwise stated.

A set of three 150mm steel cubes were used as moulds for the normally cured cubes.

A polystyrene box was constructed and used to insulate the cubes being cured electrically. The cube moulds were placed on a polystyrene slab 50mm thick which formed the base of the insulating container and the remaining cover (also 50mm thick) placed over the top.

Power, voltage and current level measurements were taken every 15 minutes during heating and after this had been completed the levels of resistance were checked at regular intervals by applying a power of 20W for a maximum of 20 seconds so as not to significantly begin heating again.

The electrical resistance was calculated by:

$$R = \frac{P}{I^2} \qquad \text{Eqn. 3.14}$$

where:

R = Total resistance of samples (Ω)

P = Power (W)

I = Current (A)

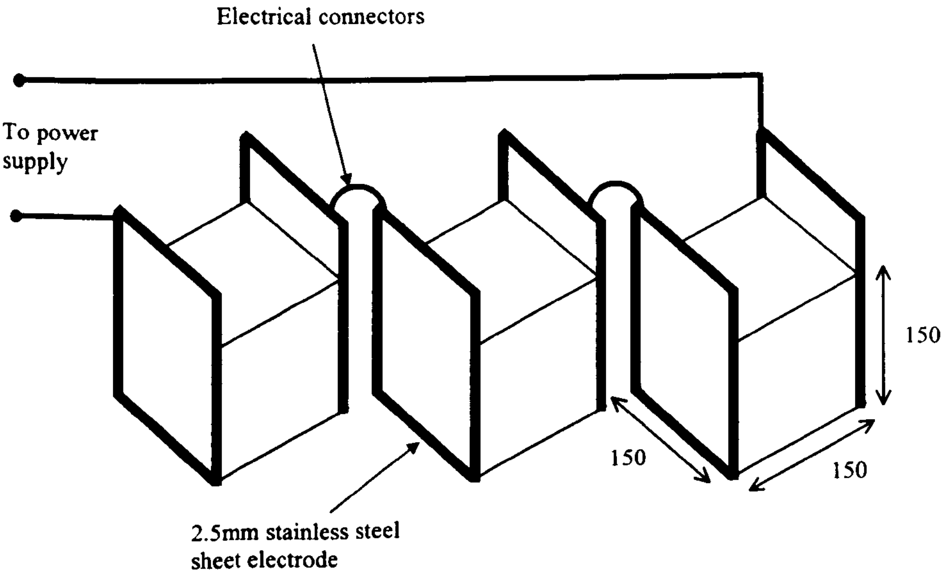

Figure 3.10 - Set-up for cube heating

3.7.3 Beam casting and curing

Four 100x100x400mm wooden moulds were used for casting the electrically cured beams. These moulds were externally reinforced to reduce deformation at higher temperatures.

Two stainless steel plates of dimensions 100x150x2.5mm were used as electrodes during the electrical curing. These were placed at opposite faces of the beam prior to the placement of the material in the mould as shown in Figure 3.11.

A thermocouple temperature sensor was embedded in the centre of each sample immediately after vibration at a depth of approximately 20mm unless otherwise stated.

Similar moulds without electrode plates were used for the normally cured beams.

A polystyrene box was constructed and used to insulate the beams being cured electrically. The beam moulds were placed on a polystyrene slab 50mm thick which formed the base of the insulating container and the remaining cover (also 50mm thick) placed over the top.

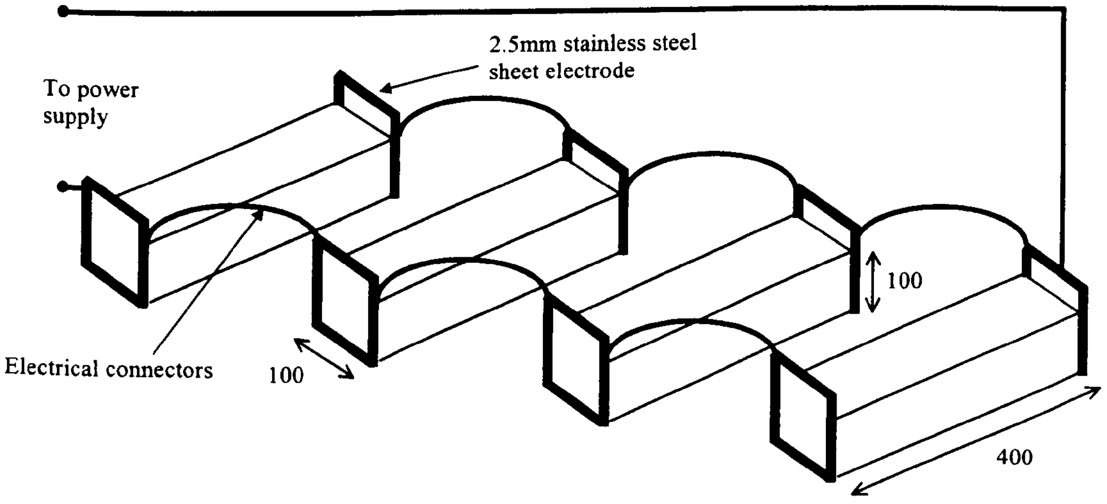

Figure 3.11 - Set-up for beam heating

3.7.4 Slab casting and curing

A 400x600x150mm wooden mould was used for casting the electrically cured slab. This mould was externally reinforced to reduce deformation at the higher temperatures used.

A stainless steel base plate of dimensions 400x600x2.5mm was used as an electrode during the electrical curing. The other electrode consisted of the internal reinforcement bars (16mm diameter) as shown in Figure 3.12.

Thermocouple temperature sensors were embedded immediately after vibration in various places within the sample at various depths.

The normally cured slabs were cast in a similar mould not containing an electrode plate.

A wooden lid was constructed to insulate the slab being cured electrically. This was solely for heat insulation and no special care was taken to make the lid airtight.

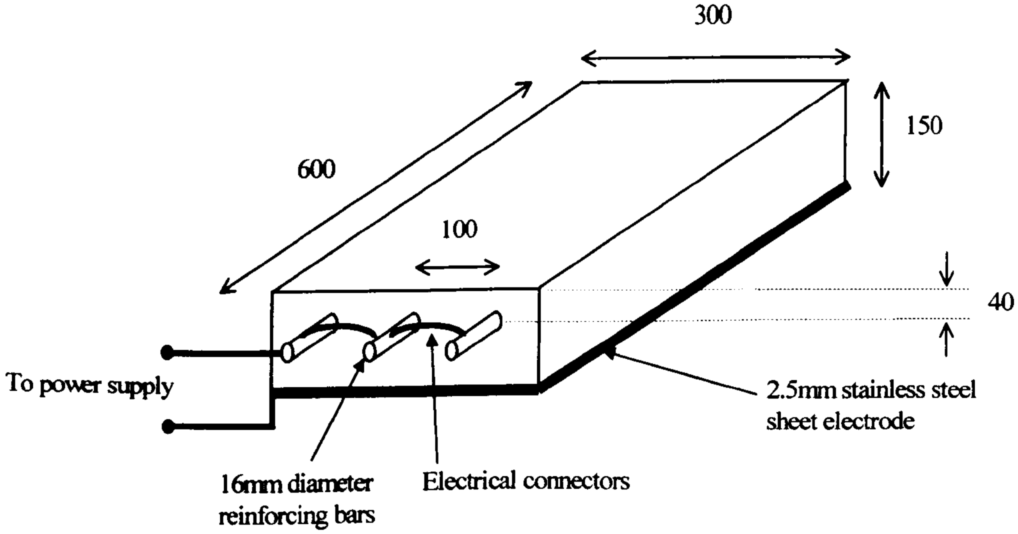

Figure 3.12 - Set-up for slab heating

3.7.5 Thermistor placement

As stated previously, in the majority of experiments carried out, a thermistor temperature sensor was manually placed in the centre of each sample approximately 20mm below the surface. However, a number of tests were carried out on cubes, beams and slabs in which more thermistors were placed to monitor temperature gradients. The thermistors were attached to 2mm diameter wooden dowel rods prior to pouring of the concrete and were mounted on an external framework for stability throughout concrete compaction. Figures 3.13-3.16 show the placement of the thermistors in the various test set-ups.

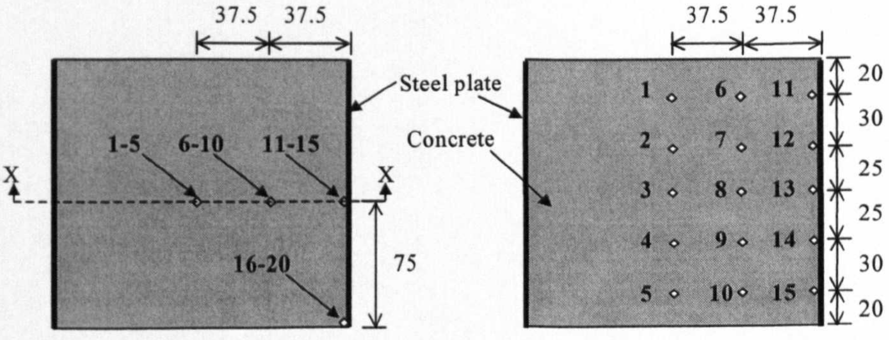

Plan view

Cross-section (X-X)

Figure 3.13 – Cube thermistor location

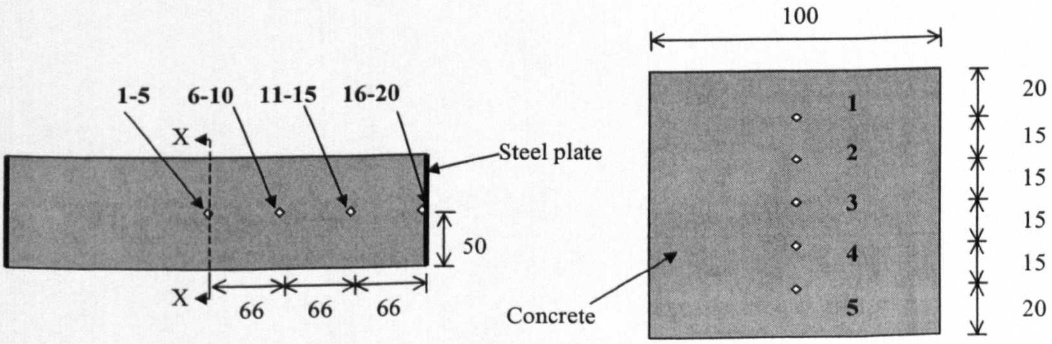

Plan view

Cross-section (X-X)

Figure 3.14 – Beam thermistor location

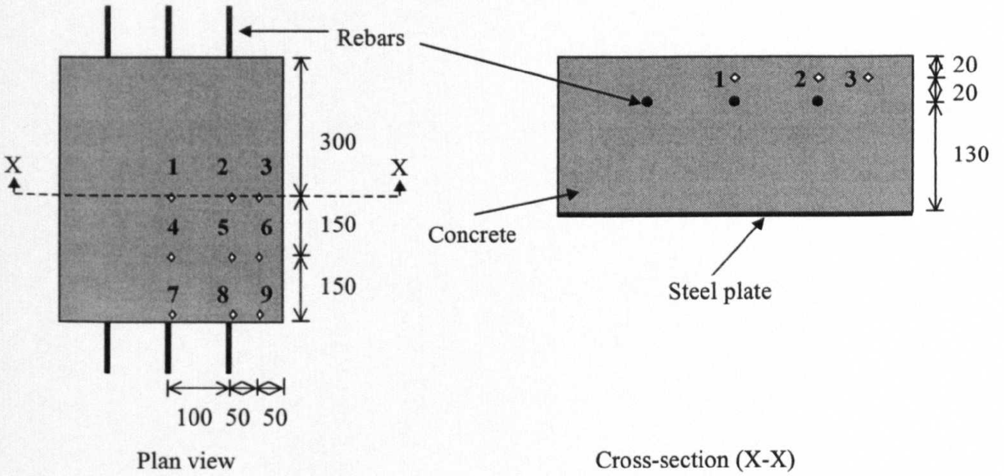

Figure 3.15 – Slab thermistor location (A)

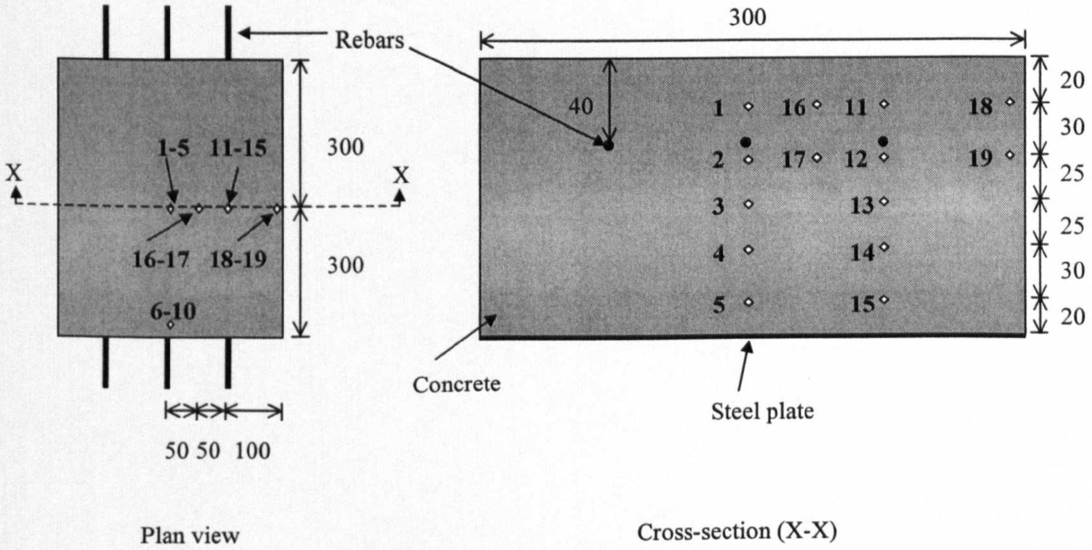

Figure 3.16 – Slab thermistor location (B)

3.7.6 Heating procedure

The experiments carried out involved the heating of samples in the arrangement shown in Figure 3.8 with the use of a Variac power controller.

The samples were heated after the addition of water at the end of a variable natural curing period (0.5-4 hours). This natural curing time was chosen to allow a degree of structural strength to develop before heating stresses were incurred. Then a rise in temperature was applied by manually varying the power input until the samples reached a maximum value. At this stage samples were either allowed to cool in situ or an isothermal period of varying length was achieved. Samples were then demoulded and placed in a water tank at a temperature of 20°C ± 1°C (BS 1881: Part 111).

Chapter 4 - DIRECT ELECTRIC CURING OF MORTAR

4.1 Introduction

This chapter provides the results and discussion of the experimental and theoretical investigation carried out on electrically cured mortar specimens. All testing was carried out on 150x150x150mm cubes unless otherwise specified. These results are summarised in Figures 4.1-4.15.

4.2 Water/Cement Ratio

Figure 4.1 shows the relationship between the compressive strength and water/cement ratio for both electrically and normally cured specimens. The figure shows that for all W/C ratios, the electrically cured specimens achieved a higher 3 days compressive strength than the normally cured specimens. Both types of specimen showed a general trend of reduction in strength as the W/C ratio increased (Neville 1988).

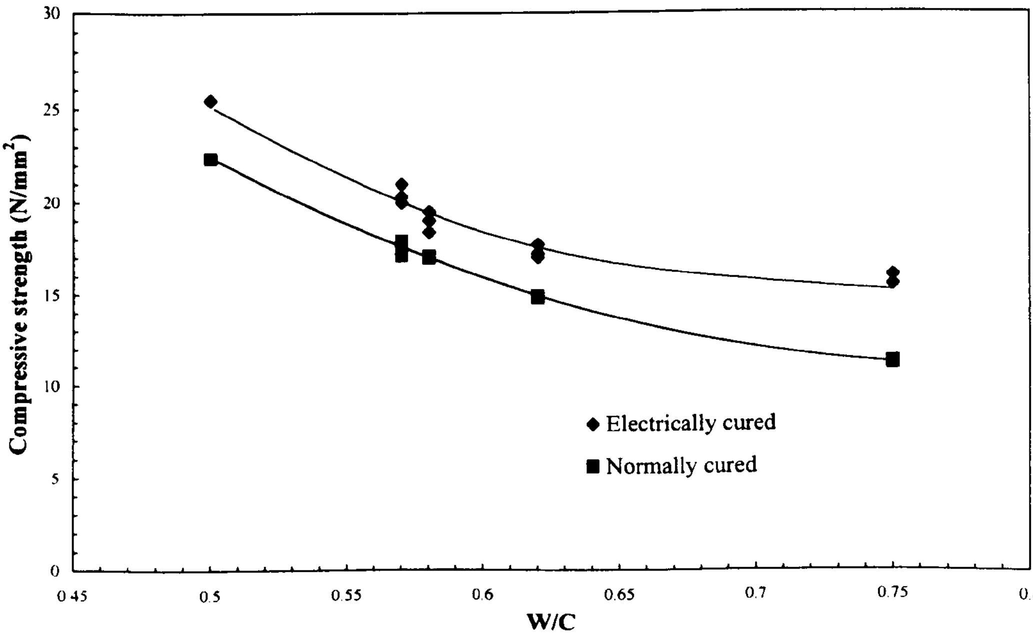

Figure 4.1 - Compressive strength at 3 days versus W/C ratio for electrically (2 hour delay, 30°C/hr rise, 80°C maximum) and normally cured samples

With the application of electrical curing, advantages concerning workability requirements were substantial. An equivalent electrical 3 days compressive strength was achievable with a 0.15 difference in W/C ratio from the normally cured specimens.

Figure 4.2 shows the relationship between the percentage strength gain of electrically cured over normally cured specimens for a range of W/C values. The figure shows that the percentage increase in strength over normally cured samples was proportionately higher at greater W/C ratios. As such the reduction of strength to be expected for increasing W/C ratios was less for the electrically heated specimens. The actual compressive strength gain at differing W/C ratios decreased slightly for the 0.50, 0.57 and 0.62 W/C ratio, showing that the actual cement content affected the strength gain.

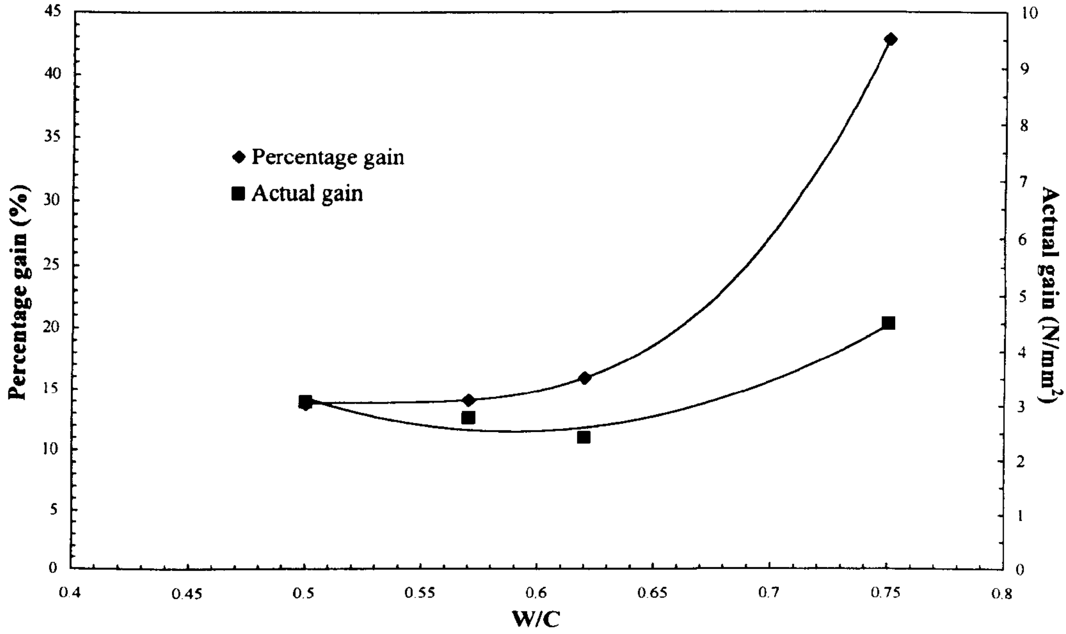

Figure 4.2 - Percentage and absolute gains of electrically cured (2hour delay, 30°C/hr rise, 80°C maximum) specimens over normally cured specimens for varying W/C ratios

From this it can be stated that the amount of cement present per m^3 reduced the apparent increased rate of hydration but it seems evident that the reduced amount of cement present was still achieving accelerated hydration reactions. The 0.75 W/C ratio points may be due to an apparent decrease in W/C ratio due to water evaporation, thus causing an equivalent strength gain. The other points, though still accelerated, may have been offset by this reduction in water content to give a partially dehydrated mix, thus reducing the apparent strength gain.

Figure 4.3 shows resistance versus time for various W/C ratios. This indicated that with a higher W/C ratio, resistance decreased. This was due to the increased conductivity of the samples for the increased amount of water present. The relationship between resistance and W/C ratio is apparent throughout heating. It can also be seen that resistance increased over time in all cases and this was due to free water being bound within hydration products, thus reducing conductivity.

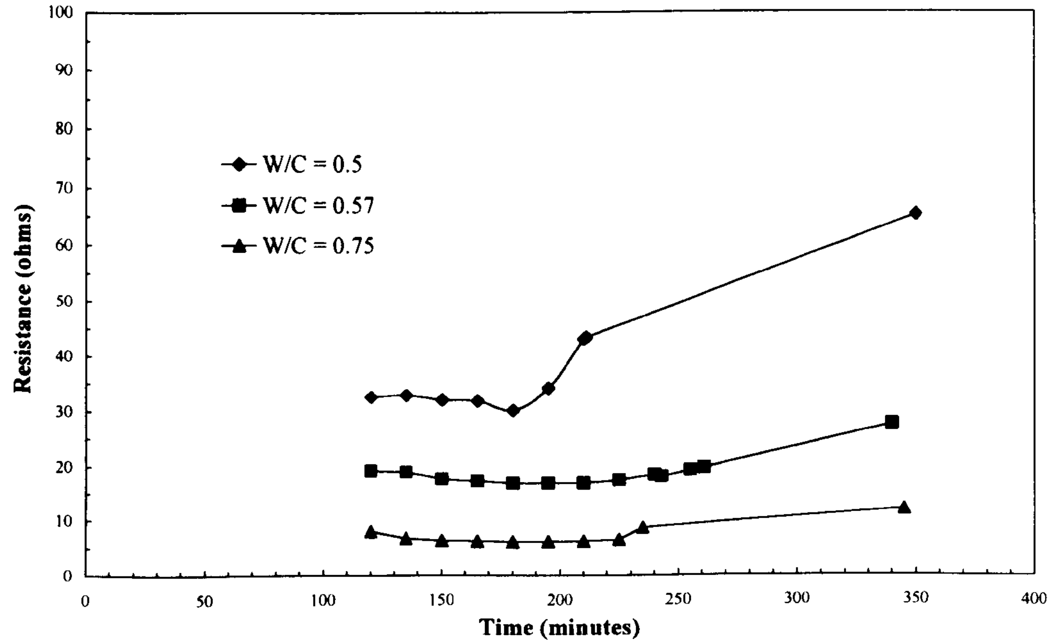

Figure 4.3 - Relationship between resistance and W/C ratio for electrically (2 hour delay, 30°C/hr, 80°C maximum) cured samples

4.3 Heating Rates

Figure 4.4 shows a typical temperature versus time curve for a mortar sample. This shows that the temperature during the linear rise can be accurately controlled and that the maximum rate of cooling was approximately 3°C/hr. This is within the allowable cooling rate given in several standards (Highways Agency 1998, Price 1969) but it may be that for other geometrys or mixes, this may not be the case. Specifically, at edges and corners, temperature losses must be minimised by the addition of a limited amount of current to reduce temperature loss or by the use of insulation (Price 1969, Kirkbride 1971). The figure also shows that for the sample used and the thermistor position, temperature time lags were not significant (Kafry 1993). This time lag is where the temperature at the thermistor position continues to increase after power has stopped being applied.

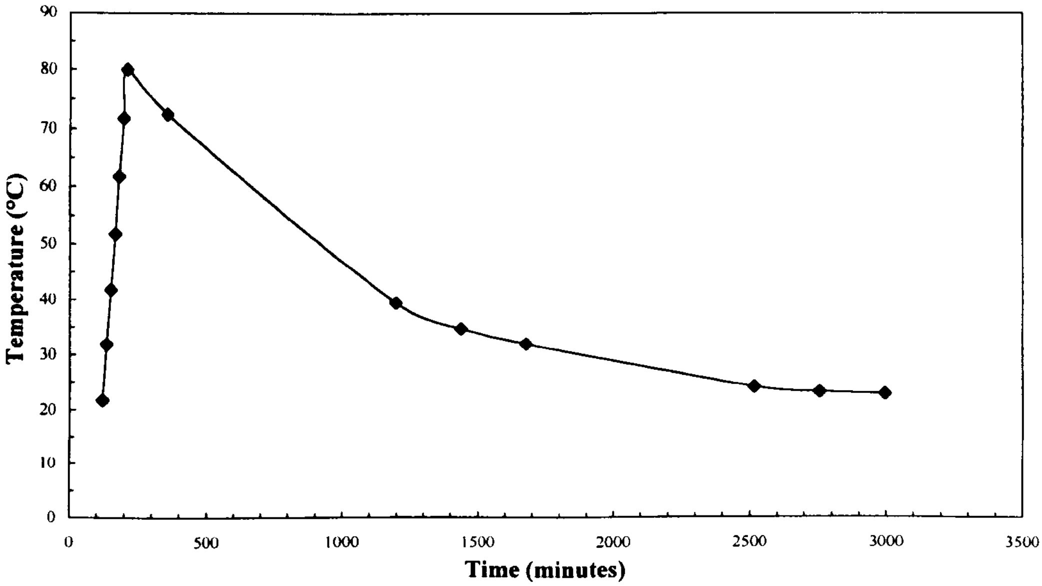

Figure 4.4 – Heating curve for mortar (W/C = 0.55, 2 hour delay, 40°C/hr rise, 80°C maximum)

Figure 4.5 shows the effects of differing heating rates (to a maximum of 80°C) on samples of W/C = 0.57. It can be seen from this relationship that the maximum 3 day compressive strength gain was achieved when a heating rate of approximately 40°C/hr was used. This suggested that above this heating rate any increase in the hydration of cement would be offset by the structural damage that would be occurring due to the higher thermal stresses imposed on the samples. Higher rates of temperature rise could not be achieved with the equipment used due to the likelihood of separation of the steel electrodes from the mortar. The actual compressive strength gain can be explained by the fact that the lower rates of temperature gain caused the samples to be at relatively high temperatures (60-80°C) for significantly longer periods, thus allowing a significantly higher rate of moisture loss. This may have caused the samples to become increasingly desiccated and as such have relatively smaller strength gains.

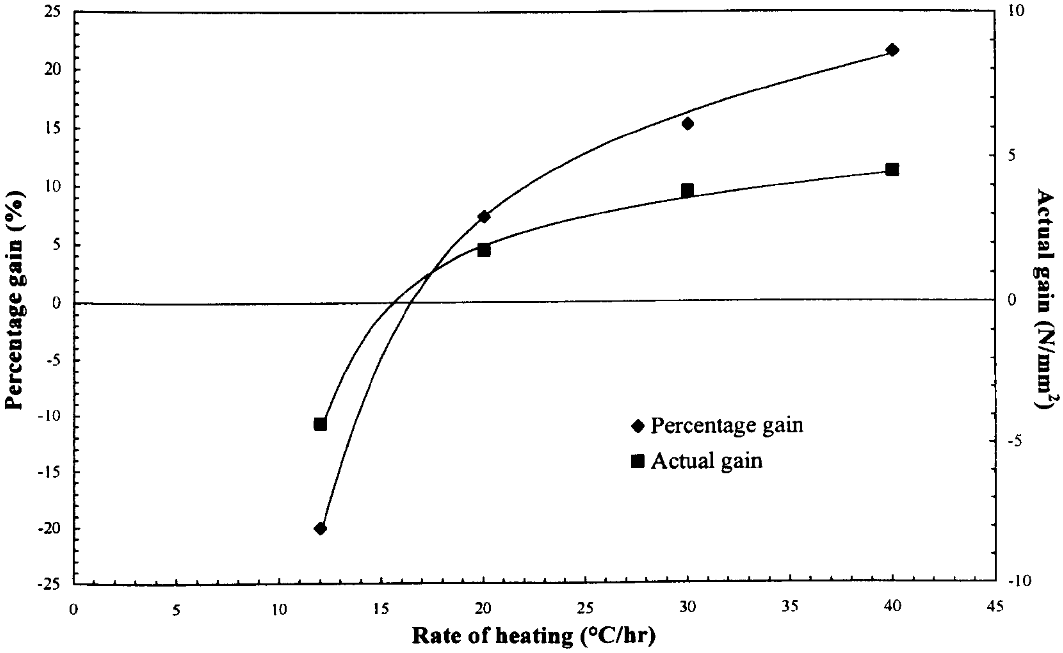

Figure 4.5 - Percentage and absolute gains of differing heating rates (2 hour delay, 80°C maximum) on samples of W/C = 0.57

4.4 Resistance

Figure 4.6 shows the relationship between the resistance of electrically cured mortar cubes measured immediately prior to compressive strength testing and the compressive strength for W/C = 0.57. The samples shown used different rates of heating rise and/or maximum temperatures. This indicated that there was no relationship between electrical resistance and compressive strength for mortars over the range tested. This was different to the behaviour of concrete and may have been due to intrinsic variability in the electrically cured test specimens or to the short length of time before testing. At 3 days, the mortar had not had time to significantly use up the excess water (the main path for conduction) in hydration product formation. As such, it would be reasonable to expect similar values of resistance for different strengths at early ages.

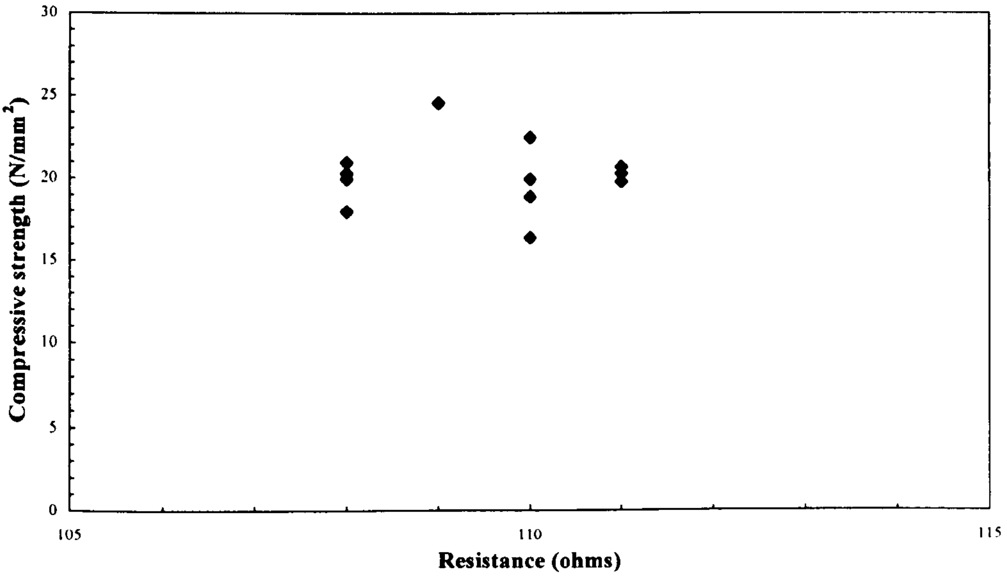

Figure 4.6 - Relationship between resistance immediately prior to compressive strength testing and 3 days compressive strength

Figure 4.7 shows a typical resistance versus time curve for W/C = 0.55 with a 2 hour delay and a 40°C/hr rate of rise to a maximum temperature of 80°C. It can be seen from this figure that the resistance initially reduced during the first 60-80 minutes of heating (Tamas 1982). This was partially due to temperature effects reducing resistance as the mortar behaves as a dielectric but was also due to water absorption by the aggregates present within the mix reducing the effective path length of the current, thus reducing resistance. This is derived from McCarter and Curran (1984) where it has been stated that current can flow in any or all of three paths:

- cement paste only
- aggregate only
- cement and aggregate combination.

It thus follows that if the aggregate starts in an initially dry state (insulator), then current will not be able to flow through it and as such will have to flow along a comparatively higher resistance path. With the absorption of water into the aggregates the resistance is reduced (conductor) within and the current can follow a path of least resistance at least partially through the aggregate, thus reducing the overall resistance. Resistance may also be reduced by the increased levels of soluble ions (Ca^{++}, OH^- and SO_4^-) in the pore water during heating.

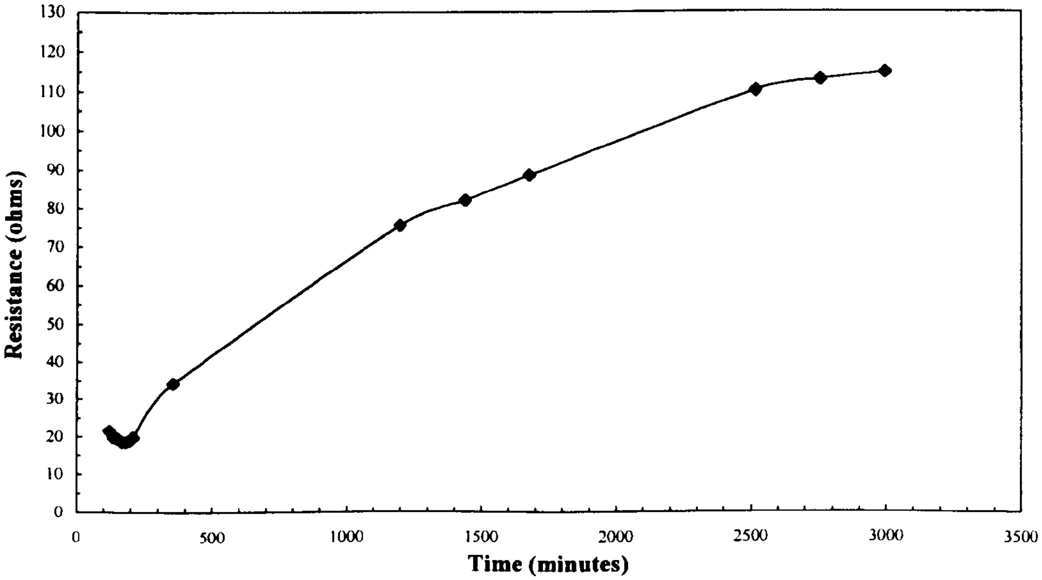

Figure 4.7 – Typical resistance graph (W/C = 0.55, 2 hour delay, 40°C/hr rise, 80°C maximum)

The resistance after approximately 200 minutes after gauging with water began to increase (Tamas 1982). This was due to the hydration of the cement reducing the amount of free water available for conduction of electricity. It was also likely to be in some extent initially to be due to direct water loss from the samples by evaporation due to the higher temperatures used.

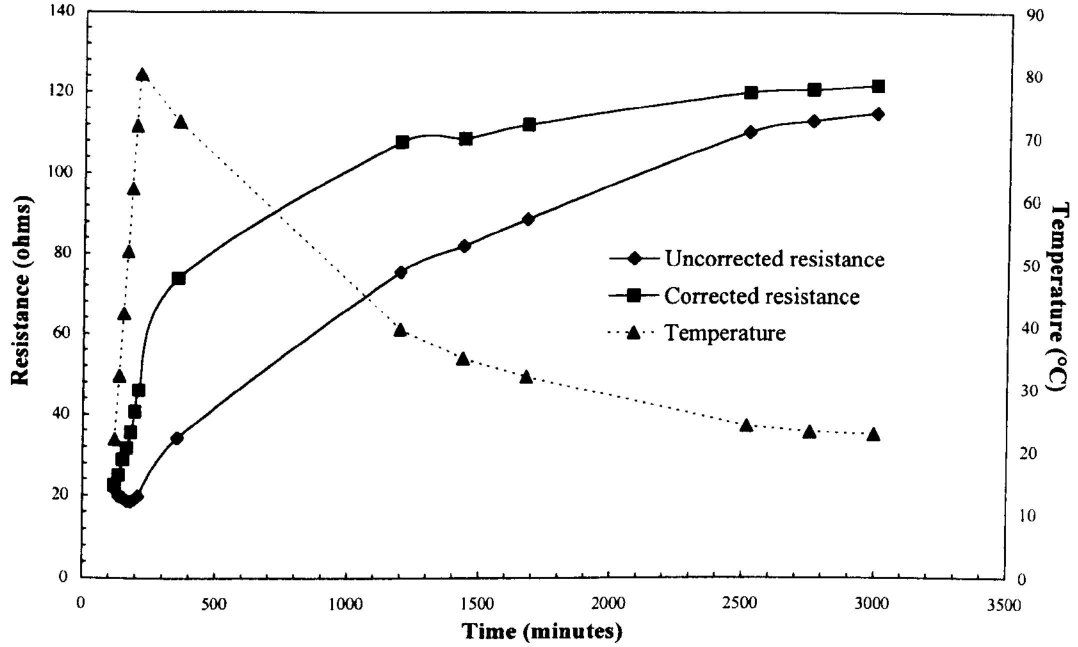

Figure 4.8 – Corrected resistance versus time (W/C = 0.55, 2 hour delay, 40°C/hr rise, 80°C maximum)

Figure 4.8 shows resistance, corrected resistance and temperature versus time. The corrected resistance was calculated using Equation 2.2 (Wilson and Gupta 1996) and using the value of α for concrete as an estimate for mortar. While likely to be relatively inaccurate, this estimation shows that the apparent resistance was likely to be seriously different to the actual resistance. This would be significant at early ages during the high temperature phase if resistance was being used to monitor the hydration reactions of the sample. The corrected values of resistance can be seen to be significantly higher than the uncorrected values of resistance. This takes into account the fact that the mortar acts as a dielectric and as such, the apparent resistance at higher temperatures reduces.

Figure 4.9 shows the initial period of heating shown in Figure 4.8. From this it can be seen that the corrected resistance did not decrease in value as did the uncorrected resistance. However, this is not a contradiction of the explanation given for Figure 4.7. This is because the corrected resistance showed a relatively slow rate of resistance rise initially as the aggregates within the sample absorbed the free water and then as the aggregates became saturated, the rate of rise of resistance was solely due to the moisture loss used in the hydration reaction. The effect of the reduced rate of resistance rise was relatively small when compared to the corrected resistance values for concrete, as within mortar, the only aggregate used is sand, with a relatively low and quick absorption of water. Also, within concrete, the large aggregate particles when acting as an insulator cause a greater effective path length than the small aggregate particles within mortar.

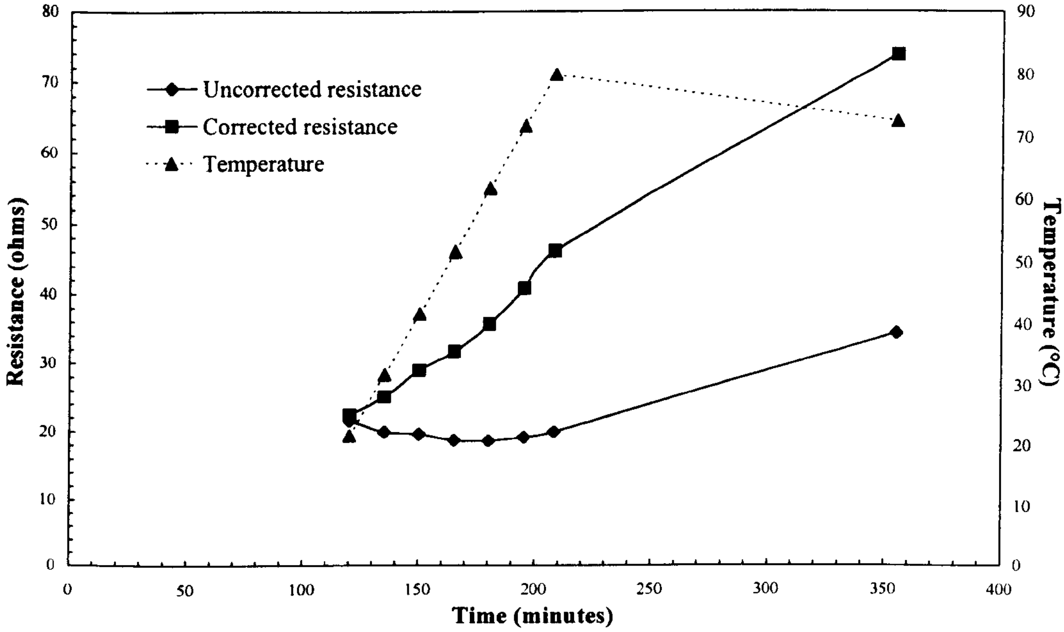

Figure 4.9 – Corrected resistance versus time (W/C = 0.55, 2 hour delay, 40°C/hr rise, 80°C maximum)

4.5 Maturity

Figure 4.10 shows values of maturity versus 3 days compressive strength for samples of W/C = 0.57. A linear best-fit line can be achieved for the tests containing no isothermal period (coefficient of determination equal to 0.72) but if the test involving a 1 hour isothermal period was taken into account then the coefficient of determination decreased to 0.64.

From this it can be stated that maturity was not a good indicator for final strength values where variable heating strategies have occurred, but was more consistent for a range of maturity values for a specific heating methodology. The range of maturity values was extremely small and indicated that the proportionally large maturity values incurred during cooling virtually overwhelmed any maturity differences incurred during the initial rapid heating.

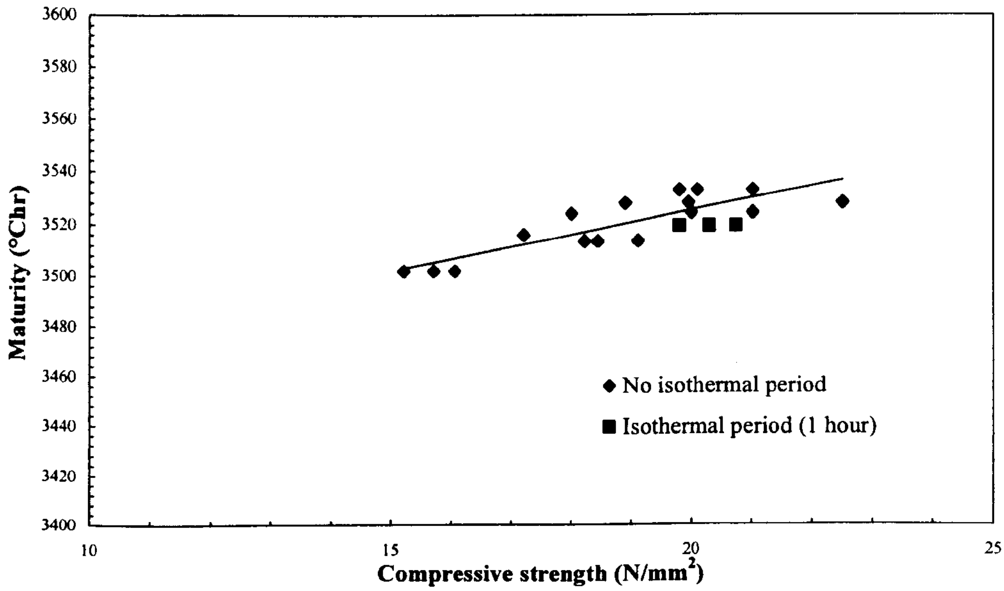

Figure 4.10 - Values of maturity versus 3 days compressive strength for samples of W/C = 0.57

4.6 Maximum Temperature

Figure 4.11 shows the relationship between maximum temperature of electrically cured specimens and compressive strength. The figure indicates that for the small range tested (approximately 15% variance), a relationship exists between maximum temperature and compressive strength. This differed to concrete based work where a maximum temperature of 80°C is not recommended (Price 1969, Kirkbride 1971). The higher temperature tolerance of mortars can be attributed to absence of coarse aggregate particles in the mix. Coarse aggregate particles have a much higher coefficient of thermal expansion (4-5x10^{-6}/°C) than fine aggregate (2x10^{-6}/°C) and as such an increase in maximum temperature creates greater thermally induced stresses between the matrix and the aggregate (El Hussein and Abd El Halim 1993).

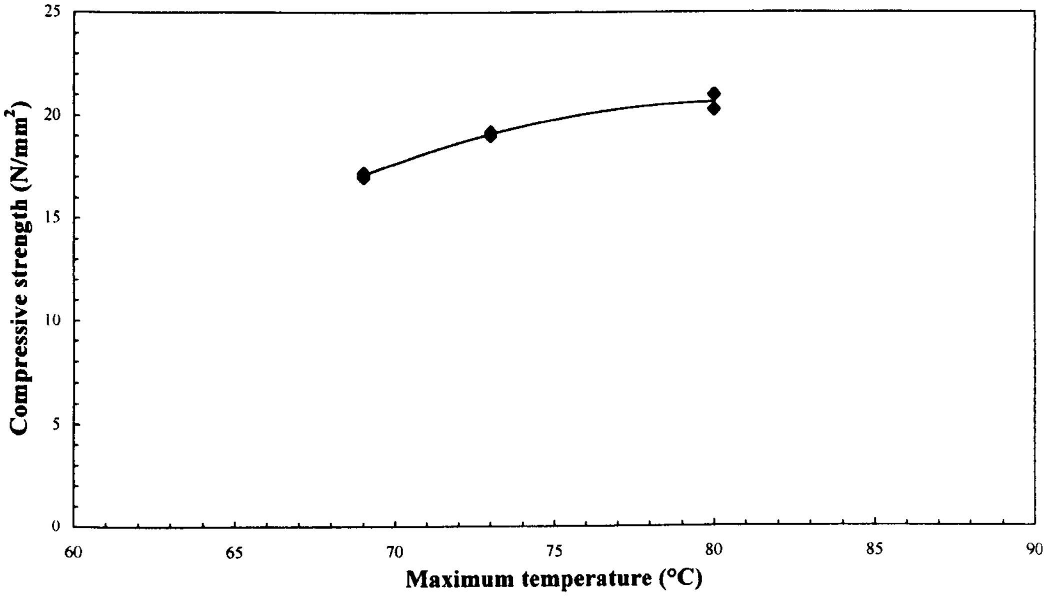

Figure 4.11 - Effect of the maximum temperature on the 3 days compressive strength (2 hours delay, 30°C/hr rise)

4.7 Long-term Compressive Strength

Figure 4.12 represents the relationship between compressive strength and age for electrical (W/C = 0.5, 2 hour delay, 40°C/hr, 80°C maximum) and normal curing. This shows that compressive strength was increased at early ages using DEC but the rate of gain of strength was decreased when compared to normal curing (Kafry 1993). This was likely to be due to microcracking caused by increased thermomechanical stresses when heating. The heating increases the rate of hydration at early ages but damages the microstructure because at the time of maximum temperature, the structure of the mortar is not strong enough to resist the differential expansion of the different constituents and as such is damaged. This thermomechanical damage was also caused by the rate of increase in temperature chosen. The fact that samples were cured for three days in air was also apparent as the normally cured samples did not achieve the long-term strength development that would be expected if the samples had been water cured after 1 day from casting (Neville 1988).

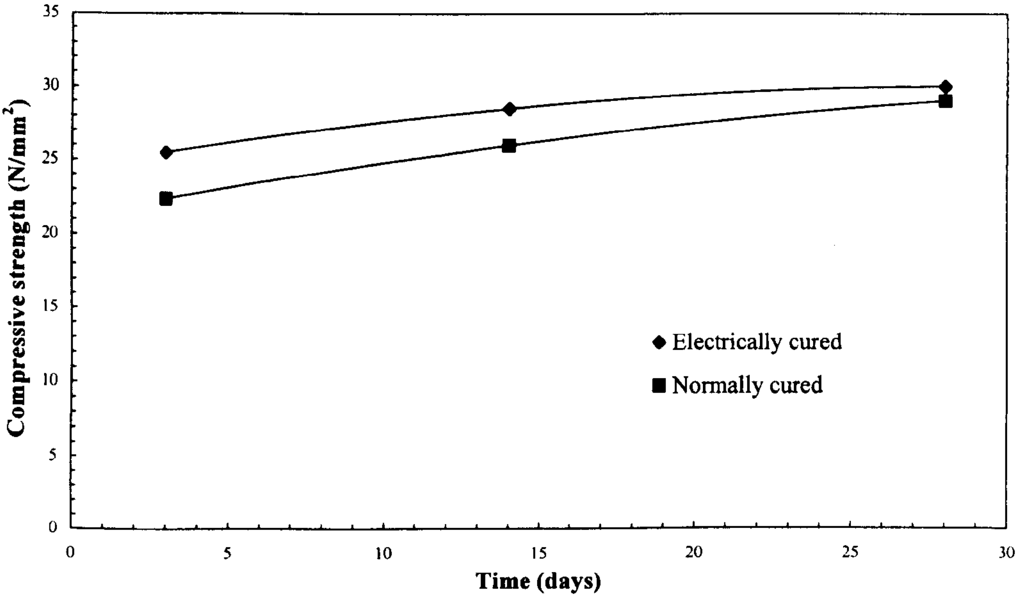

Figure 4.12 - Effect of DEC (2 hour delay, 40°C/hr rise, 80°C maximum) on long term compressive strength

4.8 Durability

Figure 4.13 shows the initial surface absorption of electrically and normally cured samples at 28 days (W/C = 0.5, 40°C/hr heating rate to a maximum of 80°C). This shows that durability was not adversely affected by DEC for the particular mix and heating regime chosen. This was likely to be due to the modification of capillary pores caused by the increased temperature used which more than offset the damage caused to the microstructure by thermomechanical stresses from the differential expansion of the constituents. The compressive strength of both the normally and electrically cured samples were approximately equivalent (4% difference), but the values of surface absorption at 10 minutes (ISA 10) were significantly different (9% difference).

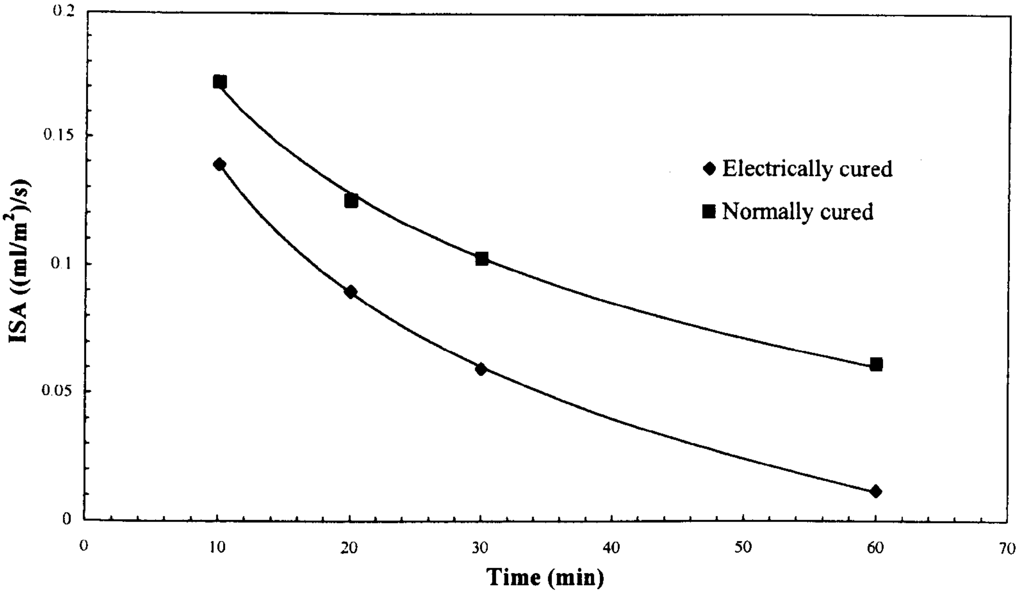

Figure 4.13 - Initial surface absorption of electrically and normally cured samples at 28 days (W/C = 0.5, 2 hour delay, 40°C/hr rise, 80°C maximum)

4.9 Isothermal Period

Figure 4.14 shows the compressive strength after 3 days (W/C = 0.55) for a non-isothermal period and an isothermal period of 1 hour at 80°C for a linear rise of 40°C/hr and a delay period of 2 hours. This shows that the non-isothermal period samples had an increased rate of compressive strength gain compared to the isothermal period samples. This small reduction in strength may have been due to excessive water loss during the isothermal period, causing desiccation of the samples. Both heating regimes achieved a compressive strength gain over the normally cured samples in the order of 8 and 15% (1.6 and 3.4N/mm^2) for isothermally and non-isothermally electrically cured samples respectively.

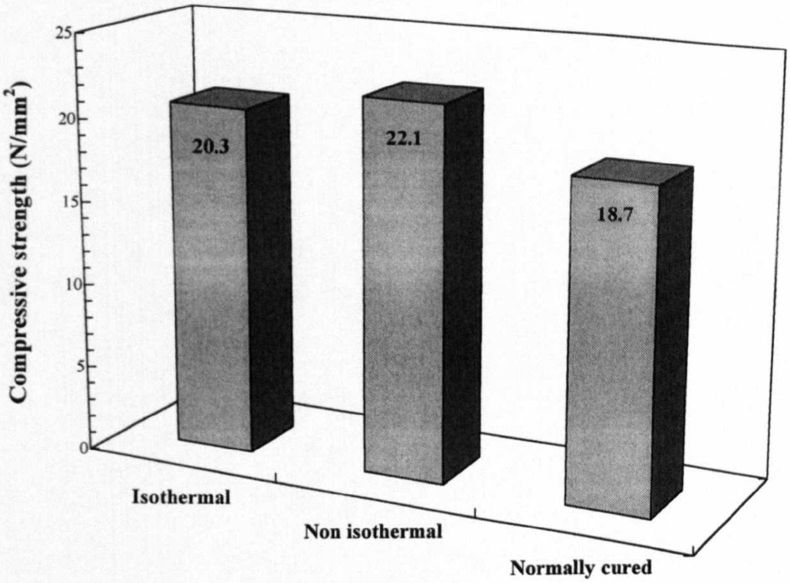

Figure 4.14 – Compressive strength after 3 days for isothermal and non isothermal electrical (2hour delay, 40°C/hr rise, 80°C maximum) curing

4.10 Delay Period

Figure 4.15 shows the compressive strength of electrically cured samples of differing delay periods at 3 days. The samples were of W/C = 0.55 with a 40°C/hr rate of rise to a maximum temperature of 80°C. This shows that the delay period determined to a large extent the expected compressive strength with the 2 hour delay attaining approximately 11% greater compressive strength than the 1 hour delay sample. This was due to the damage caused to the structurally less well-formed 1 hour delayed sample from the thermally induced stresses present during heating. Both delay periods showed a greater compressive strength at 3 days than the normally cured samples.

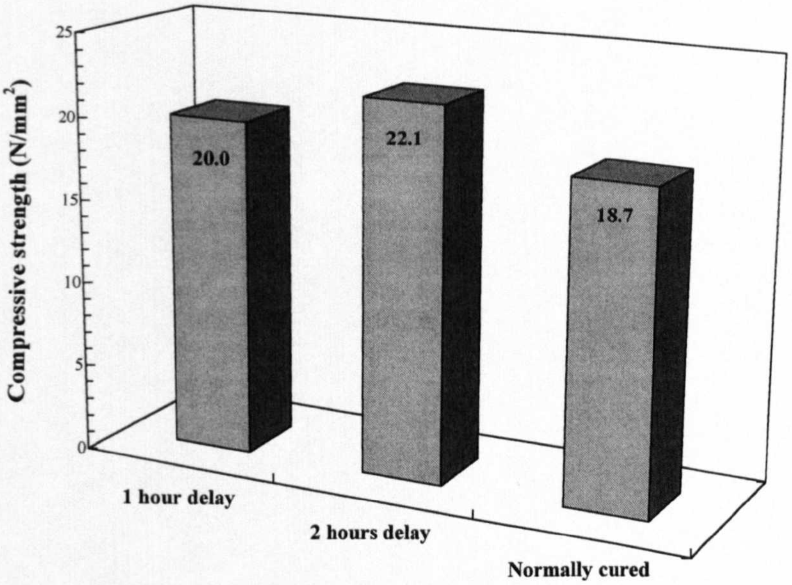

Figure 4.15 – Effect of delay period prior to heating on 3 day compressive strength (W/C = 0.55, 40°C/hr rise, 80°C maximum)

4.11 Conclusions

1. Over a range of W/C ratios electrically cured mortar samples achieved a higher initial compressive strength than normally cured samples and the proportional effectiveness of electrically cured mortar specimens was found to be increased at higher W/C ratios.

2. Resistance can be used as a guide to the amount of water in mortar with higher W/C ratios giving lower resistances at all ages.

3. For a 2 hour delay period, a rate of temperature rise of 40°C/hr gave the highest initial (3 day) compressive strength for the 0.57 W/C ratio mortar samples with a 2 hour delay.

4. There appeared to be little correlation between 3 days mortar compressive strength and resistance.

5. The initial drop in resistance during heating was due to water absorption by aggregates which reduced the effective path length of the electrical current.

6. Mortar behaved as a dielectric having a reduced apparent resistance at higher temperatures. The effect of temperature during heating seriously affected the resistance properties of the mortar samples. This effect became negligible after approximately 3 days.

7. Maturity was found to be a good indication of compressive strength when DEC was used.

8. The value of maturity during cooling was significantly higher than the maturity measured during the initial heating of samples. This meant that accurate monitoring of temperature after the initial heating concluded was required in order to estimate compressive strength.

9. For mortar, a maximum temperature of approximately 80°C provided the greatest initial (3 day) compressive strength for a 30°C/hr rise with a delay period of 2 hours.

10. Long-term (28 day) compressive strength was not adversely affected by DEC in the samples tested although the rate of compressive strength development at later ages (>28 days) was reduced when compared to normally cured samples. The reduced rate of compressive strength development at later ages in mortar was likely to be due to differential expansion of the aggregates and the cement matrix incurred by heating.

11. The durability of mortar samples (as measured by the ISAT) did not appear to be adversely effected by DEC. This was likely to be due to capillary pore modification during heating.

12. The inclusion of an isothermal period at maximum temperature appeared to have an adverse effect on initial (3 days) compressive strength. This was likely to be due to increased microstructure damage incurred at the maximum temperature and increased temperature gradients within the sample.

13. The delay period chosen had a significant effect on initial (3 days) compressive strength. Results show that a 2 hours delay produced a higher compressive strength than a 1 hour delay.

Chapter 5 - DIRECT ELECTRIC CURING OF CONCRETE

5.1 Introduction

This chapter provides the results and discussion of an experimental and theoretical investigation carried out on electrically and normally cured concrete samples. These results can be seen in Figures 5.1-5.69 and Tables 5.1-5.2.

All testing was carried out on 150x150x150mm cubes of a C30 (10-30mm slump) mix unless otherwise specified and the mixing, casting, curing and monitoring was implemented in accordance with the experimental procedures stated in Chapter 3.

5.2 Normally Cured Samples

Figure 5.1 shows compressive strength versus time relationship for normally cured samples of mix design target mean strength = 43N/mm^2 and a slump = 10-30mm. This shows the variability of mix compressive strengths used over the investigation. A logarithmic best fit curve (compressive strength = 12.03 x Ln (time) + 9.64) was used with a coefficient of determination = 0.95. This curve was used in any further comparisons of compressive strength.

A regression analysis was carried out on the data contained in Figure 5.1 as another method to determine the acceptability of the best-fit curve. To determine whether x provides information in predicting y the hypotheses for this test are:

H_0:ß=0
H_0:ß‹›0

Testing the hypothesis involved a t-test of the regression line slope with degrees of freedom = 38. From this it was found that the t-stat from the regression = 26.3. The t-stat @ 99% level = 2.42 and since 2.42<26.3 it can be said with 99% confidence that ß<>0 and the null hypothesis can be rejected. This gives an added indication that the best-fit curve used is valid.

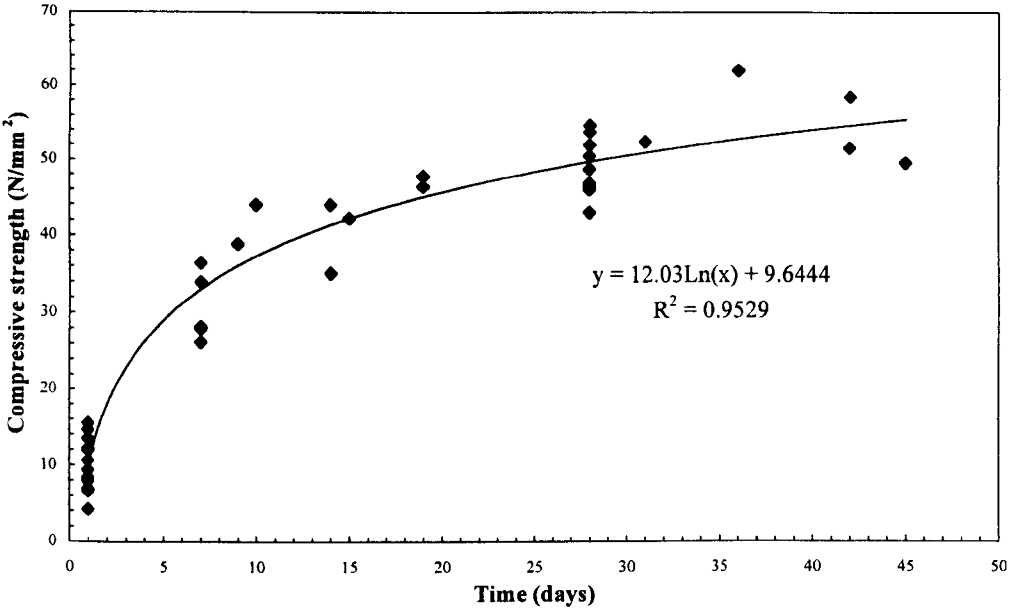

Figure 5.1 - Compressive strength versus time for normally water cured samples

5.3 Effect of Cover

Figure 5.2 shows the effect of covering of electrically cured samples on 3 day compressive strength. This shows that, for the heating regime used (1 hour delay, 40°C/hr rise to 80°C maximum), removing the 50mm thick expanded polystyrene cover reduced compressive strength by 8.3N/mm^2. The uncovered compressive strength can be seen to be lower than the equivalent age normally cured sample. This was due to the excess moisture loss incurred by the uncovered sample (Sohn and Johnson 1999). With the covered samples, moisture was retained within the covering, creating a high humidity environment that allows a degree of moist curing. With the uncovered samples, evaporation could readily escape into the atmosphere, thus allowing desiccation, particularly of the surface region of the concrete. The removal of the cover may also have effected compressive strength by the loss of thermal insulation. This created higher temperature differentials within the concrete, thus creating higher temperature induced stresses and a further reduction in compressive strength (Kirkbride 1996).

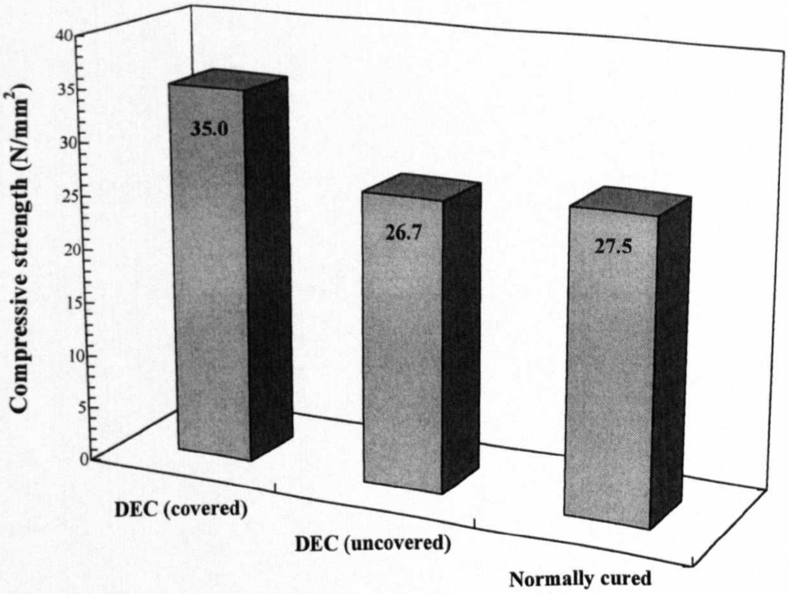

Figure 5.2 - Compressive strength versus time for covered and uncovered samples (1 hour delay, 40°C/hr rise, 80°C maximum)

Figure 5.3 shows uncorrected resistance versus time for covered and uncovered electrically cured samples of the same configuration as shown in Figure 5.2. This shows that the uncovered samples attained a significantly larger resistance value as heating occurred until approximately 1200 minutes whereupon resistance values almost ceased to rise. This was due to an increased moisture loss from the uncovered samples creating a desiccated environment which initially caused the increase in resistance. The low resistance rise after 1200 minutes was due to the lack of free water retarding hydration. This confirmed the relatively lower 3 day compressive strength of the uncovered samples shown in Figure 5.2. The covered samples showed an initially lower resistance value as the amount of free water was proportionally higher, but then continued to increase resistance as the free water was bound in hydration reactions. The final resistance values for the covered samples seemed to indicate a more fully hydrated sample and a corresponding compressive strength (Orchard 1973). These results show the importance of using identical sample environments if resistance values are to be used in assessing the degree of hydration achieved or W/C ratio of concrete.

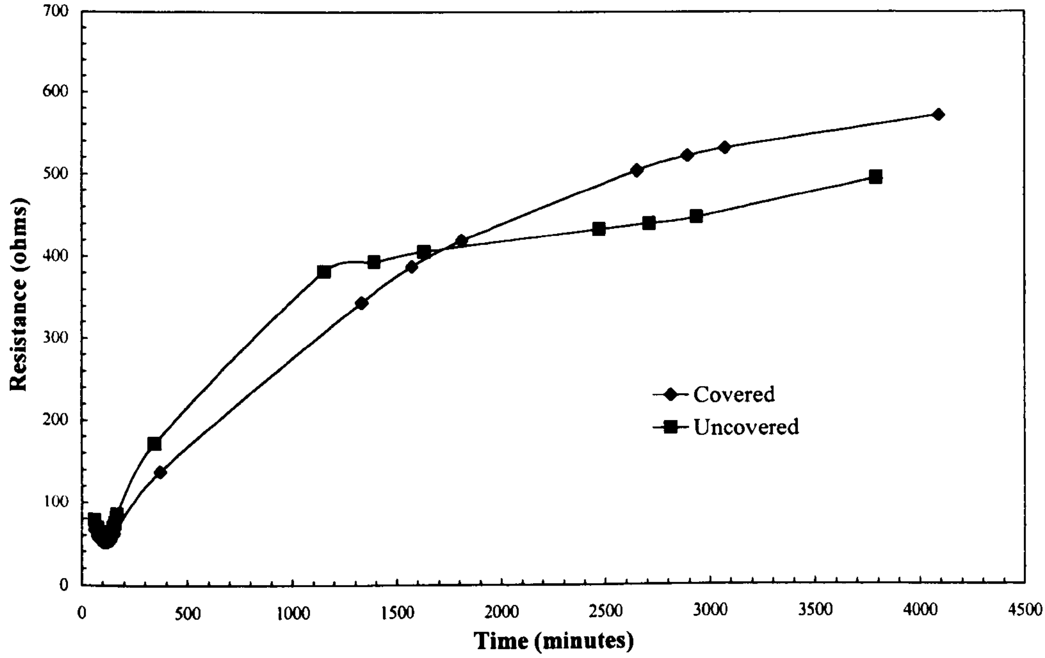

Figure 5.3 - Resistance versus time for covered and uncovered samples (1 hour delay, 40°C/hr rise, 80°C maximum)

Figure 5.4 shows the resistance for the initial period of heating for the electrical heating regimes used in Figure 5.2. This shows an initial resistance difference between the mixes which indicated that the mixes had slightly different W/C ratios. However, this difference was not believed to be significant. The figure also shows that the uncovered samples had an identical degree of change in resistance as the covered samples until the maximum temperature was approached at approximately 120 minutes and onwards (60-80°C). At this time a larger rate of rise of resistance could be observed. This was due to the fact that significant levels of evaporation can only be achieved at temperatures in the region above 60°C. This may be important in further investigations of DEC where insulation is not available and a heating regime reducing moisture loss is required.

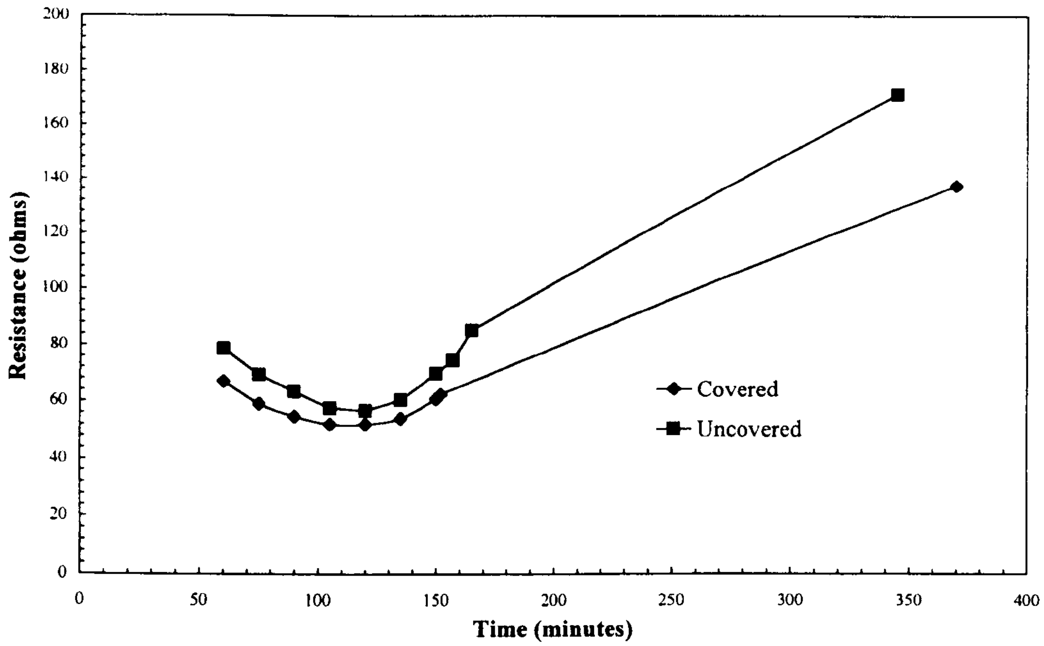

Figure 5.4 - Resistance versus time for covered and uncovered samples (1 hour delay, 40°C/hr rise, 80°C maximum)

5.4 Water/Cement Ratio

Figure 5.5 shows the relationship between the compressive strength and W/C ratio for both electrically and normally cured specimens with a heating delay of 1 hour to a maximum temperature of 80°C. The figure shows that for all W/C ratios, the electrically cured specimens achieved a higher 1 day compressive strength compared to the normally cured specimens. Both types of specimen showed the normal trend of reduction in strength as the W/C ratio increased (Goto and Roy 1981, Neville 1988).

Figure 5.6 shows that the percentage compressive strength gains of electrically cured over normally cured specimens for the above range of W/C values vary from 60% for W/C=0.55 to 219% for W/C=0.7. It can also be seen from this figure that the actual compressive strength gain was higher at higher W/C ratios. This was due to the increased water content of the mixes, which allowed a degree of moisture loss, without incurring desiccation effects. As such the reduction of strength to be expected for increasing W/C ratios at 1 day was less for the electrically heated specimens.

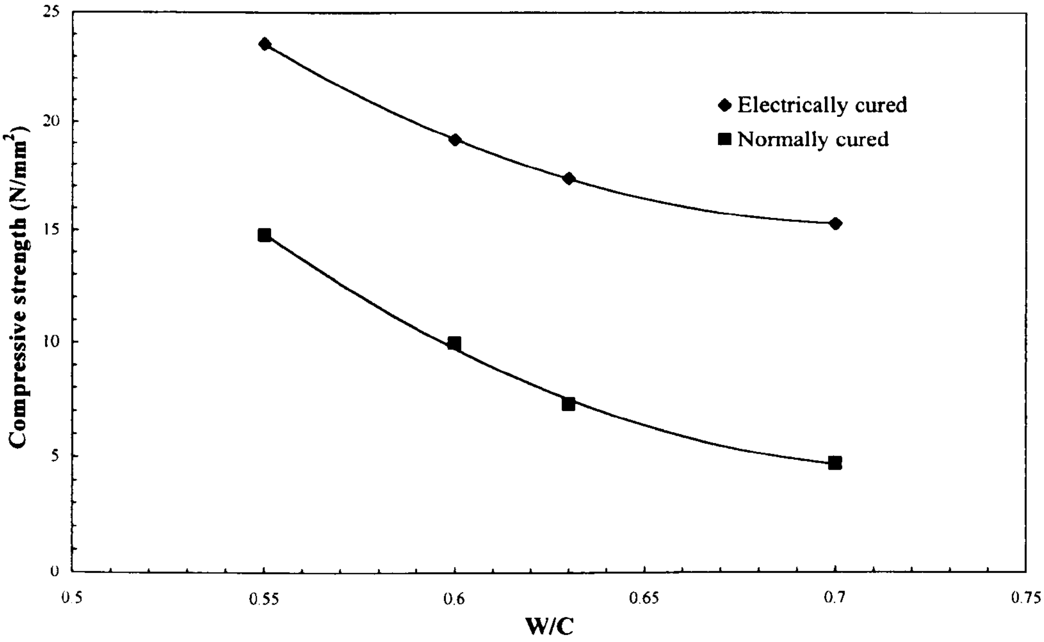

Figure 5.5 – W/C versus compressive strength at 1 day (1 hour delay, 40°C/hr rise, 80°C maximum)

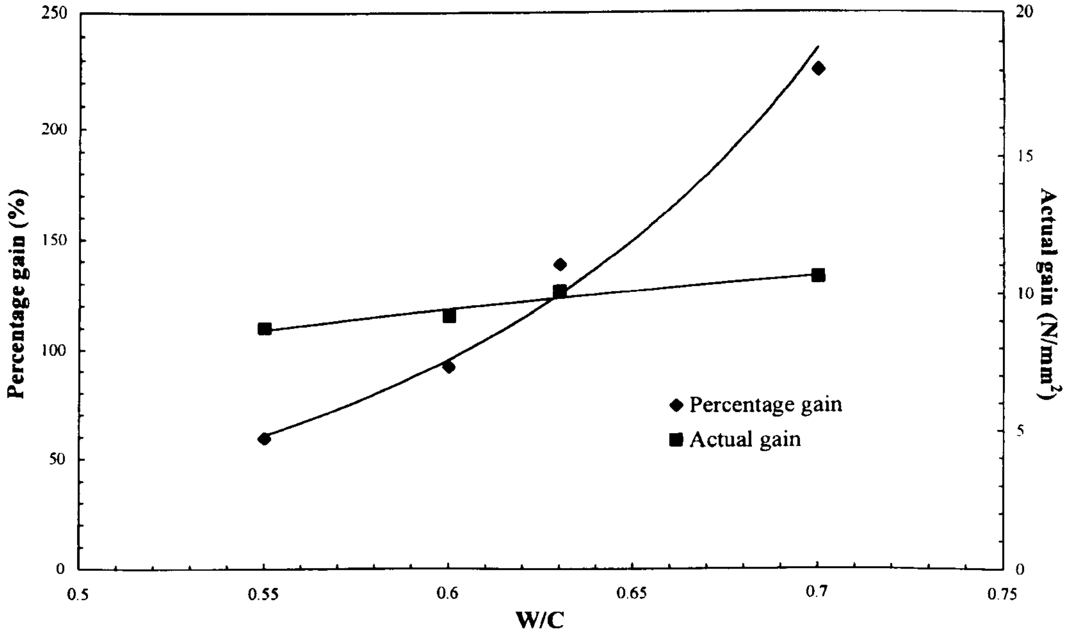

Figure 5.6 – Actual and percentage gain in compressive strength of electrically (1 hour delay, 40°C/hr rise, 80°C maximum) and normally cured samples at 1 day

Figure 5.7 represents compressive strength versus W/C ratio after 3 days of air curing. This shows the effect of low W/C ratio adversely affecting compressive strength. The assumed compressive strength for normally cured samples would be in the region of 75N/mm^2 but the actual compressive strength was 28.2N/mm^2 for normally cured and 37.2N/mm^2 for electrically cured samples. This shows the likely presence of an excessively dry mix where honeycombing and poor particle bonding is present (Neville 1988). However, the electrically cured samples still showed a comparative strength gain over the normally cured samples and as such DEC may be used to improve otherwise dry concrete.

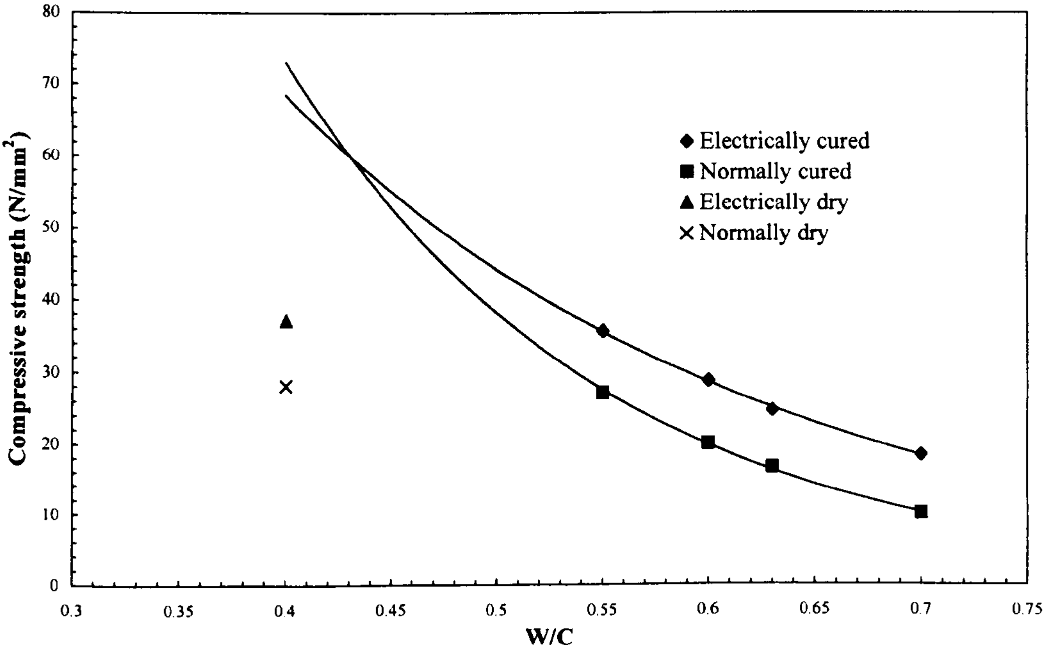

Figure 5.7 - Compressive strength versus W/C after 3 days air curing (1 hour delay, 40°C/hr rise, 80°C maximum)

Figure 5.8 shows the compressive strength versus W/C ratio for a range of mixes of adequate W/C ratio after 3 days of air curing. It can been seen from this figure that the electrically cured samples attained a significantly higher compressive strength after 3 days than the equivalent normally cured samples. This compressive strength gain was approximately equal for all W/C ratios tested and as such a compressive strength gain could be assumed for all W/C ratios used in the investigation.

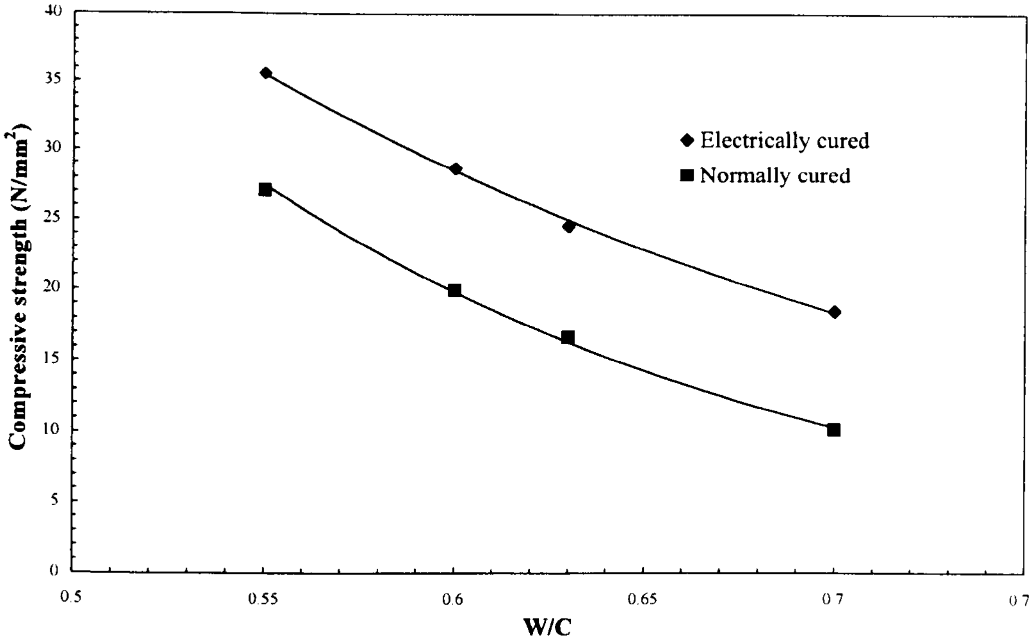

Figure 5.8 - Compressive strength versus W/C after 3 days air curing (1 hour delay, 40°C/hr rise, 80°C maximum)

Figure 5.9 shows the percentage and actual compressive strength gain after 3 days for various W/C ratios. This shows that the actual gain in compressive strength remained at approximately a constant level while the percentage gain rose proportionally with the increase in W/C ratio. This shows that DEC was proportionally more effective at higher W/C ratios and as such significantly higher performance could be gained with increasing W/C ratios.

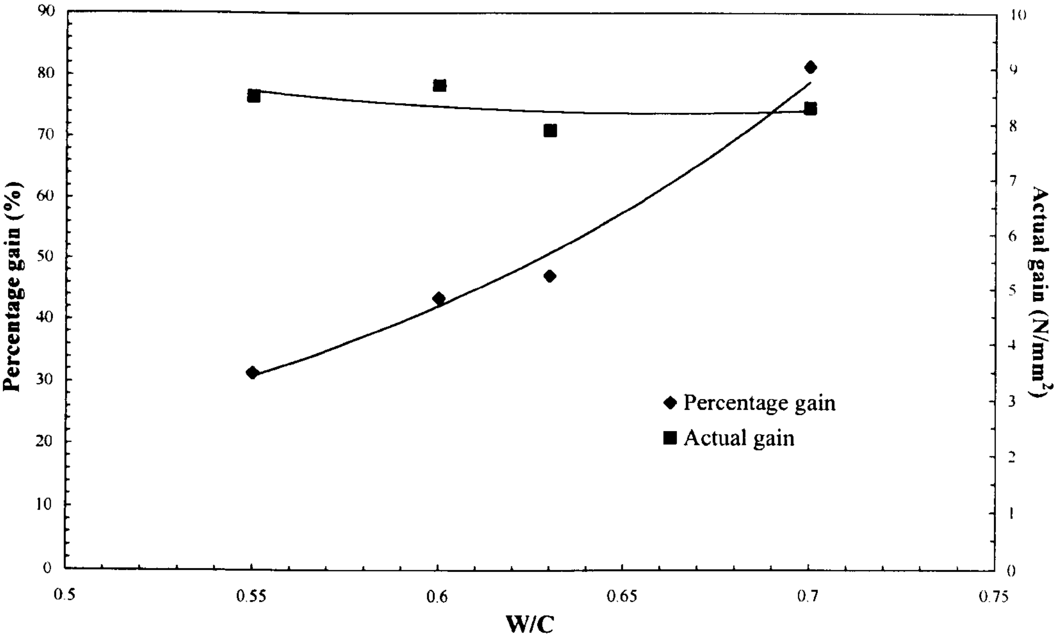

Figure 5.9 - Actual and percentage gain of electrically cured over normally cured samples for different W/C after 3 days air curing (1 hour delay, 40°C/hr rise, 80°C maximum)

Figure 5.10 shows the relationship between resistance and W/C ratio. The figure clearly shows that the resistance values were significantly affected by the amount of water present within the mix (Neville 1988). The initial reduction in resistance was due to the absorption of water by the aggregates reducing path length for the current and increased levels of soluble ions in the pore water. The temperature at demoulding was approximately equal to the reference temperature used in Equation 2.2 and as such the final resistance may be considered to be at least a guide to the water content in concrete of identical mix design, temperature history and geometry (Khalaf and Wilson 1999).

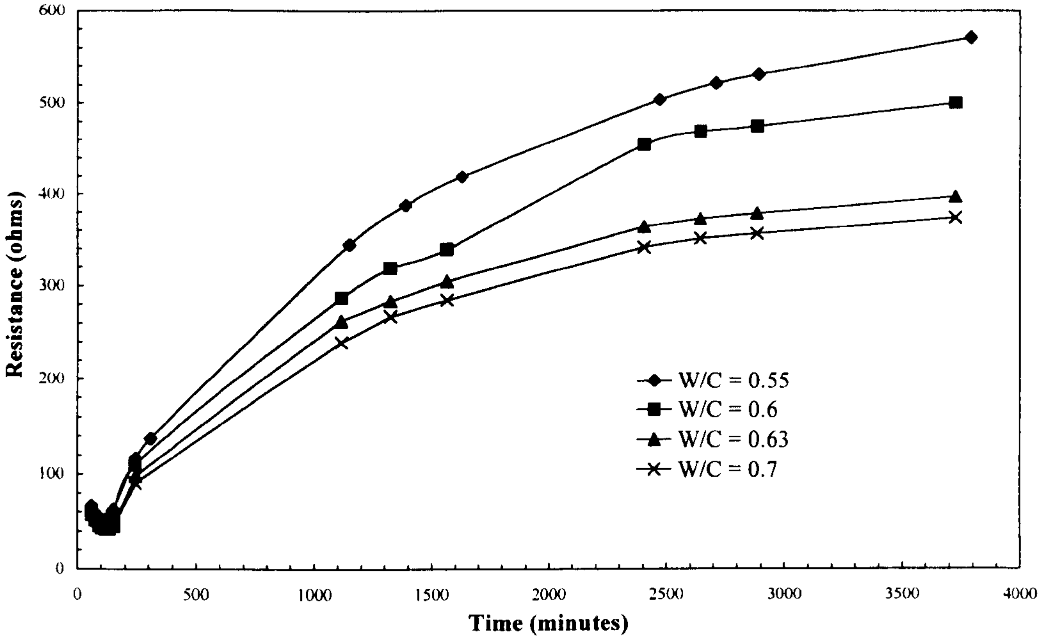

Figure 5.10 - Resistance versus time for different W/C (1 hour delay, 40°C/hr rise, 80°C maximum)

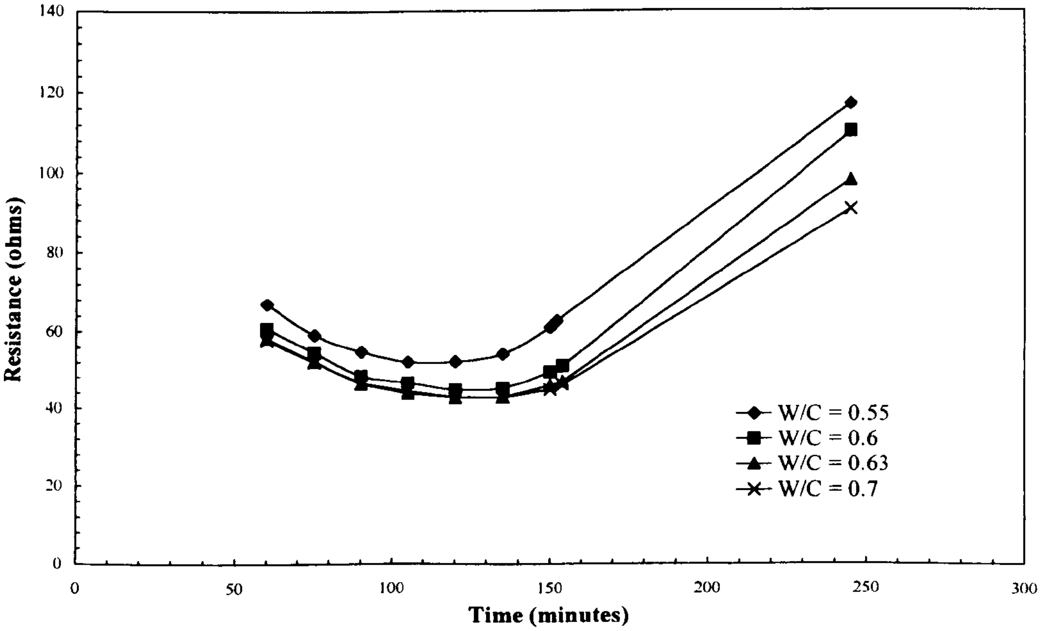

Figure 5.11 - Resistance versus time for different W/C (1 hour delay, 40°C/hr rise, 80°C maximum)

Figure 5.11 represents the resistance for varying W/C ratios over time for the first 250 minutes after gauging with water. The relationship shows that initially the W/C ratio had only a minor effect on resistance, but at later ages as hydration continued, the resistance value differences became more pronounced. At 250 minutes, compressive strength can be in the region of 1 day normally cured compressive strength and as such differences in W/C ratio and strength are more pronounced than at 60 minutes. This may be useful in accelerating the accurate assessment of W/C ratios using resistance measurements.

Figure 5.12 shows the corrected resistance using Equation 2.2 against time for differing W/C ratios.

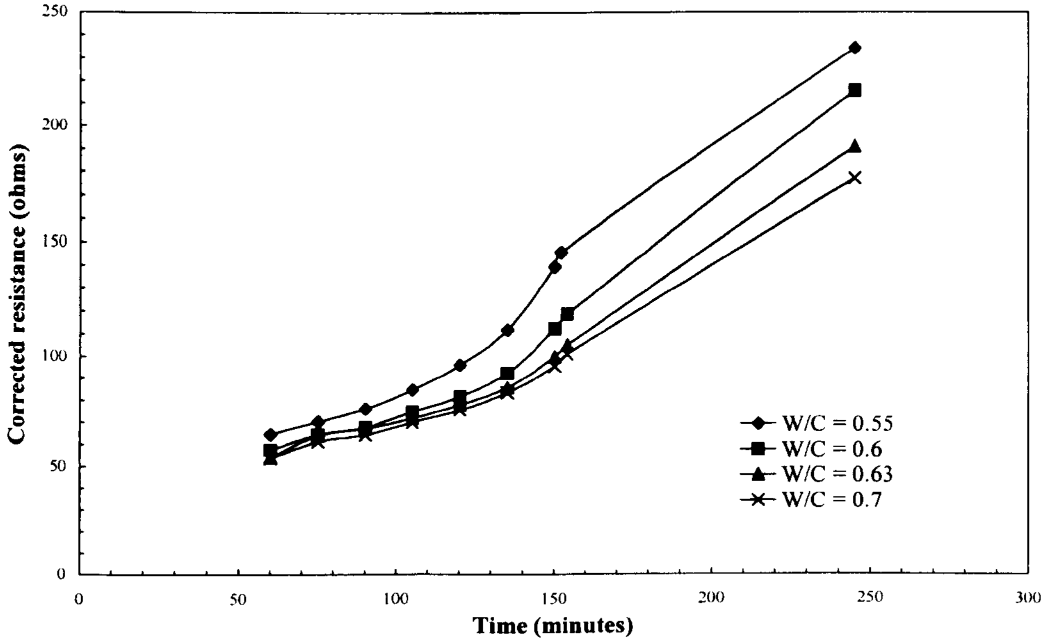

Figure 5.12 – Corrected resistance versus time for different W/C (1 hour delay, 40°C/hr rise, 80°C maximum)

This again shows a similar relationship to Figure 5.11, but without temperature dependent influences on resistance. These temperature independent resistances showed a reduced rate of gain initially caused by a combination of resistance increase due to hydration and a resistance drop caused by the absorption of free water into the aggregates (Khalaf and Wilson 1999).

5.5 Effect of Delay Period

Figure 5.13 shows the very early age strength properties for 1 stage heating with different delay periods (43N/mm^2 target mean strength mix). The delay period of 1 hour matched the normally cured compressive strength at 24 hours in only 4 hours after gauging with water. The 1 day strength of electrically cured specimens was also significantly larger than the normally cured specimens, with increases of up to 18N/mm^2 being readily achievable. The 1 hour delayed samples were of a higher 4 hour compressive strength than the other delays due to the increased maturity values (Saul 1951) at the time of testing.

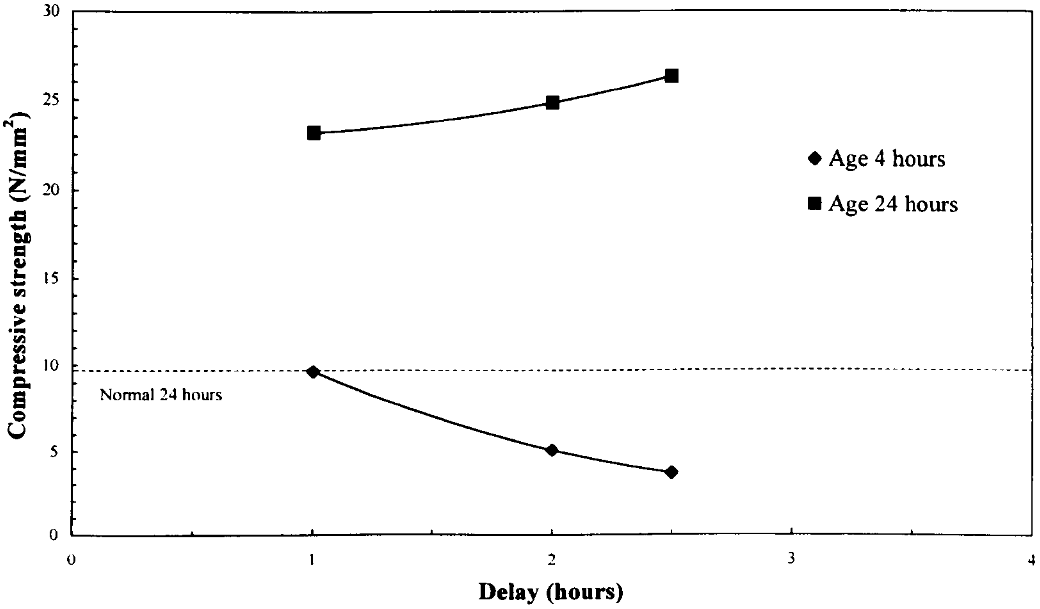

Figure 5.13 - Early age compressive strength (40°C/hr rise, 80°C maximum)

Figure 5.14 shows the relationship between compressive strength over differing ages for a 43N/mm^2 target mean strength mix with various delay periods prior to electrical curing of specimens to a maximum of 80°C. The figure shows that at 1 day the 1 hour delay time had a greater compressive strength than the 4 hours delay time, but at 7 and 28 days the situation was reversed (Pfeiffer and Landgren 1981). This was probably due to microcracks caused by thermomechanical forces exerted upon the structurally less well formed 1 hour delayed specimen that reduced the ultimate strength with age. It also shows that the 3 hours delayed specimen was the only specimen to achieve its target mean compressive strength at 28 days.

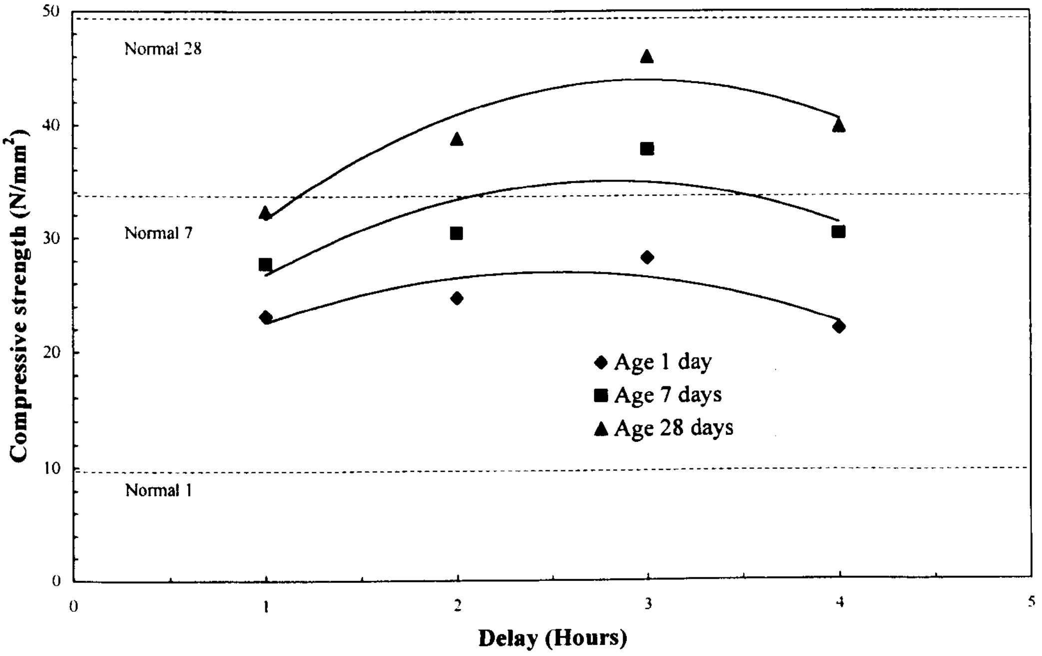

Figure 5.14 - Compressive strength versus delay period (40°C/hr rise, 80°C maximum, 1 day demoulding)

Figure 5.15 shows the percentage of compressive strength achieved at different ages relative to 28 day compressive strength for various delay periods to a maximum of 80°C. This shows that the 1 hour delay achieved the majority of its 28 day strength (71%) after only 1 day, whereas the normally cured specimens only achieved approximately 20% at the same age. The other electrically cured specimens also achieved high proportions of strength (55-65%) after 1 day. However, the 1 hour delay period had a final lower compressive strength (32N/mm^2) than any of the other regimes tested (40, 46, 41 and 49N/mm^2 for the 2, 3, 4 hours delay and normally cured specimens respectively). This was likely to be due to increased microcracking in the 1 hour delayed specimen, as the mix had not acquired enough strength to resist the thermomechanical stresses caused by heating.

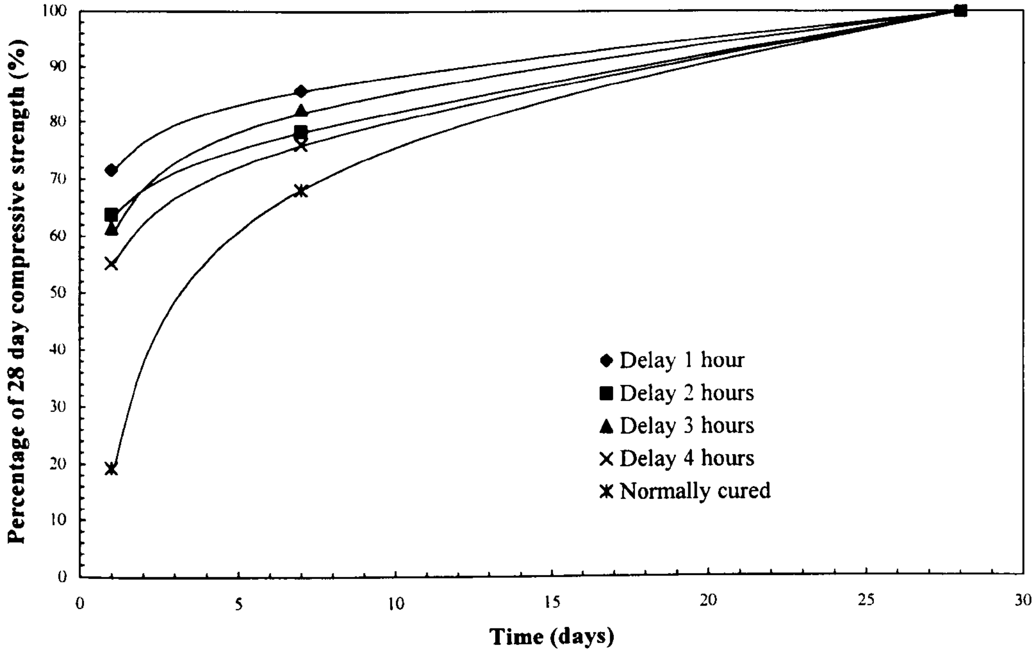

Figure 5.15 - percentage of compressive strength achieved at different ages relative to 28 day compressive strength for various delay periods (40°C/hr rise, 80°C maximum)

Figure 5.16 represents the compressive strength over differing ages for a mix with various delay periods prior to heating. The mix is a 43N/mm^2 target mean strength with slump of 10-30mm and was demoulded after 1 day. This shows that 3 hours delay prior to heating was the most beneficial to strength gain. It also shows that normal curing had a lower compressive strength than any heating regime at 1 day but had greater compressive strength than any heating regime at 28 days.

Extrapolated to ages of 100 days shows that all mixes should continue to gain compressive strength at varying rates and that all of the mixes, except the delay for 1 hour heating regime, would attain the target mean strength of $43N/mm^2$.

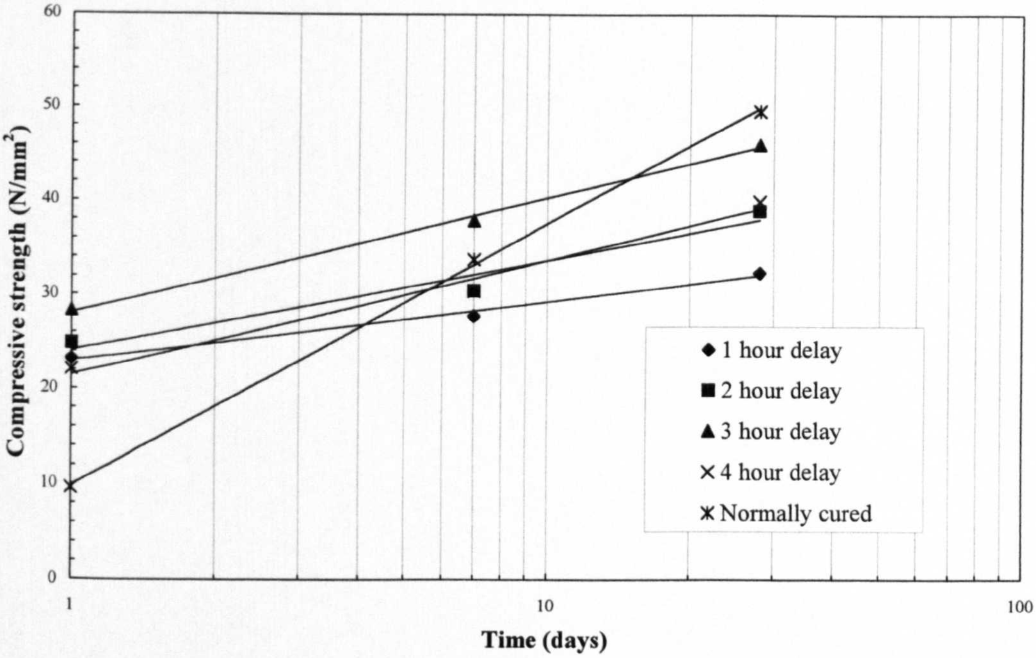

Figure 5.16 - Compressive strength versus time for various delay periods (40°C/hr rise, 80°C maximum)

Figure 5.17 shows the effect of delay period on the 3 day compressive strength. This shows that for the heating regime used, a 2 hour delay was more effective (17.1 N/mm^2, 62 % gain) than a 1 hour delay period before DEC (Xuenquan et al 1986). However, the 1 hour delay period still showed a 7.5 N/mm^2 (27%) gain in compressive strength. This may be adequate where time constraints are more important to the end user than a higher compressive strength.

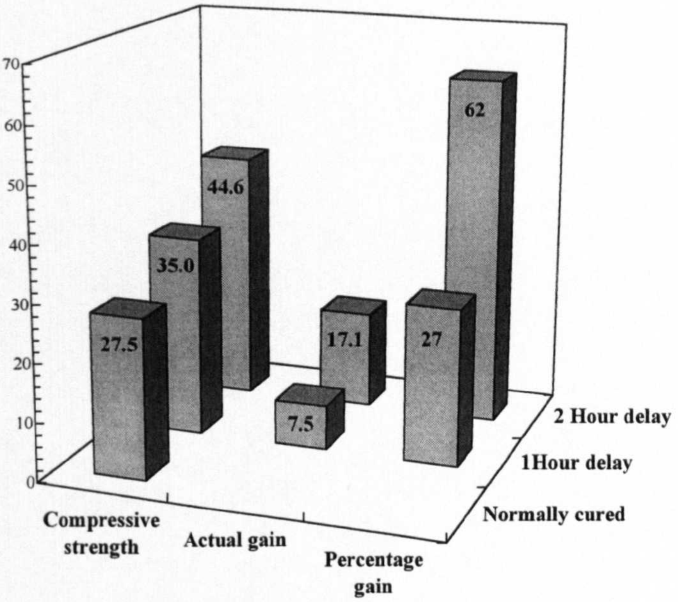

Figure 5.17 - Compressive strength versus delay period (40°C/hr rise, 80°C maximum, 3 day demoulding)

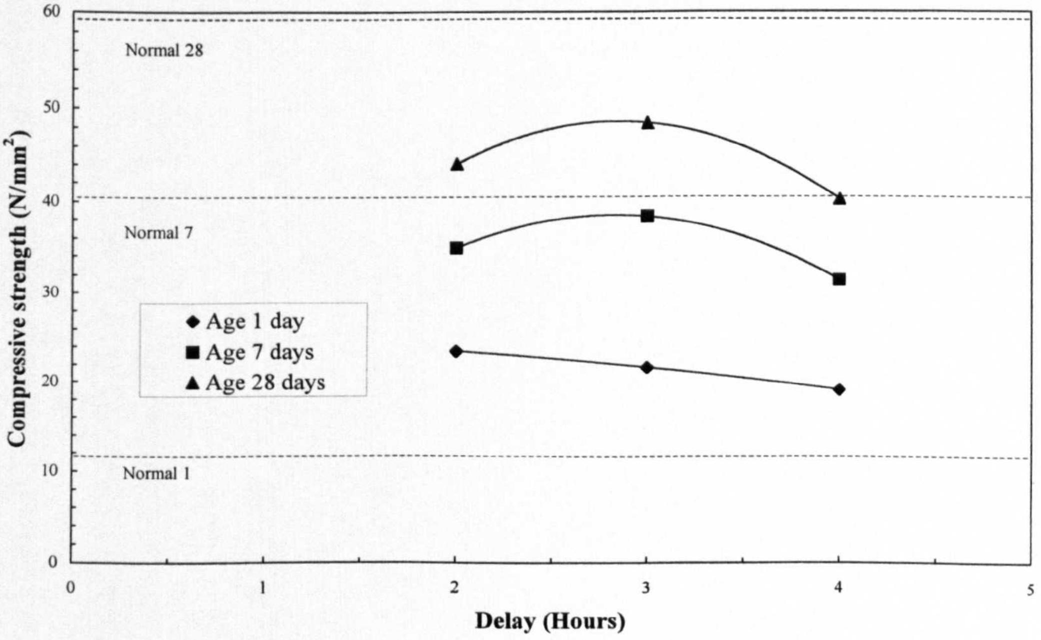

Figure 5.18 - Compressive strength versus delay period (40°C/hr rise, 60°C maximum)

Figure 5.18 shows the relationship between compressive strength over differing ages for a 43N/mm^2 mix with various delay periods prior to electrical curing of specimens to a maximum of 60°C. The figure shows a similar relationship to the differing delay periods with a maximum temperature of 80°C (Figure 5.14), but with comparatively higher electrically cured compressive strengths at 60°C for all delays at 28 days and no significant losses of compressive strength at 1 and 7 days. This was likely to be due to the reduced microstructural damage incurred by the relatively low (when compared to the 80°C maximum) temperature gradients present at 60°C.

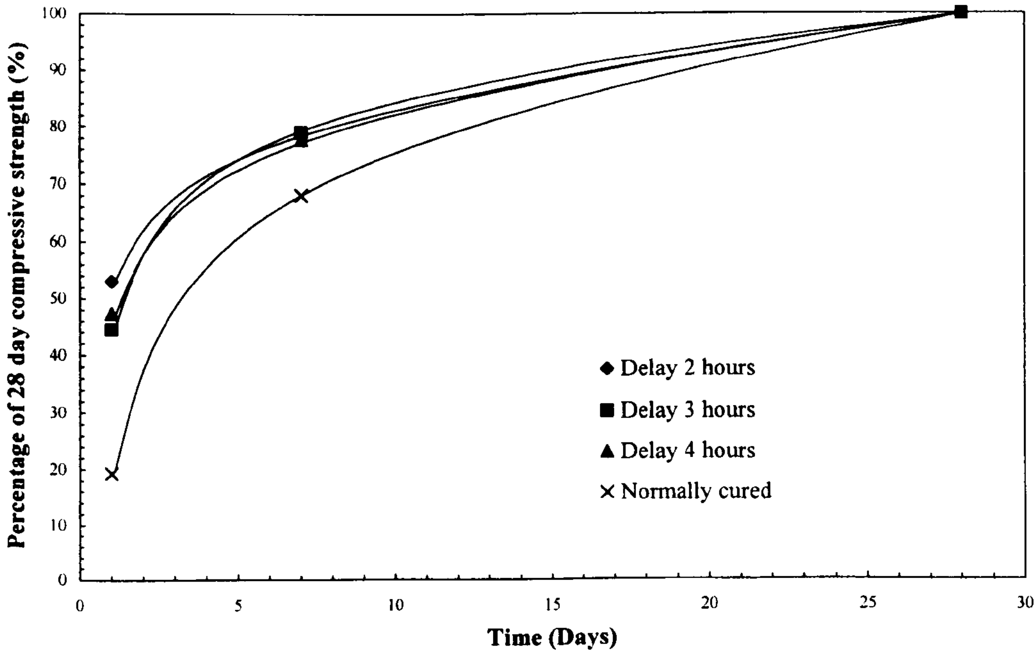

Figure 5.19 - Percentage compressive strength achieved at different ages relative to 28 day compressive strength for various delay periods (40°C/hr rise, 60°C maximum)

Figure 5.19 shows the percentage of compressive strength achieved at different ages relative to 28 day compressive strength for various delay periods to a maximum of 60°C. The figure shows a closer degree of percentage gain for the electrically cured samples of both short and long term ages than Figure 5.15. The electrically cured samples achieved approximately 50% of their respective 28 day strengths (44.1, 48.4

and 40.2N/mm^2 for the 2, 3 and 4 hour delays respectively) at 1 day. As with Figure 5.15, the 2 hours delay period achieved a larger percentage of its 28 day strength at 1 day than any other delay period, but the percentage increase after this time was not as great as the other delay periods.

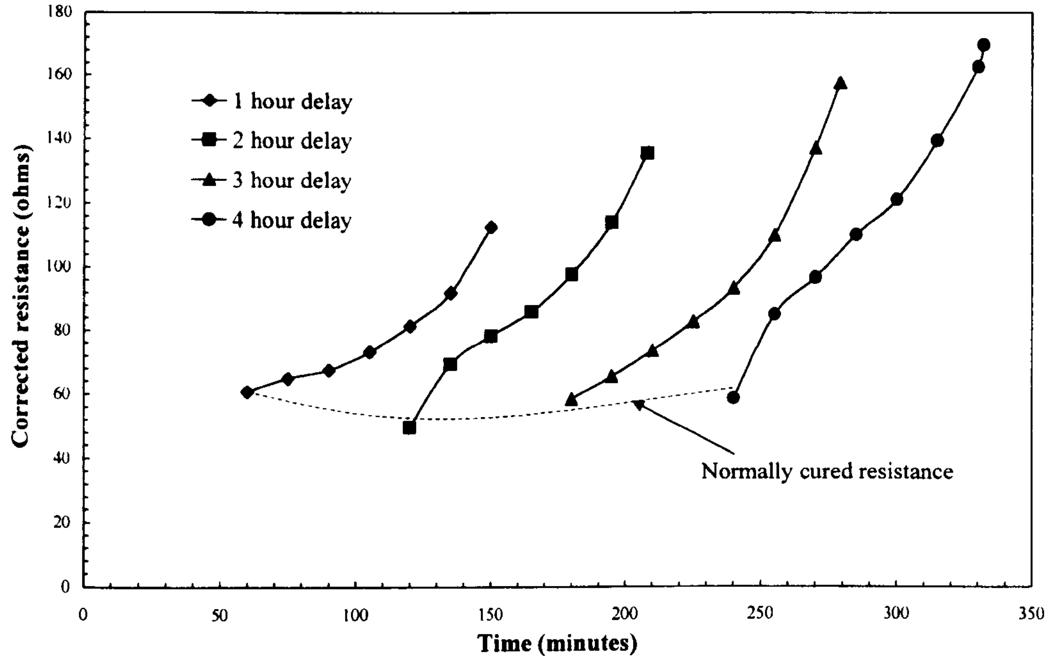

Figure 5.20 – Corrected resistance versus time for different delay periods (40°C/hr rise, 80°C maximum)

Figure 5.20 shows the corrected resistance for a number of different delay periods (40°C/hr rise, 80°C maximum). From this it can be seen that the initial resistance of each sample corresponded to the resistance at that time of a normally cured sample. This shows that the resistance of a normally cured sample reduced slightly until approximately 150 minutes after gauging with water, whereupon it rose. This was partially due to moisture absorption of water by the aggregates, thus changing them into a more conductive material, hence reducing resistance. It may also be partially due to increased levels of soluble ions (Ca^{++}, OH^- and SO_4^-) in the pore water during heating. The rise in resistance corresponded to free water being used in hydration reactions (Khalaf and Wilson 1999). The rise in resistance of the normally cured samples was not as pronounced as the rise in all of the electrically cured samples, showing that hydration was proceeding at an accelerated pace. The resistance at the end of heating can be seen to be dependent on the initial delay period. This could be used as a check to estimate the initial delay period and thus be an aid in predicting the short and long-term properties of the sample in question.

5.6 Effect of Maximum Temperature

Figure 5.21 shows the effect of maximum temperature on compressive strength for the 3 hour delayed samples. From this it can be seen that the 80°C maximum temperature achieved a higher initial 1 day compressive strength (28.3N/mm^2) than the 60°C maximum temperature (21.6N/mm^2). This situation was reversed at 28 days with the 60°C maximum attaining a compressive strength of 48.4N/mm^2 compared to 46N/mm^2 for the 80°C maximum.

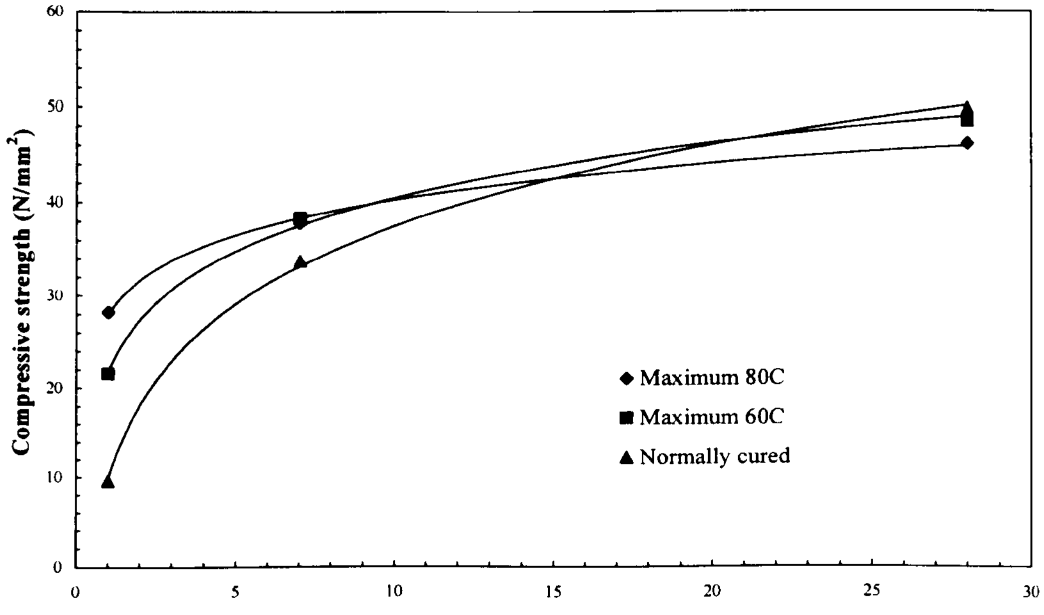

Figure 5.21 - Compressive strength versus time for 3 hour delay period samples (40°C/hr rise, 60°C and 80°C maximum)

The initial increase in strength was due to the initially increased rate of hydration achieved by using higher temperatures and the relatively higher maturity values at 1 day (Saul 1951). At later ages, damage caused by the increased thermomechanical stresses induced, reduced long-term compressive strength values. Both electrically cured samples attained their target mean strength (TMS) of 43N/mm^2 at 28 days but did not attain the same compressive strength as the normally cured samples at 28 days.

5.7 High Slump and High Strength Mixes

Figure 5.22 shows the compressive strength over time for a high slump (60-180mm) mix with TMS = 43N/mm^2. This shows a similar relationship to mixes of slump 10-30mm with the compressive strength of the electrically cured samples being initially higher (4N/mm^2) with the situation reversing after several days. From this it can be inferred that DEC could be applied to various mix designs as long as preliminary testing has been carried out on the specific mix.

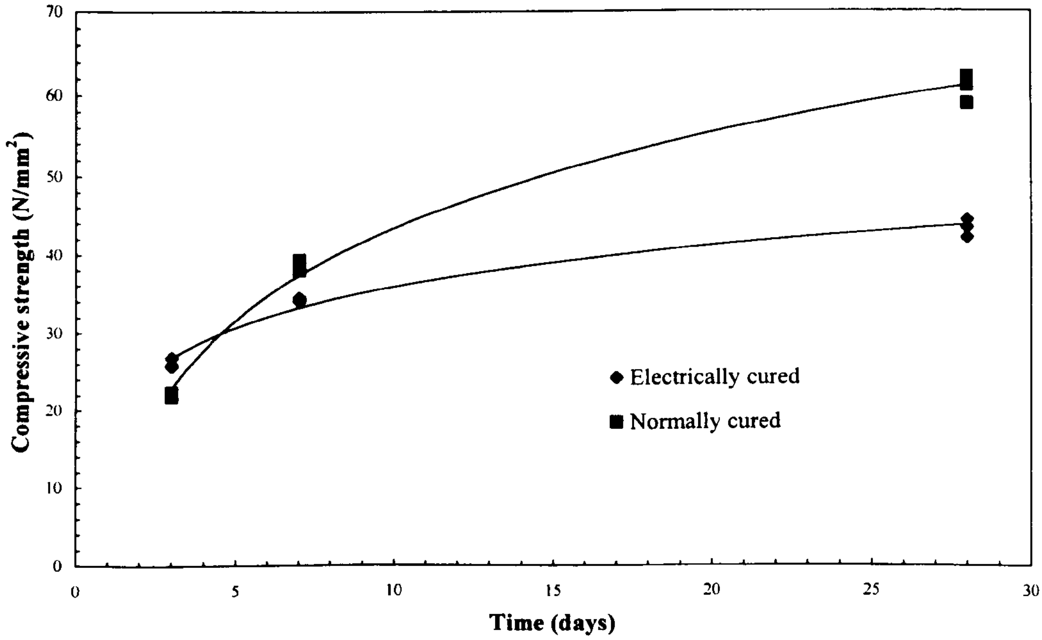

Figure 5.22 - Compressive strength versus time for a high slump mix (60-180mm) (1 hour delay, 40°C/hr rise, 80°C maximum)

Figure 5.23 shows the compressive strength over time for a high strength mix with TMS = 63N/mm^2. This shows a similar relationship to mixes of TMS = 43N/mm^2 with the compressive strength of the electrically cured samples being initially higher with the situation reversing after several days. The initial compressive strength gain of the electrically cured samples was found to be 9N/mm^2 which is equal to a 24% increase relative to normally cured samples. This larger percentage increase was thought to be due to the proportionally higher amount of cement within the mix. It gives evidence that the effectiveness of DEC is improved with the amount of cement/m^3 within the mix. This was due to the increased hydration per kg of cement associated with DEC.

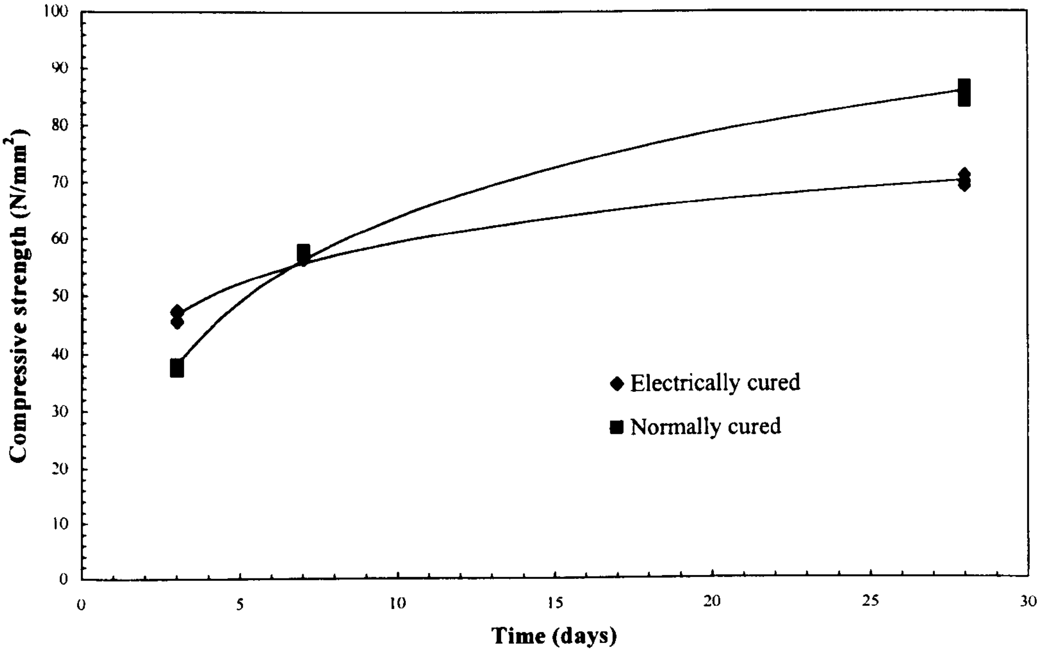

Figure 5.23 - Compressive strength versus time for a high strength mix (63N/mm^2 target mean strength) (1 hour delay, 40°C/hr rise, 80°C maximum)

Figure 5.24 shows resistance versus time for various mix types. From this it can be seen that the different mix types have a large effect on resistance. The C30 mix with 10-30mm slump had a greater resistance at later ages than the C30 mix with 60-180mm slump. This was due to the proportionally higher percentage of water to the rest of the mix constituents thus reducing the resistance of the high slump mix. The amount of water as a percentage of total constituents was 10.4% and 8.4% for the high and low slump mixes respectively. These percentages were used, as the W/C ratio in the two mixes were identical (0.55). This was not true for the C50 mix which had a water : (cement + aggregates) ratio of 8.4%, but had a greater mass of cement per m^3, thus reducing the amount of free water present in the mix after a degree of hydration had occurred, thus increasing resistance (Neville 1988).

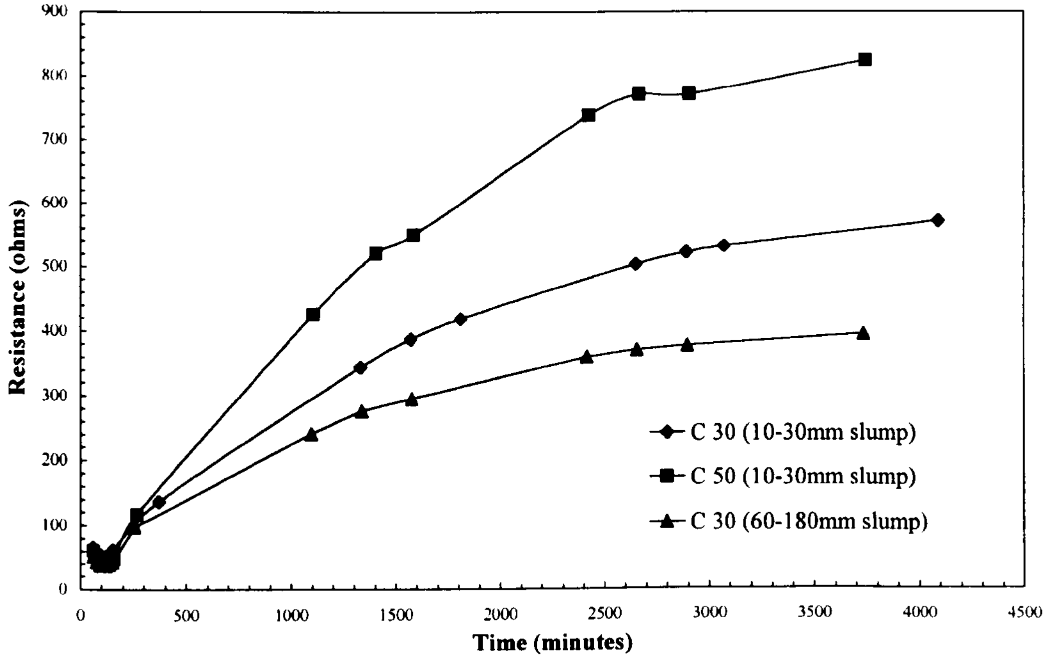

Figure 5.24 - Resistance versus time for differing mix types (1 hour delay, 40°C/hr rise, 80°C maximum)

Figure 5.25 shows the first 300 minutes of resistance measurements in Figure 5.24. This shows the time during and immediately after accelerated curing. From this it can be seen that the C50 mix had an initially similar resistance value to the other mixes, but increased at a more rapid rate, due to free water being used at an increased rate for hydration due to the proportionally higher cement in the mix. The lower resistance values of the high slump mix over time were due to the higher free water content that saturated the mix and was only partially absorbed by the aggregates at early ages, thus reducing the effective path length for the current to flow through.

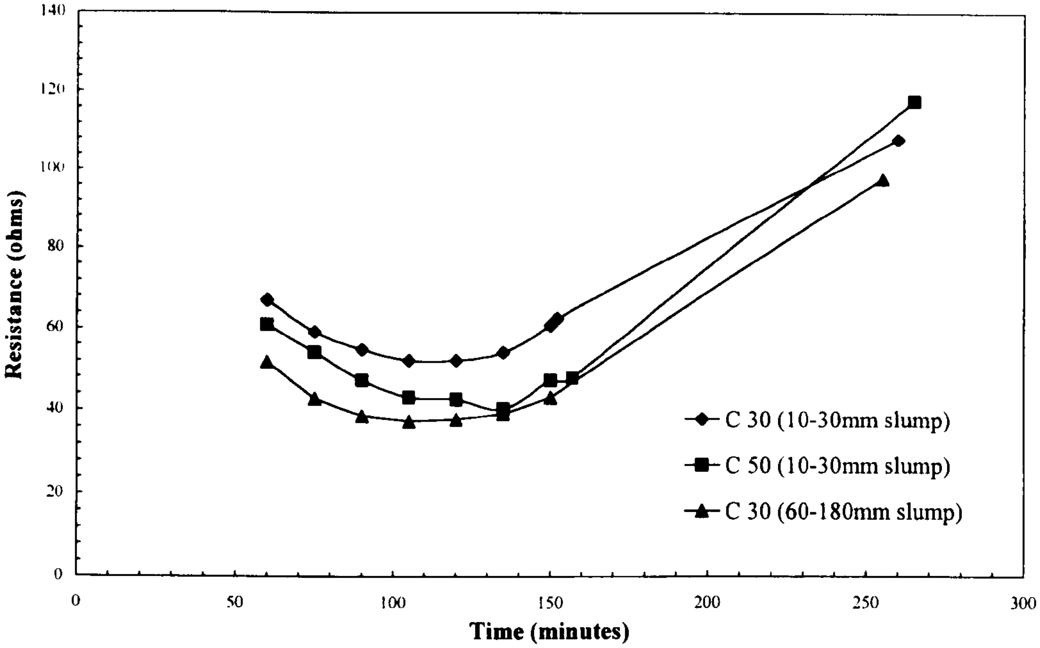

Figure 5.25 - Resistance versus time for differing mix types (1 hour delay, 40°C/hr rise, 80°C maximum)

5.8 Resistance

Figure 5.26 shows the relationship between electrical resistance of specimens at 1 day and the compressive strength for a range of curing regimes, mixes and ages. From this it can be seen that resistance was not a good indicator of compressive strength at early ages (1 day). This was because the hydration had not occurred enough to allow differences in resistance to be measured. Within the mix at this time were still large quantities of free water which allowed effectively small path lengths to be achieved by the electricity. This can be seen by the small differences in resistance measured (270-370 ohms).

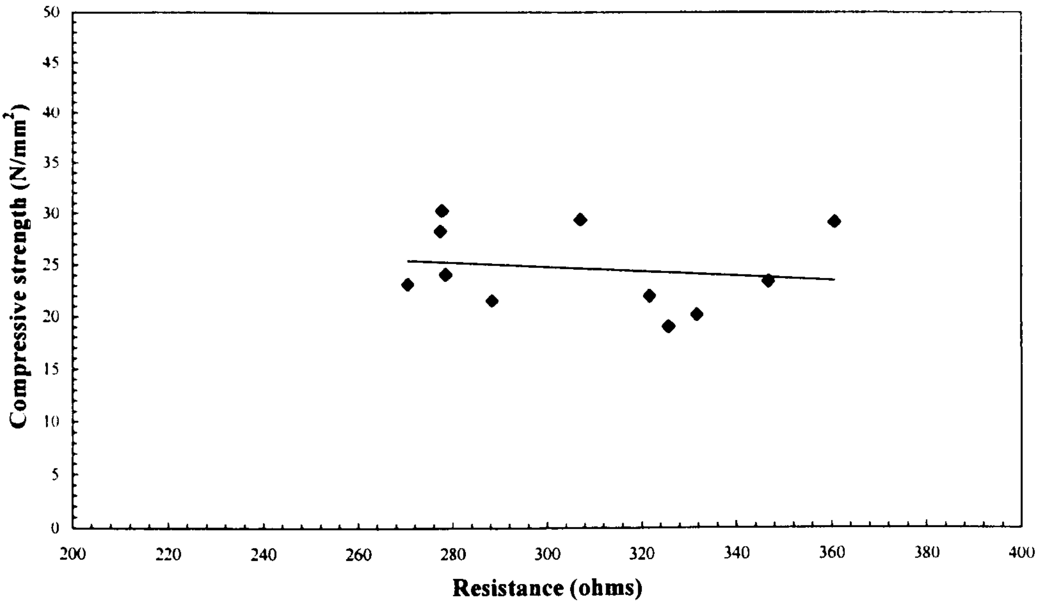

Figure 5.26 - Compressive strength versus resistance at 1 day

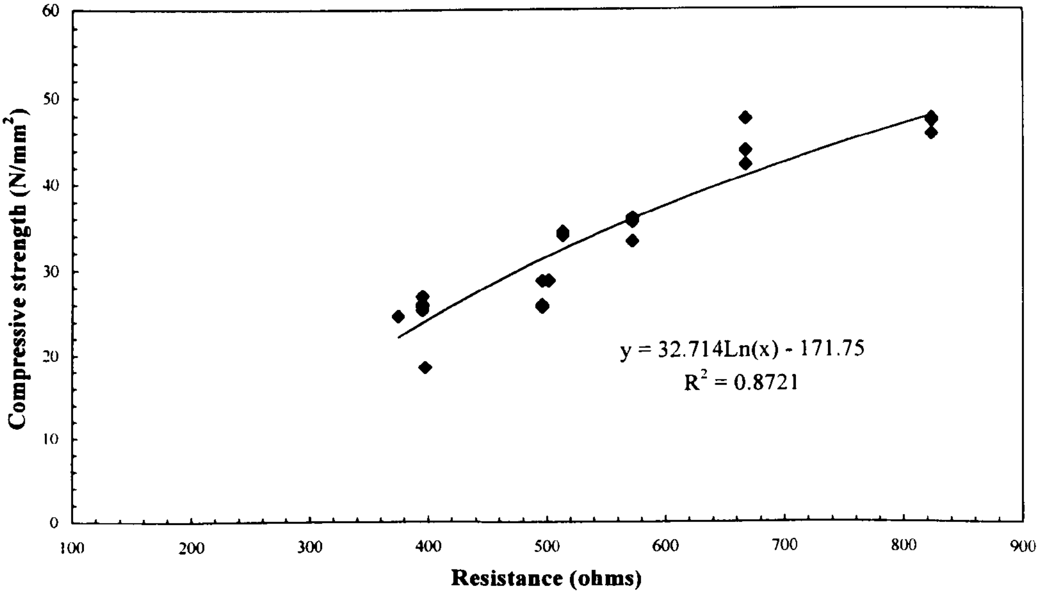

Figure 5.27 - Compressive strength versus resistance at demoulding for 3 day air cured samples

Figure 5.27 shows the relationship between electrical resistance of specimens immediately prior to testing (after 3 days of air curing) and the compressive strength for a range of curing regimes, mixes and ages. The figure shows that, for concrete, electrical resistance was a good indicator of compressive strength (compressive strength = 32.71 x Ln (resistance) + 171.75) and could be used over a range of varying mixes, heating regimes and ages. This means that the compressive strength of electrically cured specimens can be estimated indirectly from its final resistance without the need to test cubes, cores or other types of sample. The coefficient of determination (R^2) for the linear fit was found to be 0.87 with a maximum deviation from the best-fit line of $6N/mm^2$. If resistance is to be used as a non-destructive test (NDT) for geometrically different electrically cured specimens, calibration curves relating compressive strength and resistance, made of the same materials, are needed.

5.9 Effect of Temperature on Resistance

Figure 5.28 shows the effect of temperature on the resistance of concrete samples.

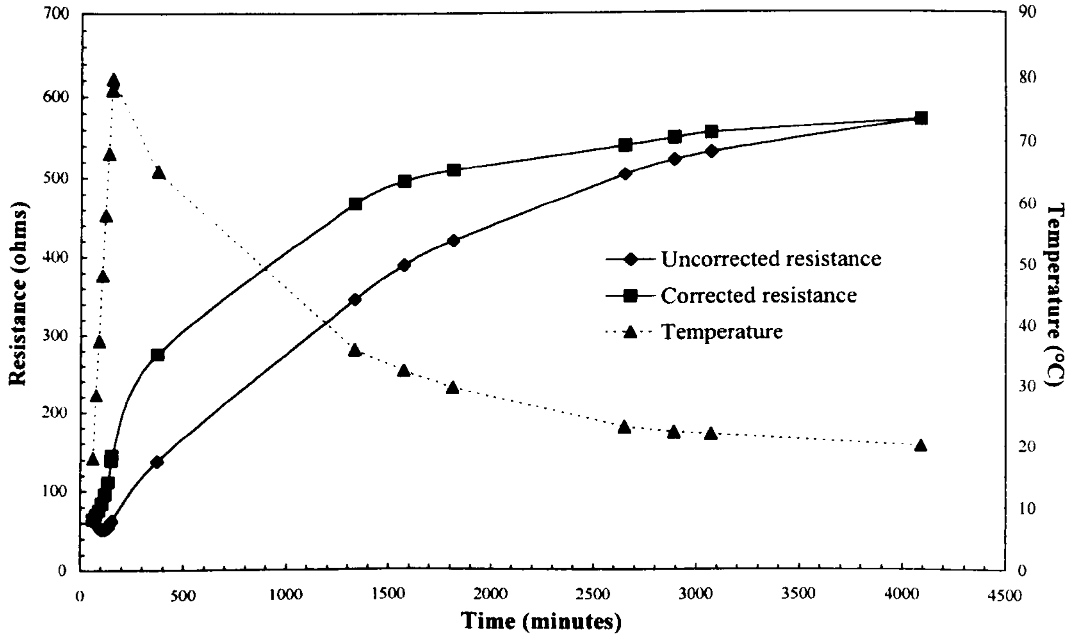

Figure 5.28 - Temperature corrected and uncorrected resistance versus time (1 hour delay, 40°C/hr rise, 80°C maximum)

The figure shows that the effect of heating on resistance was substantial with the corrected resistance being 150 ohms higher than the apparent resistance. This is important if resistance is to used in predicting concrete hydration or W/C ratio. The corrected and uncorrected resistances only converged after a period of approximately 66 hours when the temperature of the samples reduced to 20°C. It can also be seen from this figure that the maximum rate of cooling at the centre of the surface at a depth of 20mm was approximately 4°C/hr. This is within the specifications laid down by the Highways Agency (1988) but may not be true if other mix types and geometrys are chosen.

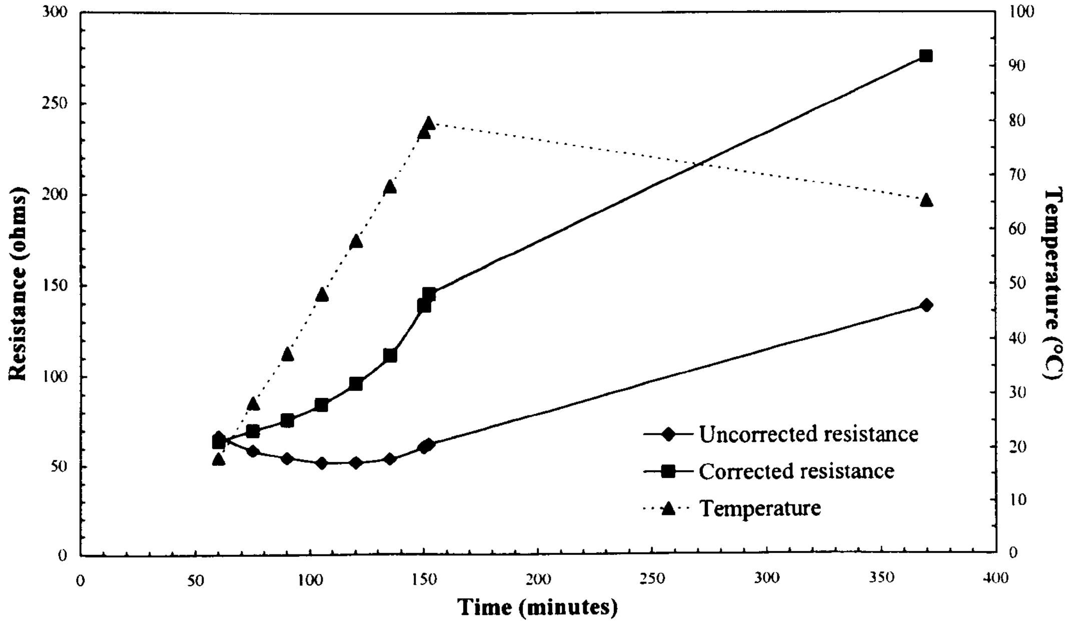

Figure 5.29 - Temperature corrected and uncorrected resistance versus time (1 hour delay, 40°C/hr rise, 80°C maximum)

Figure 5.29 shows the first 400 minutes of resistance measurement in Figure 5.28. From this it can be seen that the apparent effect of the initial lowering of resistance was reduced to a slower rise in resistance than would be expected if hydration alone was responsible for the increase. However, the effect was still present, showing that water was being absorbed by the aggregates, thus lowering the rate of rise of resistance. This also shows the need to correct for temperature when resistance is a governing factor in estimating the degree of hydration or any other derived property, such as mix type or W/C ratio (Wilson and Gupta 1996).

5.10 Two Stage Heating

The two stage heating regimes entailed a variable rate of rise in temperature. These were:

1. 15°C/hr for 1 hour with 40°C/hr to 80°C maximum (referred to as 2 stage low/high).
2. 40°C/hr for 1 hour with 20°C/hr to 80°C maximum (referred to as 2 stage high/low).

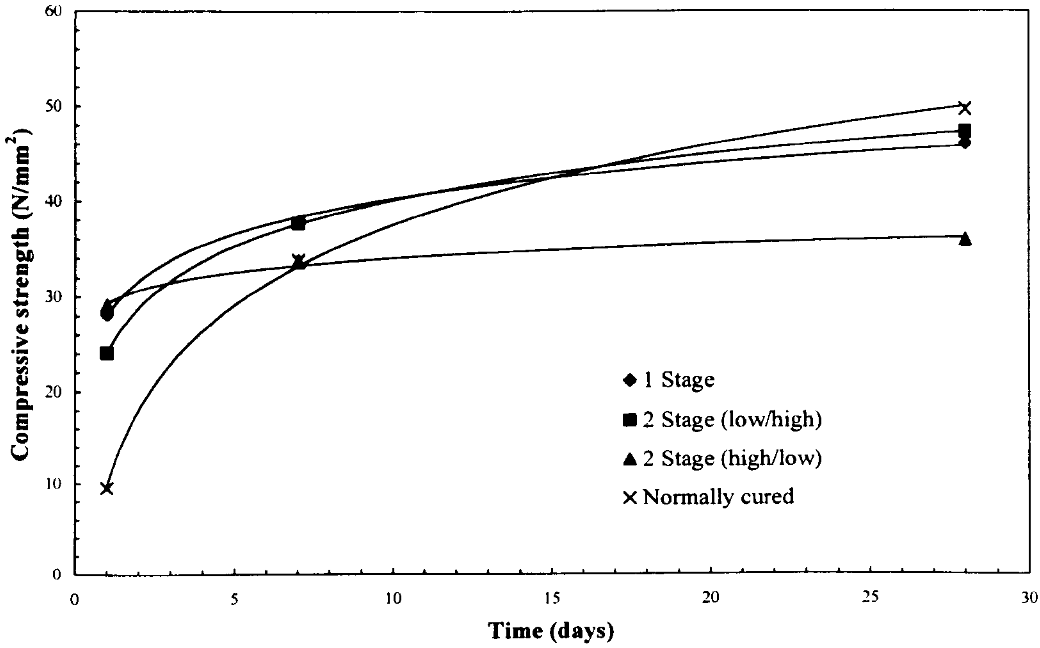

Figure 5.30 - Comparison of 1 and 2 stage heating regimes (3 hour delay)

Figure 5.30 shows a comparison of the 1 and 2 stage heating regimes used for a 3 hour delay period. This shows increased damage caused by the high/low regime at later ages and also shows the increased 1 day strength of the initially high rate of heating. The low/high regime exhibited a greater 28 day strength than the other electrically cured specimens and was almost equivalent to the normally cured mix. This illustrates the importance of the very early stages of curing during heating and the need to be able to monitor temperature throughout the specimen were relatively minor differences have large, long term ramifications to compressive strength.

Figure 5.31 shows a comparison of the 1 and 2 stage heating regimes used for a 2 hour delay period. This shows increased damage to the structure of concrete at later ages in all electrically cured samples due to the lack of strength present after 2 hours delay to resist the thermomechanical stresses imposed during heating. The 2 stage heating regimes showed a slightly increased compressive strength after 1 day when compared to the 3 hour delay period in Figure 5.30, but the 1 stage linear heating regime did not. This may be because with the 2 stage heating regime, the concrete did not achieve its maximum temperature until later than the 1 stage regime. This would increase the maturity value of the concrete at 1 day, but the affect on maturity at later ages is negligible when compared to the damage caused to the structure of the concrete by the earlier delay period.

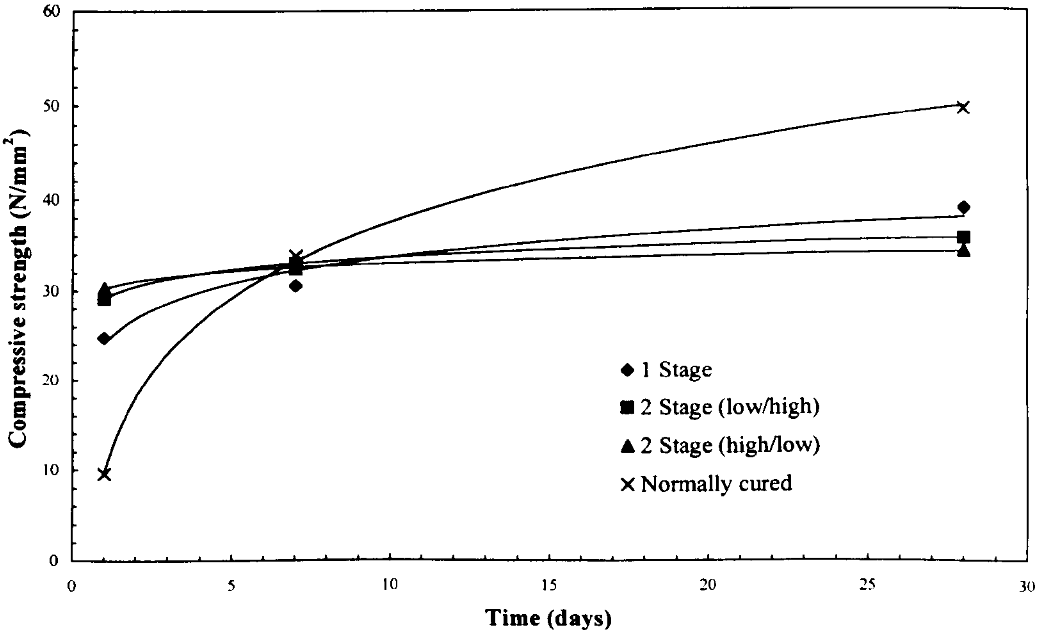

Figure 5.31 - Comparison of 1 and 2 stage heating regimes (2 hour delay)

Figure 5.32 shows the importance of the delay period for 2 stage curing (low/high). The difference of only 1 hour delay period significantly altered both the short and long term strength development of concrete. With a relatively early delay period (2 hours), 1 day strength was increased when compared to a 3 hour delay period. This situation was then reversed as the initial damage caused to the structure of the early delay period specimen significantly reduced its long-term strength (Xuenquan et al 1986).

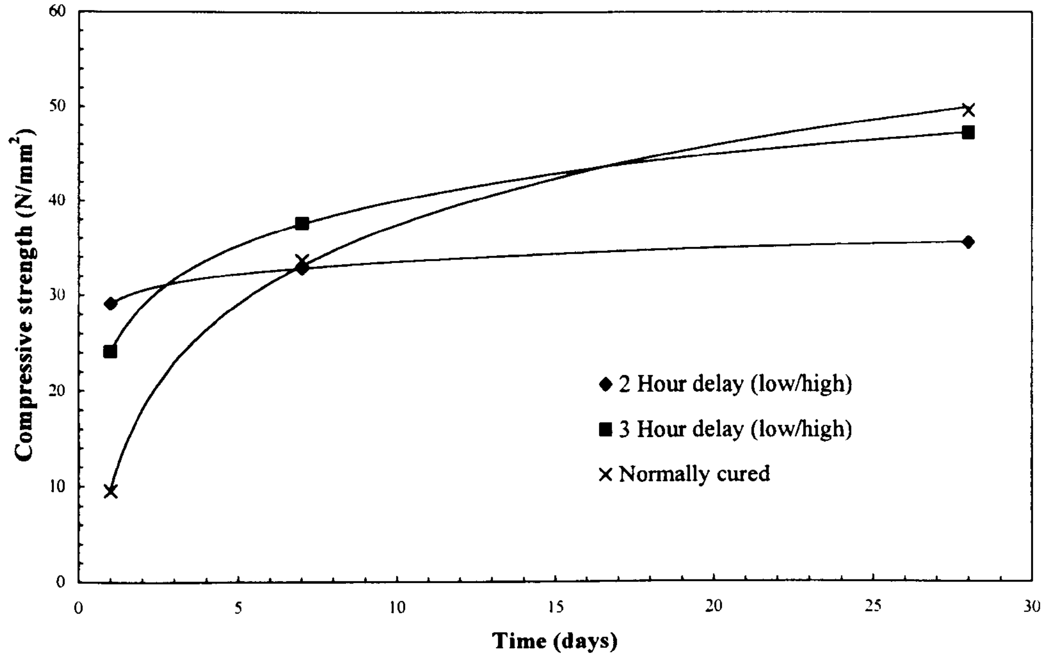

Figure 5.32 - Compressive strength versus time for different delay periods for two stage heating (15°C/hr rise for 1 hour + 40°C/hr rise, 80°C maximum)

Figure 5.33 shows the importance of the delay period for 2 stage curing (high/low). From this it can be seen that the high/low regime for a delay period of 3 hours significantly reduced long-term compressive strength when compared to the low/high regime shown in Figure 5.32. This was likely to be due to the higher temperatures being reached at an earlier stage with the high/low regime, thus causing greater damage at later ages. The 1 day compressive strengths for equivalent delay periods were similar due to the similar maturity values achieved (Saul 1951).

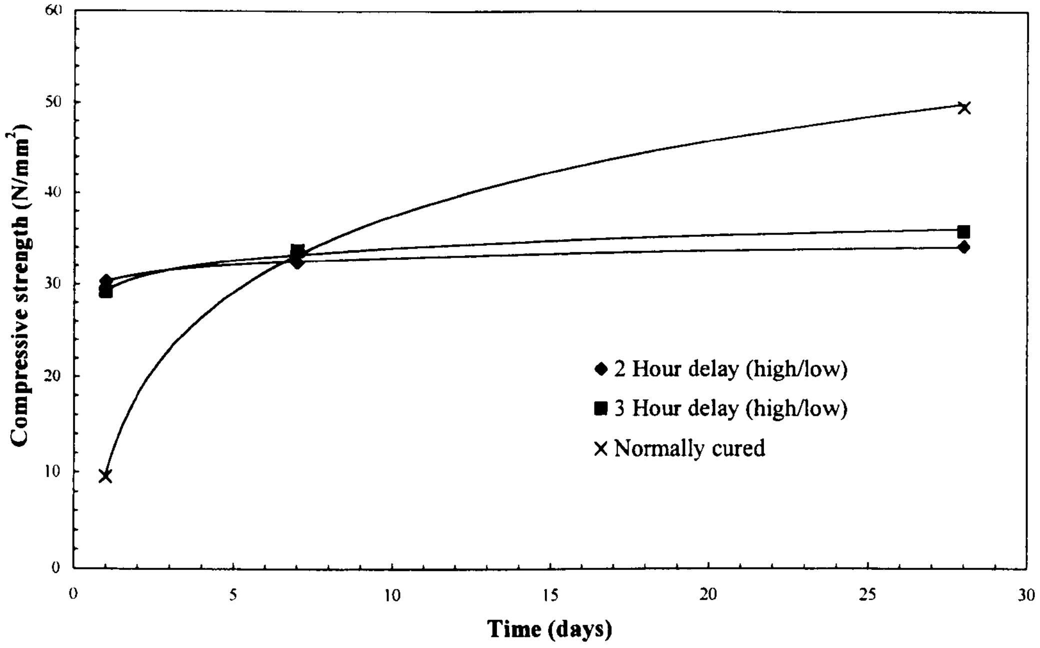

Figure 5.33 - Compressive strength versus time for different delay periods for 2 stage heating (40°C/hr rise for 1 hour + 20°C/hr rise, 80°C maximum)

Figure 5.34 shows the percentage compressive strength gain of 1 and 2 stage electrically cured samples (3 hour delay) over normally cured samples. From this it can be seen that 1 stage and 2 stage (high/low) achieved approximately 200% of the compressive strength of the normally cured samples at 1 day. The 2 stage (low/high) achieved approximately 150% of the normally cured compressive strength at the same age. This was likely to be due to the time at which the samples reach maximum temperature. With both the 1 stage and the 2 stage (high/low) temperatures in excess of 60°C were reached within 1 hour of heating (4 hours after gauging with water), but this temperature was not reached until 1.75 hours after heating for the 2 stage (low/high) heating rate. This is critical to the effect on the acceleration of hydration where later higher temperatures have a reduced effect on the initial strength (Orchard and Barnett 1971). The 2 stage (high/low) heating rate attained a slightly higher percentage gain at 1 day than the 1 stage heating rise due to the 2 stage samples being at higher temperatures for longer, thus having increased maturity. The normally cured samples attained a greater degree of compressive strength than the electrically cured samples between 7 and 10 days. The 28 day compressive strength of the electrically cured samples were all lower than the normally cured samples. This was due to thermomechanical damage caused to the structure of the concrete. This was confirmed by the greater reduction of the 2 stage (high/low) heating rise. This was because this 2 stage heating rate maintained high temperatures (60-80°C) for a comparatively longer period than the other heating rates, thus causing more damage. This was also confirmed by the 2 stage (low/high) heating rate that allowed a greater degree of structural formation to occur before attaining high temperatures (60-80°C), thus allowing less damage to occur and allowing a comparatively high 28 day compressive strength.

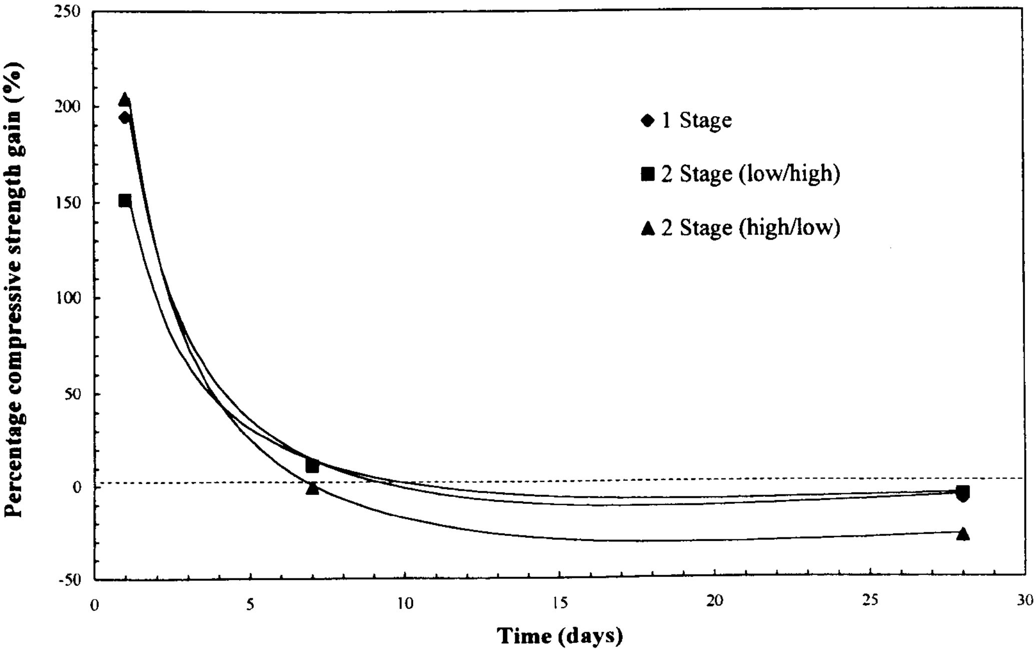

Figure 5.34 - Percentage compressive strength gain versus time for 1 and 2 stage heating regimes (3 hour delay)

Figure 5.35 shows the corrected resistance for 2 stage heating regimes, with a delay period of 3 hours. From this it can be seen that the low/high rise had reduced resistance values when compared to the high/low rise. This reflected the degree of accelerated hydration present within the samples (Wilson and Gupta 1996). The high/low rise attained a higher temperature earlier and as such the degree of hydration was increased, thus reducing the free water content and increasing resistance. The low/high rise increased resistance substantially after 60°C had been reached and the rate of resistance rise was greater than the equivalent temperature rise in the high/low sample. This was also true of the low rise section of the high/low heating regime. After approximately 60°C the rise in resistance of the high/low regime was significantly greater than the resistance increase in the initial low section of the low/high regime. This was likely to be due to a combination of the following two factors:

1. At temperatures above 60°C, water loss through evaporation may significantly affect resistance values.
2. The increase in the rate of hydration may be temperature specific, with greater increases over certain temperature regions.

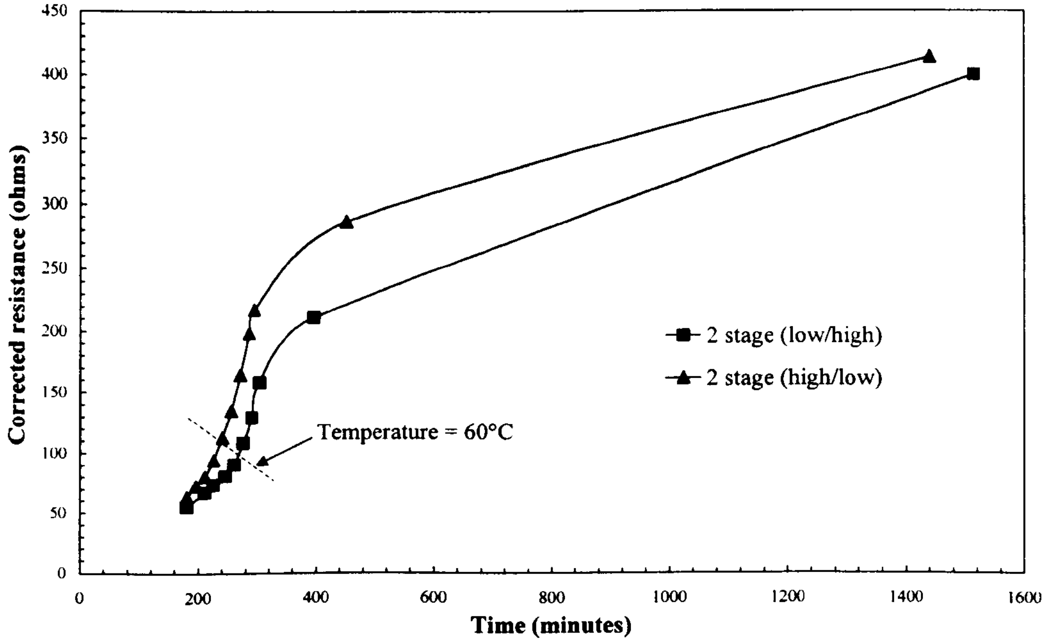

Figure 5.35 – Corrected resistance versus time for 2 stage heating regimes (3 hour delay)

The resistance values after heating reflected the relative compressive strengths of the samples after 1 day with the low/high regime having a lesser resistance, thus indicating a lower degree of hydration and a lower compressive strength. At demoulding, the rate of resistance increase in the low/high regime was greater than the high/low which would indicate a greater degree of hydration at later ages (Wilson and Gupta 1996). This was in agreement with the later 28 day compressive strength values which showed the low/high regime having greater compressive strength.

5.11 Splitting Tensile Strength

Figure 5.36 shows the splitting tensile strength of beams over time. From this it can be seen that tensile strength of electrically cured samples followed a similar relationship to that of compressive strength as shown in Figure 5.21 (Neville 1988) with an initial increase over normally cured samples at 1 day and a reduction of tensile strength at 28 days.

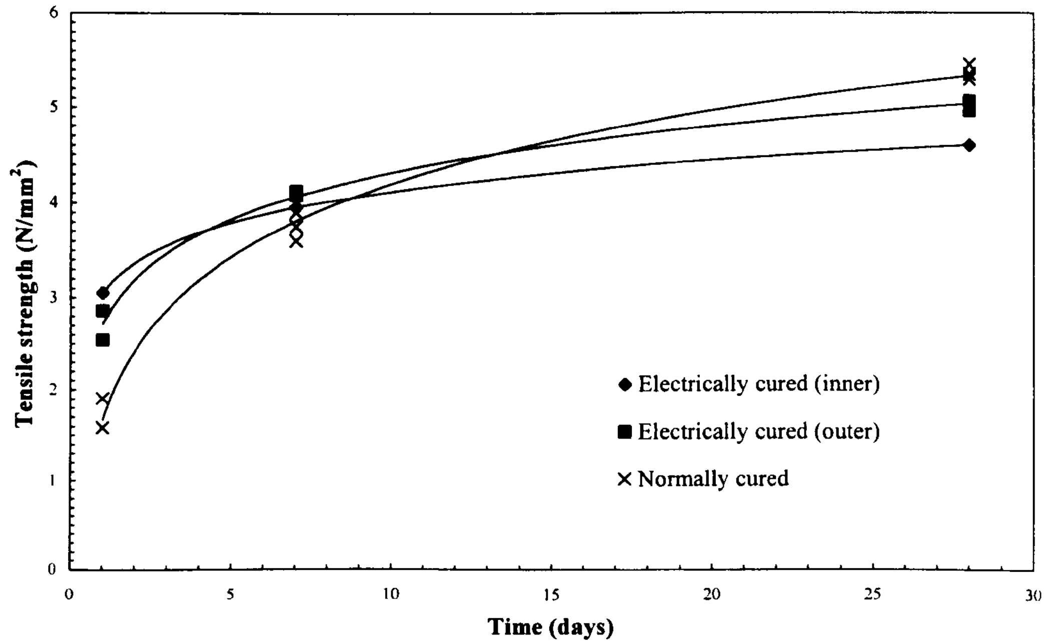

Figure 5.36 – Splitting tensile strength versus time electrically (3 hour delay, 40°C/hr rise, 80°C maximum) and normally cured samples

It can also be seen that the inner (centre) section attained a higher tensile strength when compared to the outer (1/4) section. This was due to the higher temperatures achieved in the centre section, thus increasing the initial rate of hydration and maturity. The outer sections eventually attained a higher tensile strength due to the increased thermomechanical damage caused to the inner section by the relatively higher temperatures used.

Figure 5.37 shows the splitting tensile strength against position on an electrically cured beam for various ages. From this it can be clearly seen that the position that tensile strength is tested is crucial to both short and long-term properties. This shows that the inner section attained the greatest initial tensile strength, but the lowest long-term tensile strength. The situation was reversed as the distance from the centre increased and the figure shows an extrapolated maximum tensile strength of approximately 6.4N/mm^2 at 28 days for the extreme edges of the beam. This shows the importance of the testing position of accelerated cured beams where temperature histories are certainly different for each section (Figure 5.57).

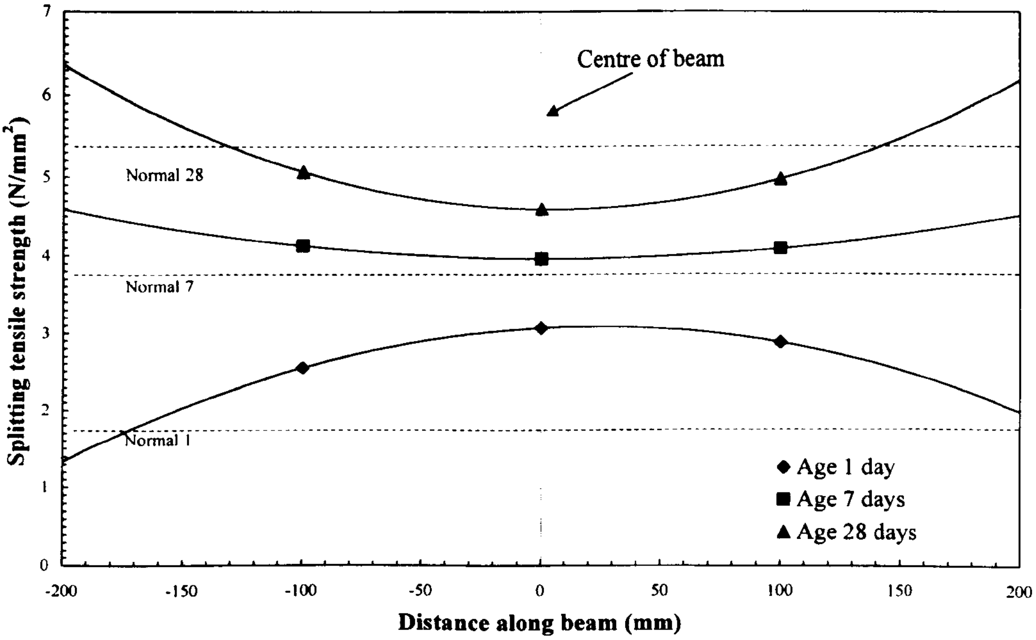

Figure 5.37 – Splitting tensile strength versus distance along beam at differing ages

Figure 5.38 shows the percentage gain in splitting tensile strength of electrically cured beams (3 hour delay, 40°C/hr rise, 80°C maximum) for inner and outer sections. It can again be seen that the inner sections attained a significantly greater gain in tensile strength over normally cured concrete at earlier ages than the outer sections. Both outer and inner electrically cured samples attained significantly higher tensile strengths at 1 day than the normally cured samples (60-80%), thus indicating that the rate of hydration had been increased. The 28 day tensile strength can be seen to be 14.5% less than the normally cured samples. This was at the worst case of the centre of the beam were temperature induced stresses were highest, thus reducing tensile strength to the greatest degree.

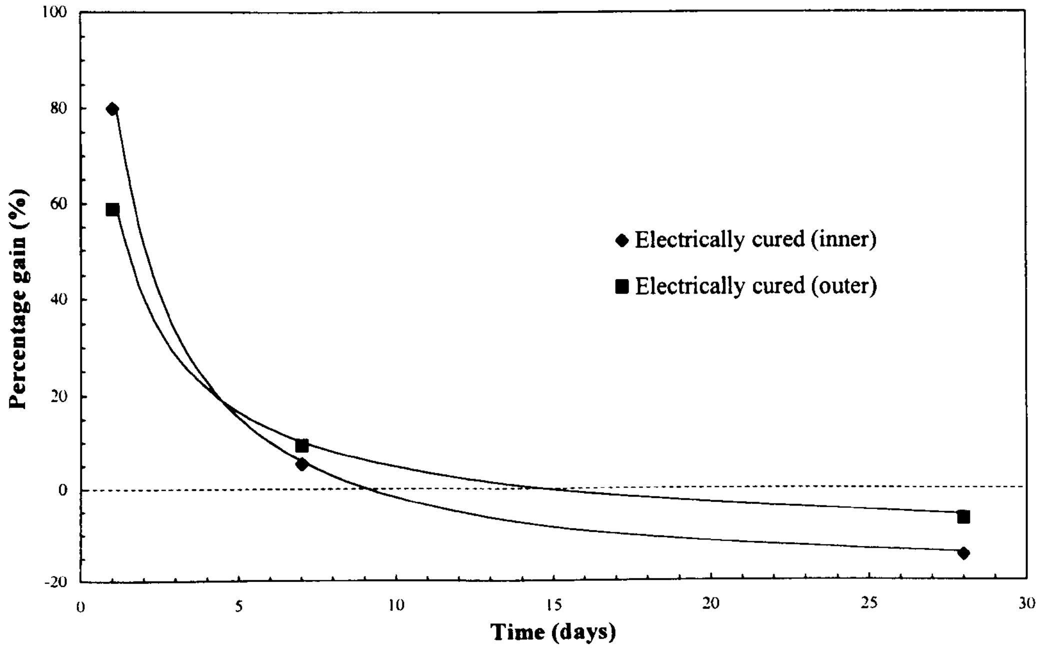

Figure 5.38 - Percentage increase of splitting tensile strength at differing ages

Figure 5.39 shows the percentage gain of tensile strength of electrically cured beams and compressive strength of equivalently cured cubes (3 hour delay, 40°C/hr rise, 80°C maximum). The percentage gains for tensile strength at 1, 7 and 28 days were substantially lower than the compressive strength gains for an equivalent mix and heating regime (195%, 12% and –7.3% gain). This was due to the amount of microcracks present within the mix. During compressive testing, these cracks were forced to close, thus not affecting the compressive strength greatly, but during tensile testing, these microcracks acted as stress concentrators and allowed larger crack propagation to occur, thus decreasing the tensile strength to a greater degree. This decrease in tensile strength from what would normally be expected means that extra consideration needs to be given to the design of concrete in tension when using electrically accelerated curing. Substantial pretesting to derive the tensile properties of the concrete along the length of the beam would certainly need to be carried out prior to any assumptions being made about tensile strength (Neville 1988).

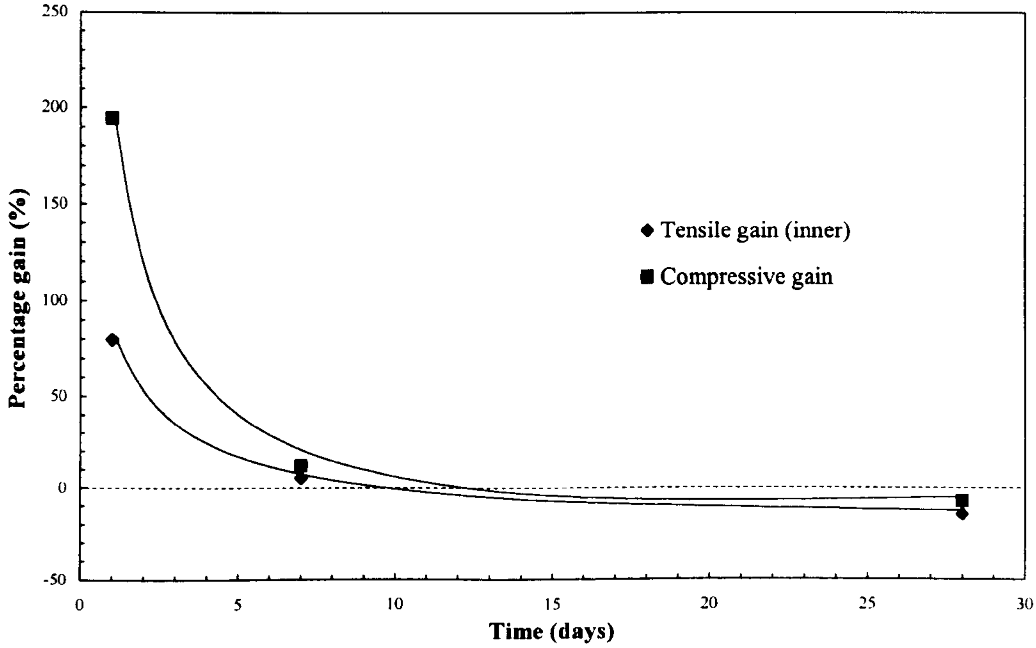

Figure 5.39 - Comparison of percentage gain of compressive and splitting tensile strength (3 hour delay, 40°C/hr rise, 80°C maximum)

5.12 Flexural Tensile Strength

Figure 5.40 shows the effect of electrical curing on 28 day flexural tensile strength. This shows an equivalent reduction in flexural tensile strength (15%) as with splitting tensile strength when compared to normally cured samples. This was again due to microcracks acting as stress concentrators as tensile forces occur during loading.

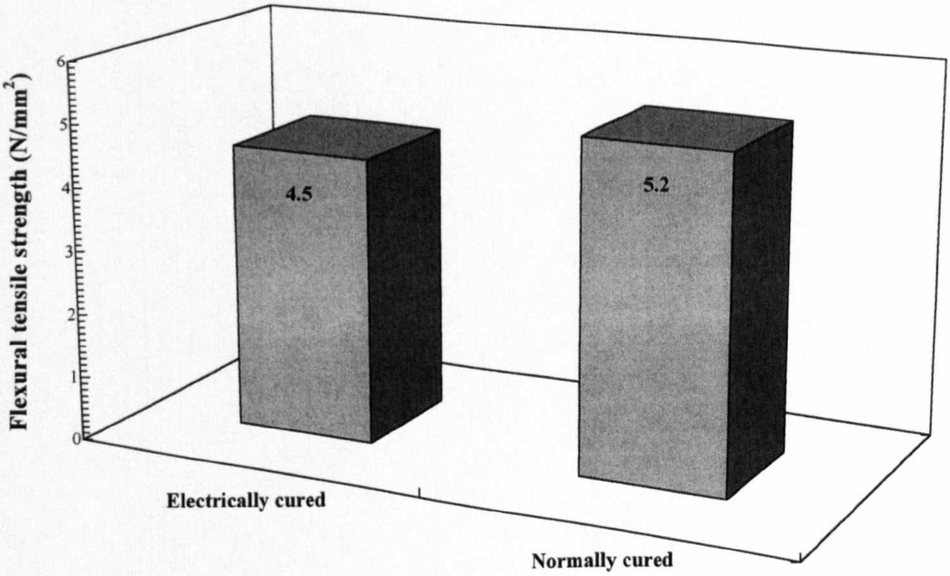

Figure 5.40 - Flexural tensile strength of electrically (3 hour delay, 40°C/hr rise, 80°C maximum) and normally cured samples at 28 days

5.13 Maturity

Figure 5.41 shows compressive strength of normally cured samples versus maturity. From this it can be seen that compressive strength for the C30 mix followed a logarithmic curve of equation:

$$\text{compressive strength} = 11.244 \times \text{Ln (maturity)} - 63.038 \qquad \text{Eqn. 5.1}$$

The coefficient of determination ($R^2 = 0.9241$) was only slightly less than the coefficient of determination for the logarithmic curve used to describe Figure 5.1 ($R^2=0.9529$) and may be ascribed to minor temperature fluctuations within the curing tank (20°C±1°C) that is allowed in BS 1881. This shows that for the mix used, log maturity was a good indicator of compressive strength (ASTM C1074). This was to be expected, as compressive strength at constant temperatures and moisture conditions generally follows a logarithmic curve (Neville 1988).

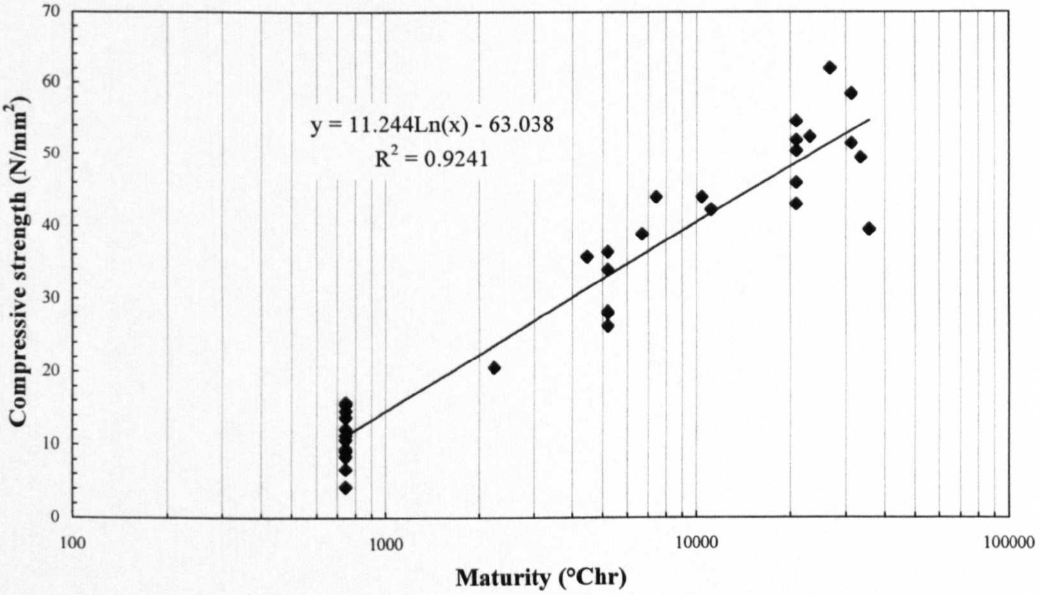

Figure 5.41 - Compressive strength versus maturity (normally cured)

Figure 5.42 shows compressive strength of electrically cured samples of various heating regimes versus maturity. From this it can be seen that compressive strength for the C30 mix followed a logarithmic curve of equation:

$$\text{compressive strength} = 6.244 \times \text{Ln (maturity)} - 20.35 \qquad \text{Eqn. 5.2}$$

The coefficient of determination (R^2) was equal to 0.8459. The gradient of the best-fit line can be seen to be significantly less than the equivalent normally cured samples indicating that in general, the rate of compressive strength gain in electrically cured samples was lower than normally cured samples. Also, the intercept for the electrically cured samples is shown to be at a greater level indicating that initial strength was higher. The coefficient of determination was reduced when compared to normally cured maturity because classical maturity calculations do not take account of extreme temperatures or the time at which they occur (Saul 1951). However, it can be seen that classical maturity values can at least give an indication of compressive strength providing previous data has been acquired concerning the particular mix.

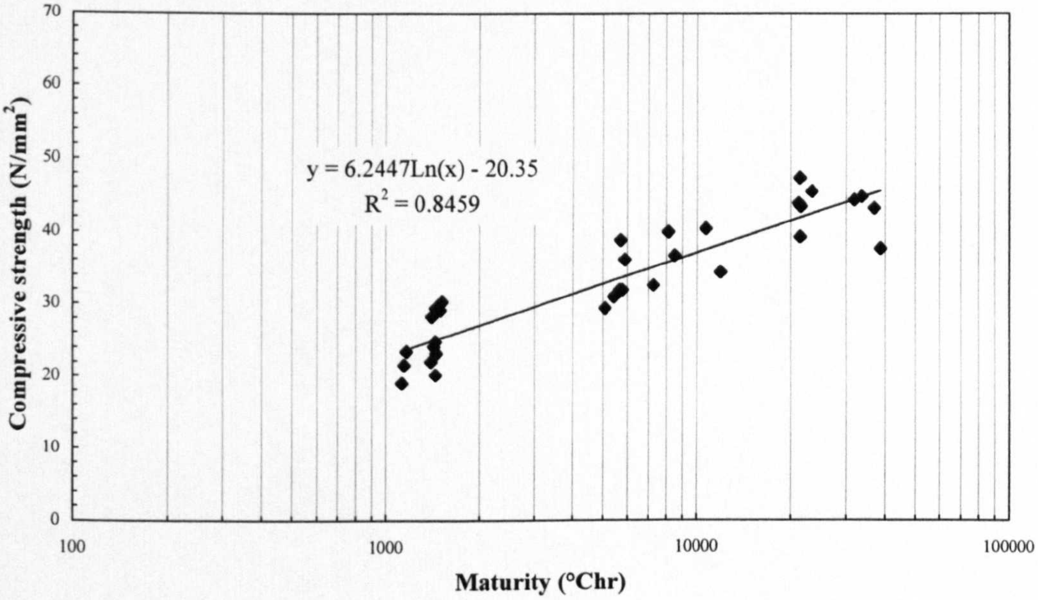

Figure 5.42 - Compressive strength versus maturity (electrically cured)

Figure 5.43 shows compressive strength of both electrically cured samples of various heating regimes and normally cured samples versus maturity. From this it can be seen that standard maturity values for normally cured concrete underestimated electrically cured compressive strength at early ages and overestimated electrically cured compressive strength at later ages. This was because classical maturity values do not account for the greater effect of early age temperature rises on hydration (Saul 1951), nor do they take into account damage caused to the structure of the concrete at these early ages by thermally induced stresses.

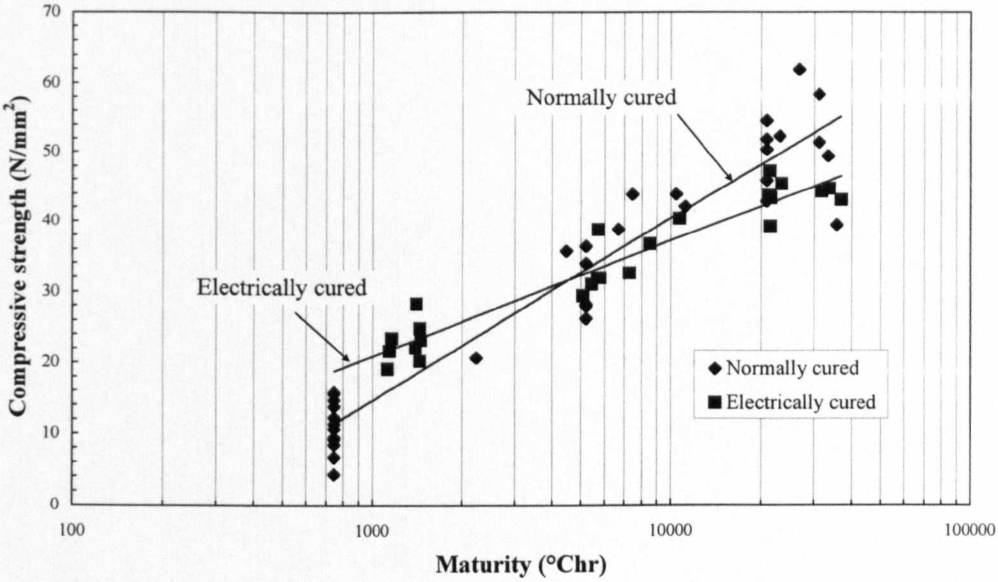

Figure 5.43 - Compressive strength versus maturity (normally and electrically cured)

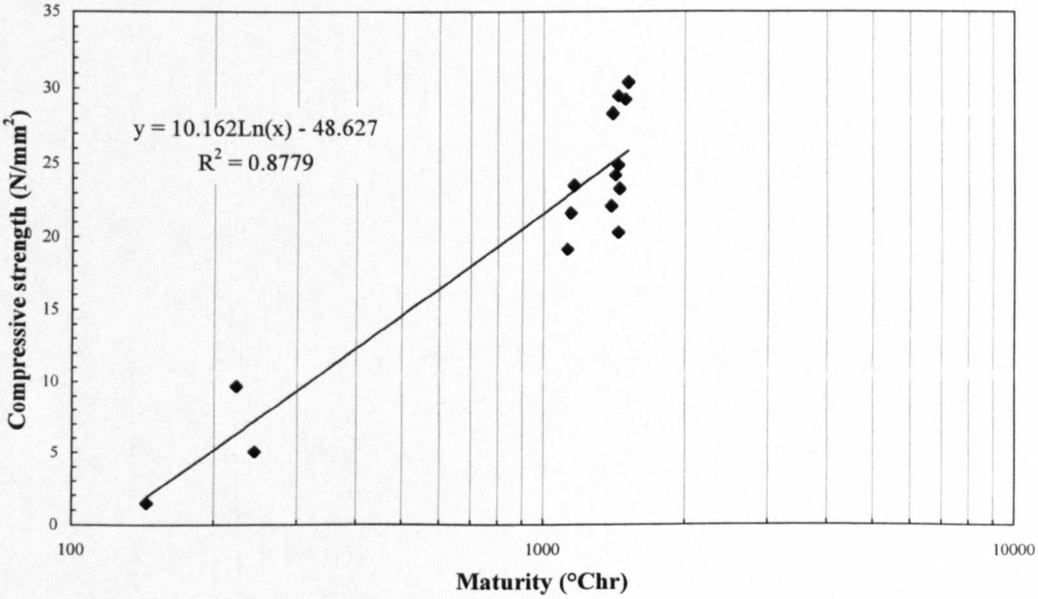

Figure 5.44 - Early age (≤ 1 day) compressive strength versus log maturity

Figure 5.44 shows the early age compressive strength of electrically cured samples of various heating regimes versus maturity. From this it can be seen that compressive strength for the C30 mix followed a logarithmic curve of equation:

$$\text{compressive strength} = 10.162 \times \text{Ln (maturity)} - 48.627 \qquad \text{Eqn. 5.3}$$

The coefficient of determination (R^2) was equal to 0.8779. From this it can be seen that although compressive strength of electrically cured samples did rise with maturity, the variability caused by the effects of temperature at certain times caused a large degree of variability. As such, classical maturity values can only give an indication of the early age compressive strength of electrically cured samples (ASTM C1074).

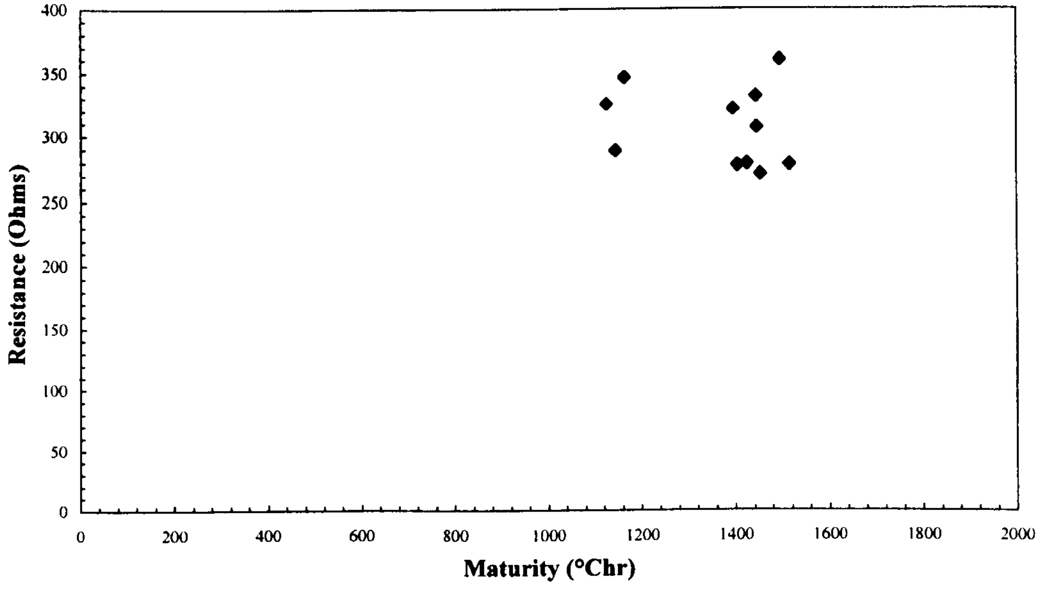

Figure 5.45 - Resistance versus maturity

Figure 5.45 shows the relation between electrical resistance and maturity values for electrically cured samples. From this it can be seen that there appeared to be no correlation between resistance and maturity. This would seem to be a contradiction to previous results, which showed that both resistance and maturity can be used to indicate compressive strength. The reason for the apparent lack of correlation was that all resistance measurements shown were taken at very early ages (1 day) and as such the effectiveness of changes in resistance predicting compressive strength due to hydration progression was reduced.

5.14 Initial Surface Absorption Test

Figure 5.46 shows the Initial Surface Absorption Test (ISAT) (Levitt 1969) results for a 1 stage heating period with a 1 hour delay period after 28 days. This shows that the surface absorption of electrically cured concrete was significantly lower than the equivalent normally cured specimen. This would seem to be in contradiction with the comparatively lower compressive strength results for the electrically cured specimens and may have been due to the refinement of the capillary pores during heating, thus causing a reduction in moisture flow.

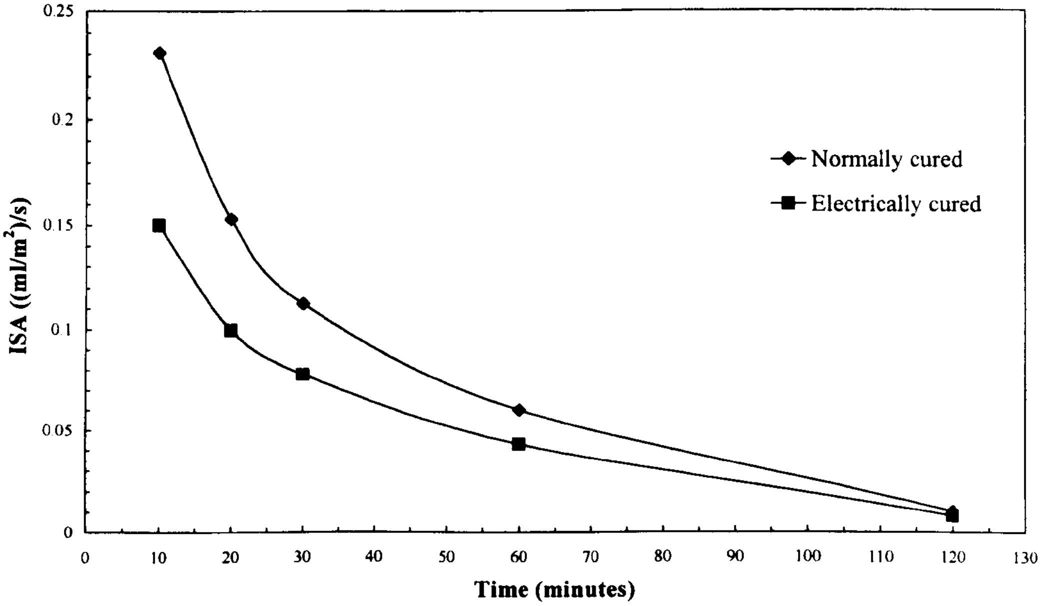

Figure 5.46 - ISA of electrically (3 hour delay, 40°C/hr rise, 80°C maximum) and normally cured samples at 28 days

Other aspects of durability, especially Delayed Ettringite Formation (Lawrence 1993), have not been considered at the present time. This is an important area of concern with the relatively high temperatures used in the presented test set-up and needs to be fully evaluated before larger scale practical applications can be developed.

Figure 5.47 shows the relationship between compressive strength at various ages and the 10 minute surface absorption result (ISA 10) for both electrically and normally cured samples for a C30 (10-30mm slump) mix design. From this it can be seen that the normally cured samples followed the expected relationship of a lowering of compressive strength as ISA 10 increased (Dhir and Byars 1991). This was due to compressive strength being related to the degree of hydration experienced. As hydration progressed, the capillary pore structure of normally cured samples gradually filled with hydration products, thus reducing the absorption of water.

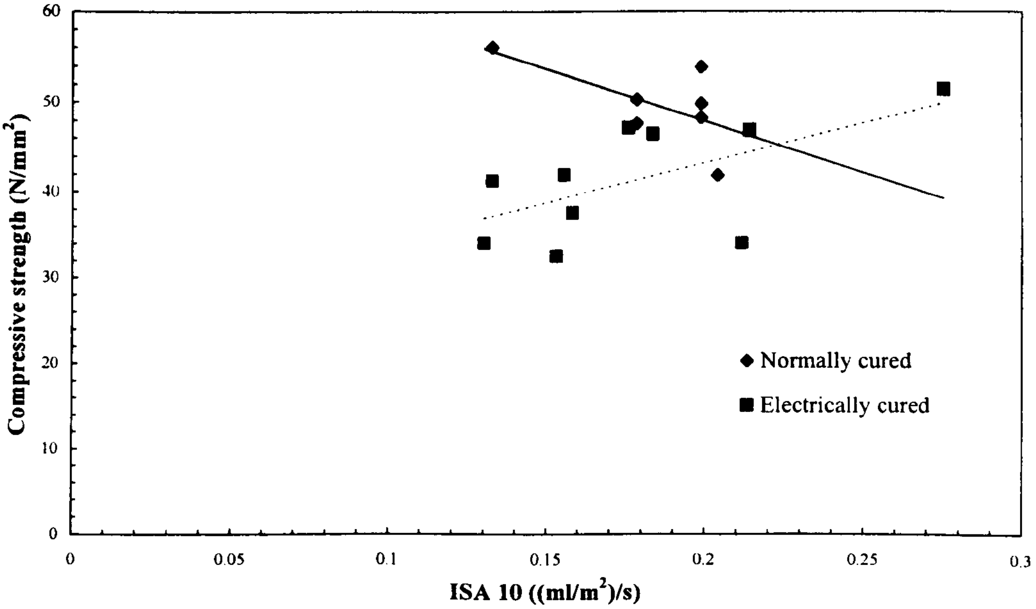

Figure 5.47 - Compressive strength versus ISA 10

The electrically cured samples, however, follow the opposite trend (dotted line). This is because the ISA readings were all been taken at relatively high ages (>28 days). Electrically cured samples that achieved high long-term compressive strengths generally had relatively little damage to the structure of the cement matrix due to the thermal stresses induced. The electrically cured samples that attained relatively low long-term compressive strengths were generally the ones with a shorter initial delay period (1-2 hours) or high maximum temperature, thus incurring a larger amount of cement matrix damage by the thermally induced stresses. The damage occurred because the cement matrix was still fluid when heating occurred and as such had little inherent strength to counteract the induced stresses. For these mixes, the stresses induced a refinement of the capillary pore structure, thus reducing the amount of water flow through the hardened concrete.

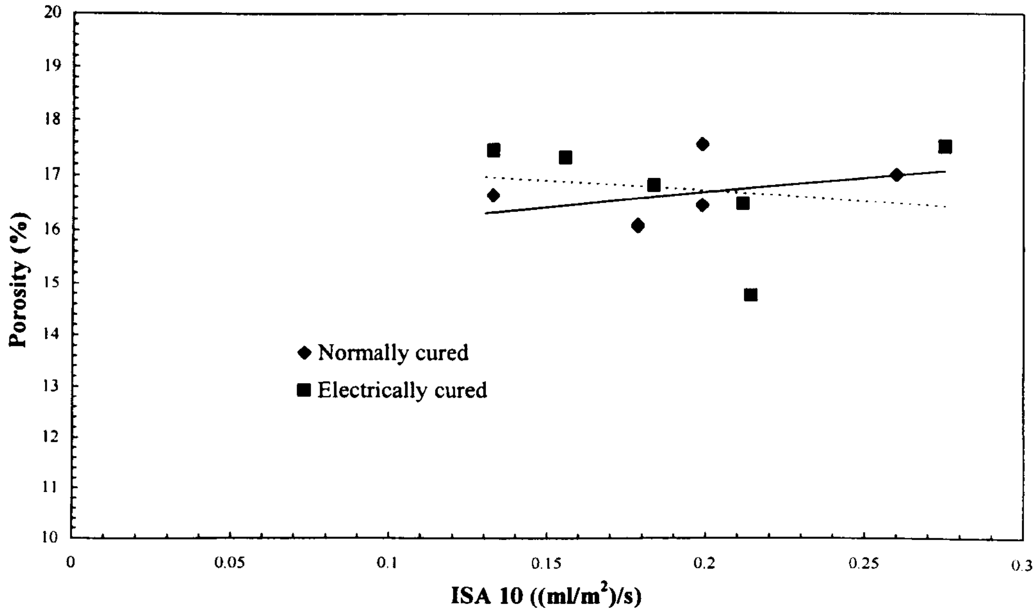

Figure 5.48 - Porosity versus ISA 10

Figure 5.48 shows the relationship between porosity and ISA 10 for electrically and normally cured samples. From this it can be seen that relatively small changes in porosity occurred. However, even with this small range there appeared to be opposite trends in the electrically (dotted line) and normally (solid line) cured relationships. The normally cured samples appeared to have the expected increase in ISA 10 value as porosity increased (Neville 1988). This was to be expected, as with increased voids, surface absorption of water should increase. The electrically cured samples followed the opposite trend with ISA 10 increased as porosity decreased. This may have been because, with short delay periods (before the initial set), air bubbles trapped within the mix were free to expand from the increase in temperature. This caused an increase in porosity but also corresponded with a refinement of capillary pores, thus reducing ISA 10. If heating occurred at later delay periods (after the initial set), then the air bubbles were constrained from expanding, thus causing expansion stresses, which in turn created microcracks which can readily increase the network of connected pores and capillaries.

5.15 Porosity

Figure 5.49 shows the change in porosity over time for C30 mixes of both electrically and normally cured samples.

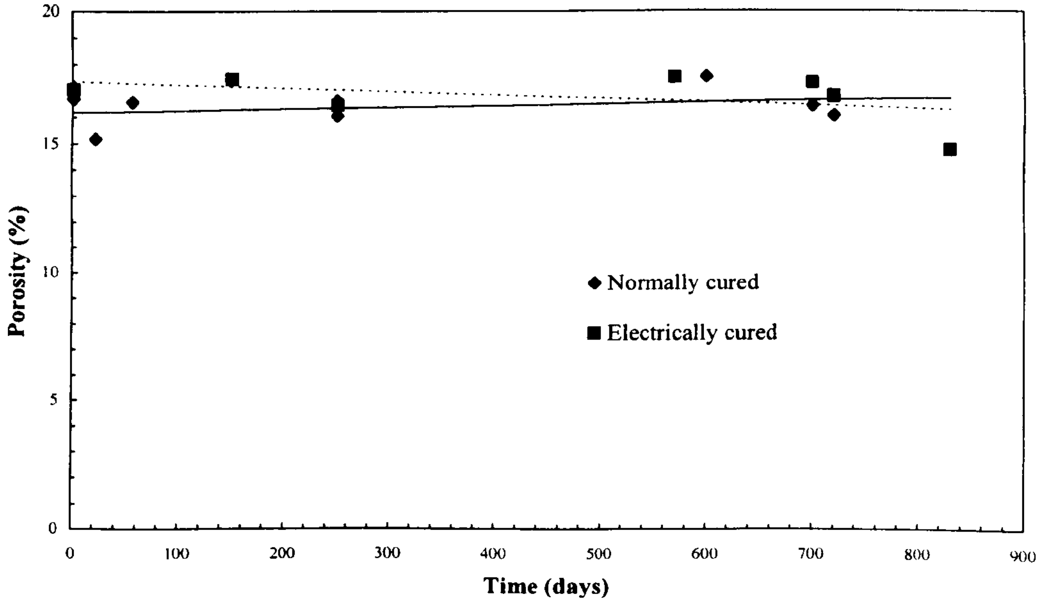

Figure 5.49 - Porosity versus time for electrically and normally cured samples

The electrically cured samples (dotted line) were of various heating regimes. Both showed little difference in porosity up to periods of 800 days and remained around 16-18% porosity. This shows that porosity, as measured by the experimental set-up used (DeVenny and Khalaf 1998), was not adversely affected by the use of electrical curing.

Figure 5.50 shows the relationship between porosity and compressive strength for a C30 mix for electrically and normally cured mixes. The electrically cured samples were of various heating regimes. From this, it can be seen that porosity did not appear to change significantly with changes in compressive strength. Both electrically (dotted line) and normally (solid line) cured mixes had a porosity of 14-17% over the range of compressive strengths tested. This was likely to be due to the age of the samples (>28 days) by which time porosity changes little.

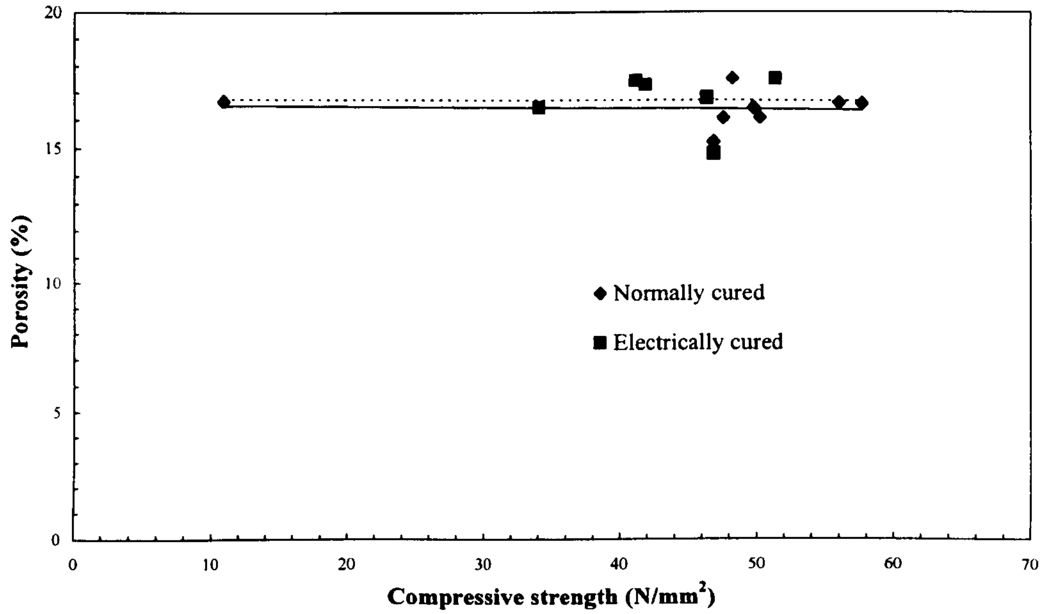

Figure 5.50 – Porosity versus compressive strength for electrically and normally cured samples

5.16 Density

Figure 5.51 shows the changes in density over time for electrically and normally cured concrete samples. The electrically cured samples were of various heating regimes. From this it can be seen that both normally (solid line) and electrically (dotted line) cured samples had virtually identical densities (2300-2400kg/m^3) over periods up to 800 days. This was clearly due to the fact that identical mixes (C30) were used in both circumstances and although electrical curing does inevitably lead to initial water losses, in the long-term this did not affect density.

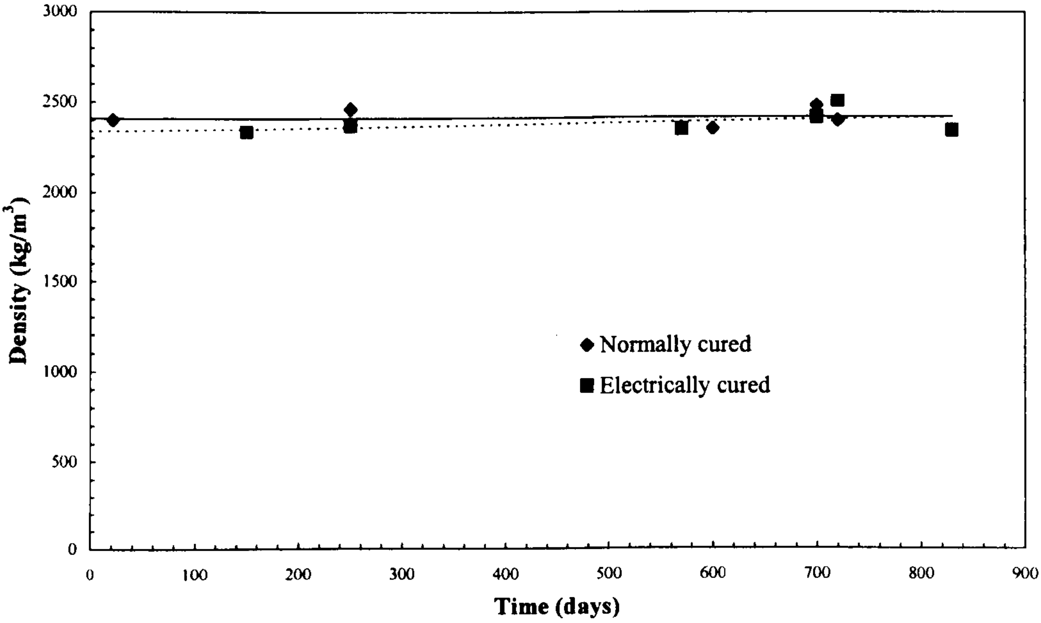

Figure 5.51 - Density versus time for electrically and normally cured samples

5.17 Water Absorption

Figure 5.52 shows the water absorption of electrically (dotted line) and normally (solid line) cured samples at various ages. The electrically cured samples were of various heating regimes and all mixes are designed as C30 (slump 10-30mm). From this it can be seen that water absorption remained fairly constant over the long-term, though a slight reduction was apparent. This was to be expected, as with the time scale used (up to 800 days), relatively little reduction in pore volume occured.

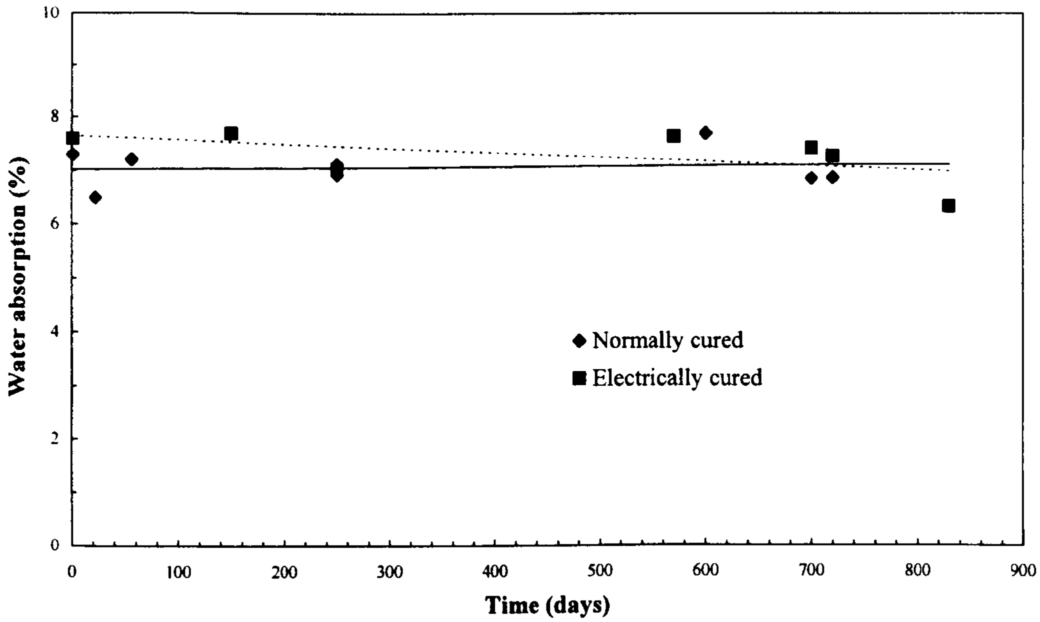

Figure 5.52 – Water absorption versus time for normally and electrically cured samples

5.18 Temperature Profiles

A full list of temperatures for a 150x150x150mm cube heated to 80°C at a rate of 40°C/hr with a delay period of 3 hours over various ages can be seen in Table 5.1.

Figure 5.53 shows the colour temperature scale used for defining the temperatures in Figures 5.57, 5.54, 7.16 and 7.27. Each colour represents a range of 1°C.

Figure 5.54 shows a graphical representation of Table 5.1. From this it can be seen that prior to heating, the temperature distribution was approximately uniform (±1°C) across the sample at each time period selected. At 60 minutes, it can be seen that the exterior regions were at a higher temperature than the internal regions. This was due to the ambient temperature (20°C) being higher than the temperature of the concrete. This allowed heat conduction through the electrode plates into the concrete but did not occur at the base due to the cubes sitting on 50mm thick expanded polystyrene which acted as a thermal barrier to the lower ambient temperatures. The overall temperature did rise from approximately 12°C immediately after mixing to 17°C prior to heating. This was due to exothermic hydration reactions occurring as the concrete cures normally (Neville 1988).

Table 5.1 - Temperature of 150mm cube at various ages

Time after gauging with water (min)	**Sensor number (from Chapter 3)**									
	1	**2**	**3**	**4**	**5**	**6**	**7**	**8**	**9**	**10**
0	12.4	12.4	12.4	12.4	12.5	12.5	12.5	12.5	12.5	12.4
60	14.1	13.8	13.7	13.7	13.7	14.3	14.0	14.0	13.9	13.9
160	17.1	17.1	17.0	17.0	17.0	17.2	17.2	17.3	17.2	17.2
180	17.5	17.5	17.5	17.5	17.4	17.6	17.7	17.7	17.7	17.6
195	27.5	27.4	27.1	26.1	24.7	27.2	27.6	27.1	26.3	24.7
210	37.5	37.6	37.1	35.4	33.1	36.5	37.3	36.6	35.2	32.6
225	47.5	48.6	47.9	45.7	42.6	46.0	47.7	46.9	45.1	41.6
240	57.5	60.1	59.6	56.9	53.2	55.5	58.7	58.0	56.0	51.7
255	67.5	71.9	71.6	68.8	64.5	64.9	69.6	69.1	67.2	62.5
270	77.5	84.3	84.4	81.8	77.2	75.0	82.0	81.8	80.1	75.0
274	80.0	88.0	88.0	85.5	81.0	77.3	84.6	84.9	83.3	78.2
285	75.6	84.4	85.7	84.7	81.6	73.2	81.1	82.5	82.1	78.7
300	72.0	80.7	82.7	83.3	81.9	70.6	78.0	80.4	81.1	79.6
510	52.0	54.1	54.1	53.4	52.2	51.4	53.1	54.2	52.6	51.6
1550	26.0	26.2	26.2	26.3	26.3	26.0	26.1	26.2	26.3	26.3
1710	25.7	25.8	25.8	25.9	25.9	25.4	25.8	25.8	25.9	25.9
	Sensor number									
	11	**12**	**13**	**14**	**15**	**16**	**17**	**18**	**19**	**20**
0	12.4	12.5	12.5	12.5	12.6	12.6	12.7	12.7	12.8	12.7
60	15.0	14.6	14.4	14.4	14.4	15.3	15.1	15.1	15.0	15.0
160	17.6	17.5	17.5	17.5	17.4	17.8	17.9	17.9	17.9	17.8
180	18.1	17.9	17.9	17.9	17.9	18.1	18.2	18.3	18.3	18.1
195	27.2	27.2	26.8	25.6	24.3	26.6	26.7	27.1	27.4	25.1
210	34.9	36.0	35.3	33.6	31.4	33.7	34.4	34.9	35.0	31.8
225	43.6	45.6	44.9	42.9	39.9	41.5	43.4	43.7	43.5	39.8
240	52.7	56.0	55.3	52.8	49.3	50.0	53.1	53.8	53.6	48.6
255	61.8	66.4	66.0	63.2	59.3	58.9	63.3	64.4	64.2	58.1
270	71.2	77.6	77.6	75.0	70.8	67.9	74.0	75.2	75.8	69.0
274	73.8	80.7	80.9	78.1	73.8	70.6	77.1	79.1	79.3	72.3
285	70.3	77.7	79.3	78.2	75.3	67.7	75.5	77.4	77.2	73.0
300	68.4	75.5	77.9	77.9	76.4	66.3	74.1	76.5	76.9	74.1
510	51.4	52.2	52.2	51.6	50.7	50.1	51.5	51.9	51.9	51.2
1550	25.9	26	26.1	26.1	26.1	25.8	26.0	26.1	26.1	26.1
1710	25.5	25.7	25.7	25.7	25.7	25.5	25.6	25.7	25.6	25.7

During heating, it can be seen that the maximum temperature was always in the central region and 'sank' as the temperature increased. This may have been due to the increased insulation on the bottom surface. As the temperature increased, a greater amount of heat was lost through the exposed upper surface, thus requiring higher currents to attain the same rate of heating which increased the temperature gradients and thus increased the temperature of the lower, better insulated regions.

After heating, the cube gradually cooled, with a greater rate of cooling and higher temperature gradients at the surface which was due to the thermal insulating properties of the plastic mould. After 1 day the temperature had again reached an approximate equilibrium condition across the section at a temperature of 25°C.

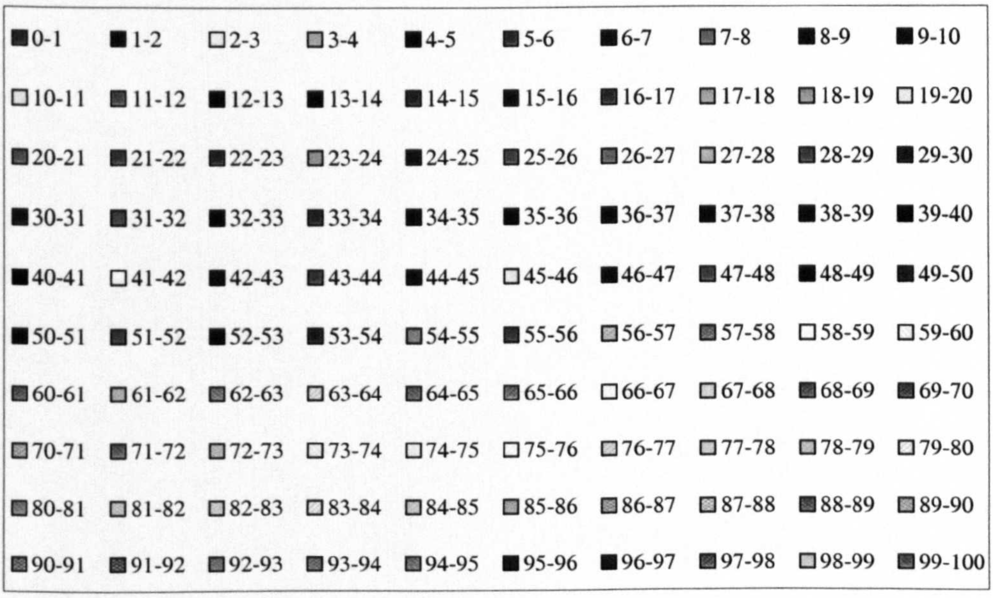

■0-1	■1-2	□2-3	▨3-4	■4-5	■5-6	■6-7	▨7-8	■8-9	■9-10
□10-11	■11-12	■12-13	■13-14	■14-15	■15-16	■16-17	▨17-18	▨18-19	□19-20
▨20-21	■21-22	■22-23	▨23-24	■24-25	■25-26	▨26-27	▨27-28	■28-29	■29-30
■30-31	■31-32	■32-33	■33-34	■34-35	■35-36	■36-37	■37-38	■38-39	■39-40
■40-41	□41-42	■42-43	■43-44	■44-45	□45-46	■46-47	■47-48	■48-49	■49-50
■50-51	■51-52	■52-53	■53-54	▨54-55	■55-56	▨56-57	▨57-58	□58-59	□59-60
▨60-61	▨61-62	▨62-63	□63-64	▨64-65	▨65-66	□66-67	□67-68	▨68-69	▨69-70
▨70-71	▨71-72	▨72-73	□73-74	□74-75	□75-76	▨76-77	□77-78	▨78-79	□79-80
▨80-81	▨81-82	□82-83	□83-84	□84-85	▨85-86	▨86-87	▨87-88	▨88-89	▨89-90
▨90-91	▨91-92	▨92-93	▨93-94	▨94-95	■95-96	■96-97	▨97-98	□98-99	▨99-100

Figure 5.53 –Temperature (°C) colour key to Figures 5.54, 5.57, 7.16 and 7.27

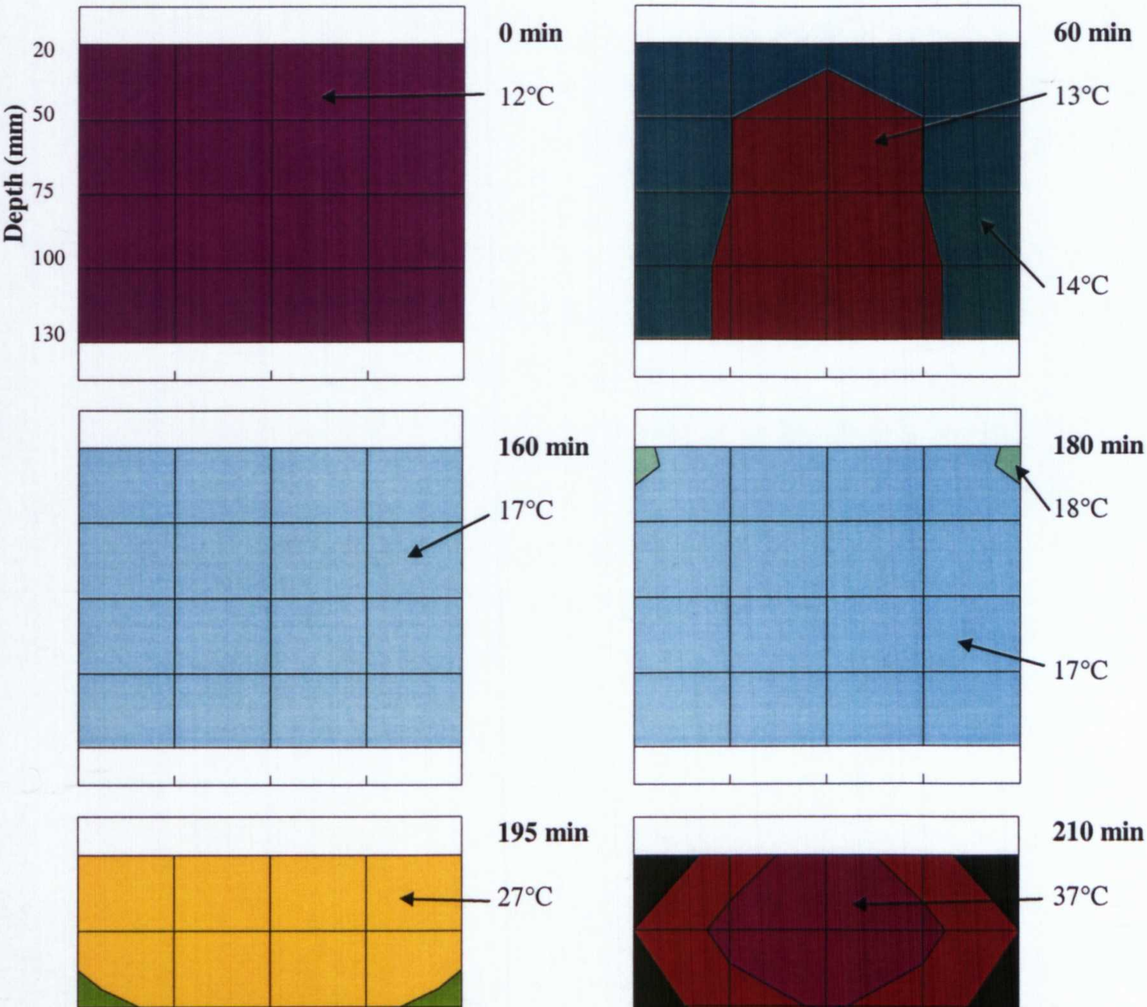

Figure 5.54 – Temperature cross section centrally perpendicular to electrodes

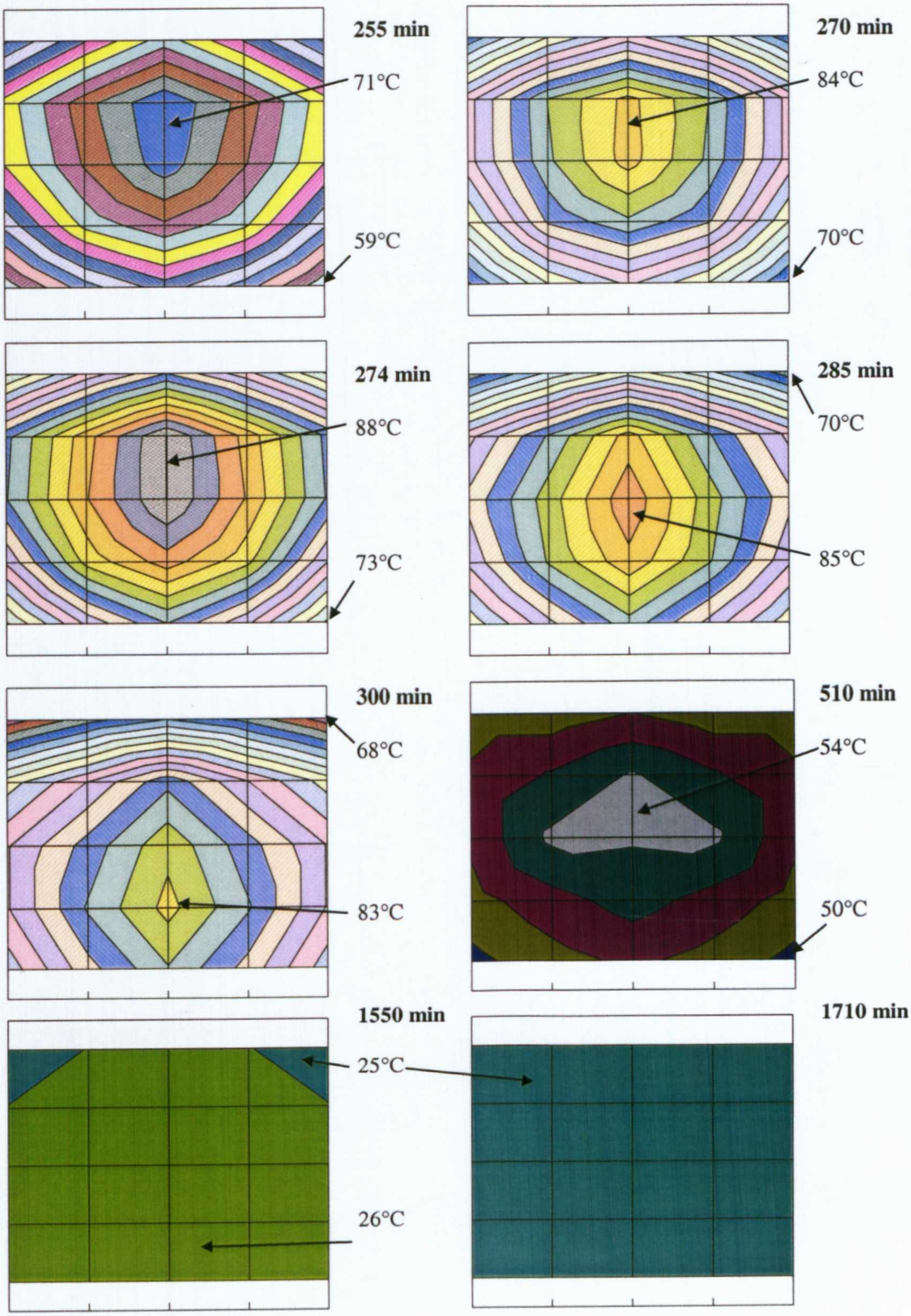

Figure 5.54 – Temperature cross section centrally perpendicular to electrodes (continued)

Figure 5.55 shows the temperature profile along the beam (400x100x100m) at various ages during heating (3 hour delay, 40°C/hr rise to a maximum of 80°C) at a depth of 50mm. From this it can be seen that the central region, at the end of heating, attained a higher temperature (89.6°C) than the outside regions (81.3°C) and the point where the temperature datum was calculated from (80°C at a depth of 20mm). This was due to the relatively small temperature gradients that were present laterally (Figure 5.57) and the relatively high thermal insulating properties of concrete which resulted in the highest temperature being within the internal central region (Bazant and Kaplan 1996).

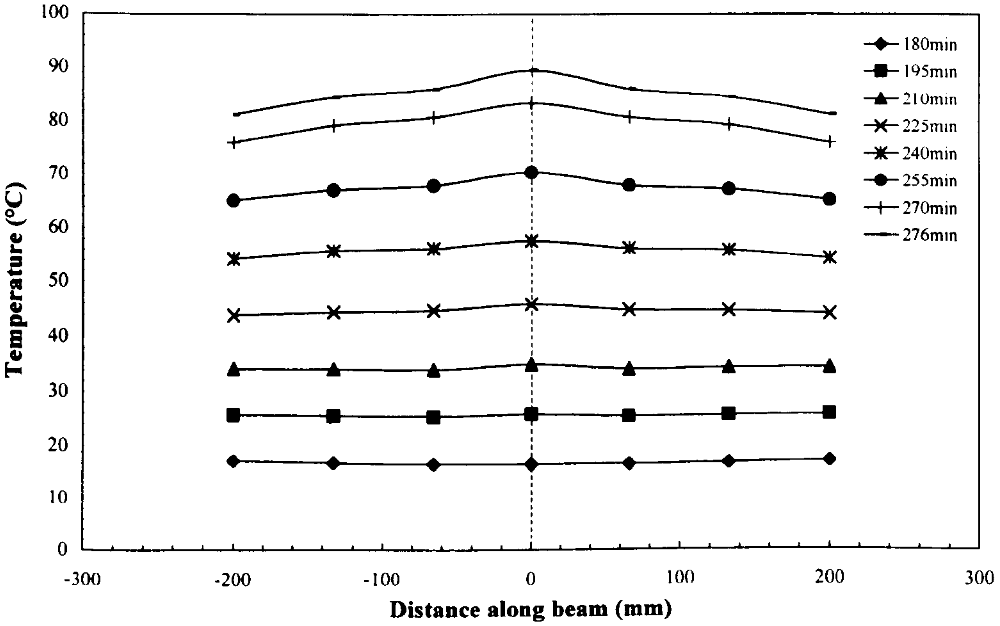

Figure 5.55 – Temperature distribution along centre of beam at a depth of 50mm (3 hour delay, 40°C/hr rise, 80°C maximum)

Figure 5.56 shows the temperature profile along the beam (400x100x100mm) at various ages during heating at a depth of 20mm. From this it can be seen that the maximum temperature at the surface was always lower than the temperature within the concrete (Figure 5.55). This was due to the vertical temperature gradients inherent within electrically heated concrete that show the transfer of heat from the 'hot' core to the relatively cool ambient atmosphere. It can also be seen that immediately prior to heating

(180 minutes), the outside regions were at a slightly higher temperature than the inner regions. This was again due to the influence of the ambient temperature, which at this time was higher than the concrete temperature and as such heated up the concrete from the outside inwards.

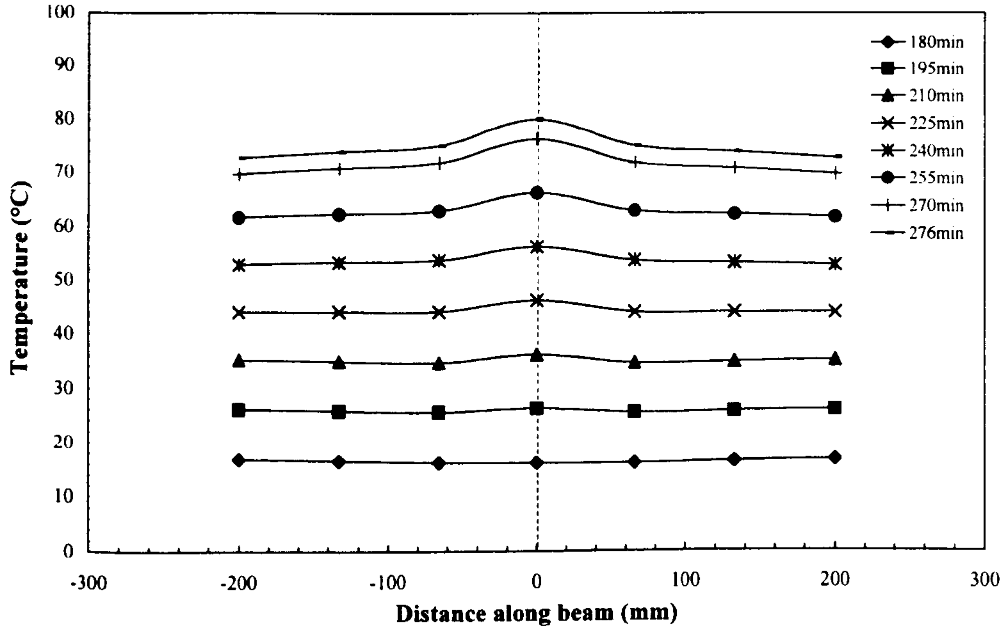

Figure 5.56 – Temperature distribution along centre of beam at a depth of 20mm (3 hour delay, 40°C/hr rise, 80°C maximum)

A full list of temperatures for a beam (400x100x100mm) with a 3 hour delay period heated to 80°C at a 40°C/hr rise over various ages can be seen in Table 5.2. From this it can be seen that the temperature gradients present increased during heating, especially near the upper surface, but decreased after heating ended until after 1 day where a uniform temperature of 25°C (±1°C) was attained.

Table 5.2 - Temperature of beam (400x100x100mm) at various ages

Time after gauging (min)	Sensor number (from Chapter 3)									
	1	**2**	**3**	**4**	**5**	**6**	**7**	**8**	**9**	**10**
180	16.3	16.5	16.6	16.8	16.9	16.3	16.4	16.6	16.8	17.1
195	26.3	26.25	25.8	25.5	25.1	25.6	25.7	25.4	25.0	24.4
210	36.3	36.0	35.0	34.1	33.2	34.8	34.9	34.1	33.1	31.7
225	46.3	46.5	45.8	45.0	44.0	44.2	45.0	44.7	43.6	42.1
240	56.3	57.5	57.7	57.0	56.1	53.8	55.9	56.2	55.3	53.8
255	66.3	69.1	70.5	70.4	69.5	62.9	66.7	68.0	67.8	66.6
270	76.3	79.8	83.4	84.0	83.9	71.9	78.0	80.8	81.8	81.2
276	80.0	84.6	89.6	91.2	90.1	75.1	82.4	86.1	88.0	88.1
285	76.9	82.8	88.1	90.2	90.4	73.0	80.5	84.9	87.7	88.6
300	72.6	77.4	82.8	85.6	86.6	69.3	75.7	80.3	83.8	85.8
345	66.9	69.4	72.4	74.1	74.5	65.1	68.3	70.8	72.9	74.3
1375	25.5	25.6	25.6	25.6	25.6	25.5	25.6	25.6	25.7	25.7
1515	25.2	25.3	25.3	25.3	25.3	25.2	25.3	25.3	25.3	25.3
	Sensor number									
	11	**12**	**13**	**14**	**15**	**16**	**17**	**18**	**19**	**20**
180	16.6	16.6	16.8	16.9	17.1	16.9	17.1	17.2	17.3	17.4
195	25.8	25.8	25.6	25.0	24.7	26.1	26.1	25.8	25.4	24.8
210	35.1	35.0	34.3	33.1	32.3	35.3	35.0	34.4	33.5	32.2
225	44.2	44.9	44.5	43.5	42.5	44.1	44.4	44.0	43.1	41.8
240	53.4	55.4	55.8	55.0	54.0	52.9	54.2	54.3	53.6	52.0
255	62.3	65.8	67.2	67.2	66.5	61.7	64.2	65.3	64.9	63.3
270	70.8	76.3	79.3	80.6	80.4	69.7	73.8	76.1	76.6	75.1
276	74.0	80.6	84.5	86.7	86.9	72.8	78.0	81.3	82.0	81.2
285	71.9	78.6	83.0	86.0	86.6	69.7	75.0	78.5	80.1	79.5
300	68.0	73.6	78.1	81.9	83.4	65.7	70.2	73.8	75.9	76.0
345	63.2	65.9	68.3	70.7	71.6	60.1	62.1	64.1	65.2	65.1
1375	25.4	25.4	25.5	25.5	25.5	25.3	25.3	25.4	25.4	25.4
1515	25.1	25.2	25.2	25.2	25.2	25.1	25.1	25.1	25.1	25.1

Figure 5.57 shows a cross section temperature map of the beam (400x100x100mm) at the end of heating (276 minutes). From this it can be seen that the central point of maximum temperature has ‘sunk’ in a similar manner to Figure 5.54 to a point 20mm above the bottom surface. It can also be seen that the maximum temperature gradients occurred vertically near to the upper surface with comparatively small temperature gradients appearing laterally. This was due to the current flowing uniformly laterally throughout the beam and the relatively low ambient temperature present.

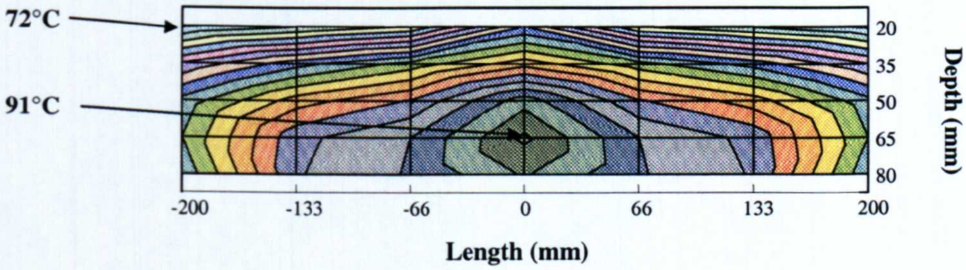

Figure 5.57 - Cross section temperature map of the beam at the end of heating (276 minutes) (3 hour delay, 40°C/hr rise, 80°C maximum)

5.19 Scanning Electron Microscopy

Three curing regimes were chosen for analysis by the use of a Scanning Electron Microscope (SEM). These were:

1. Normally cured (sample A)
2. DEC: 3 hour delay, 40°C/hr rise, maximum 60°C (sample B)
3. DEC: 2 hour delay, 40°C/hr rise, maximum 80°C (sample C)

After 1 day all samples were transferred to a water tank in accordance with the procedures stated in Chapter 3.

5.19.1 Microstructure

Figures 5.58, 5.59 and 5.60 show scanning electron microscope images of concrete samples cured according to curing regime A, B and C respectively, 1 day after mixing. All samples showed a dense microstructure associated with the development of C-S-H gel. At 1 day normally cured concrete showed a more uniform microstructure as seen in Figure 5.58 than the concrete heated to 80°C maximum (Figure 5.60) which exhibited a much coarser microstructure. Sample C also showed a much higher level of hydration than the other two samples with ettringite crystals clearly visible in Figure 5.60 as filamentous structures growing out from the cement grains into the water filled pores.

This was the result of the high maximum temperatures applied, which accelerated the initial hydration process.

Sample A showed a higher degree of unhydrated cement particles at 1 day than samples B and C which implied that elevated temperature speeds up the hydration process of OPC cement.

At higher magnifications, shown in Figures 5.61 and 5.62 respectively, it can be seen that the ettringite crystals have become larger in sample C when compared to sample A. The larger needle-like crystals (ettringite) form at this stage of hydration as a result of the reaction of C_3A and gypsum in solution. It can also be seen that the microstructure in sample C is coarser and more obviously crystalline in form.

At 28 days there is little difference in the microstructure of all of the concrete samples scanned as shown in Figures 5.63, 5.64 and 5.65, but the heat cured samples appeared less uniform. The C-S-H gel had grown during the continued hydration and had became more compact in all samples. There was also a relative scarcity of residual unhydrated cement grains in all samples showing that a high proportion of the possible hydration had taken place by 28 days in both electrically and normally cured samples.

5.19.2 Pore structure

It can be observed from Figures 5.58, 5.60 and 5.66 respectively that all samples had a visible pore structure. The larger pores of the concrete samples can be seen to be of the hollow shell type, but the samples also contained capillary pores and spaces.

It appears from Figures 5.58, 5.60 and 5.66 that sample C had a coarser pore structure than sample B, which in turn had a coarser pore structure than sample A. Heat curing has generally been reported to result in a coarsening of the pore structure (Kjellsen 1995).

At 28 days, the pores in the normally cured concrete appeared to be less numerous (Figure 5.63) but the pores in the heated concrete (Figures 5.64 and 5.67) appeared to be more apparent but not as extensive as at 1 day. The high decrease in porosity of sample A was because during hydration calcium ions may have diffused into the previously formed hollow shells and precipitated as calcium hydroxide (portlandite). This was likely not to have happened in the heat cured concrete due to the greater maturity at the time of exposure to water curing which may have caused less production of portlandite to fill the hollow shells.

5.19.3 Microcracking

Figures 5.63, 5.67, 5.68 and 5.69 respectively show images of the concrete samples in the aggregate/concrete matrix region. All of the concrete samples exhibited microcracking in the bulk cement paste and especially at the aggregate/cement matrix zone. However, the extent of the cracks at the aggregate interface was found to be more prevalent in the mixes that had been electrically cured. No apparent differences in crack number and width seemed apparent between the electrically cured mixes. This may have been due to the small sample sizes available. This kind of microcracking is likely to be caused as a result of the differential expansion of the aggregate during heat curing and the subsequent cooling period.

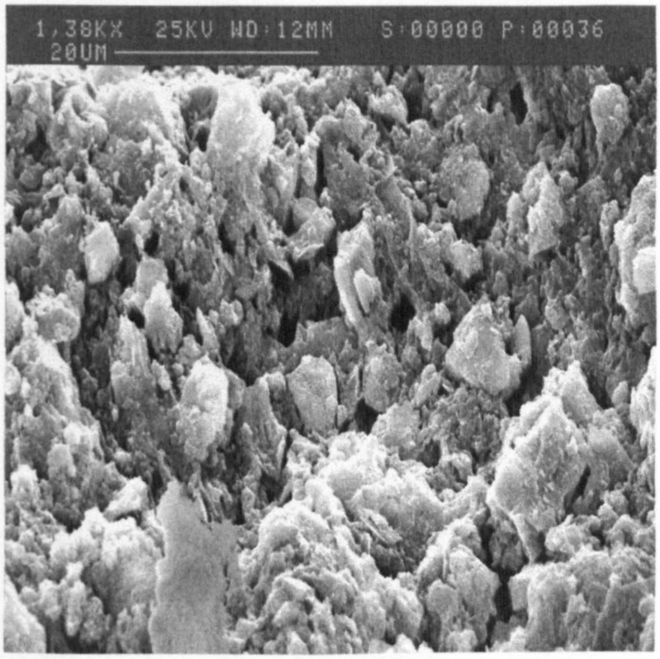

Figure 5.58 – 1380X magnification of normally cured concrete (1 day)

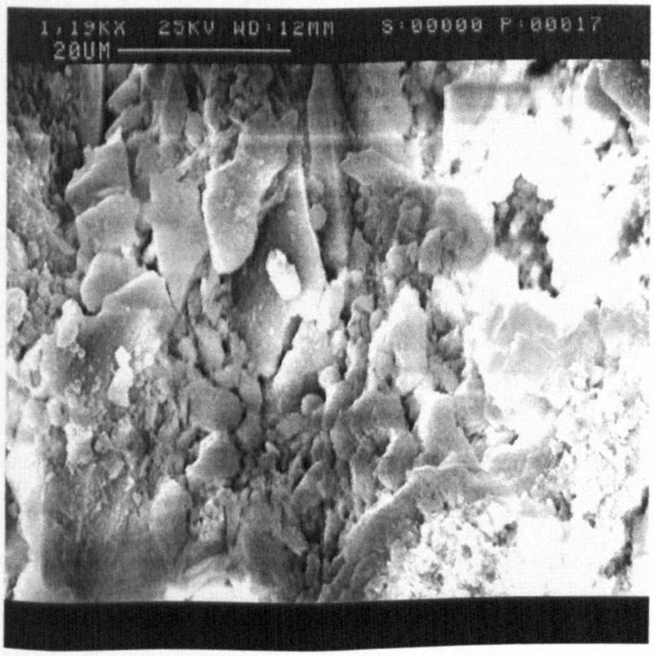

Figure 5.59 – 1190X magnification of electrically cured (40°C/hr rise, 60°C maximum, 3 hour delay) concrete (1 day)

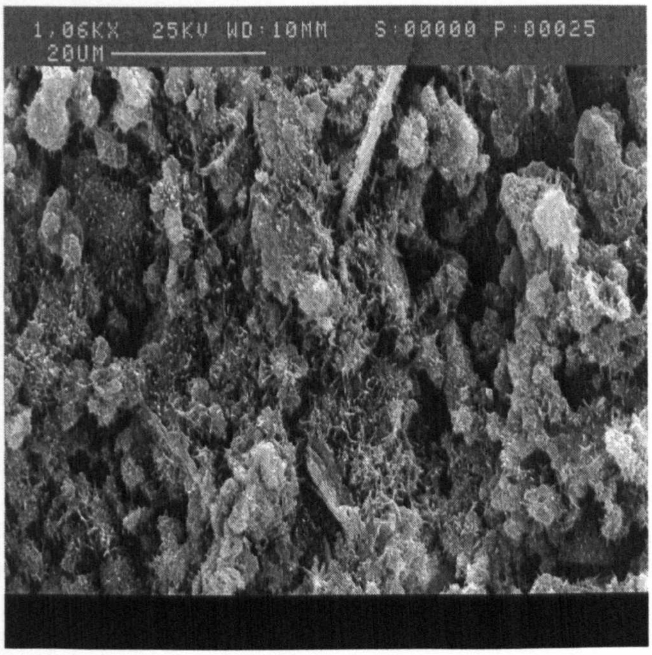

Figure 5.60 – 1060X magnification of electrically cured (40°C/hr rise, 80°C maximum, 2 hour delay) concrete (1 day)

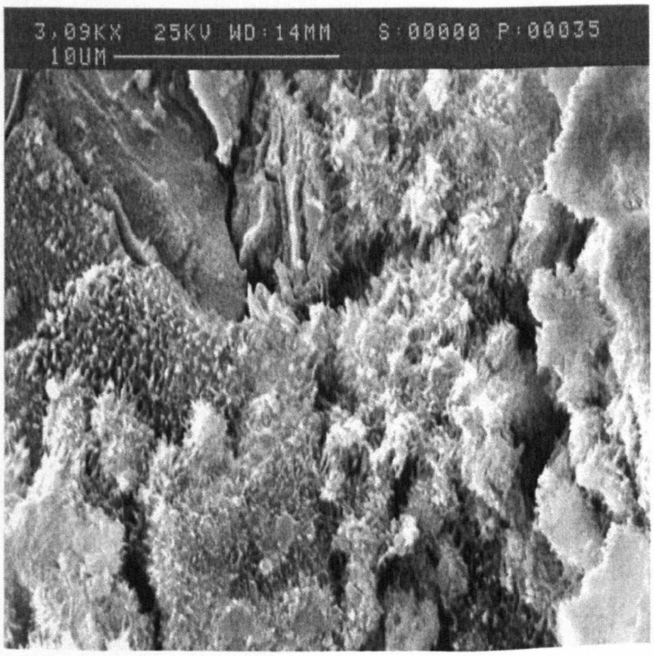

Figure 5.61 – 3090X magnification of normally cured concrete (1 day)

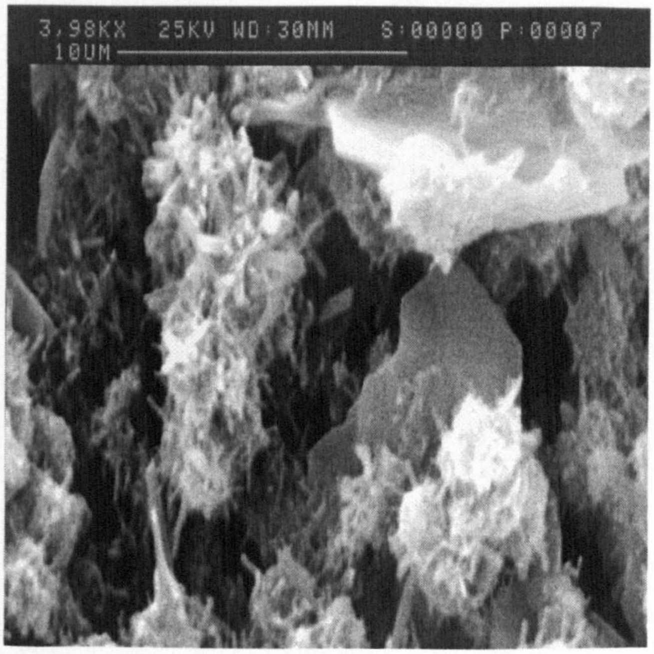

Figure 5.62 – 3980X magnification of electrically cured (40°C/hr rise, 80°C maximum, 2 hour delay) concrete (1 day)

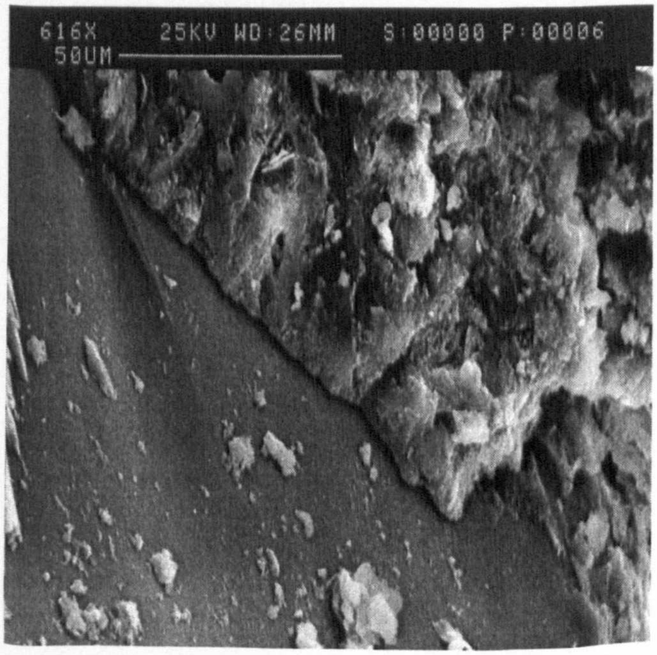

Figure 5.63 – 616X magnification of normally cured concrete (28 days)

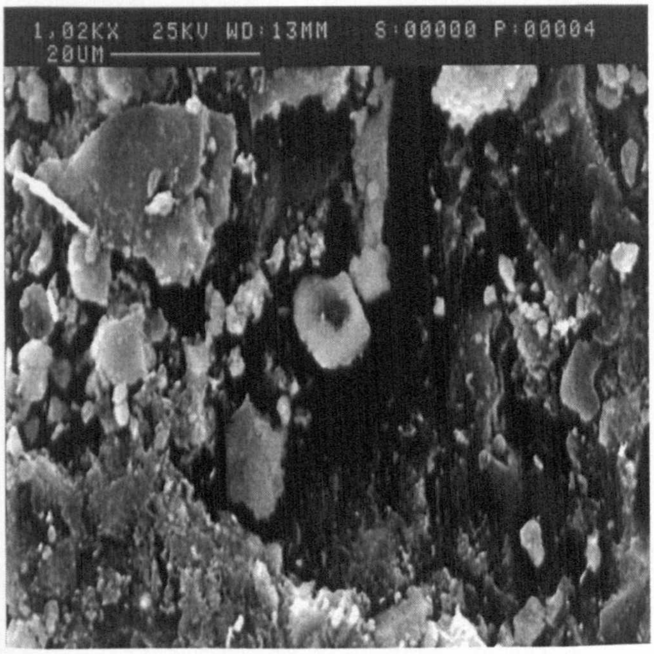

Figure 5.64 – 1020X magnification of electrically cured (40°C/hr rise, 60°C maximum, 3 hour delay) concrete (28 days)

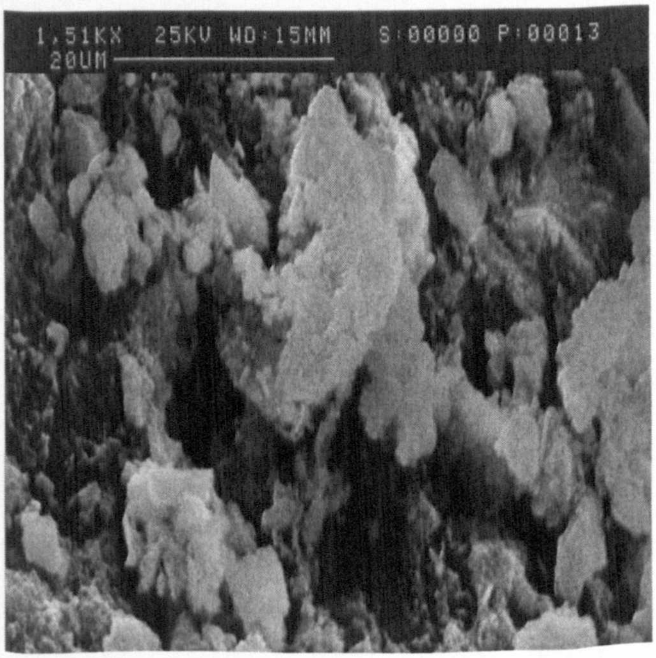

Figure 5.65 – 1510X magnification of electrically cured (40°C/hr rise, 80°C maximum, 2 hour delay) concrete (28 days)

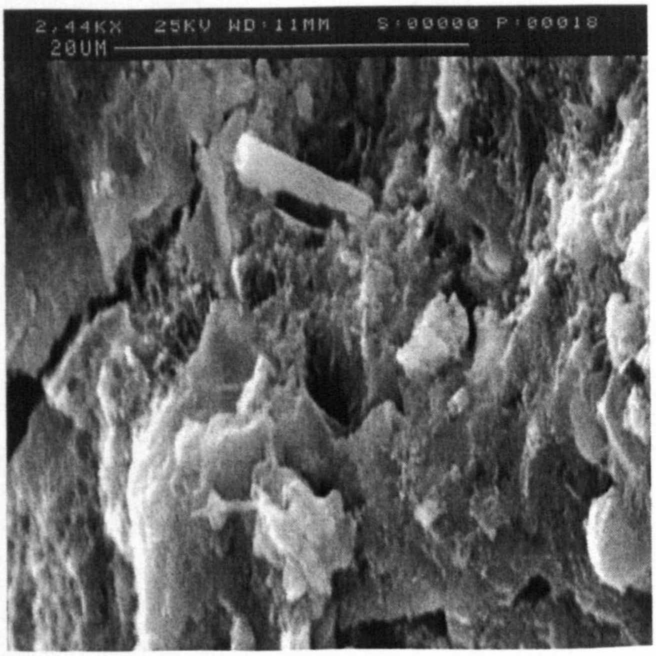

Figure 5.66 – 2440X magnification of electrically cured (40°C/hr rise, 60°C maximum, 3 hour delay) concrete (1 day)

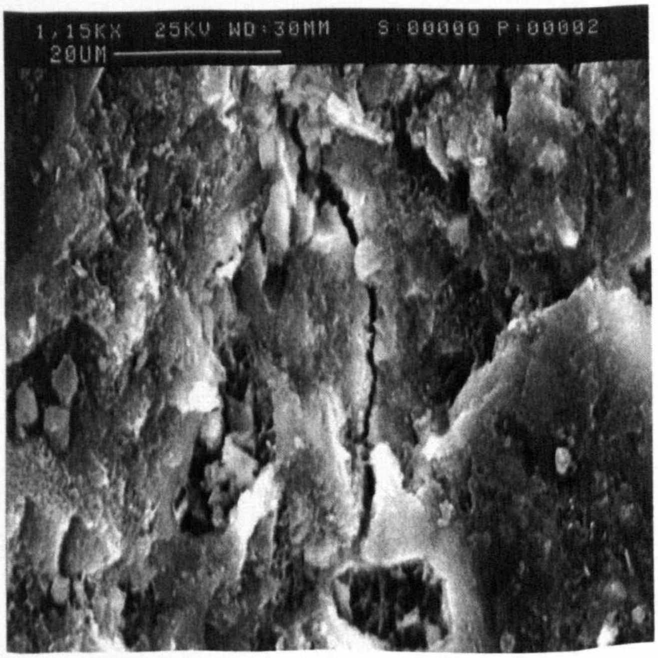

Figure 5.67 – 1150X magnification of electrically cured (40°C/hr rise, 80°C maximum, 2 hour delay) concrete (28 days)

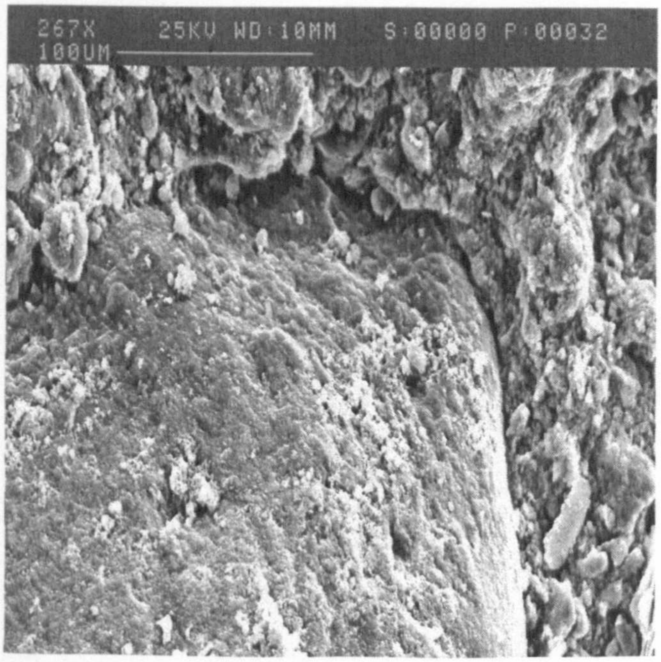

Figure 5.68 – 267X magnification of normally cured concrete (1 day)

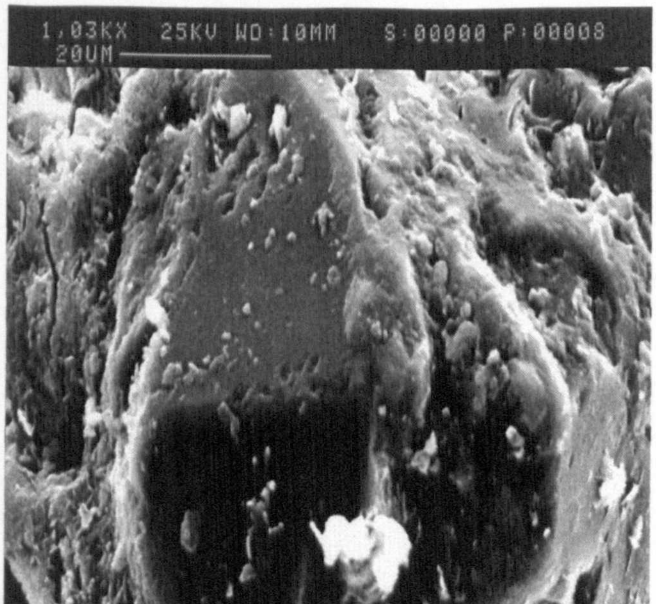

Figure 5.69 – 1030X magnification of electrically cured (40°C/hr rise, 60°C maximum, 3 hour delay) concrete (28 days)

5.20 Conclusions

1. The effect of removing the 50mm thick polystyrene cover was found to cause a reduction in initial strength of DEC concrete when compared to normally cured concrete. This was likely to be due to excessive moisture loss from the concrete and higher internal temperature gradients necessary to maintain the same heating regime as for DEC concrete cured under insulation cover.

2. The resistance of uncovered samples was found to attain a higher value than covered samples up to 1800 minutes after mixing, but after that time covered samples were found to have a higher resistance. This was likely to be due to the loss of moisture from the uncovered samples which initially increased resistance but reduced further hydration due to desiccation.

3. At 1 day, all samples of varying W/C ratios cured using DEC attained a higher compressive strength than normally cured samples. The increase became slightly higher with increases in W/C ratios but this effect was not apparent for compressive strength at 3 days.

4. The effect of W/C ratio on resistance values was seen to be apparent, with higher W/C ratios producing lower resistance values.

5. The compressive strength of normally cured concrete at 24 hours was attained using DEC in 4 hours and compressive strengths of up to 26N/mm^2 were readily achievable using DEC after 1 day.

6. Short delay periods (1 hour) tended to give higher initial compressive strengths, but reduced long-term compressive strengths when compared to longer delay periods (4 hours). The reduction in long-term compressive strengths was likely to be due to increased microcracking in the short delay period samples which reduce long-term strength. The greatest long-term compressive strength (≥28 days) was found to

occur when heating commenced at 3 hours after mixing. This was due to high early age compressive strengths combining with limited microstructural damage to produce relatively high long-term compressive strengths.

7. DEC concrete attained a large proportion (up to 71%) of its 28 day compressive strength within 1 day.

8. The temperature corrected resistance (Equation 2.2) at the end of heating was found to be dependent on the delay period chosen prior to heating.

9. For equivalent mixes and heating regimes, a higher maximum temperature produced higher 1 day compressive strengths but lower long-term (≥28 day) compressive strengths. This was likely to be due to increased thermomechanical damage and moisture loss at the higher temperatures.

10. DEC was found to be applicable to different mix designs with initial (≤1 day) increases but long-term (≥28 days) reductions in compressive strength, when compared to equivalent normally cured concrete. This was found to be the case for both high slump and high strength mixes.

11. The resistance at 1 day was not found to be proportional to compressive strength but at 3 days a logarithmic relationship was found to exist.

12. Concrete was found to behave as a dielectric with a lower apparent resistance at higher temperatures. This implies that concrete temperature should be closely monitored if resistance is to be used in predicting the progress of hydration.

13. Significantly different short and long-term compressive strengths were found to be achievable using a 2 stage heating rise with a high/low heating regime producing higher short-term (1 day) but lower long-term (28 days) compressive strengths.

14. It was found that the effect of the delay period prior to heating of the 2 stage samples effected the short and long-term compressive strength in a similar manner to 1 stage heating regimes.

15. The splitting tensile strength of concrete cured using DEC was found to follow a similar trend as compressive strength of DEC cubes with higher initial temperatures causing increased initial tensile strength but lower long-term tensile strength.

16. It was found that, when compared to normally cured samples, the DEC splitting tensile strength had a lower percentage tensile strength increase at 1 day and a higher percentage tensile strength loss at 28 days than the equivalently cured DEC compressive strength tests. This was likely to be due to microcracks acting as stress concentrators during tensile loading.

17. Flexural tensile strength was found to act in a similar manner to splitting tensile strength.

18. Saul's maturity values were found to be more accurate in determining the compressive strength of normally cured samples than electrically cured samples. Maturity values were also found to underestimate the compressive strength of electrically cured samples at early ages and overestimate compressive strength at later ages.

19. There was found to be no direct relationship between resistance and maturity for the samples tested.

20. Durability of concrete (as measured by ISAT) did not appear to be adversely effected when using DEC. This was likely to be due to the refinement of capillary pores during heating.

21. It was found that ISA 10 values were related to compressive strength. For normally cured samples, ISA 10 values increased as compressive strength decreased, but for electrically cured samples, the opposite was true. This was due to low compressive strengths in electrically cured concrete being related to microstructural damage which also caused capillary pores to alter, thus reducing water absorption.

22. Porosity, density and water absorption was found to be similar for both electrically and normally cured samples.

23. Natural temperature rises within the concrete were apparent prior to heating and were due to exothermic hydration reactions.

24. Temperature gradients increased during heating and also the maximum temperature within the electrically heated (150x150x150mm) cubes and (400x100x100mm) beams were in the central region with minimum temperatures immediately adjacent to the exposed concrete surface.

25. Within the (400x100x100mm) beams, larger temperature gradients were seen to occur vertically (parallel to the electrodes) than laterally (perpendicular to the electrodes). This was thought to be due to the thermal insulating properties of the concrete and mould and the relatively low ambient temperatures.

26. Using a scanning electron microscope (SEM), both normally and electrically cured samples were found to exhibit a dense microstructure associated with C-S-H formation at all ages, but electrically cured samples tended to have a less uniform structure with coarser pores being more prevalent.

27. Results show that higher concentrations and lengths of ettringite were found after 1 day in electrically cured samples.

28. The microstructure at 28 days appeared to be similar for normally and electrically cured samples with little unhydrated cement present.

29. All samples have a degree of aggregate/cement matrix fracturing, but the electrically cured samples were found to have wider, more numerous aggregate/cement matrix cracking. No differences in the degree of this cracking could be found between different heating regimes used to electrically cure samples. The increased cracking was thought to be caused by differential thermal expansion during initial heat curing.

Chapter 6 - DIRECT ELECTRIC CURING OF CONCRETE CONTAINING ADMIXTURES AND ADDITIVES

6.1 Introduction

This chapter provides the results and discussion of an experimental and theoretical investigation of electrically cured concrete containing admixtures and additives. All testing was carried out on 150x150x150mm, C30 (10-30mm slump) cubes unless otherwise specified. These results can be seen in Figures 6.1-6.18.

The mixing, casting, curing and monitoring was implemented in accordance with the experimental procedures stated in Chapter 3.

6.2 Air Entraining Admixture

Figure 6.1 shows the relationship between density at 28 days and ultrasonic pulse velocity (UPV) for both electrically and normally cured concretes containing different amounts of air entrainment. The percentage of air entrainment for each sample can be seen to be adjacent to the data points on Figure 6.1. From this, it can be clearly seen that, as expected, the UPV tended to increase with density. The relationship (density = 253.3 x (UPV) + 1381) between the two properties was not strong (coefficient of determination (R^2) = 0.64) and so only gave an indication of the density for a particular concrete. It also appeared that, for the small range tested, the electrically cured and normally cured samples could be said to have separate linear changes in UPV as density increased. This may have been due to differences in pore structure in the electrically cured samples which locally increased density but did not affect UPV because they did not form a continuous structure within the cement matrix (Patel et al 1994, Kjellsen 1995).

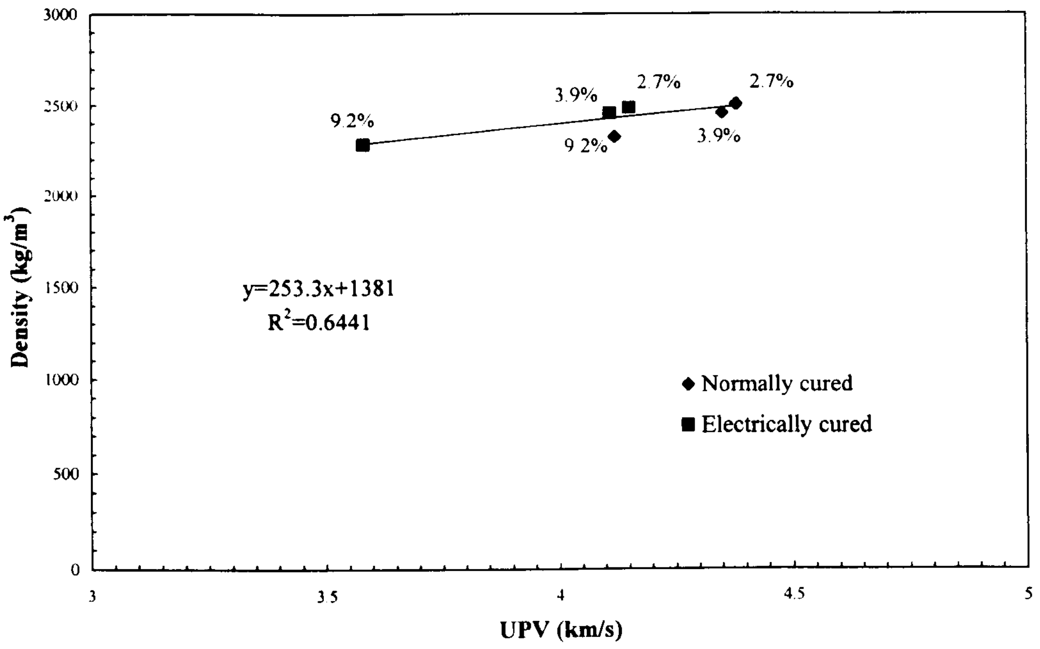

Figure 6.1 – Density versus ultrasonic pulse velocity at 28 days (0.5 hour delay, 40°C/hr rise, 80°C maximum for 4 hours)

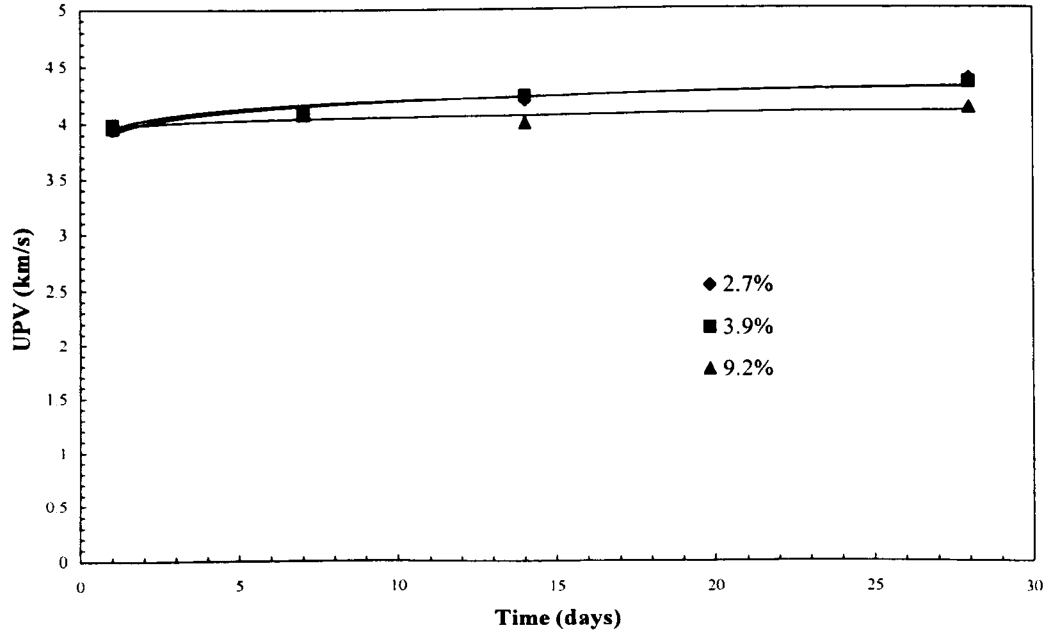

Figure 6.2 – Ultrasonic pulse velocity for normally cured samples of different percentages of air entrainment

Figure 6.2 shows the relationship between UPV and age for normally cured samples of different air entrainment. From this it can be seen that UPV increased slightly over time for the samples tested. This was due to minor increases in density as the concrete continued hydration. It can also be seen that the 9.2% air entrainment mix had a reduced UPV value at later ages. This was due to the relatively large amount of air entrainment reducing density. The difference between the 2.7% and 3.9% air entrainment could not be identified within the accuracy of the instrumentation used (Bungey 1982).

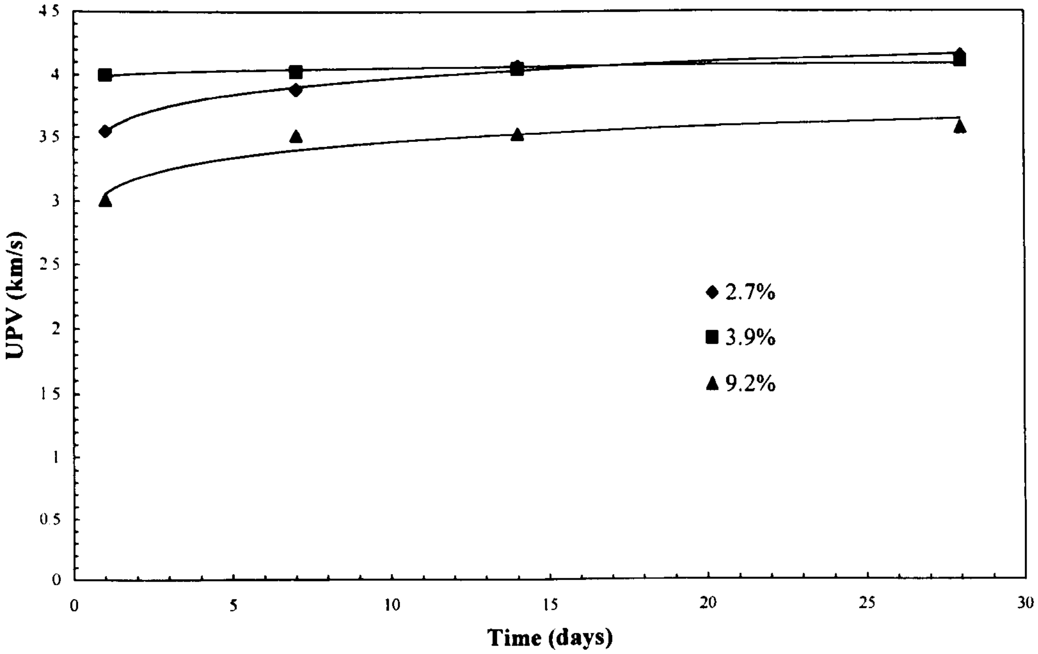

Figure 6.3 – Ultrasonic pulse velocity for electrically (0.5 hour delay, 40°C/hr rise, 80°C maximum for 4 hours) cured samples of different percentages of air entrainment

Figure 6.3 shows the relationship between UPV and age for electrically cured (0.5 hour delay, 40°C/hr rise, 80°C maximum, isothermal period for 4hrs) samples of different air entrainment. This shows a similar trend to Figure 6.2 by which UPV increased over time. The differences between samples appeared far greater than Figure 6.2 with the mix containing no air entraining agent (2.7%) having a lesser UPV than the 3.9% air entrainment. This may have been due to variability of the samples or the difference in microstructure of adding bubbles affecting UPV. The mix containing 9.2% air entrainment had a significantly lower UPV at all ages than any of the other samples. At 28 days it appeared that UPV gave an indication of the proportion of air entrained within the electrically cured mixes.

Figure 6.4 shows the relationship between compressive strength and UPV for electrically and normally cured samples of differing air entrainment and ages. From this it can be seen that a relationship exists (Bungey 1982) between the two variables (compressive strength = $0.007 \times (\mathrm{UPV})^{5.9782}$) for a combination of electrically and normally cured mixes (coefficient of determination (R^2) = 0.8478) with differing air entrainment and ages.

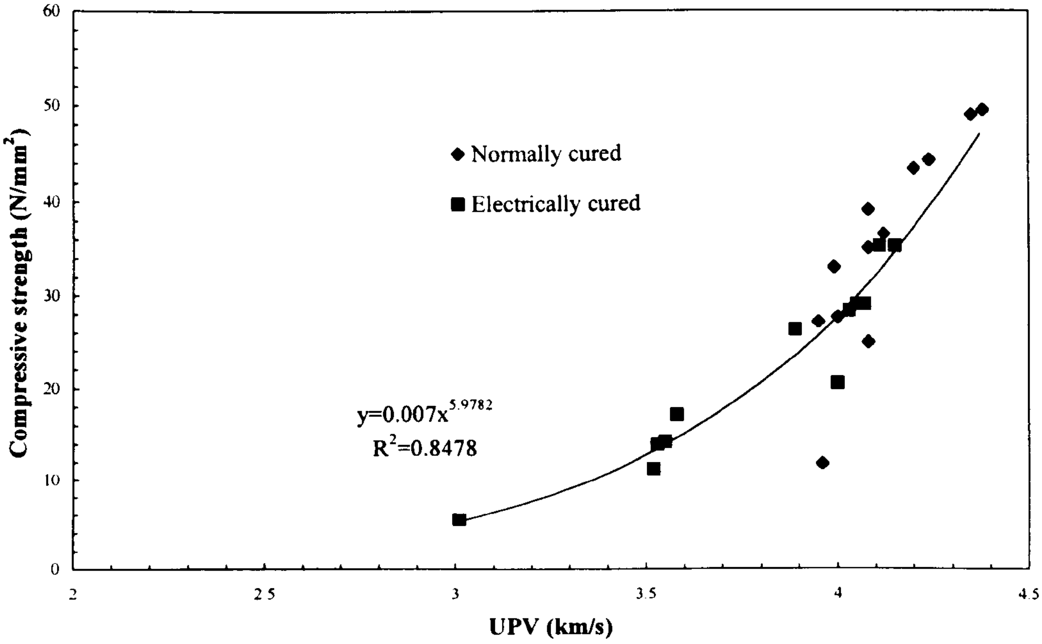

Figure 6.4 – Compressive strength versus ultrasonic pulse velocity for electrically (0.5 hour delay, 40°C/hr rise, 80°C maximum for 4 hours) and normally cured samples

Figure 6.5 shows the relationship between compressive strength and time for normally and electrically (0.5hr delay, 40°C/hr rise, 80°C maximum, isothermal period for 4hrs) cured samples of 9.2% air entrainment. From this it can be seen that the expected increase in initial (1 day) compressive strength did not occur. The electrically cured samples did not attain the normally cured compressive strength at any age and the rate of compressive strength gain over time was proportionally reduced. This was due to the extreme heating regime used together with the large proportion of air entrained. With only 0.5 hours delay prior to heating combined with a 4 hour isothermal period at 80°C, the large percentage of air entrained caused a large amount of damage to the structurally unformed cement matrix. This damage reduced the initial strength and also seriously retarded the subsequent compressive strength development of the electrically cured sample (El Hussein and Abd El Halim 1993).

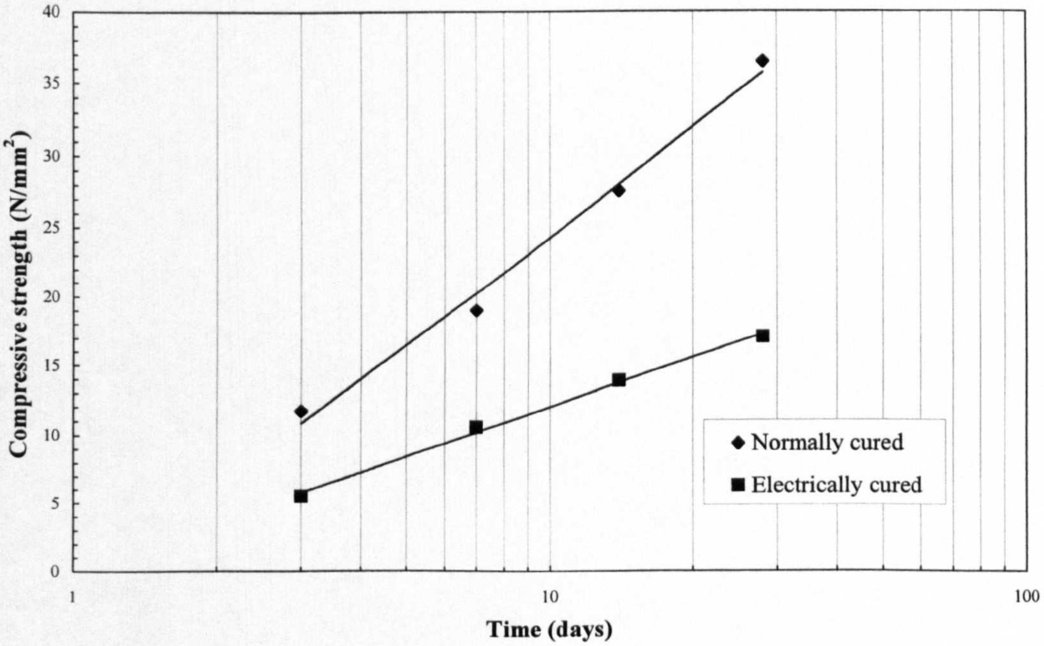

Figure 6.5 – Compressive strength versus time for electrically (0.5hr delay, 40°C/hr rise, 80°C maximum for 4hrs) and normally cured samples with 9.2% air entrainment

Figure 6.6 represents the effect of air entrainment on 28 day compressive strength for normally and electrically (0.5hr delay, 40°C/hr increase, 80°C maximum for 4hrs) cured concrete. From this it can be clearly seen that the 28 day strength of the 3.9% and 9.2% air entrained concrete was lower than the 2.7% concrete. This was because the 2.7% air entrained concrete did not contain an air entraining admixture and the 3.9% and 9.2% mixes were originally designed (Department of the Environment 1992) for an equivalent TMS of 43N/mm^2 with an estimated air entrained content of 2% and 5% respectively. It can be seen that as the percentage of air entrainment increased the difference between the normally and electrically cured concrete became greater. This could be due to increased microcracking in the electrically cured samples as the amount of air entrainment increased. During heating, the air within the entrained bubbles attempts to expand causing tensile stresses in the surrounding cement shell and thus microstructural damage (El Hussein and Abd El Halim 1993).

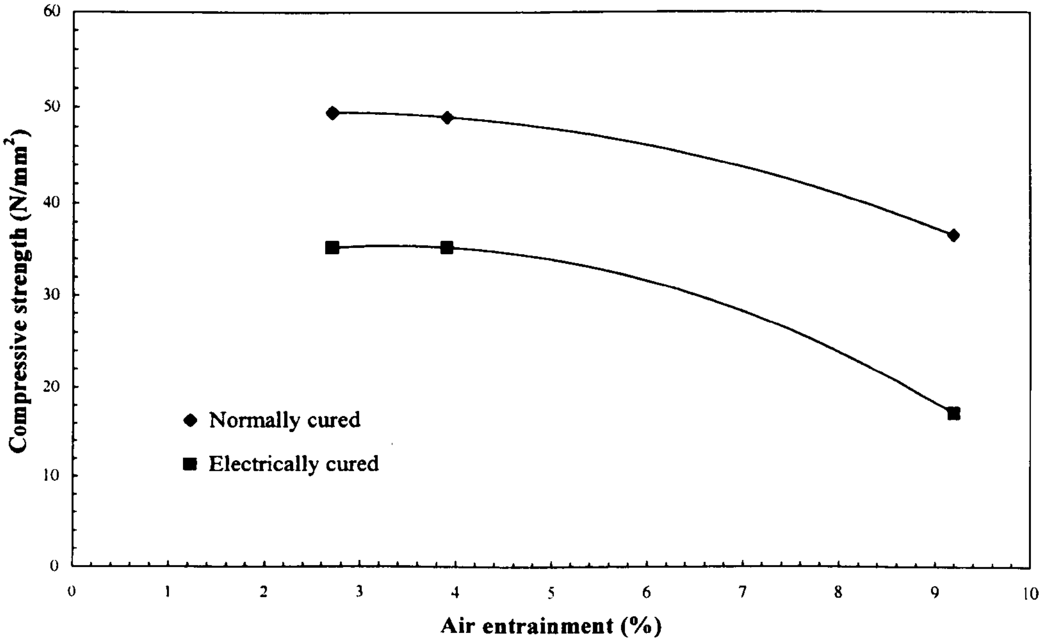

Figure 6.6 – Compressive strength at 28 days versus percentage air entrainment (0.5 hour delay, 40°C/hr rise, 80°C maximum for 4 hours)

Figure 6.7 represents the effect of maximum temperature on electrically cured (3hr delay, 40°C/hr rise) samples with 5.0% air entrainment. From this it can be seen that the mix electrically cured to a maximum of 60°C attained a slightly increased compressive strength at all ages. This was likely to be due to the increased stresses incurred at 80°C. This caused microfractures upon the entrained air cement shells which caused structural damage. This was not apparent in mixes not containing air entrainer (Figure 5.21) and was because the extra damage incurred by the microfracturing of the entrained air bubble shells outweighed the usual gains in hydration (maturity) at early ages.

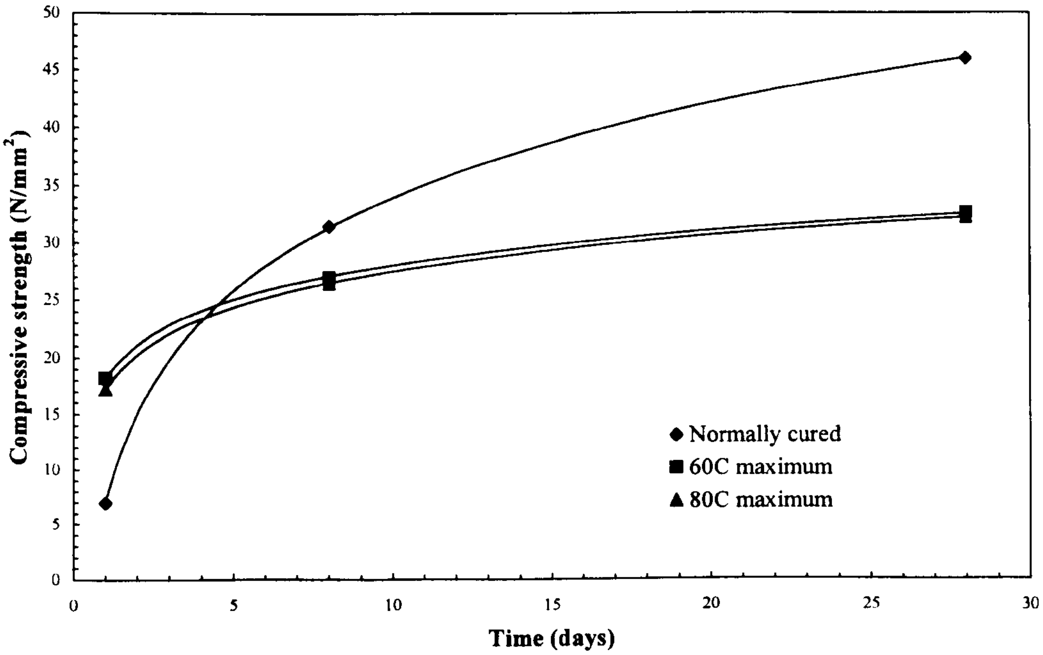

Figure 6.7 – Compressive strength for normally and electrically (3hr delay, 40°C/hr rise) cured samples with 5.0% air entrainment heated to different maximum temperatures

Figure 6.8 shows the effect over time of 5.0% air entrainment for equivalent strength mixes (Department of the Environment 1992) for normally and electrically (3hr delay, 40°C/hr rise, 80°C maximum) cured samples. From this it can be seen that the 5.0% air entrained normally cured samples attained a similar compressive strength at all ages, thus indicating that air entrainment was approximately 5.0%. It can also be seen that the usual degree of compressive strength gain of electrically cured samples did not occur in the air entrained samples. This was due to the effect of the large number of bubbles entrained within the cement matrix. During heating, the air contained within the bubbles attempts to expand, thus causing a far greater degree of structural damage to the surrounding cement matrix. This caused an initial reduction in the expected compressive strength gain and also significantly affected the long-term compressive strength. This shows that extra care and test samples need to be considered when using admixtures combined with DEC to ensure that properties are not assumed on the basis of previous non-admixture mixes (Highways Agency 1998).

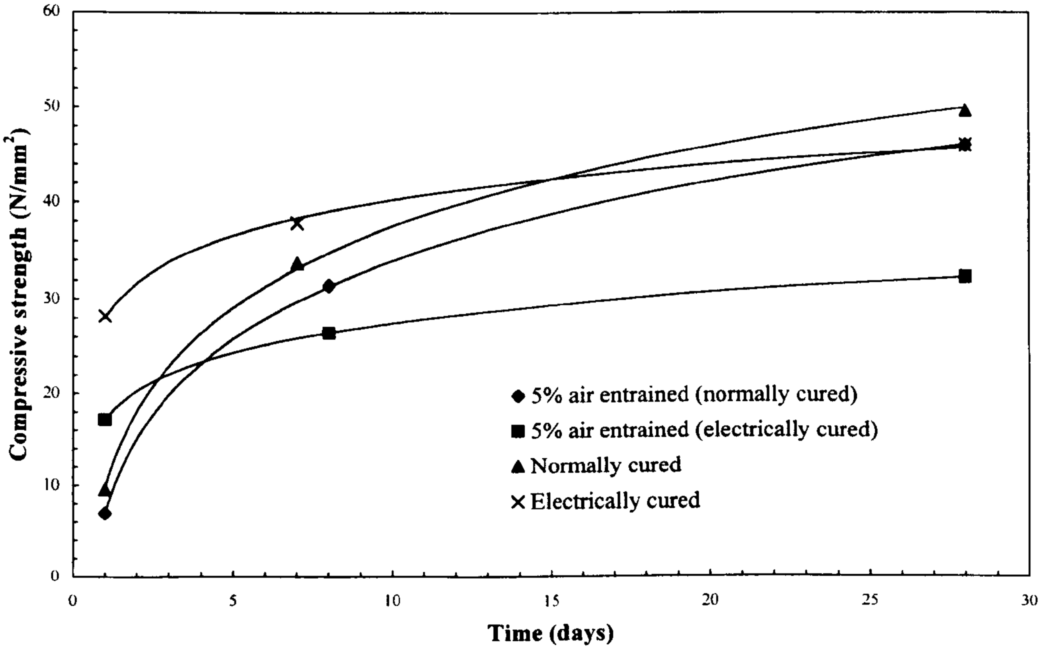

Figure 6.8 – Air entrained (5.0%) compressive strength versus time for electrically (3hr delay, 40°C/hr rise, 80°C maximum) and normally cured samples

Figure 6.9 represents the effect of air entrainment on resistance for electrically (0.5hr delay, 40°C/hr increase, 80°C maximum, isothermal period for 4hrs) cured concrete during heating. From this it can be seen that an initial reduction in resistance was apparent in all samples. This was likely to be due to water absorption by the coarse and fine aggregates after mixing (Khalaf and Wilson 1999) and increases in the level of soluble ions (Ca^{++}, OH^- and SO_4^-) in the pore water during heating.. There appeared to be no direct relationship between the amount of air entrainment and resistance but this apparent effect may have been due to the altered (when compared to water alone) electrical properties of the air entraining agent.

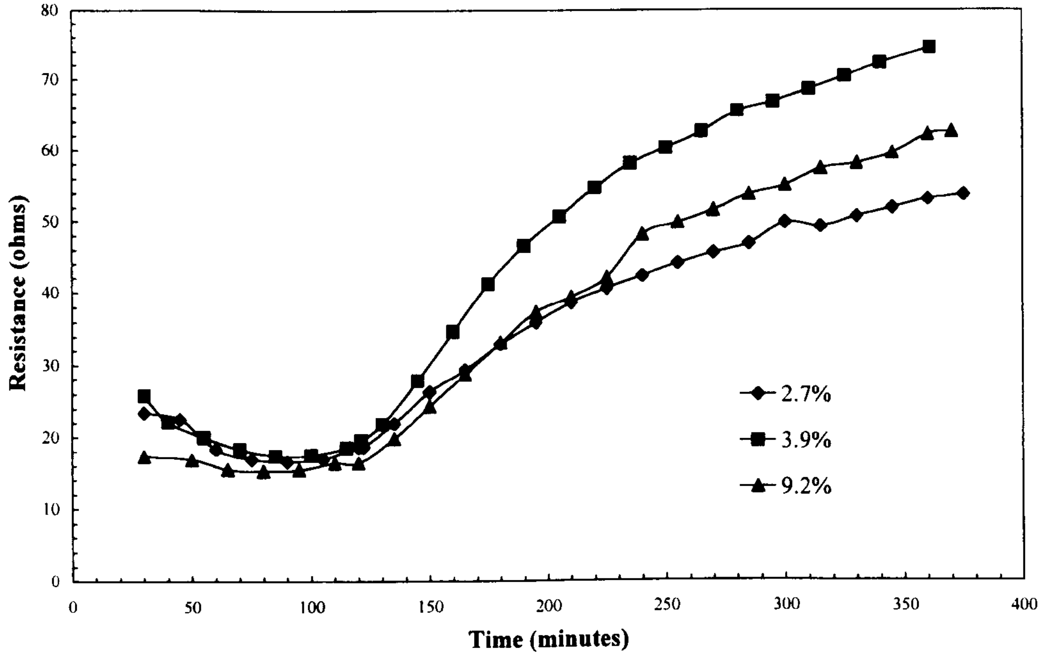

Figure 6.9 – Resistance versus time for different percentages of air entrainment (0.5 hour delay, 40°C/hr rise, 80°C maximum for 4 hours)

Figure 6.10 shows the effect of 5.0% air entrainment on resistance during (3hr delay, 40°C/hr rise, 60°C maximum) and after heating. It can be seen that the mix containing air entrainment had a higher resistance value at all ages. This was likely to be due to the larger proportion of voids within the mix that dry out during hydration, thus causing localised pockets of high resistance and thus increasing overall resistance. Both air entrained and non-air entrained samples showed the expected initial reduction in resistance associated with the absorption of water into the aggregates within the mix (Khalaf and Wilson 1999) and increases in the level of soluble ions in the pore water.

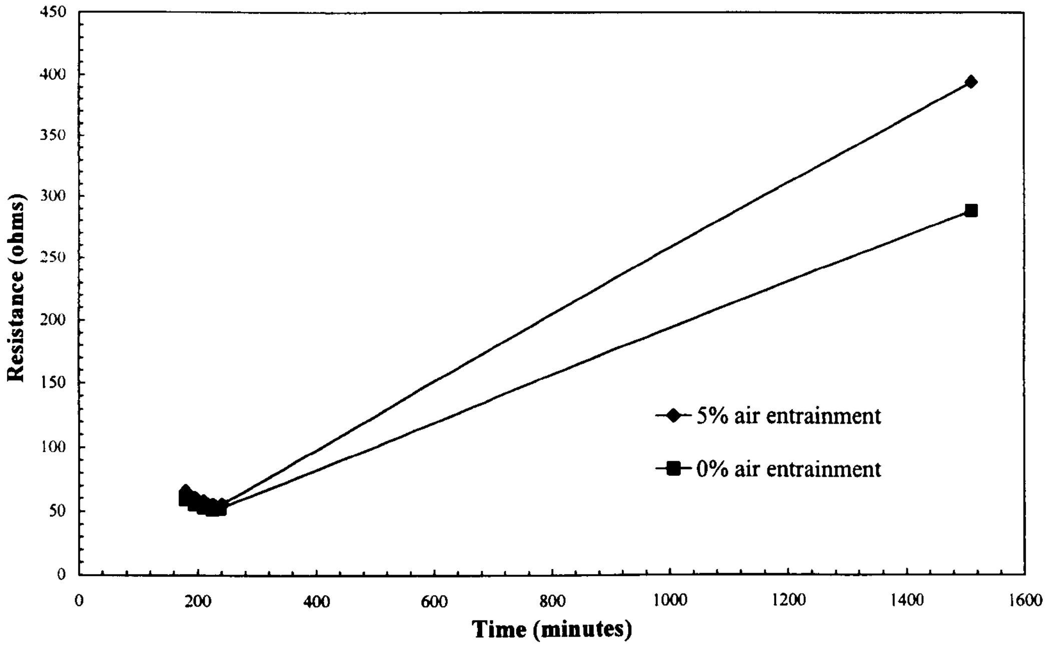

Figure 6.10 – Resistance versus time for air entrained and non-air entrained samples (3hr delay, 40°C/hr rise, 60°C maximum)

6.3 Superplasticising Admixture

Figure 6.11 shows the effect of replacing water with 2 litres of superplasticiser per 100kg of cement. From this it can be seen that, for normally cured concrete, the mix containing superplasticiser attained a higher compressive strength over all ages.

For electrically cured concrete (3hr delay, 40°C/hr rise, 60°C maximum) it can be seen that the mix containing no superplasticiser attained a slightly greater compressive strength at 28 days than the equivalent electrically cured sample containing superplasticiser. The opposite was true for normally cured mixes. This was due to the setting time being increased when superplasticiser was added and thus the mix containing the superplasticiser acted at 3 hours as a mix not containing superplasticiser at 1 or 2 hours. This means that greater microstructural damage occurred during heating resulting in long-term (28 days) compressive strength reductions.

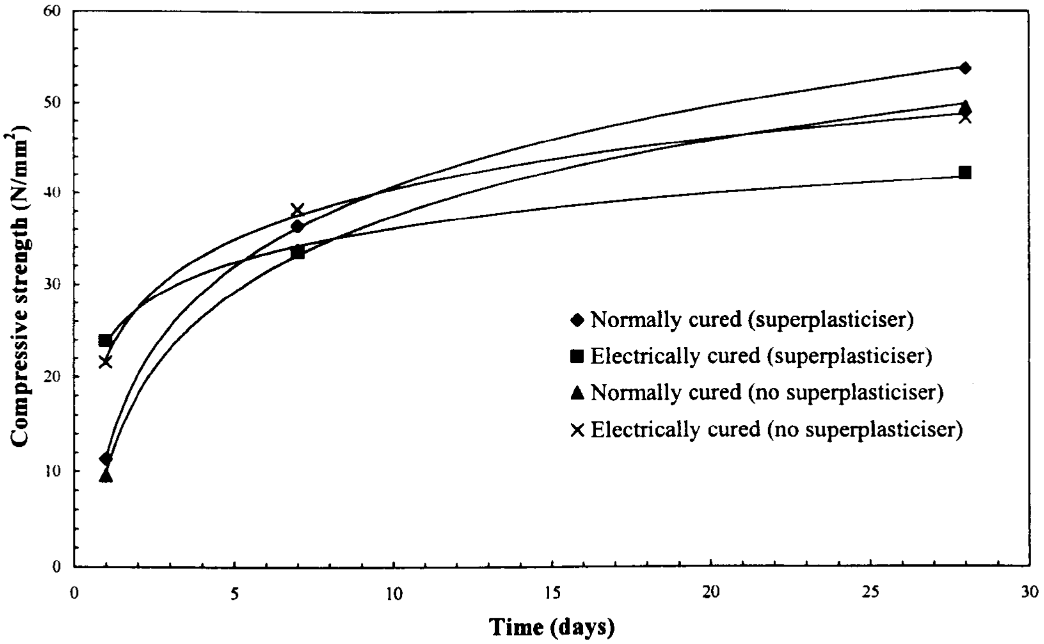

Figure 6.11 – Compressive strength versus time for electrically (3hr delay, 40°C/hr rise, 60°C maximum) and normally cured samples with and without superplasticiser

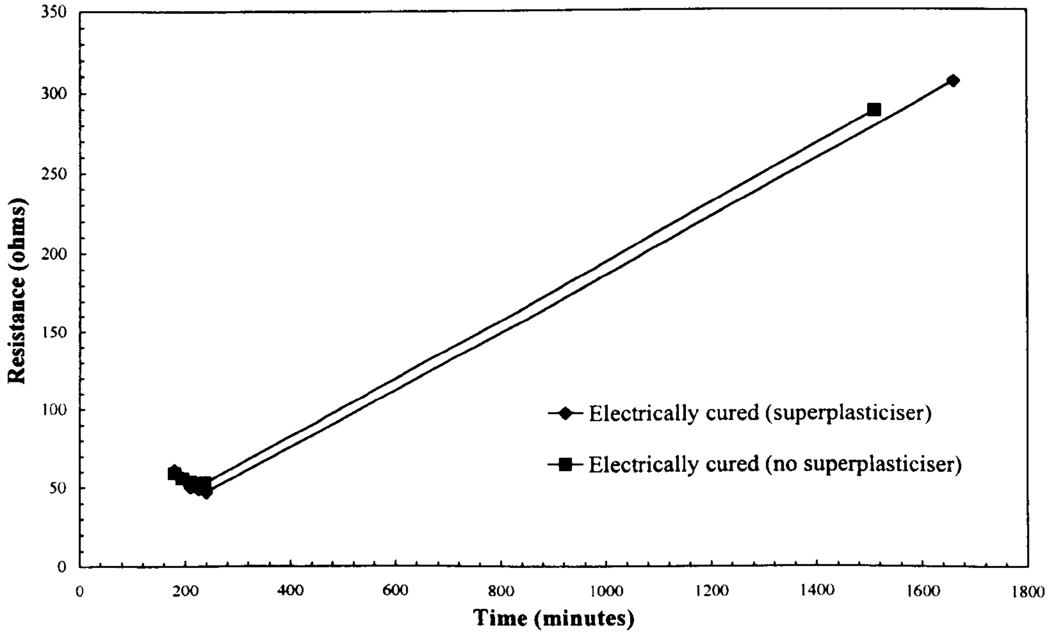

Figure 6.12 – Resistance versus time of electrically (3hr delay, 40°C/hr rise, 60°C maximum) cured concrete samples with and without superplasticiser

Figure 6.12 shows the effect of replacing water with 2l of superplasticiser per 100kg of cement upon resistance during (3hr delay, 40°C/hr rise, 60°C maximum) and after heating. From this it can be seen that the mix containing the superplasticiser initially had a slightly higher resistance but at later ages the mix not containing superplasticiser had a slightly higher value. This initially higher resistance may have been due to the inherent superplasticiser resistance properties which then acted as a water reducer, thus lowering the resistance of the more workable concrete. The lower final resistance of the superplasticiser mix may indicate the relative level of hydration between the two samples.

6.4 Accelerating Admixture

Figure 6.13 shows the effect of replacing water with 0.4 litres of accelerator per 100kg of cement. From this it can be seen that the normally cured mix containing the accelerator achieved a higher compressive strength at all ages than the mix containing no accelerator.

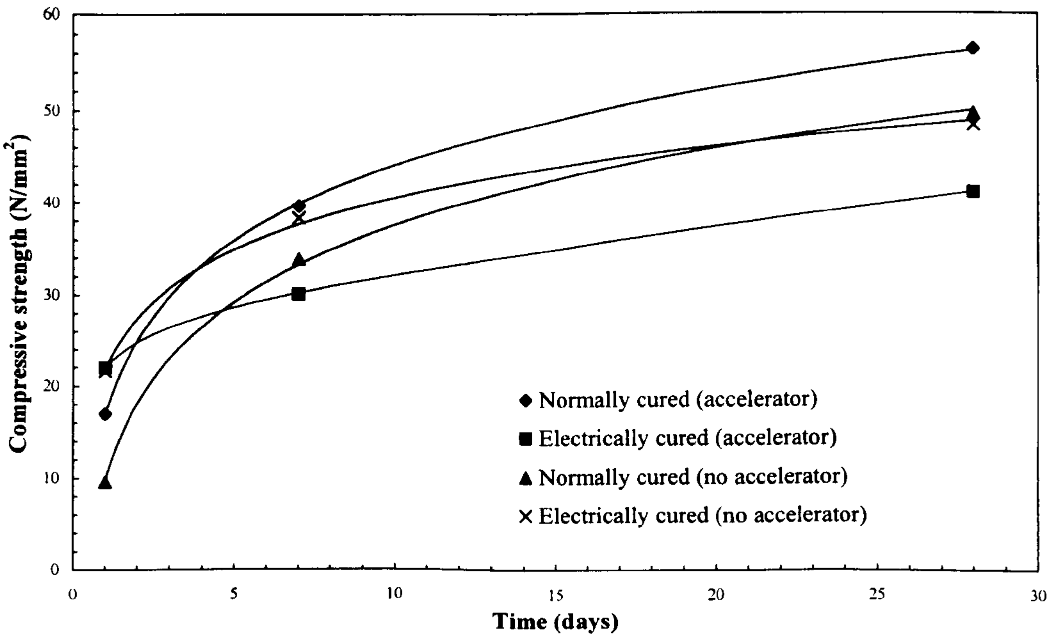

Figure 6.13 – Compressive strength versus time for electrically (3hr delay, 40°C/hr rise, 60°C maximum) and normally cured samples with and without accelerator

The electrically cured (3hr delay, 40°C/hr rise, 60°C maximum) mix containing the accelerator achieved a lower compressive strength increase (when compared to the equivalent normally cured mix) at early ages (1 day) than the mix not containing accelerator. At later ages (28 days) both mix types attained a similar compressive strength loss when compared to the equivalent normally cured samples. This was because the setting time of the mix containing accelerator was reduced, thus the mix containing the accelerator acted at 3 hours after mixing in a similar manner to the mix not containing the accelerator at 4 or 5 hours. This means that the effect of heating upon hydration was reduced at early ages, but microstructural damage was also reduced due to the relatively increased structural strength at the beginning of heating.

6.5 Retarding Admixture

Figure 6.14 shows the effect of replacing water with 0.4 litres of retarder per 100kg of cement.

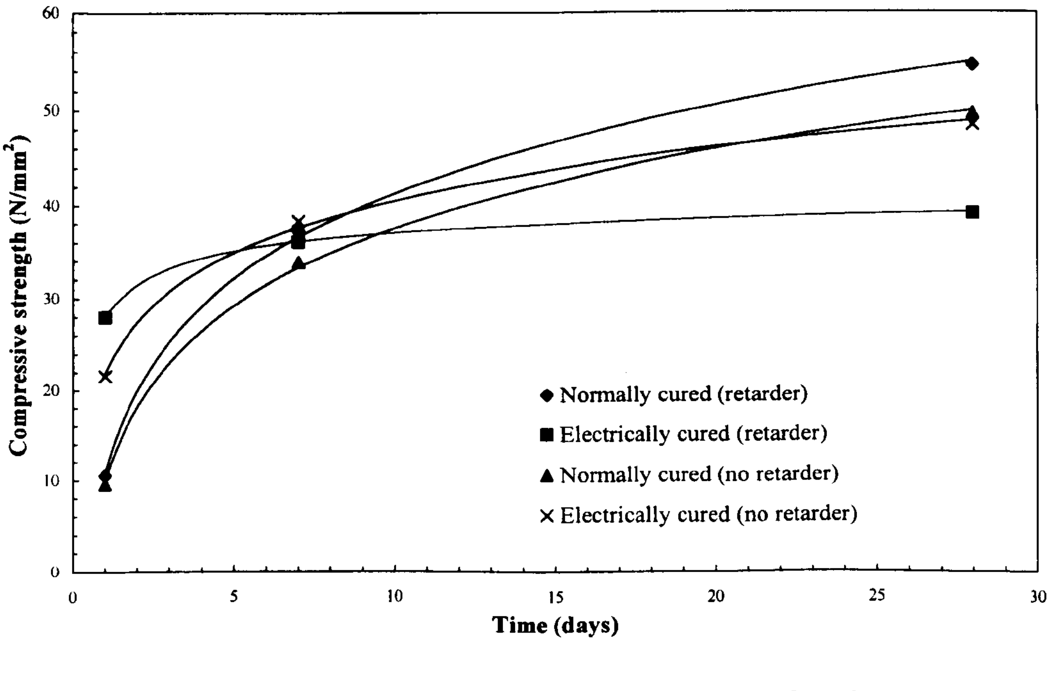

Figure 6.14 – Retarder compressive strength versus time for electrically (3hr delay, 40°C/hr rise, 60°C maximum) and normally cured samples

It can be seen that the effect of adding a retarder was similar to that of adding a superplasticiser. It can be seen that with electrical curing (3hr delay, 40°C/hr rise, 60°C maximum) the mix containing the retarder attained a relatively higher initial compressive strength increase (compared to an equivalent normally cured mix) than an electrically cured mix not containing retarder. This situation was reversed at 28 days with the electrically cured mix containing retarder incurring the lowest compressive strength of the samples tested. This was due to the same reasons as Figure 6.11.

6.6 Pulverised Fuel Ash Addition

Figure 6.15 shows the effect of 30% PFA cement replacement on compressive strength over time for normally and electrically (2hr delay, 40°C/hr rise, 60°C maximum) cured concrete.

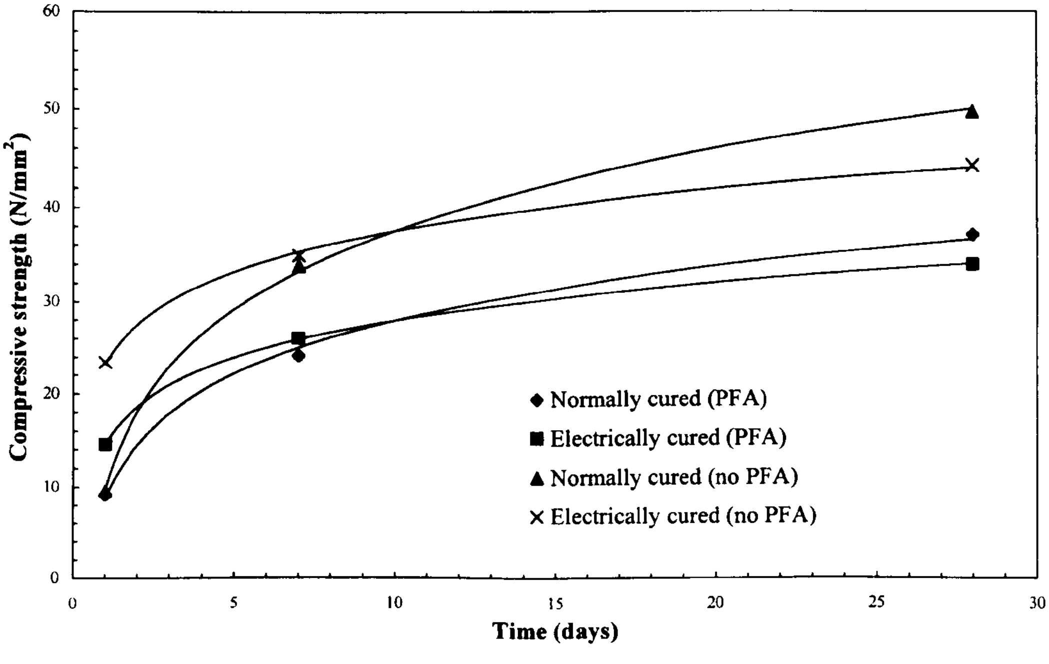

Figure 6.15 – Compressive strength versus time for electrically (2hr delay, 40°C/hr rise, 60°C maximum) and normally cured samples with and without PFA

From this it can be seen that the normally cured mix containing PFA attained a significantly lower compressive strength at later ages (28 days) than the sample not containing PFA (Berry and Malhotra 1980). This was likely not to be the case at much later ages where PFA has been shown to have increased compressive strength over concrete not containing PFA (Neville 1988). The initial compressive strength gain of the electrically cured PFA samples was reduced when compared to the electrically cured mix not containing PFA. This may have been due to damage incurred during heating, where the PFA mix had an increased setting time and thus did not attain the same degree of strength to be able to resist the thermomechanical stresses imposed during heating as the mix not containing PFA. It may also have been due to the addition of another solid material with a different coefficient of thermal expansion to the other mix components.

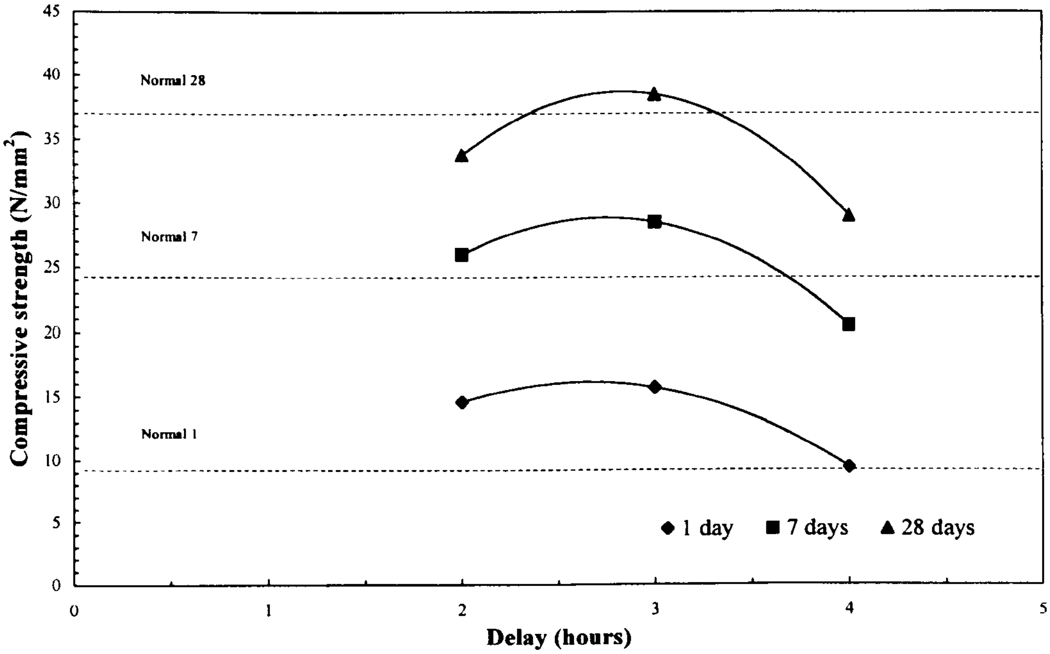

Figure 6.16 – Effect of delay period on compressive strength for 30% PFA cement replacement (40°C/hr rise, 60°C maximum)

Figure 6.16 shows the effect of delay period on the compressive strength of electrically (40°C/hr rise, 60°C maximum) cured mixes containing 30% PFA cement replacement. From this it can be seen that the 3 hour delayed samples performed best in both the short and long-term. The 4 hour delayed samples did not attain a significant degree of compressive strength improvement at early ages. This was a similar result to Figure

5.18 and was due to similar reasons. The differences between the two figures were likely to be due to the different setting times between mixes with and without PFA (Bamforth 1992).

Figure 6.17 shows the effect of 30% PFA cement replacement upon resistance during and after heating (2hr delay, 40°C/hr rise, 60°C maximum). From this it can be seen that the initial resistance of the mix containing PFA was higher than the mix not containing PFA. This was likely to be due to the physical form and resistance properties of PFA (Dhir 1986) which may have increased the resistance of the cement/PFA matrix. The final resistance of the PFA mix was lower than the equivalent mix not containing PFA. This reflected the relatively reduced level of hydration present and the reduced final compressive strength of the mix containing PFA.

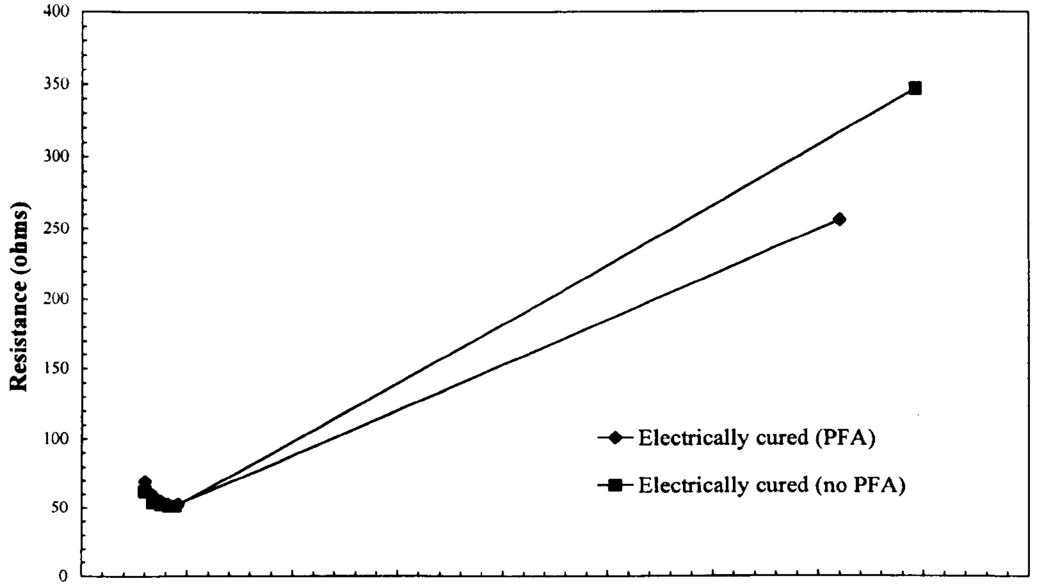

Figure 6.17 – Resistance versus time for electrically (2hr delay, 40°C/hr rise, 60°C maximum) cured samples with and without PFA

Figure 6.18 shows the initial surface absorption characteristics of normally and electrically (2hr delay, 40°C/hr rise, 60°C maximum) cured samples at 28 days. From this it can be seen that the electrically cured samples attained a lower ISA value throughout the test than the normally cured samples. This was a similar result to Figure 5.46 and was again likely to be due to collapsed capillary pores incurred during heating.

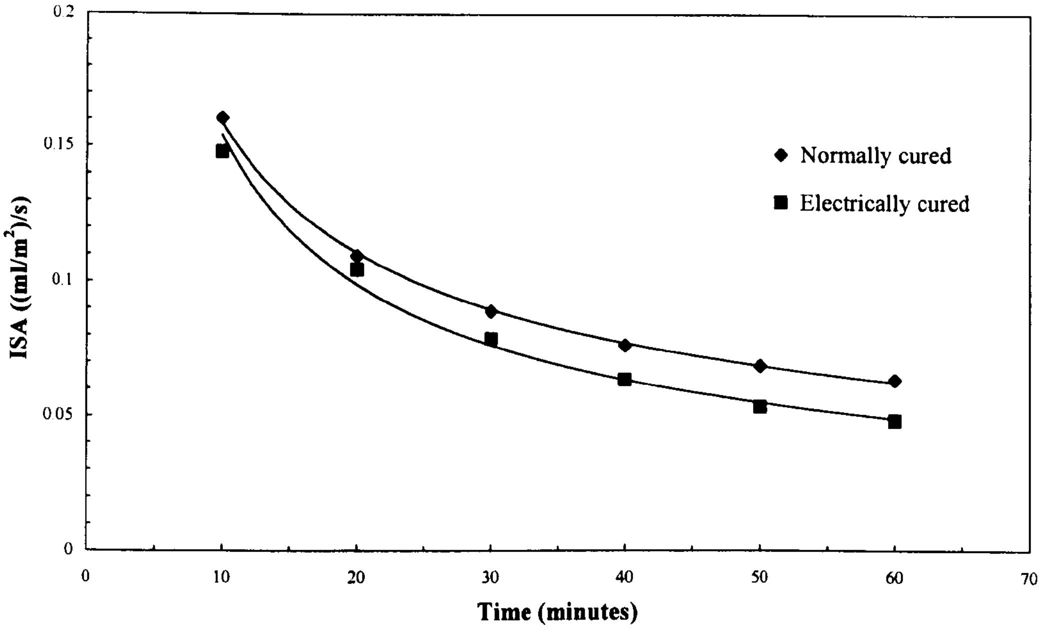

Figure 6.18 – ISA for electrically (2hr delay, 40°C/hr rise, 60°C maximum) and normally cured concretes containing PFA

6.7 Conclusions

1. There exists a relationship between ultrasonic pulse velocity (UPV) and density for both normally and electrically cured concrete samples.

2. The UPV values for both electrically and normally cured samples were found to give an approximate estimation of percentage of air entrainment in concrete at 28 days.

3. It was found that UPV could be used to give an indication of compressive strength for all concrete samples tested.

4. It was found that a compressive strength loss of electrically cured samples containing high levels of air entrainment could be achieved in extreme circumstances if very short delay periods were chosen and a 4 hour isothermal period was applied at 80°C. This was likely to be due to increased microstructural damage incurred around the entrained air bubble cement paste shells during heating and cooling.

5. The reduction of compressive strength at 28 days for electrically cured air entrained concrete when compared to normally cured concrete was found to be dependent on the percentage of air entrainment, with higher levels of air entrained producing greater reductions in compressive strength.

6. The maximum temperature of electrically cured air entrained concrete was found to influence compressive strength at all ages, with higher temperatures producing lower compressive strength. This was likely to be due to increased microcracking around the entrained air bubbles at the higher temperatures.

7. The effectiveness of electrical curing in improving compressive strength on mixes containing air entrainment was found to be reduced when compared to similarly designed mixes not containing air entrainment. This was also due to increased microcracking around the entrained air bubbles incurred during heating.

8. Resistance during heating was found not to be a good indicator of percentage of air entrainment.

9. Results show that normally cured samples containing a superplasticiser attained a higher compressive strength at all ages than a similar mix without superplasticiser. The electrically cured concrete samples containing superplasticiser cured after a delay of 3 hours acted in an identical manner to a heated mix without superplasticiser with a delay period of 1 or 2 hours. This was due to the

superplasticiser mix having a greater period before the initial set which effectively reduced the delay period.

10. Resistance was not found to be a good indicator of the presence of superplasticiser added to the mix.

11. It was found that normally cured samples containing an accelerator attained a higher compressive strength at all ages than a similar mix without accelerator. The electrically cured mix with accelerator cured after a delay of 3 hours acted in a similar manner to a heated mix without accelerator with a delay period of 4 hours. This was due to the mix with accelerator having a reduced period before initial set which effectively reduced the delay period.

12. It was found that both normally and electrically cured concrete containing a retarder behaved in a similar manner to concrete containing a superplasticiser.

13. It was found that with cement replacement by PFA the effectiveness of electrical curing in improving compressive strength was reduced at 1 day. This was likely to be due to the concrete containing PFA having an extended period before initial set, thus being less able to resist the thermomechanical stresses incurred during heating.

14. Resistance was not found to be a good indicator of the presence of PFA but may be used as an indication of the extent of hydration.

Chapter 7 - DIRECT ELECTRIC CURING OF CONCRETE CONTAINING REINFORCEMENT

7.1 Introduction

This chapter provides the results and discussion of an experimental and theoretical investigation of normally and electrically cured concrete containing reinforcement. These results can be seen in Figures 7.1-7.27 and Tables 7.1-7.2

The mixing, casting, curing and monitoring was implemented in accordance with the experimental procedures stated in Chapter 3.

Electrically cured slabs A and B and the normally cured slabs all consisted of a C30 mix with a TMS = 43N/mm^2 and a slump of 10-30mm. The electrically cured slabs had a delay period of 4 hours, with a linear temperature rise of 40°C/hr to a maximum of 60°C. The temperature datum was taken from position 1 for Slab A and position 3 for Slab B (see Figures 3.15 and 3.16).

7.2 Normally Cured Slab

7.2.1 Schmidt hammer

Figure 7.1 shows Schmidt hammer number for normally cured slab and 150x150x150mm cube compressive strength versus time. From this it can be seen that both Schmidt hammer and compressive strength followed a similar trend of increased strength over time (Xuenquan et al 1986). There was a variability inherent in the Schmidt hammer results due to only the immediate surface of the concrete being tested (Bungey 1982). As such, aggregate particles or air voids immediately below the surface could significantly higher or lower the Schmidt hammer number respectively.

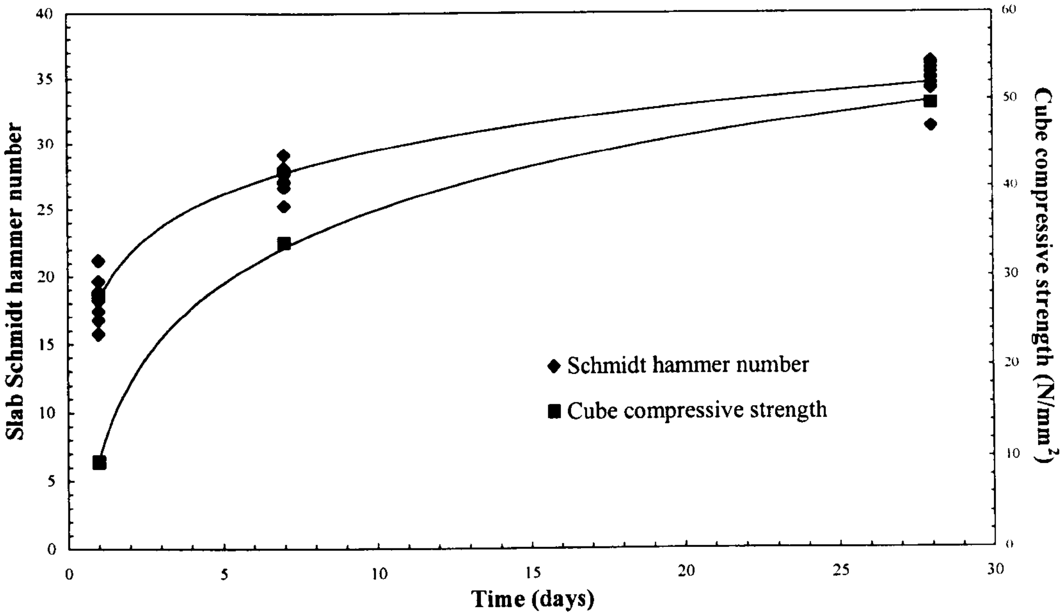

Figure 7.1 – Schmidt hammer number and 150mm cube compressive strength versus time for normally cured slab

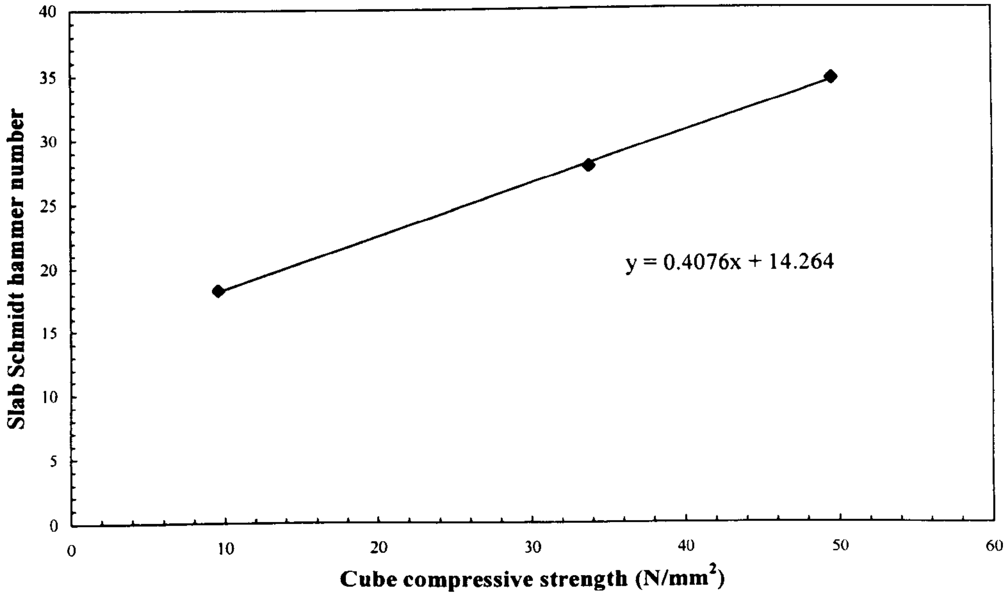

Figure 7.2 – Slab Schmidt hammer number versus 150mm cube compressive strength for normally cured samples

Figure 7.2 shows the relationship between average Schmidt hammer number and compressive strength of 150mm cubes for normally cured samples over time. From this it can be seen that the relationship can be assumed to be approximately linear which is given by:

Schmidt hammer number = 0.407 x (cube compressive strength) + 14.264 Eqn. 7.1

From this, approximate actual compressive strengths for the mix used (C30) could be derived from the Schmidt hammer results gained from the electrically cured slabs.

7.2.2 Core failure load

Figure 7.3 shows the average core failure load for a normally cured slab and cube compressive strength versus time.

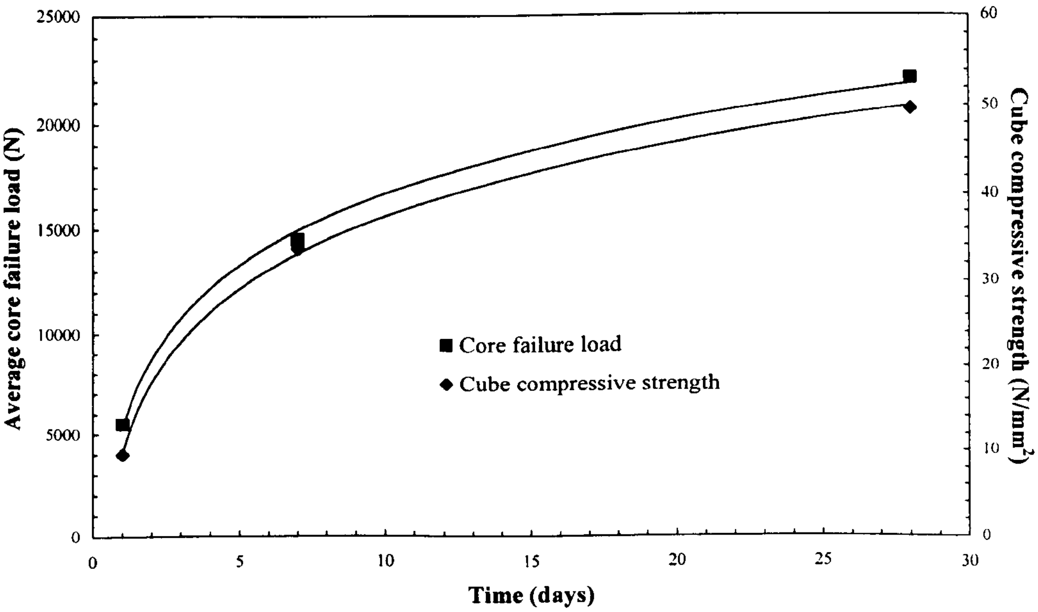

Figure 7.3 – Core failure load and 150mm cube compressive strength versus time for normally cured samples

From this it can be seen that both core failure load and compressive strength followed a similar trend of increased strength over time. This increase was due to the continued hydration incurred by both samples which increased the strength of the cement matrix and thus increased both the cube and core crushing values (Neville 1988).

Figure 7.4 shows the relationship between average core failure load and cube compressive strength for normally cured samples over time. From this it can be seen that the relationship can be assumed to be approximately linear and can be given by:

core failure load = 414 x (cube compressive strength) +1279.9 Eqn. 7.2

From this, approximate actual compressive strengths for the mix used (C30) could be derived from the core failure load gained from the electrically cured slabs.

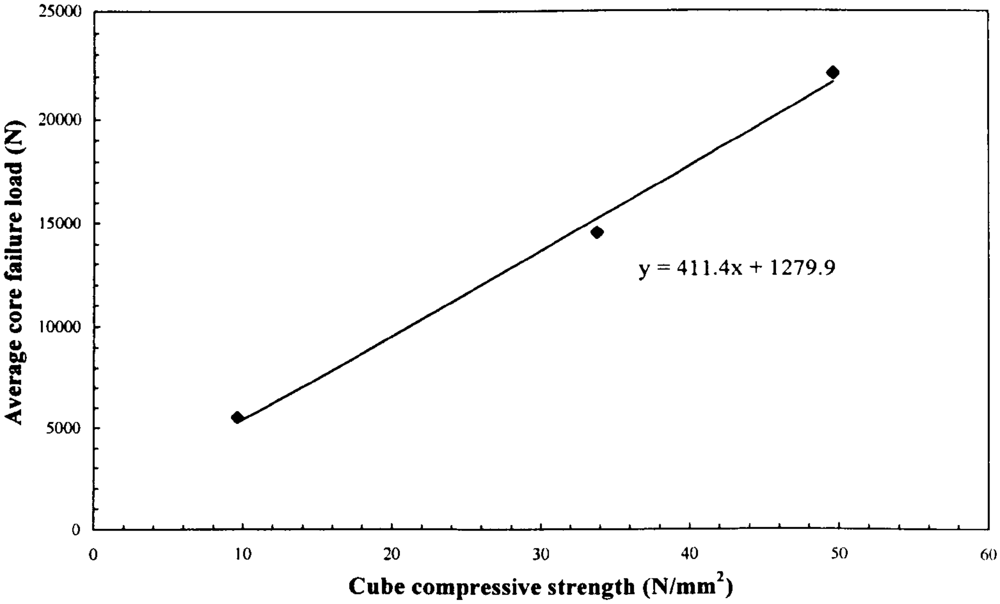

Figure 7.4 – Core compressive strength versus actual compressive strength for normally cured slab

7.2.3 Temperature history

Figure 7.5 shows the temperature changes in a normally cured slab. The thermistor temperature sensors were placed in a similar arrangement to the electrically cured Slab A. Individual sensor placements have not been identified due to the similarity of all results. From this it can be seen that the temperature rose for approximately the first 300 minutes after gauging with water, whereupon a slight lowering of temperature could be seen to occur by 1300 minutes. This was due to Alite (impure C_3S) hydration reactions producing an exothermic chemical reaction (Neville 1988, Gibbon and Ballam 1998). The temperature rise was slight due to the placement of the thermistors on the surface of the normally cured slab. This reduced the apparent heating effect due to the effect of surface cooling by the atmosphere and the thermal insulation of the concrete. Within the centre of the slab, temperature rises would be expected to be slightly higher. All thermistor placements showed approximately the same temperature at all ages (±2°C) and the average temperature over the entire time tested was approximately 23°C.

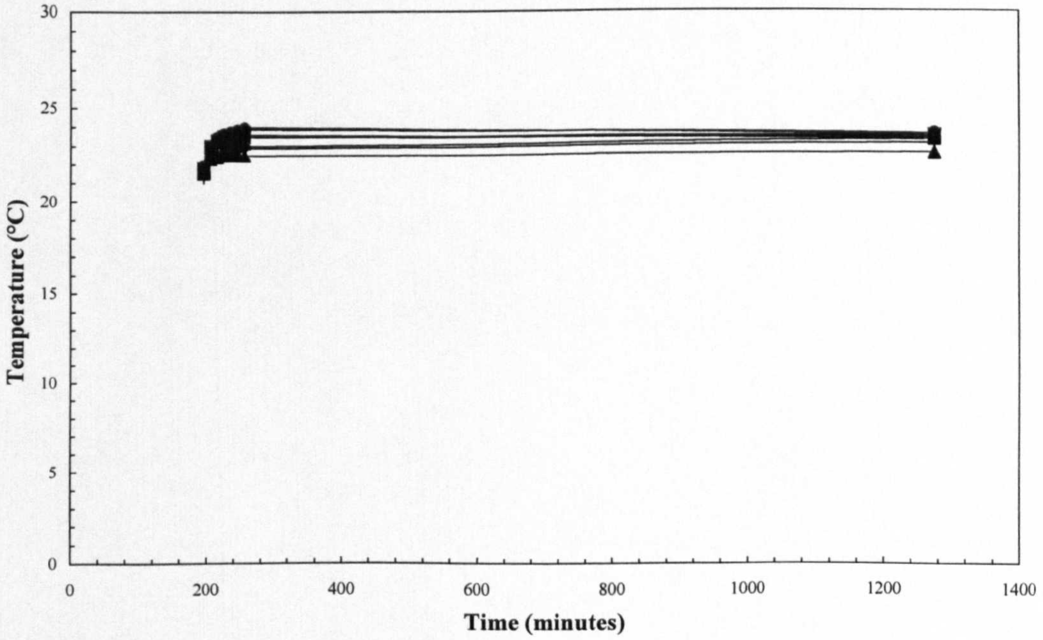

Figure 7.5 – Temperature versus time for a normally cured slab

7.3 Electrically Cured Slab A

7.3.1 Visual inspection

Visual observations were carried out on the slab during and after heating. It was observed that during heating, visible surface cracks along the reinforcement bars (approximately 1mm wide) occurred after the first 15 minutes and subsequently steam was seen to be rapidly emitted from the underside of the slab. Concurrent to this audible 'splintering' sounds were heard to be coming from the sample and air bubbles were seen to be emitted from specific points across the surface. The bubble emission sites remained in a fixed position throughout the test and as such it can be assumed that pathways of gas were present in the body of the concrete that allowed the heated air and steam to escape. This would damage the structure of the concrete in specific regions, whilst leaving relatively undamaged sections between the emission points. This was likely to be due to the placement of the temperature sensors near the surface of the slab which resulted in the internal overheating of the sample in order to achieve the 60°C maximum temperature. This required excessive voltages to be applied initially and as such caused localised boiling which induced the observed cracks, bubbles and sounds.

7.3.2 Schmidt hammer

Figure 7.6 shows the derived average (70 results per point) Schmidt compressive strength for electrically cured Slab A and the normally cured compressive strength over time. From this it can be seen that the electrically cured slab attained (on average) a higher initial compressive strength than the normally cured samples. This situation was reversed at later ages (>7 days) were the normally cured samples continued to gain compressive strength at a greater rate than the electrically cured slab (Hutchinson et al 1991). This showed the same trend as the electrically cured cube samples not containing reinforcement. The percentage gain, when compared to the normally cured slab, for the electrically cured slab was 167.5% at 1 day and –28.5% at 28 days. The percentage gain for the electrically cured cube, when compared to the normally cured cube, was 98.8% at 1 day and –18.9% at 28 days. The greater increase in percentage gain initially and the greater decrease in percentage gain at 28 days of the electrically cured slab was due to the increased temperature internally required to achieve the superficially similar heating regime to the cube. This extra temperature within the slab was due to the electric field density around the reinforcement bars being substantially higher than the surrounding areas. This field density then heated up the surrounding concrete at a much higher rate than the surface areas and then heat was transferred solely by conduction to the thermistors placed at 20mm below the surface. The increased temperature internally was slowly distributed (Gibbon and Ballam 1998) throughout the sample after heating had ended, thus increasing the early age maturity, but at later ages, the higher initial internal temperatures caused greater structural damage than the cube heating regime.

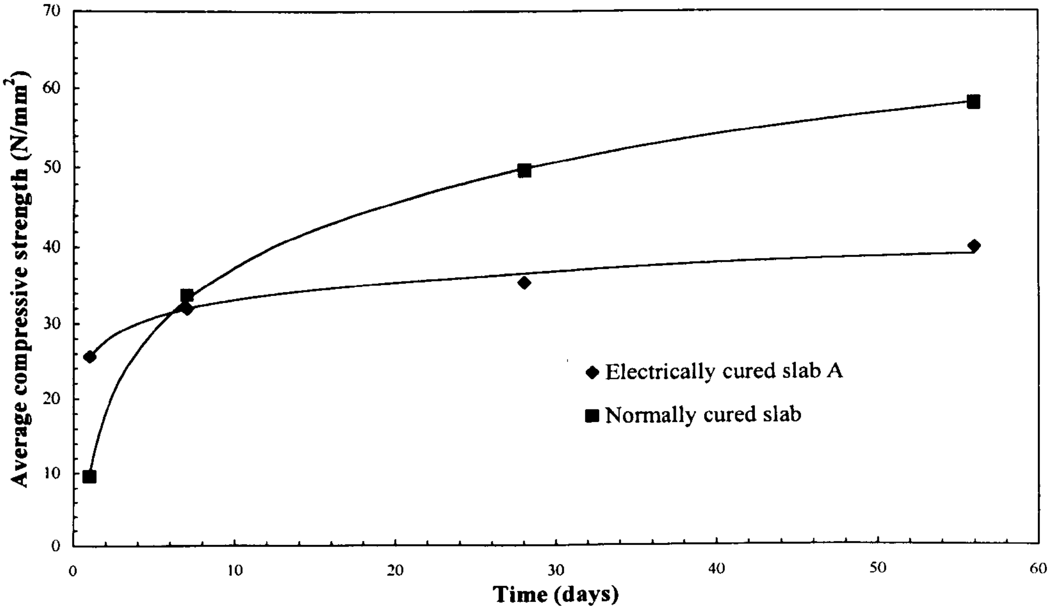

Figure 7.6 – Average compressive strength versus time for electrically and normally cured slab (derived from Schmidt hammer)

Figure 7.7 represents the average (10 results per data point) compressive strength (derived from Schmidt hammer) perpendicular to the reinforcement bars (along the length of the slab) of Slab A at various ages. The centre of the slab is marked by the vertical dotted line. From this it can be seen that the 1 day compressive strength varied significantly across the width of the slab. Where reinforcement bars are present (-100, 0 and 100mm), a greater degree of 1 day compressive strength was achieved than in the regions between the reinforcement bars. This was due to the extra heating to be expected around the reinforcement bars as electric field density is increased. This trend was reversed at later ages (28 and 56 days) where the regions between the reinforcement bars showed a greater compressive strength. This was likely to be due to the damaging effects of temperature gradients causing thermomechanical damage in the regions adjacent to the reinforcement bars, thus reducing long term strength. This trend was similar to cube samples electrically cured containing no reinforcement, where greater temperatures at an early age result in long-term structural damage.

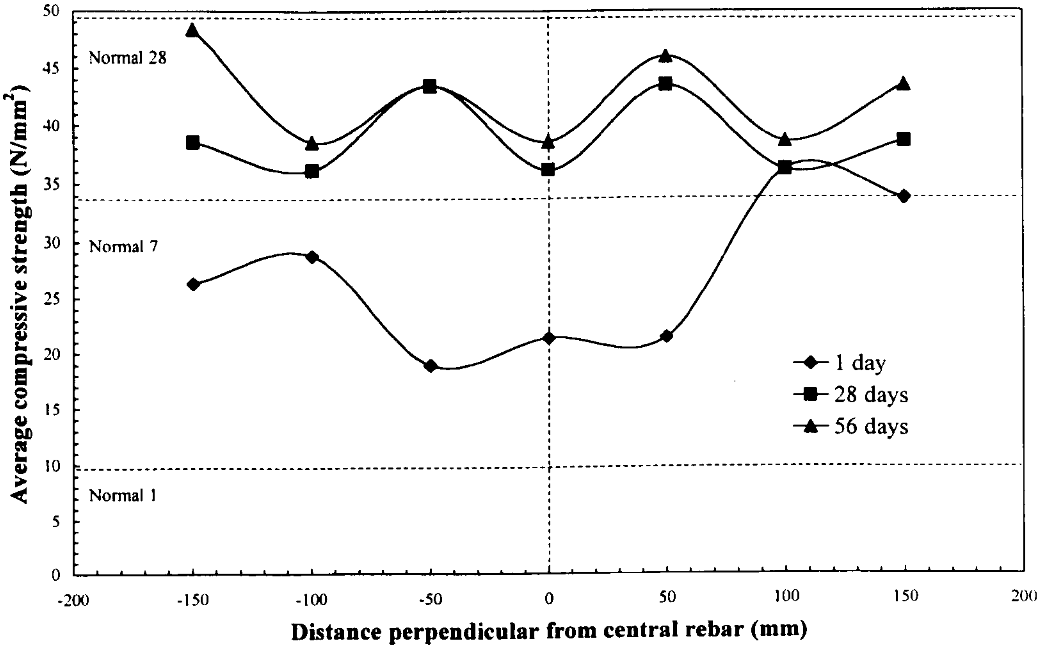

Figure 7.7 – Average compressive strength versus distance from centre reinforcement bar (derived from Schmidt hammer)

It can also be seen from the figure that all regions of the slab (at the surface) achieved the characteristic design strength (C30) but only two sections achieved the TMS (43N/mm^2) at 28 days (-50 and 50mm) (Wilson and Gupta 1996). There was a degree of overlap present where it appeared the 1 day compressive strength was greater than the 28 day compressive strength. This was likely to be due to the innate variability of the Schmidt hammer apparatus. However, confidence can be given to the general results due to the apparent symmetry on either side of the centre reinforcement bar.

Figure 7.8 represents the average (7 results per data point) compressive strength (derived from Schmidt hammer) parallel to the reinforcement bars of Slab A at various ages. From this it can be seen that at all ages there was a greater similarity in results when compared to the compressive strength perpendicular to the reinforcement bars. This was due to a more uniform temperature distribution in this direction. The temperature parallel to the reinforcement bars would be expected to be similar apart from excess heating towards the centre of the sample (Gibbon and Ballam 1998). This was confirmed by the slightly higher compressive strengths in the central region at 1 day and the reduced compressive strengths at 28 days. The outer regions showed a comparatively higher compressive strength at 28 days, due to reduced microstructural damage from heating effects.

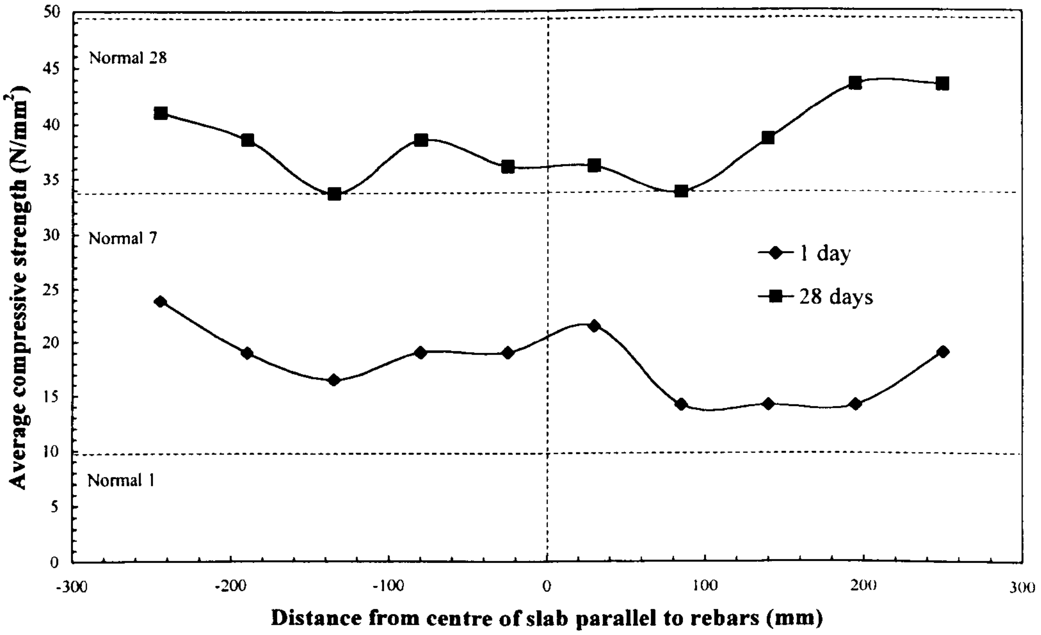

Figure 7.8 – Average compressive strength versus distance from centre of slab parallel to reinforcement bars (derived from Schmidt hammer)

7.3.3 Core failure load

Figure 7.9 shows the average (14 results per data point) core compressive strength for electrically cured Slab A and the normally cured slab over time. From this it can be seen that the electrically cured slab attained (on average) a higher initial compressive strength than the normally cured samples (Wilson and Gupta 1996). This situation was reversed at later ages (>3 days) were the normally cured samples continued to gain compressive strength at a greater rate than the electrically cured slab. This showed the same general trend as the electrically cured samples not containing reinforcement. The percentage gain, when compared to the normally cured slab, for the electrically cured slab was 129.2% at 1 day and -38.5% at 28 days whereas the percentage gain for the electrically cured cube was 98.8% at 1 day and −18.9% at 28 days.

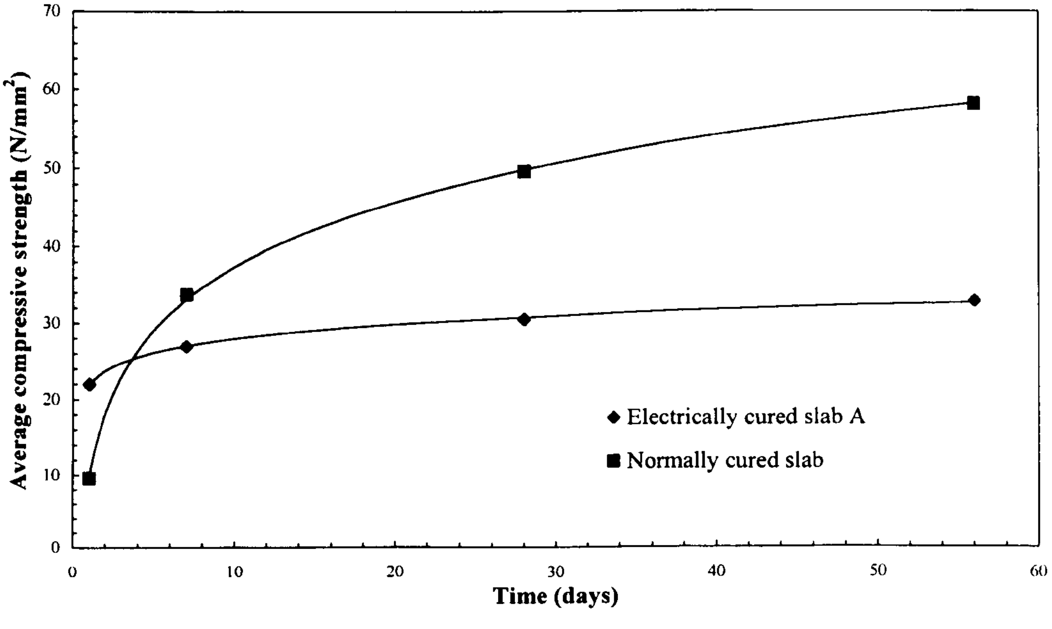

Figure 7.9 – Average core compressive strength versus time for electrically and normally cured slab (derived from core results)

Figure 7.10 shows the compressive strength (derived from core results) at 56 days perpendicular to the reinforcement bars at various locations along the length of Slab A.

From this it can be seen that the central region attained a significantly lower compressive strength than the outer regions (Owens 1985). This was due to the long-term damage caused to the central region by thermomechanical stress caused by the initial heating.

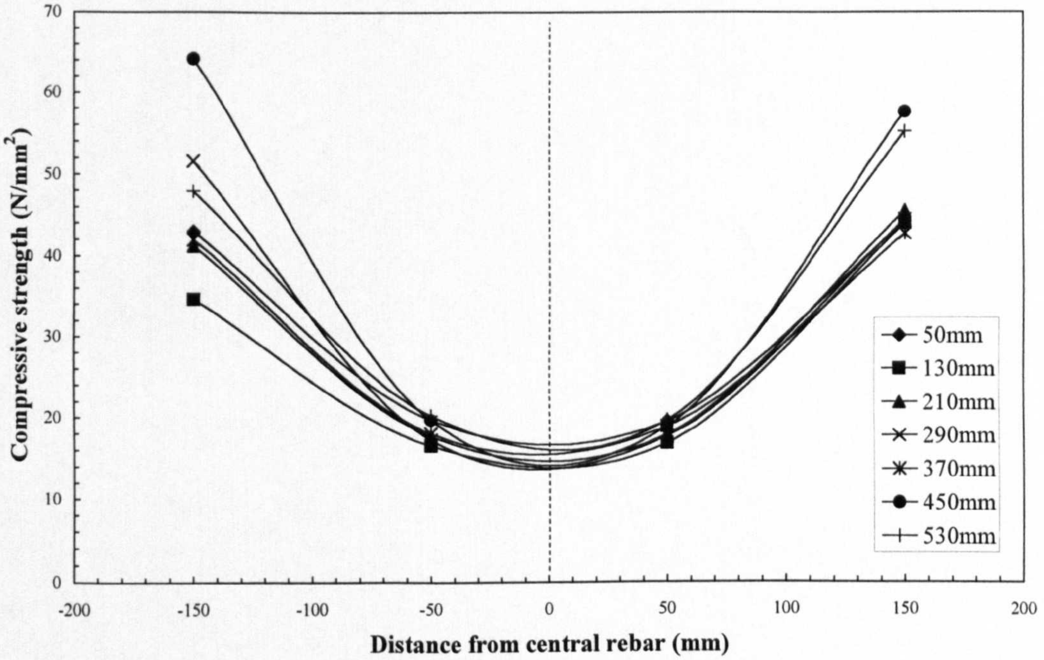

Figure 7.10 – Compressive strength at 56 days perpendicular to reinforcement bars (derived from core results)

Figure 7.11 shows the differing compressive strengths (N/mm^2) (derived from core results) over the surface of Slab A at 56 days. From this it can be clearly seen that compressive strength was approximately uniform parallel to the reinforcement bars along the entire length of the slab. The central region clearly showed a reduced compressive strength as in Figure 7.10. From this it can be stated that, for the particular slab tested, compressive strength was mainly dependent on the distance perpendicular to the reinforcement bars and once this has been estimated, then the compressive strength can be assumed to be approximately equal throughout the length of the slab. This would not be valid for larger sections where heat insulation effects could significantly increase the temperatures in the central region, thus affecting structural damage. It would also not be valid for different geometrys (Leung and Pheeraphan 1994) or reinforcement bar layouts.

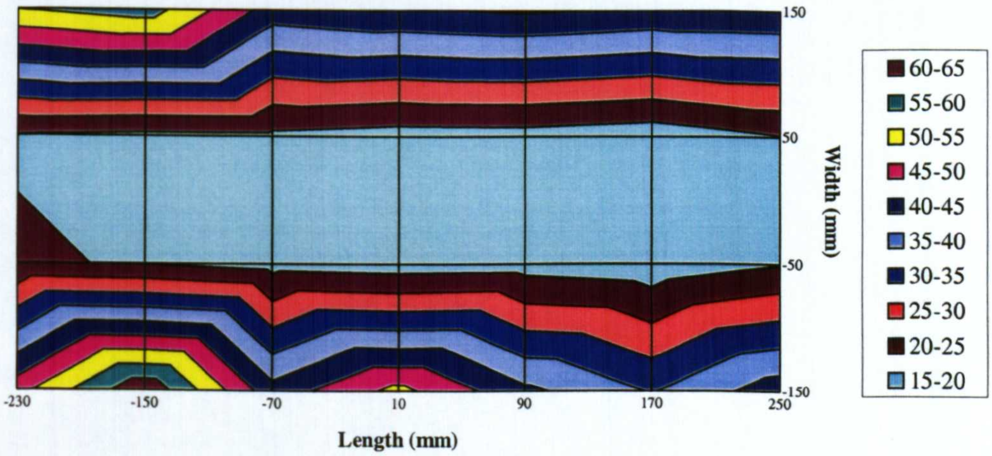

Figure 7.11 – Compressive strength at 56 days (derived from core results)

Figure 7.12 shows a comparison of the average derived compressive strengths for Slab A for both core and Schmidt hammer results over time. From this it can be seen that the compressive strength derived from the cores was lower than the compressive strength derived from the Schmidt hammer results over the entire time tested (56 days). This was due to the cores being taken from a greater depth than the Schmidt hammer which is only a surface measurement of strength. Thus the cores contained a different temperature history throughout their length and as such were going to fail under load at the weakest point. This was at the point closest to the surface at early ages (1 day) and at the point closest to the reinforcement bars at later ages (>28 days). This implied that extra care should be taken when deciding upon a method for testing compressive strength in electrically cured samples as normally cured concrete (excluding mass concrete) tends to have a similar temperature history within its structure and as such tends to have a more uniform compressive strength throughout.

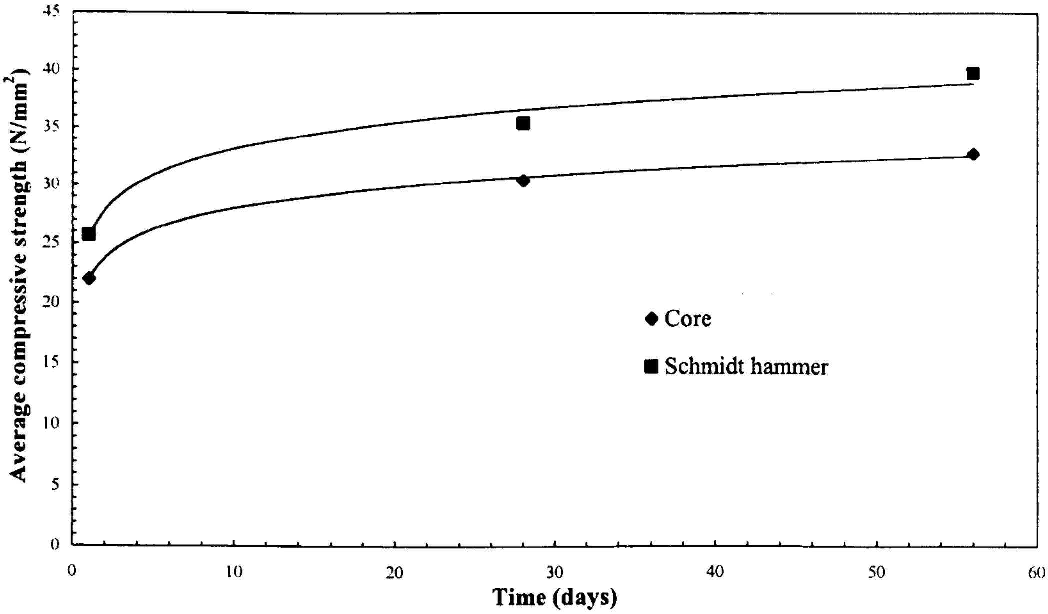

Figure 7.12 – Average compressive strength versus time (derived from core and Schmidt hammer results)

7.3.4 Porosity

Figure 7.13 shows the porosity (%) at different points over Slab A at 56 days. From this it can be seen that the porosity only varied between 13.8% and 17.4% over the entire surface of the slab. This was similar to the porosity of the normally cured concrete at the same age (approximately 16%). It can also be seen that porosity appeared to be roughly similar parallel to the reinforcement bars, with areas of greatest porosity corresponding roughly to the area along the reinforcement bars. This was not for certain, however, due to the small differences that were apparent. The apparent increase in porosity may have been due to localised boiling of the free water within the mix, causing an increase in pore size and microcracks through the expansion of water (through conversion to steam) and air. However, this may have been in conjunction with the collapse of capillary pores during heating which would lower the porosity around the reinforcement bars (Parcevaux 1983).

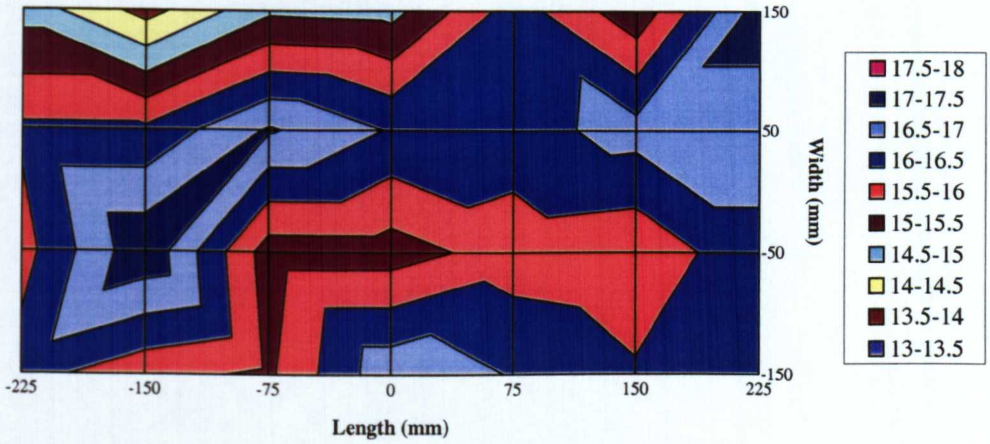

Figure 7.13 – Porosity over slab surface at 56 days

7.3.5 Density

Figure 7.14 represents the distribution of density (kg/m^3) over the surface of Slab A at 56 days. From this it can be seen that the density was approximately equal over the entire slab (2225-2350kg/m^3). This confirmed the results from Figure 5.51, which showed that the heating regime used did not significantly affect density. This was clearly due to the fact that the concrete used was of a uniform initial density and although electrical curing did inevitably lead to initial small water losses, in the long-term this did not affect the overall density.

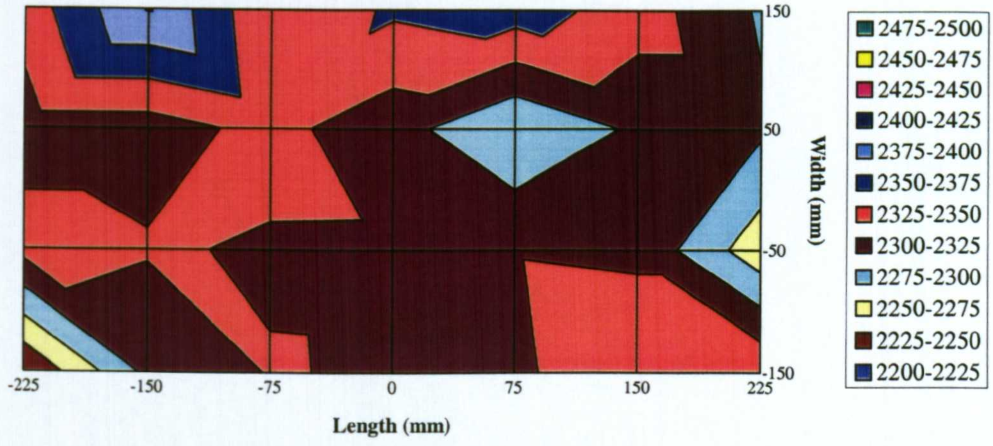

Figure 7.14 – Density over slab surface at 56 days

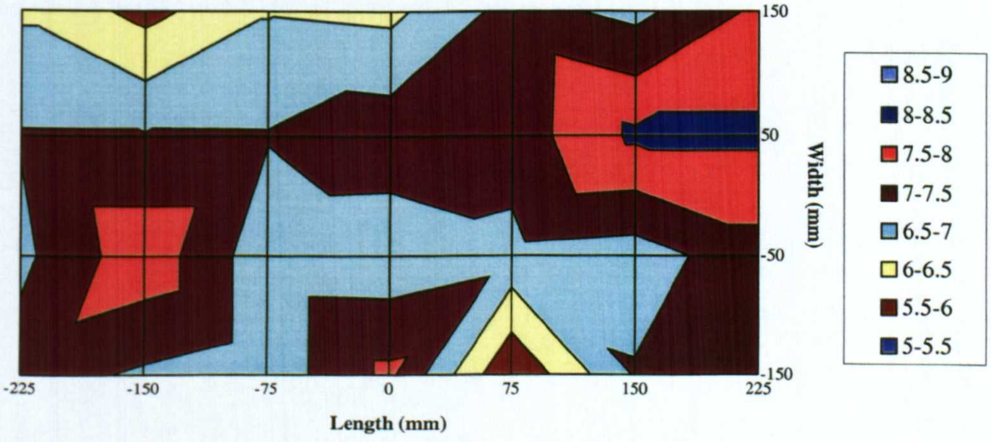

Figure 7.15 – Water absorption over slab surface at 56 days

7.3.6 Water Absorption

Figure 7.15 shows the distribution of water absorption (%) characteristics over the surface of Slab A at 56 days. From this it can be seen that the water absorption showed a similar distribution to the porosity given in Figure 7.13. This also showed relatively small differences in water absorption over the entire surface and was due to porosity and water absorption being closely related (Neville 1988).

7.3.7 Temperature profile

The temperature profile along the surface of Slab A was found to be inaccurate. This was due to the manual placement of the thermistors at a depth of approximately 20mm. Thus a small deviation from this depth incurred a relatively large distortion of the temperature profile due to the temperature gradients inherent during electrically accelerated curing.

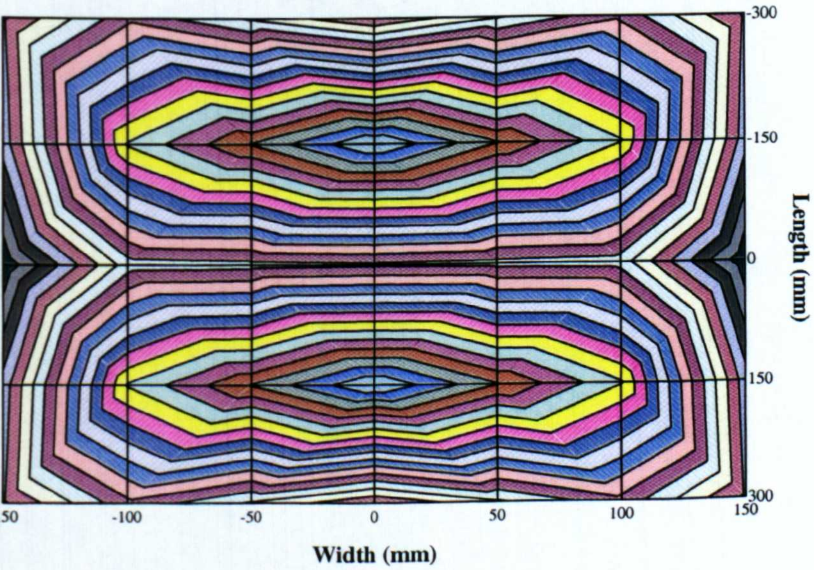

Figure 7.16 – Temperature profile along Slab A at 320 minutes after gauging with water

An example of the surface profile at 320 minutes after the gauging with water can be seen in Figure 7.16 (same colour key as Figure 5.53) and a full list of temperatures over various ages can be seen in Table 7.1. These showed that temperature generally tended to be relatively decreased at the outside edges when compared to the central region.

Table 7.1 - Temperature of Slab A at various ages

Time after gauging with water (min)	**Sensor number (from Chapter 3)**									
	1	**2**	**3**	**4**	**5**	**6**	**7**	**8**	**9**	**10**
240	15.8	15.8	15.7	15.7	15.7	15.6	15.7	15.6	15.5	20.6
250	23.1	24.6	22.2	36.5	23.1	23.0	22.2	24.0	26.5	22.2
260	33.1	35.4	28.1	43.2	35.7	29.3	30.8	34.5	32.4	22.5
270	38.5	39.3	31.8	46.1	41.9	33.2	35.6	38.8	34.7	23.1
280	45.4	45.0	37.1	57.5	48.6	39.2	41.6	44.7	40.8	23.8
290	51.0	50.5	41.5	62.7	55.4	43.9	46.6	50.0	44.4	24.8
300	55.3	56.1	47.2	70.6	62.0	50.3	51.6	56.2	51.0	24.9
305	56.9	57.9	48.8	72.1	64.7	51.9	53.7	58.4	52.5	23.8
310	58.1	59.0	51.1	72.9	66.3	54.2	55.2	59.9	54.8	24.2
315	59.1	59.4	52.3	73.1	67.0	55.5	56.3	60.6	56.0	24.2
320	59.8	59.5	53.2	73.0	67.1	56.4	57.0	60.7	56.8	24.3
1165	36.6	35.7	31.0	36.6	35.9	34.2	33.5	33.0	34.6	20.9
1370	29.7	29.2	25.2	29.9	29.0	28.1	28.2	27.8	28.4	22.0

7.4 Electrically Cured Slab B

7.4.1 Visual inspection

Visual observations were carried out on the slab during and after heating. It was observed that at no time did visible cracks appear on the surface of the slab and no 'excessive' localised steam was seen to be emitted from the slab.

7.4.2 Schmidt hammer

Figure 7.17 represents the average (70 results per data point) compressive strength (derived from Schmidt hammer results) for Slab B and the compressive strength of normally cured cubes. From this it can be seen that the electrically cured slab attained a higher initial compressive strength but at later ages (>4 days) the normally cured samples attained a higher compressive strength. The initial compressive strength gain of the electrically cured slab was due to the increased hydration caused by the higher temperatures and the later reduction in strength was due to damage (Kirkbride 1996) caused to the structure of the cement matrix incurred during the initial heating phase. This followed the same trend as that of an equivalently cured cube containing no reinforcement. The percentage gain, when compared to equivalent normally cured samples, for the electrically cured slab was 153.6% at 1 day and –38.7% at 28 days whereas the percentage gain for the electrically cured cube not containing reinforcement was 98.8% at 1 day and –18.9% at 28 days. This was again likely to be due to the greater heating surrounding the reinforcement bars which increased the early age maturity of the slab but induced long-term structural damage.

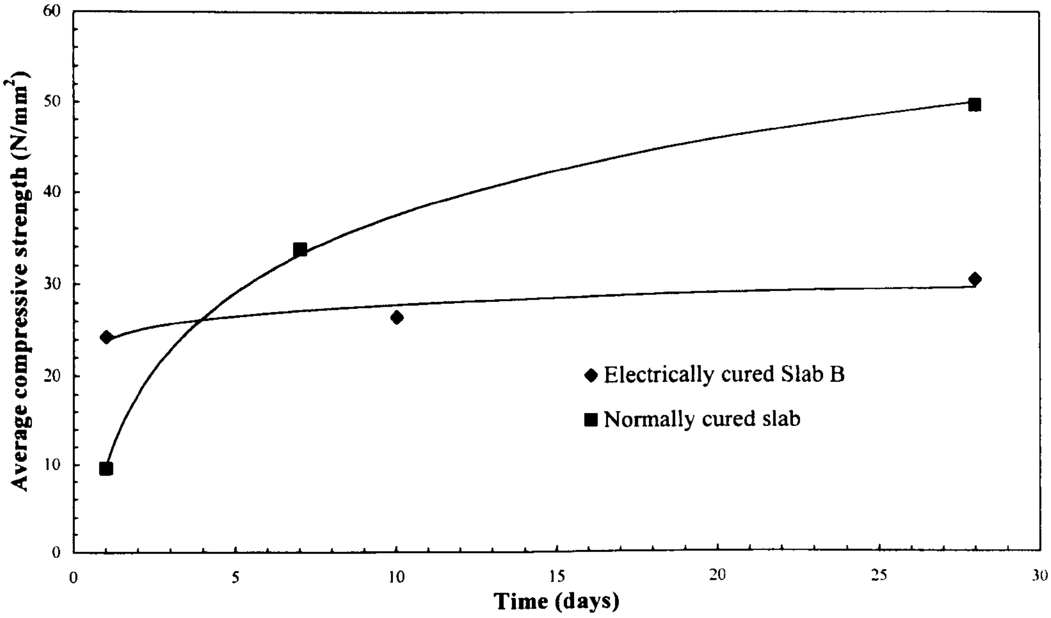

Figure 7.17 – Average compressive strength versus time for electrically and normally cured slab (derived from Schmidt hammer results)

Figure 7.18 represents the average (10 results per data point) compressive strength (derived from Schmidt hammer) perpendicular to the reinforcement bars at various distances from the central reinforcement bar at various ages. From this it can be seen that at 1 day the compressive strength above the reinforcement bars (-100, 0, 100mm) tended to be higher than the compressive strength between the reinforcement bars. This effect was reduced as the Schmidt hammer is a surface measurement of compressive strength (Bungey 1982) and temperature effects were minimised due to the thermal insulation of the concrete (Gibbon and Ballam 1998). This reduced temperature differences at the surface, which in turn reduced the effective differences in maturity. The situation was reversed at 10 days where the compressive strength was lower in the areas adjacent to the reinforcement bars when compared to the areas between reinforcement bars. At 28 days the compressive strength appeared to be contradictory to the 10 days result. This may have been due to a combination of the innate variability of the Schmidt hammer test and the relatively minor differences in surface temperature. However, the highest reduction in compressive strength at 28 days was apparent above the reinforcement bars at -100 and 100mm distance from the central reinforcement bar.

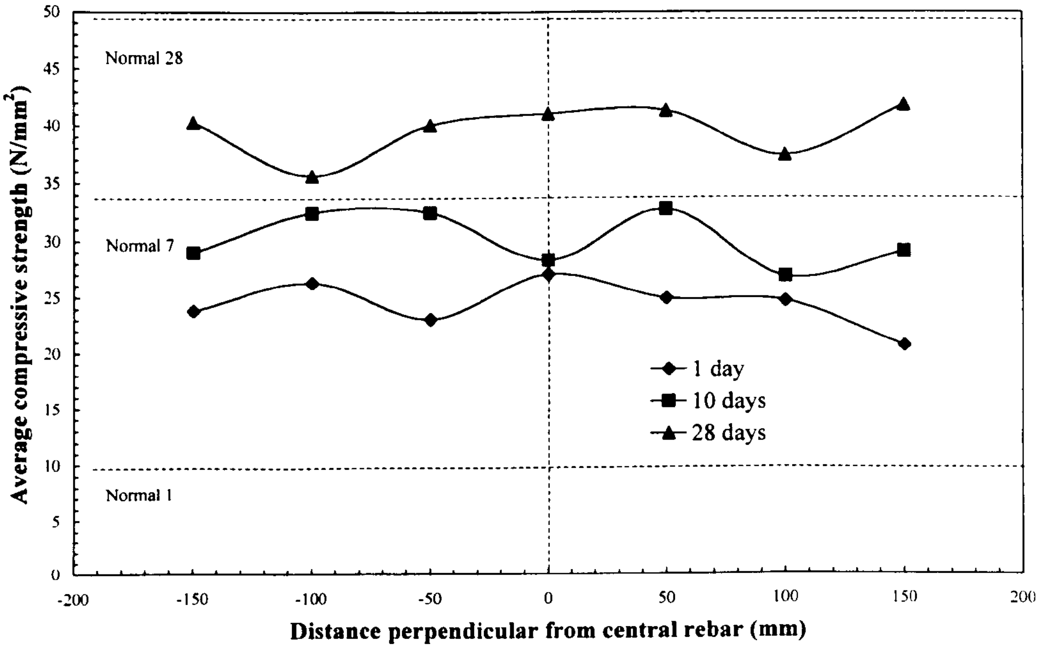

Figure 7.18 – Average compressive strength versus perpendicular distance from central reinforcement bar (derived from Schmidt hammer results)

Figure 7.19 represents the average (7 results per data point) compressive strength (derived from Schmidt hammer results) parallel to the reinforcement bars at various ages. The compressive strength at 1 day showed a similar compressive strength along the reinforcement bars (20N/mm^2). This may have again been due to the small temperature differences that occurred on the surface (Figure 7.27). At 10 and 28 days the compressive strength appeared to be slightly reduced in the central region. This was due to the slightly higher temperatures present at the central region which caused a greater degree of structural damage than the outer regions. The effect was not as pronounced as for the compressive strength of cubes containing no reinforcement because compressive strength derived from crushing values was a more accurate method than compressive strength derived from Schmidt hammer (Bungey 1982).

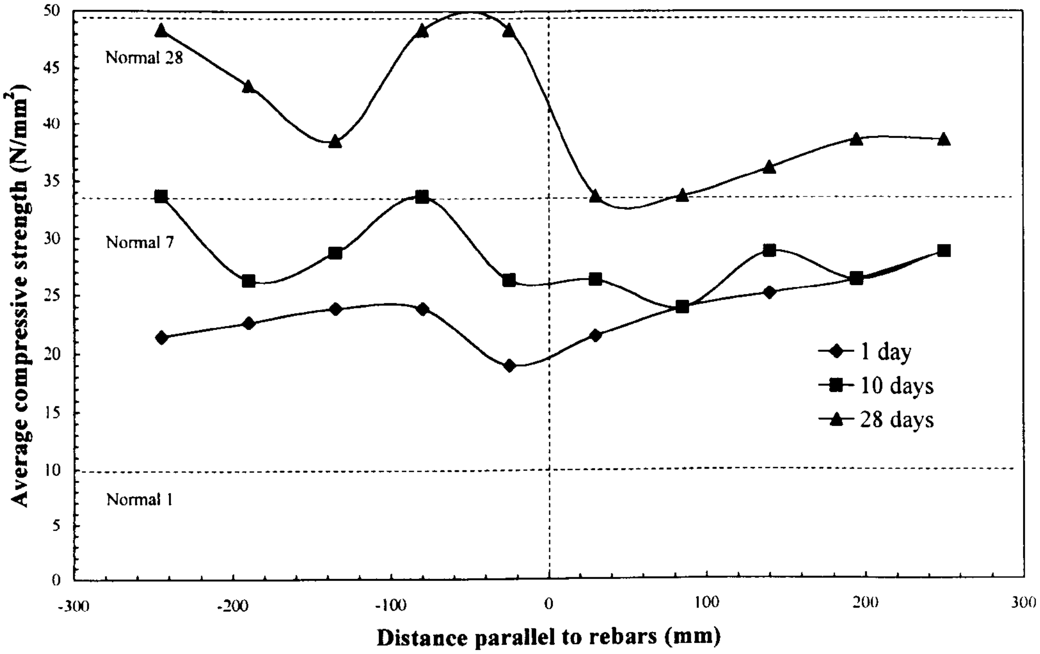

Figure 7.19 – Average compressive strength versus distance from centre of Slab B parallel to reinforcement bars (derived from Schmidt hammer results)

7.4.3 Core failure load

Figure 7.20 shows the average (14 results per data point) electrically cured Slab B (derived from core results) and normally cured slab compressive strengths over time. From this it can be seen that the electrically cured compressive strength attained a significantly higher value at initial ages (1 day) than the normally cured slab. Though the compressive strength of the electrically cured slab did not achieve the same rate of strength increase after 1 day, the 28 day compressive strength of both samples were approximately the same (50 N/mm^2). This long-term strength equivalence was due to the averaging effect of the core failure loads, as within the outer region, compressive strengths were significantly higher than the inner regions. Also, the alteration of the depth at which the maximum temperature was measured for this slab was different to that of the cube set-up.

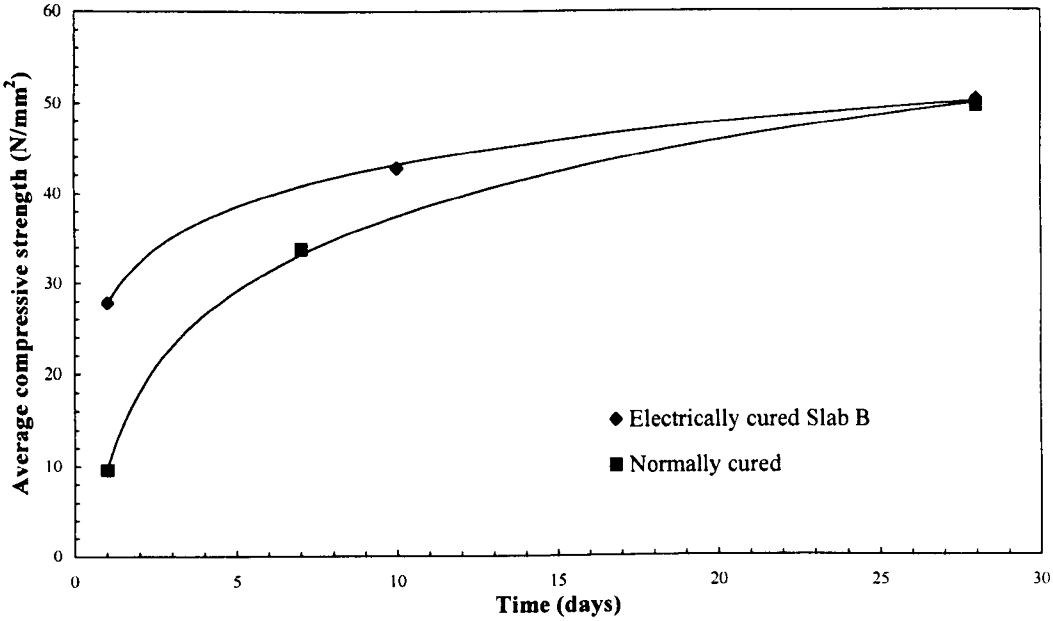

Figure 7.20 – Average compressive strength versus time for electrically and normally cured slab (derived from core results)

Within the cubes the maximum temperature differed by a maximum of 8.2°C when the assumed temperature was 60°C at a depth of 20mm, but within the slab a difference of up to 22.5°C occurred when a depth of 75mm was chosen as a datum and as such a greater degree of temperature range can be assumed to occur within a slab. This shows that the position of the temperature sensors used to determine the heating regime is critical to the short and long-term properties of the concrete, especially when complex geometrys and/or reinforcement bars are used.

Figure 7.21 shows the distribution of compressive strength perpendicular to the reinforcement bars from the central reinforcement bar along the length of Slab B at 28 days. From this it can be seen that over the entire length of the slab, compressive strength at the centre was significantly less than at the outer edges. This was due to the long-term damage to the central structure of the concrete that attained significantly higher temperatures, and thus higher thermomechanical stresses, than the outer regions (Orchard and Barnett 1971).

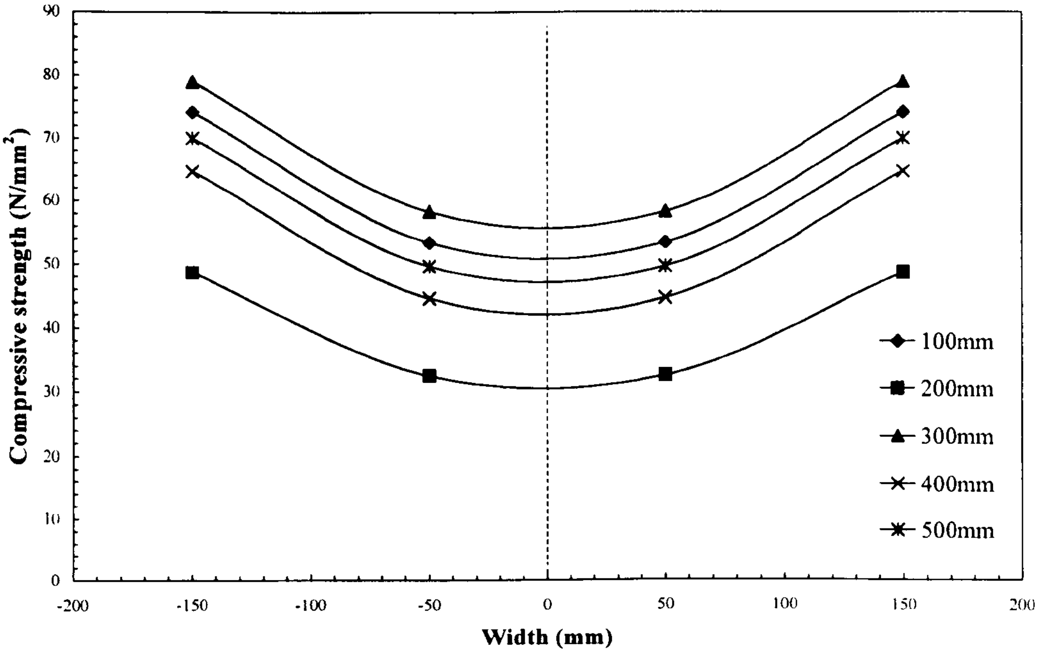

Figure 7.21 – Compressive strength at 28 days perpendicular to reinforcement bars (derived from core results)

The compressive strength profile parallel to the reinforcement bars may have been more complicated than the figure shows. This was due to the fact that no cores could be taken immediately above the reinforcement bars. However, it could be expected from previous results (Figure 7.18), that the 28 day compressive strength was lower in the regions directly above the reinforcement bars. This was again due to the increased temperatures in the region causing increased thermomechanical damage to the long-term structure of the concrete. The effect on internal compressive strength was likely to be greater than the effect on surface compressive strength (derived from Schmidt hammer results) due to the higher temperature gradients internally (Figures 7.24 and 7.25).

Figure 7.22 shows the compressive strength (N/mm^2) distribution (derived from core results) over the surface of Slab B at 28 days. This again shows that the compressive strength was higher in the outer regions than the inner regions reaching a maximum of 75N/mm^2 and a minimum of 30N/mm^2. This minimum value was equivalent to the characteristic strength but did not reach the target mean strength (TMS = 43N/mm^2).

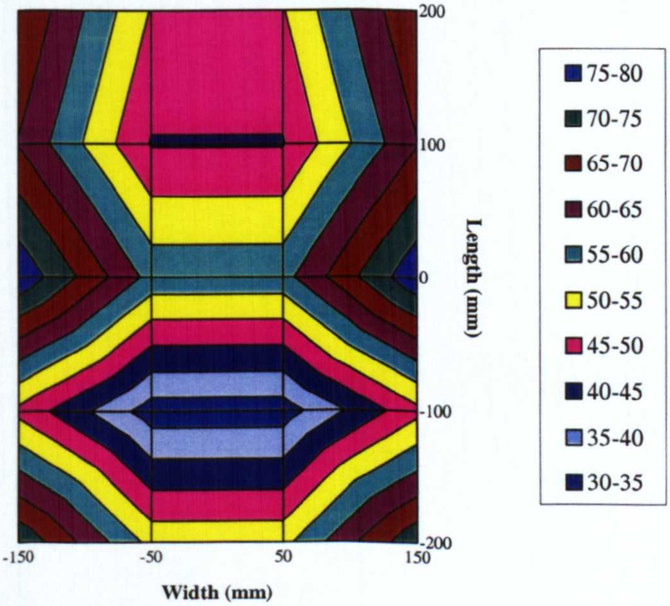

Figure 7.22 – Compressive strength at 28 days (derived from core results)

Figure 7.23 shows the comparison of the average compressive strength derived from the Schmidt hammer and core failure load results for Slab B over time. From this it can be seen that the compressive strength results were significantly different for the two methods of estimating compressive strength. The compressive strength derived from the core failure load results attained a higher value than the values derived from the Schmidt hammer results. This was the opposite result to Figure 7.12 and was due to the position of placement of the temperature sensors. In Slab B, the temperature sensor used to determine the heating regime was placed at a depth of 75mm at the centre of the surface of the slab. This means that the temperature in the centre of the slab did not reach temperatures at which excessive structural damage may occur (approximately >60°C) but did have a higher maturity value than the corresponding surface points. In Slab A the temperature was measured at a depth of 20mm which was likely to cause an excessive degree of structural damage in the centre of the slab where the expected higher temperatures (Orchard and Barnett 1971) were not monitored.

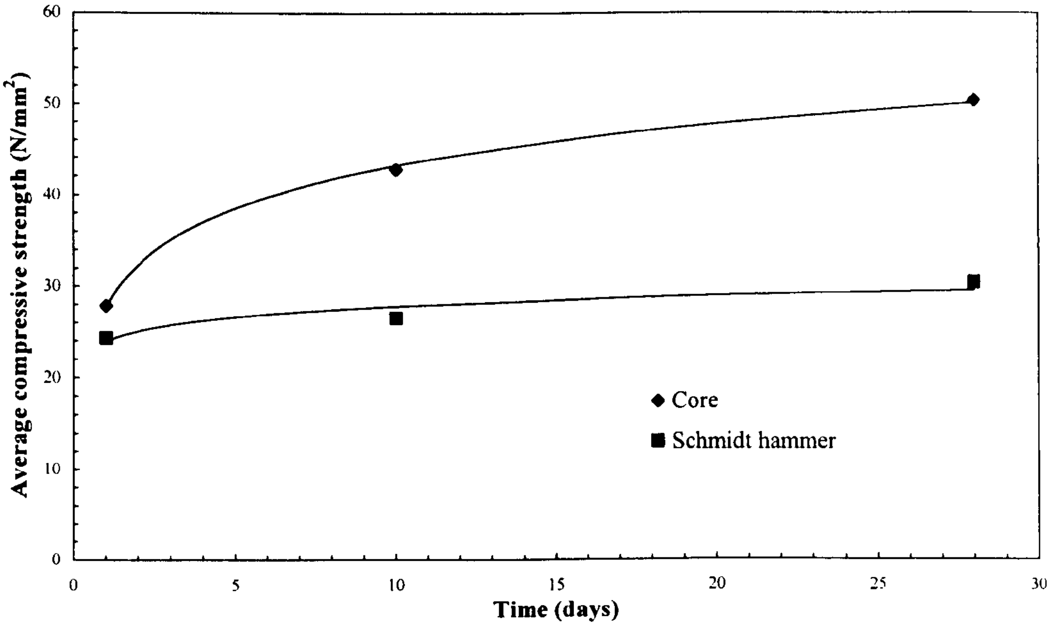

Figure 7.23 – Average compressive strength versus time (derived from core and Schmidt hammer results)

7.4.4 Temperature history

Figure 7.24 shows the temperature profile at various distances from the central reinforcement bar perpendicular to the reinforcement bars at a depth of 75mm at the centre of the Slab B during heating. From this it can be seen that in the vicinity of the reinforcement bars (-100, 0, 100mm) a significantly higher temperature was attained. This was due to the concentration of the field density around the reinforcement bars which thus increased the temperature. It can also be seen that the outer edges attained a lower temperature at all ages than the sensors placed between the reinforcement bars. This was due to cooling incurred at the external surface (Orchard and Barnett 1971) and shows the importance of adequate monitoring of the temperature gradients, thermal stresses and maturity. A possibility of reducing these gradients may be to reduce the spacing between reinforcement bars.

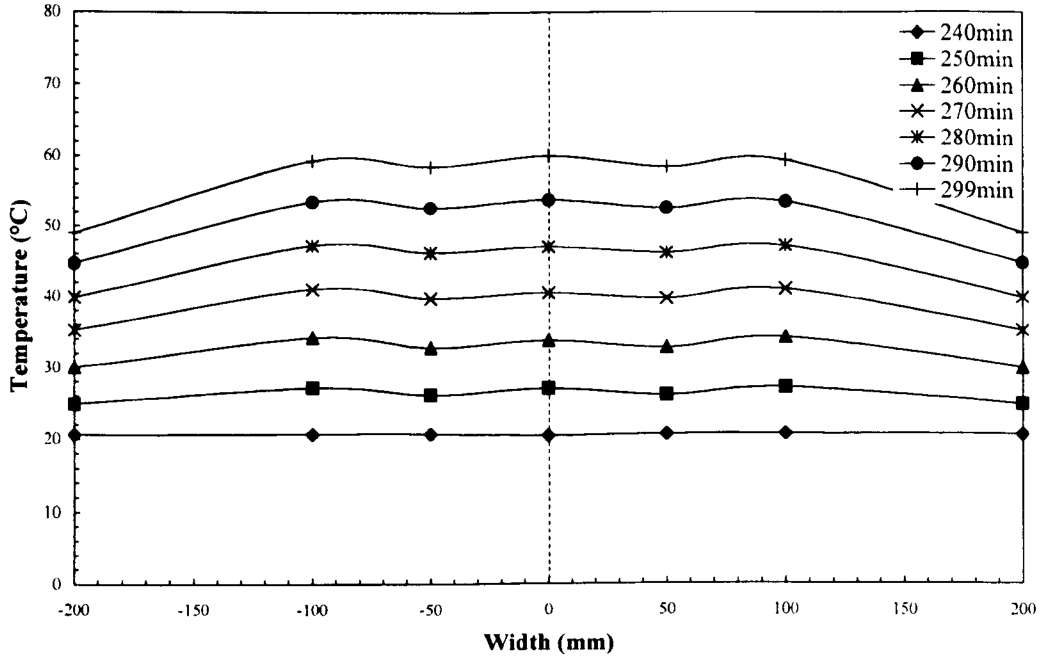

Figure 7.24 - Temperature profile perpendicular to the reinforcement bars at the centre of Slab B at a depth of 75mm

Figure 7.25 shows the temperature profile at various distances from the central reinforcement bar perpendicular to the reinforcement bars at a depth of 20mm at the centre of the slab during heating. From this it can be seen that the overall temperatures and temperature gradients present near the surface were greatly reduced when compared to the equivalent temperature gradients at greater depths. This was due to the insulating thermal properties of concrete (Gibbon and Ballam 1998) and also by the comparatively similar field densities that were likely to be present away from the immediate vicinity of the reinforcement bars. This again shows the importance of knowing the temperature history of the entire sample in order to estimate its short and long-term properties.

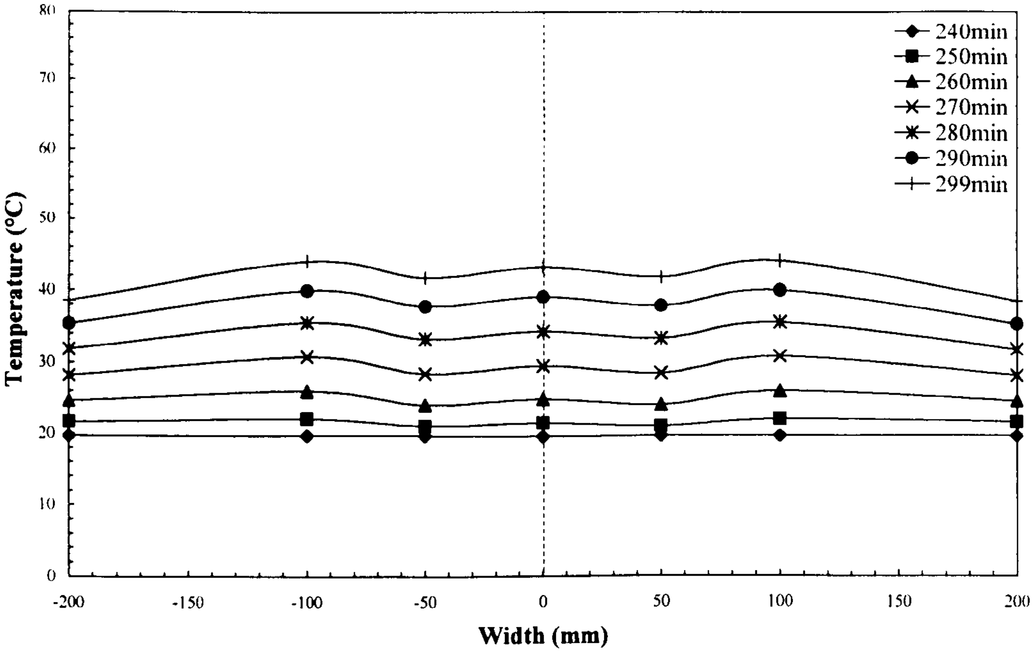

Figure 7.25 - Temperature profile perpendicular to the reinforcement bars at the centre of Slab B at a depth of 20mm

Figure 7.26 shows the temperature profile of certain depths at the centre of the slab and of a thermistor directly in contact with the reinforcement bar. From this it can be seen that the reinforcement bar did not attain as high a temperature as the concrete immediately above it. This shows that the reinforcement bar did not act significantly in heating directly the concrete. This was due to its low electrical resistance which did not allow significant heating (Wilson and Gupta 1996). The reinforcement bar may have acted as a cooling agent, allowing the heat to escape into the environment by direct heat conduction to the external portion of the reinforcement bar surface which was exposed to the ambient temperatures present (approximately 20°C).

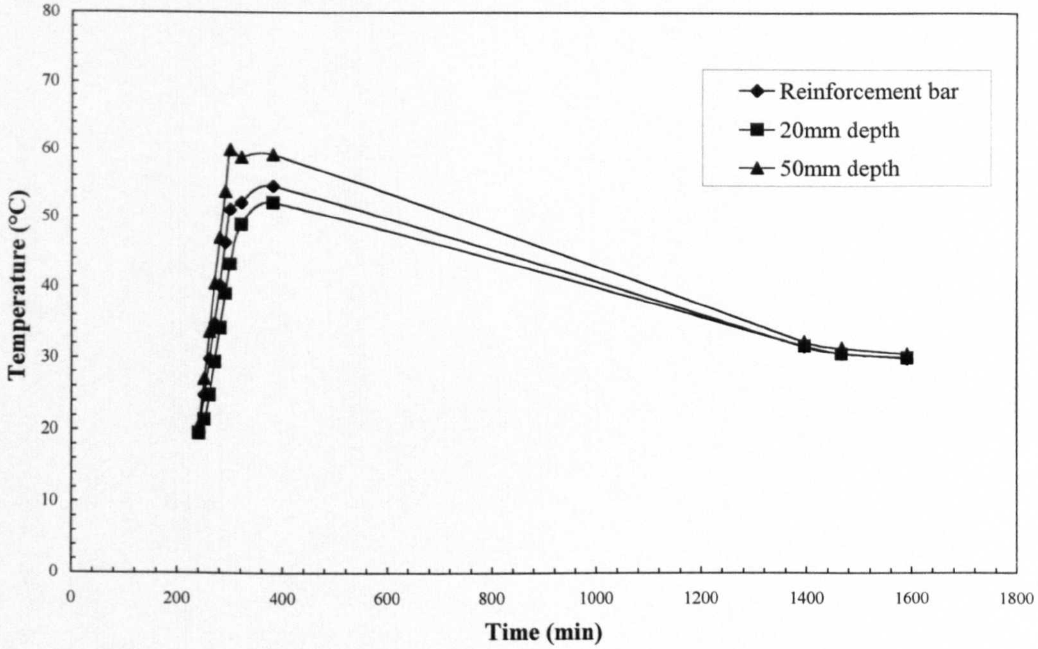

Figure 7.26 – Temperature history of differing depths at the centre of Slab B and reinforcement bar

Figure 7.27 shows the cross sectional temperature along the length of the central reinforcement bar for various ages. From this it can be seen initially (prior to heating at 240 min), temperatures were evenly distributed with a minimum temperature of 19°C in the upper region (<50mm) and a maximum temperature of 21°C in the lower region (>100mm depth). This initial variation was caused by the exothermic hydration reactions as the concrete cured normally and the increase at lower depths was due to the added insulation of the mould shuttering.

During heating, the maximum temperature was always between the reinforcement bar (40mm) and the bottom electrode (150mm). This was due to the current being passed only between the two electrodes, thus increasing the temperature rise of the concrete in this area. The maximum temperature throughout heating was also always in the central region of the slab. This was due to the thermal insulating properties of concrete (0.6-2.6 W/m°C) (Gibbon and Ballam 1998) which did not allow the temperature to be quickly distributed.

The maximum temperature gradient could be seen to occur vertically in the central region and decreases with depth. This attained a maximum of approximately 0.25°C/mm at 299 minutes and was due to the comparatively low ambient temperature (approximately 21°C at the surface). The vertical temperature gradients were not as large at the lower surface due to the thermal insulating properties of the mould shuttering.

The temperature gradient along the length of the reinforcement bar was relatively minor in comparison (maximum of 0.05°C/mm at 380 minutes). This was due to the similarity of the layout along the length of the slab, with a reinforcement bar always in the same relative position. Thus, the only thermal gradients that could occur laterally were those influenced by the bulk thermal insulation properties of the concrete and as such the concrete tended to have a higher central temperature (Orchard and Barnett 1971).

Relatively high temperature gradients could be seen 1.5 hours after heating had ended. The temperature contours were not centred upon the central reinforcement bar position, but instead spread evenly throughout the length of the sample. The equivalent temperature regions could be seen to be enlarging as heat is dissipated to the ambient atmosphere at the edges of the sample (Orchard and Barnett 1971). After 1 day, the temperature recorded at the central region was 32°C, which was still significantly higher than the ambient temperature.

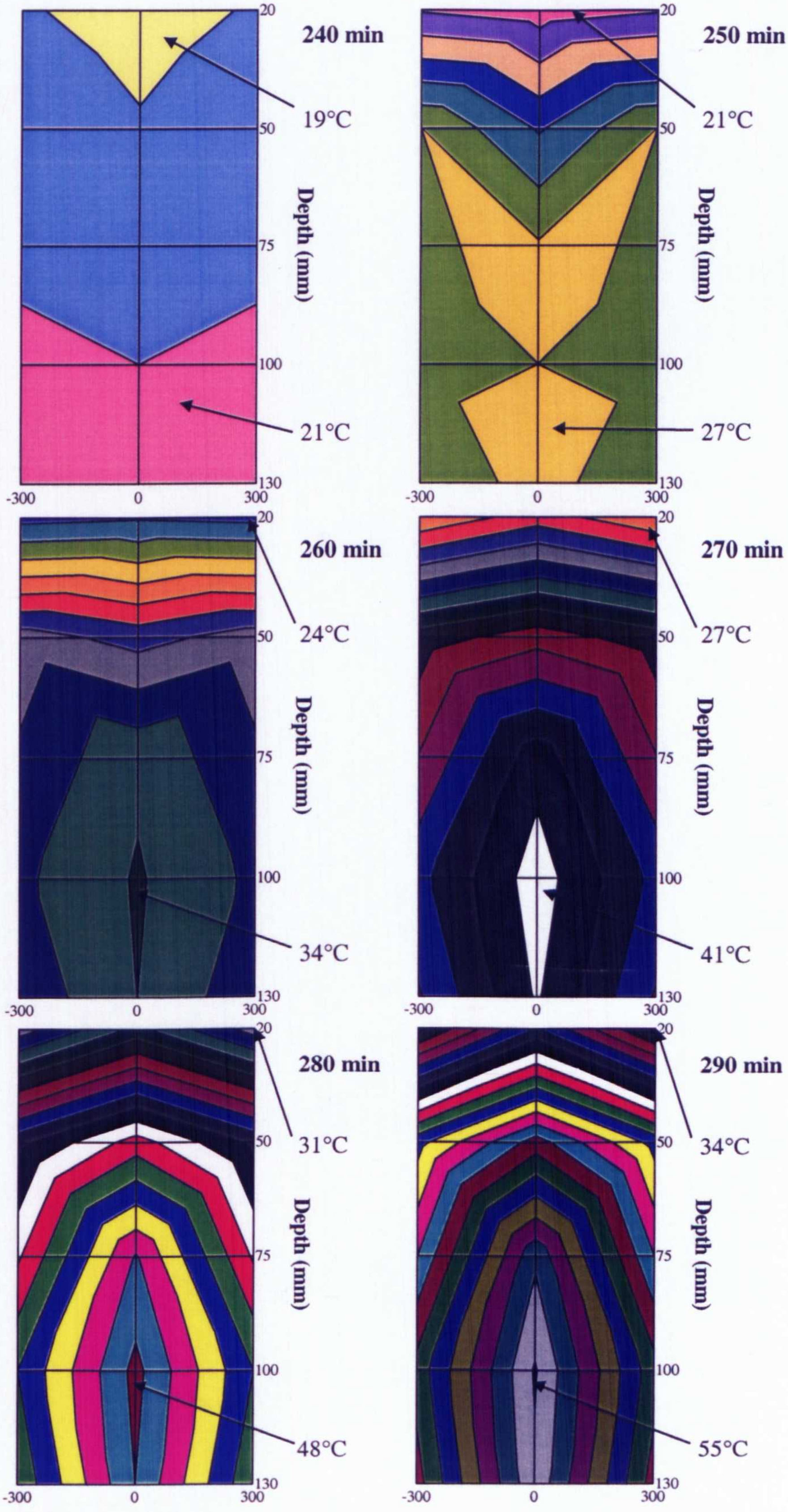

Figure 7.27 – Cross-sectional temperature profile over time along the length of the central reinforcement bar

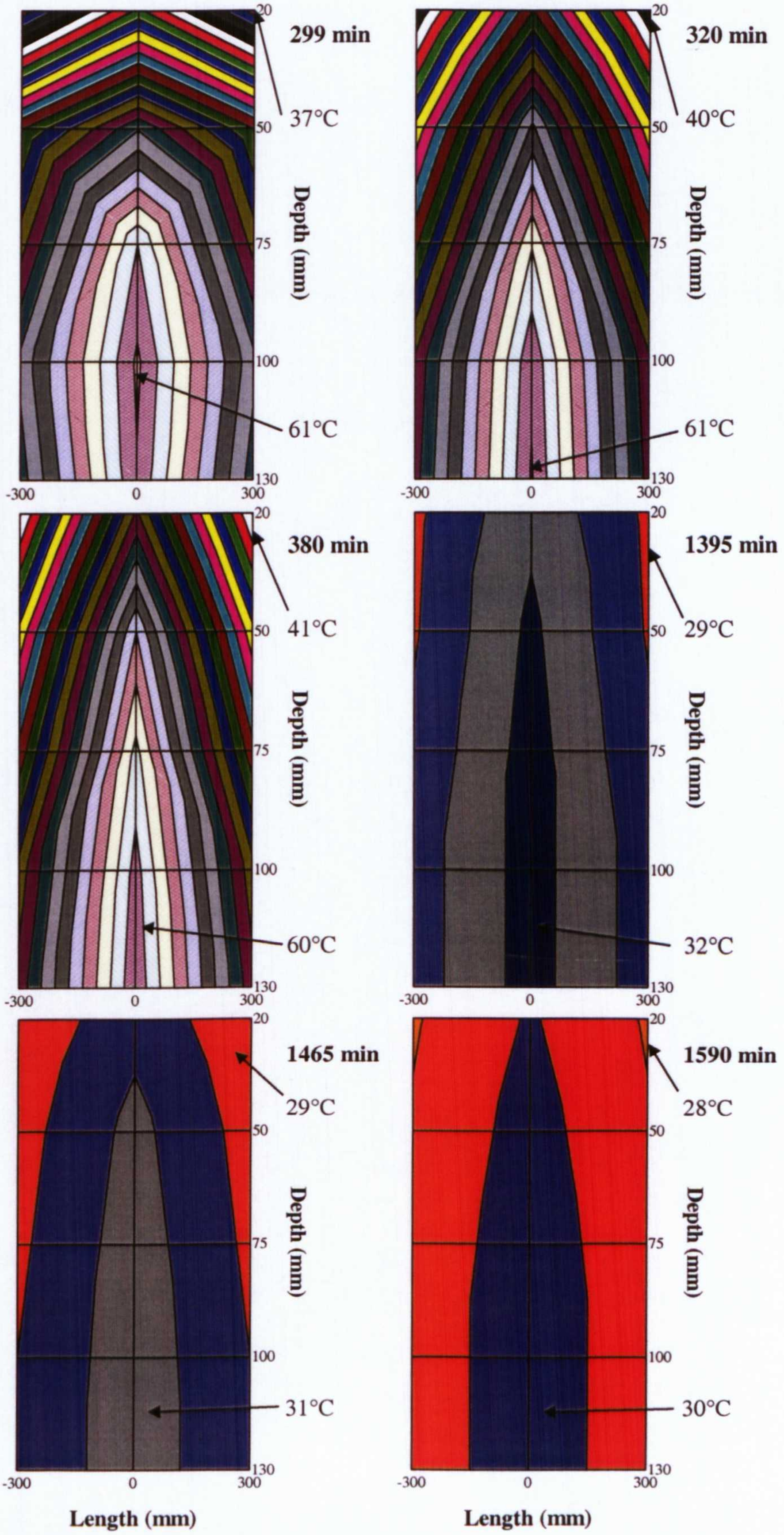

Figure 7.27 – Cross-sectional temperature profile over time along the length of the central reinforcement bar (continued)

A full list of temperatures over various ages can be seen in Table 7.2.

Table 7.2 - Temperature of Slab B at various ages

Time after gauging (min)	**Sensor number (from Chapter 3)**									
	1	**2**	**3**	**4**	**5**	**6**	**7**	**8**	**9**	**10**
240	19.6	20.1	20.5	21.0	21.4	20.1	20.7	20.9	21.1	21.3
250	21.5	24.9	27.1	27.0	27.2	21.9	27.0	26.9	26.9	26.6
260	24.9	30.6	33.8	34.1	34.0	24.7	31.5	32.2	32.8	32.3
270	29.5	36.6	40.6	41.5	41.1	28.1	35.4	37.0	38.7	37.9
280	34.3	42.5	47.1	48.3	48.0	31.5	39.7	31.8	44.0	43.2
290	39.1	48.5	53.8	55.1	54.8	34.7	44.6	47.0	49.4	48.6
299	43.3	53.9	60.0	61.2	60.9	37.5	48.9	51.6	54.3	53.5
320	49.0	55.2	58.9	60.8	61.1	40.0	45.3	48.7	52.2	52.6
380	52.2	57.0	59.3	60.4	60.8	40.9	45.3	48.3	51.4	52.4
1395	31.8	32.2	32.4	32.4	32.4	29.8	29.9	30.2	30.5	30.5
1465	30.7	31.3	31.5	31.6	31.6	29.2	29.6	29.8	30.0	30.1
1590	30.1	30.4	30.6	30.6	30.6	28.9	29.1	29.2	29.4	29.4
	Sensor number									
	11	**12**	**13**	**14**	**15**	**16**	**17**	**18**	**19**	**20**
240	19.7	20.2	20.7	21.1	21.4	19.7	20.7	19.7	20.6	19.9
250	22.1	25.8	27.2	27.4	27.3	21.1	26.2	21.7	24.9	24.9
260	26.0	31.8	34.2	34.5	33.9	24.1	32.8	24.6	30.0	29.9
270	30.8	37.7	41.1	41.8	40.6	28.5	39.8	28.2	35.2	34.9
280	35.5	43.3	47.2	48.3	47.0	33.3	46.2	31.8	39.9	40.3
290	40.0	49.1	53.5	54.8	53.5	37.8	52.6	35.3	44.7	46.4
299	44.1	54.3	59.3	60.7	59.2	41.8	58.4	38.5	49.0	51.2
320	47.9	53.2	56.9	59.0	58.6	48.2	58.4	42.0	49.1	52.2
380	49.9	54.1	56.6	58.2	58.3	50.9	58.4	45.0	50.9	54.6
1395	31.6	31.9	32.1	32.2	32.1	31.7	32.3	31.0	31.5	31.7
1465	30.8	31.1	31.4	31.4	31.4	30.8	31.4	30.4	30.8	30.7
1590	29.9	30.2	30.3	30.4	30.3	30.0	30.5	29.5	29.9	30.0

7.5 Conclusions

1. Both the Schmidt hammer and core failure load was found to be acceptable in estimating compressive strength for electrically cured slabs.

2. Cracks were found to be present on the surface of the concrete slab which used a depth of 20mm as a temperature datum during heating but no cracks were found on the slab that used a depth of 75mm as a temperature datum.

3. Similar compressive strength trends were found for both the electrically cured slabs and cubes with higher initial compressive strength and reduced compressive strength at later ages (when compared to normally cured samples).

4. It was found from the Schmidt hammer results that the regions directly above the reinforcement bars attained a higher initial compressive strength but a lower long-term compressive strength when compared to the regions between the reinforcement bars. This was due to higher temperatures in the immediate vicinity of the reinforcement bars as the electric field density increased around the electrodes.

5. The results show that compressive strength was similar along the entire length of the concrete slab and that a slight increase was apparent in the central region at early ages. This was due to the increased temperature of the central region because of the thermal insulating properties of concrete.

6. Core derived compressive strength showed higher strengths parallel to the reinforcement bars in the outer regions at 56 days than the inner regions. This was due to the reduced thermomechanical damage in the outer regions from relatively low temperatures incurred during heating.

7. Differences were found between the strength predicted from the Schmidt hammer and core failure load. This was found to be due to the Schmidt hammer being a surface measurement and the cores being taken from within the concrete where different temperature histories occurred during heating which resulted in different values of compressive strength.

8. Porosity, density and water absorption were found to be approximately similar over the entire surface of the slab.

9. The temperature immediately above the reinforcement bars was found to be greater than the temperature in the region between the reinforcement bars. This was due to electric field density increases around the reinforcement bars which increased the heating rate in this area.

10. The temperature of the reinforcement bar was approximately the same as the surrounding concrete at the depth at which it was placed. This implied that the reinforcement bars did not heat up directly, but instead acted as pure electrodes. This was likely to be due to the relatively low resistance of reinforcement bars which precluded ohmic heating.

11. The maximum temperatures were seen to be present between the reinforcement bars and the plate electrode. This was found to be due to current passing only through this region between the electrodes. The area above this region was only heated by thermal conduction and as such attained relatively high thermal gradients between the reinforcement bar and the ambient exposed surface.

Chapter 8 – SUMMARY OF CONCLUSIONS AND FUTURE RESEARCH

8.1 Introduction

This chapter provides a summary of conclusions from the results and discussions of Chapters 4-7 and also suggestions for future research in the field of Direct Electric Curing (DEC).

8.2 Summary of Conclusions

The experimental and theoretical results presented in this thesis prove that mortar and concrete can be successfully produced using DEC with a wide range of strength and durability properties using alternative heating regimes, mixes and reinforcement. In general, it was found that the initial strength properties of both mortar and concrete were substantially improved using DEC. The samples show higher initial strengths but slightly lower long-term strengths.

8.2.1 DEC of mortar

It was found that both the short-term (3 days) and long-term (28 days) compressive strengths could be favourably altered using DEC by the use of variable delay periods, rates of temperature rise, maximum temperatures and isothermal periods.

Over a range of W/C ratios electrically cured mortar samples achieved substantially higher initial (3 days) compressive strengths than normally cured samples and the proportional effectiveness of electrically cured mortar specimens was found to be increased at higher W/C ratios.

Long-term (28 day) compressive strength was not adversely affected by DEC in the samples tested although the rate of compressive strength development at later ages (>28 days) was reduced when compared to normally cured samples. The reduced rate of compressive strength development at later ages in mortar was likely to be due to differential expansion of the aggregates and the cement matrix incurred by heating.

The initial drop in resistance during heating was due to water absorption by aggregates which reduced the effective path length of the electrical current. Resistance can be used as a guide to the amount of water in mortar with higher W/C ratios giving lower resistances at all ages but there appeared to be little correlation between 3 days mortar compressive strength and resistance. Mortar behaved as a dielectric having a reduced apparent resistance at higher temperatures. This effect became negligible after approximately 3 days when the sample temperature approached ambient levels.

Maturity was found to be a good indication of compressive strength when DEC was used. The value of maturity during cooling was significantly higher than the maturity increase measured during the initial heating of samples. This meant that accurate monitoring of temperature after the initial heating was concluded was required in order to estimate compressive strength.

The durability of mortar samples (as measured by the ISAT) did not appear to be adversely effected by DEC. This was likely to be due to capillary pore refinement during heating.

8.2.2 DEC of concrete

It was found that, for a range of different concrete mixes, short-term compressive strengths could be substantially improved by using DEC and varying delay periods, rates of temperature rise and maximum temperatures.

The compressive strength of normally cured concrete at 24 hours was attained using DEC in 4 hours and compressive strengths of up to 26N/mm^2 were readily achievable using DEC after 1 day. At 1 day, all samples of varying W/C ratios cured using DEC attained a higher compressive strength than normally cured samples.

Short delay periods (1 hour) tended to give higher initial compressive strengths, but reduced long-term compressive strengths when compared to longer delay periods (4 hours). The reduction in long-term compressive strengths was likely to be due to increased microcracking in the short delay period samples which reduce long-term strength. The greatest long-term compressive strength (≥28 days) was found to occur when heating commenced at 3 hours after mixing. This was due to high early age compressive strengths combining with limited microstructural damage to produce relatively high long-term compressive strengths.

For equivalent mixes and heating regimes, a higher maximum temperature produced higher 1 day compressive strengths but lower long-term (≥28 day) compressive strengths. This was likely to be due to increased thermomechanical damage and moisture loss at the higher temperatures.

The splitting tensile strength and flexural tensile strength of concrete cured using DEC was found to follow a similar trend as compressive strength of DEC cubes with higher initial temperatures causing increased initial tensile strength but lower long-term tensile strength.

Concrete was found to behave as a dielectric with a lower apparent resistance at higher temperatures. This implied that concrete temperature should be closely monitored if resistance is to be used in predicting the progress of hydration. The resistance at 1 day was not found to be proportional to compressive strength but at 3 days a logarithmic relationship was found to exist.

It was found that, when compared to normally cured samples, the DEC splitting tensile strength had a lower percentage tensile strength increase at 1 day and a higher percentage tensile strength loss at 28 days than the equivalently cured DEC compressive strength tests. This was likely to be due to microcracks acting as stress concentrators during tensile loading.

Saul's maturity values were found to be more accurate in determining the compressive strength of normally cured samples than electrically cured samples. Maturity values were also found to underestimate the compressive strength of electrically cured samples at early ages and overestimate compressive strength at later ages.

Durability of concrete (as measured by ISAT) did not appear to be adversely effected when using DEC. This was likely to be due to the refinement of capillary pores during heating. It was also found that ISA 10 values were related to compressive strength.

Porosity, density and water absorption was found to be similar for both electrically and normally cured samples.

Temperature gradients increased during heating and also the maximum temperature within the electrically heated (150x150x150mm) cubes and (400x100x100mm) beams were in the central region with minimum temperatures immediately adjacent to the exposed concrete surface.

Using a scanning electron microscope (SEM), both normally and electrically cured samples were found to exhibit a dense microstructure associated with C-S-H formation at all ages, but electrically cured samples tended to have a less uniform structure with coarser pores being more prevalent. It was also found that higher concentrations and lengths of ettringite were found initially in electrically cured samples.

8.2.3 DEC of concrete containing admixtures and additives

Using combinations of DEC and admixtures or additives for a similar mix design could achieve a large variability of the short-term (1 day) and long-term (28 days) compressive strengths.

The maximum temperature of electrically cured air entrained concrete was found to influence compressive strength at all ages, with higher temperatures producing lower compressive strength. This was likely to be due to increased microcracking around the entrained air bubbles at the higher temperatures. The effectiveness of electrical curing in improving compressive strength on mixes containing air entrainment was found to be reduced when compared to similarly designed mixes not containing air entrainment.

The reduction of compressive strength at 28 days for electrically cured air entrained concrete when compared to normally cured concrete was found to be dependent on the percentage of air entrainment, with higher levels of air entrained producing greater reductions in compressive strength.

Normally cured samples containing a superplasticiser attained a higher compressive strength at all ages than a similar mix without superplasticiser. The electrically cured concrete samples containing superplasticiser cured after a delay of 3 hours acted in an identical manner to a heated mix without superplasticiser with a delay period of 1 or 2 hours. This was due to the superplasticiser mix having a greater period before the initial set which effectively reduced the delay period. It was also found that both normally and electrically cured concrete containing a retarder behaved in a similar manner to concrete containing a superplasticiser.

It was found that normally cured samples containing an accelerator attained a higher compressive strength at all ages than a similar mix without accelerator. The electrically cured mix with accelerator cured after a delay of 3 hours acted in a similar manner to a heated mix without accelerator with a delay period of 4 hours. This was due to the mix with accelerator having a reduced period before initial set which effectively reduced the delay period.

It was found that with cement replacement by PFA the effectiveness of electrical curing in improving compressive strength was reduced at 1 day. This was likely to be due to the concrete containing PFA having an extended period before initial set, thus being less able to resist the thermomechanical stresses incurred during heating.

There exists a relationship between ultrasonic pulse velocity (UPV), density, percentage of air entrainment and compressive strength for both normally and electrically cured concrete samples.

8.2.4 DEC of concrete containing reinforcement

The compressive strength of the slabs tested after accelerated curing by DEC was found to be dependent on the method of testing (Schmidt hammer or cores) and the placement of the temperature datum.

Similar compressive strength trends were found for both the electrically cured slabs and cubes with higher initial compressive strength and reduced compressive strength at later ages (when compared to normally cured samples).

Both the Schmidt hammer and core failure load was found to be acceptable in estimating compressive strength for electrically cured slabs although differences were found between the strength predicted from the Schmidt hammer and core failure load. This was found to be due to the Schmidt hammer being a surface measurement and the cores being taken from within the concrete where different temperature histories occurred during heating which resulted in different values of compressive strength.

It was found from the Schmidt hammer results that the regions directly above the reinforcement bars attained a higher initial compressive strength but a lower long-term compressive strength when compared to the regions between the reinforcement bars. This was due to higher temperatures in the immediate vicinity of the reinforcement bars as the electric field density increased around the electrodes.

The results showed that compressive strength was similar along the entire length of the concrete slab and that a slight increase was apparent in the central region at early ages. This was due to the increased temperature of the central region because of the thermal insulating properties of concrete.

Porosity, density and water absorption were found to be approximately similar over the entire surface of the slab.

The temperature immediately above the reinforcement bars was found to be greater than the temperature in the region between the reinforcement bars. This was due to electric field density increases around the reinforcement bars which increased the heating rate in this area. The maximum temperatures were seen to be present between the reinforcement bars and the plate electrode. This was found to be due to current passing only through this region between the electrodes.

8.3 Recommendations for Future Research

Further research will be required in order to produce workable standards for the use of DEC in producing concrete. Until this is achieved and a recognition of the benefits of DEC over more traditional forms of accelerated curing become more widespread, the DEC of concrete will remain a highly specialised and relatively unused procedure.

The durability of concrete cured using DEC could be further investigated by testing of specimens for resistance to frost damage. This would involve freezing and thawing specimens for a specified number of cycles and then comparing results with other forms of curing. DEC undoubtedly has major benefits compared to normal curing in resistance to frost attack due to the heating of concrete in the process. However, investigations need to completed to study the effect of edges and corners present in most cementitious products.

The resistance of DEC cured specimens should also be tested regarding other aspects of durability including sulphate attack, chloride ingress and carbonation. This can be achieved by utilising a number of standard testing procedures to again compare DEC results with other forms of curing.

A special area for concern regarding heat accelerated hydration is delayed ettringite formation. Long-term testing is required to ensure DEC is not especially susceptible to this form of durability problem.

The concerns considering shrinkage of specimens cured using DEC need to be assessed and compared to other forms of accelerated and normal curing. This is due to the relatively large amount of moisture lost with DEC. The effects of shrinkage may be reduced by the increased early age strength but the long term effects of DEC need to be investigated.

The long term creep of specimens cured using DEC also needs to be considered. This will be greatly influenced by the relatively low gain in strength after the initial curing as well as the usual factors affecting the creep of concrete.

The further development of DEC into practical applications such as precast products requires research. This should concentrate on the innate variability of specimens due to reinforcement and geometry affecting the electrical field density and heat generation.

The investigation of DEC as relating to in-situ situations needs to be considered. Health and safety issues and practicality of use are of importance due to the inherently dangerous nature of passing large currents through specimens in the relatively uncontrolled environment of a construction site. This could be achieved by small scale field trials and the analysis of previous in-situ procedures used in different countries.

A detailed investigation of the economical aspects of DEC in real situations is required to understand the feasibility of using DEC as compared to other accelerating curing methods. This will require an analysis of capital expenditure, maintenance, training, cost of use, resale value and productivity levels.

A computer modelling of DEC as applied to differing geometrical forms and mixes by the use of finite element analysis (FEA) is necessary. This will require the modelling specifically of the changing electrical field density and resistance. The resistance is affected by time, properties of the mix constituents, varying temperature and moisture content. The electrical field density is affected by the placement of reinforcement, the geometry of the specimen, the resistance and the required temperature rise.

REFERENCES

ABBASI, A.F. and AL-TAYYIB, A.J. 'Effect of hot weather on modulus of rupture and splitting tensile strength of concrete'. Cement and Concrete Research, Vol. 15, 1985, pp. 233-244.

ACI COMMITTEE 308. 'Recommended practice for hot weather concreting'. American Concrete Institute, Detroit, ACI 305R-77, 1992.

AL-GAHTANI, H.J., ABBASI, A.G.F. and AL-AMOUDI, O.S.B. 'Concrete mixture design for hot weather: experimental and statistical analyses'. Magazine of Concrete Research, Vol. 50, No. 2, 1998, pp. 95-105.

AMERICAN SOCIETY FOR THE TESING OF MATERIALS. ASTM C1074-1998. 'Standard practice for estimating concrete strength by the maturity method'.

AMERICAN SOCIETY FOR THE TESING OF MATERIALS. ASTM C1202-1997. 'Standard test method for electrical indication of concretes ability to resist chloride ion penetration'.

BAJZA, A. and ROUSEKOVA, I. 'Effect of heat treatment conditions on the pore structure of cement mortar'. Cement and Concrete Research, Vol. 13, 1983, pp. 747-750.

BAKKER, R.F.M. 'Permeability of blended cement structures'. Proceedings of the 1st International Conference on the use of Fly Ash, Silica Fume, Slag and Other Mineral By-products in Concrete, ACI Special Publication SP-79, 1983, pp. 589-605.

BAMFORTH, P.B. 'Performance of concrete structures'. Proceedings from the National Seminar on the Use of PFA in Construction, February 1992.

BAZANT, Z.P. and KAPLAN, M.F. 'Concrete at high temperatures'. Longman, 1996.

BERGE, O. 'Improving the properties of hot-mixed concrete using retarding admixtures'. ACI Journal, Vol. 73, No. 29, 1976, pp. 394-398.

BERHANE, Z. 'The behaviour of concrete in hot climates'. Materials and Structures, Vol. 25, 1992, pp. 157-162.

BERRY, E.E., and MALHOTRA, V.M. 'Fly ash for use in concrete - a critical review', American Concrete Institute Journal, Vol. 77, No. 8, 1980, pp. 59-73.

BREDENKAMP, S., KRUGER, D. and BREDENKAMP, G.L. 'Direct electric curing of concrete'. Magazine of Concrete Research, Vol. 45, No. 162, March 1993, pp. 71-74.

BRITISH STANDARDS INSTITUTION. BS 12: 1996. 'Portland cement'.

BRITISH STANDARDS INSTITUTION. BS EN 196: Part 2: 1995. 'Chemical analysis of cement'.

BRITISH STANDARDS INSTITUTION. BS 451: Part 2: 1994. 'Method of testing fly ash: determination of fineness by wet sieving'.

BRITISH STANDARDS INSTITUTION. BS 812: Part 2: 1995. 'Method for determination of physical properties'.

BRITISH STANDARDS INSTITUTION. BS 812: Part 103: 1985. 'Method for determination of particle size distribution'.

BRITISH STANDARDS INSTITUTION. BS 812: Part 112: 1995. 'Method for determination of aggregate impact value (AIV)'.

BRITISH STANDARDS INSTITUTION. BS 882: 1983. 'Aggregates from natural sources for concrete'.

BRITISH STANDARDS INSTITUTION. BS 890: 1995. 'Specification for building limes'.

BRITISH STANDARDS INSTITUTION. BS 1377: Part 2: 1990. 'Methods of testing for soils for civil engineering purposes. Classification tests'.

BRITISH STANDARDS INSTITUTION. BS 1881: Part 5: 1970. 'Methods of testing hardened concrete for other than strength'.

BRITISH STANDARDS INSTITUTION. BS 1881: Part 102: 1983. 'Method for determination of slump'.

BRITISH STANDARDS INSTITUTION. BS 1881: Part 104: 1983. 'Method for determination of Vebe time'.

BRITISH STANDARDS INSTITUTION. BS 1881: Part 106: 1983. 'Method for determination of air content of fresh concrete'.

BRITISH STANDARDS INSTITUTION. BS 1881: Part 108: 1983. 'Method for making test cubes from fresh concrete'.

BRITISH STANDARDS INSTITUTION. BS 1881: Part 111: 1983. 'Method of normal curing of test specimens'.

BRITISH STANDARDS INSTITUTION. BS 1881: Part 112: 1983. 'Methods of accelerated curing of test cubes'.

BRITISH STANDARDS INSTITUTION. BS 1881: Part 114: 1983. 'Methods for determination of density of hardened concrete'.

BRITISH STANDARDS INSTITUTION. BS 1881: Part 115: 1986. 'Specifications for compression testing machines for concrete'.

BRITISH STANDARDS INSTITUTION. BS 1881: Part 116: 1986. 'Method for determination of compressive strength of concrete cubes'.

BRITISH STANDARDS INSTITUTION. BS 1881: Part 117: 1983. 'Method for determination of tensile splitting strength'.

BRITISH STANDARDS INSTITUTION. BS 1881: Part 118: 1983. 'Method for determination of flexural strength'.

BRITISH STANDARDS INSTITUTION. BS 1881: Part 125: 1986. 'Methods for mixing and sampling of fresh concrete'.

BRITISH STANDARDS INSTITUTION. BS 1881: Part 202: 1986. 'Recommendations for surface hardness testing by rebound hammer'.

BRITISH STANDARDS INSTITUTION. BS 1881: Part 203: 1986. 'Recommendations for measurement of velocity of ultrasonic pulses in concrete'.

BRITISH STANDARDS INSTITUTION. BS 3148: 1980. 'Water for making concrete'.

BRITISH STANDARDS INSTITUTION. BS 4550: Part 3: 1978. 'Methods of testing cement'.

BUNGEY, J. H. 'The testing of concrete in structures'. Surrey University Press, 1982.

CARINO, N.J., LEW H.S. and VOLZ, C.K. 'Early age temperature effects on strength prediction by the maturity method'. ACI Journal, Vol. 80, No. 10, 1983, pp. 93-101.

CATHER, B. 'Curing: the true story?'. Magazine of Concrete Research, Vol. 46, No. 168, March 1994, pp. 157-161.

CZERNIN, W. 'Cement chemistry and physics for civil engineers'. Georg Godwin Ltd, 1980.

DANISH MINISTRY OF TRANSPORT. 'The road directorate: the concrete of the Faroe bridges'. 1985, pp. 156.

DAVIS, R.E., CARLSON, R.W., KELLY, J.W. and DAVIS, H.E. 'Properties of cements and concrete containing fly ash'. Proceedings ACI 33, 1937, pp. 577-612.

DE BORST, R., VAN DEN BOOGARD, A.H., VAN DEN BOGERT, P.A.J. and SLUYS, L.J. 'Computational issues in time-dependent deformation and fracture of concrete'. Proceedings 5th RILEM International Symposium on Creep and Shrinkage of Concrete, 1993.

DEPARTMENT OF THE ENVIRONMENT. 'Design of normal strength concrete mixes'. Building Research Establishment, 1992.

DEVENNY, A.S and KHALAF, F.M. 'New tests for brick porosity and water absorption'. 5th International Masonry Conference, British Masonry Society, No. 8, 1998, pp. 13-15.

DHIR, R.K. 'Pulverized-fuel ash'. Cement Replacement Materials, Surrey University Press, 1986, pp. 197-255.

DHIR, R.K. and BYARS, E.A. 'PFA concrete: near surface absorption properties'. Magazine of Concrete Research, Vol. 43, No. 157, December 1991, pp. 219-232.

DIAMOND, S. 'Processes and problems'. Cement and Concrete Composites, Vol. 18, No. 3, 1996, pp. 205-215.

DOUBLE, D.D. 'New developments in understanding the chemistry of cement hydration'. Proceedings of a Royal Society discussion meeting, 16-17 February 1983, pp. 53-66.

EL HUSSEIN, H.M. and ABD EL HALIM, A.O. 'Differential thermal expansion and contraction: a mechanistic approach to adhesion in asphalt concrete'. Canadian Journal of Civil Engineering, Vol. 20, 1993, pp. 366-373.

EREN, O., BROOKS, J.J. and CELIK, T. 'Setting times of fly ash and slag-cement concretes as affected by curing temperature'. Cement, Concrete and Aggregates, CCAGDP, Vol. 17, No. 1, 1995, pp. 11-17.

FARRAR, J.R. 'Electrically conductive concrete'. GEC Journal of Science and Technology, Vol. 45, No. 1, 1978, pp. 45-48.

FEDERATION INTERNATIONALE DE LA PRECONTRAINTE. 'Acceleration of concrete hardening by thermal curing: guide to good practice'. 1982, pp. 1-16.

GAYNOR, R.D., MEININGER, R.C. and KHAN, T. S. 'Effect of temperature and delivery time on concrete proportions'. Temperature Effects on Concrete, ASTM STP 858, 1985, pp. 68-87.

GEBLER, S.H. and KLIEGER, P. 'Effect of fly ash on physical properties of concrete'. Proceedings 2nd International Conference on Fly Ash, Silica Fume, Slag and Natural Pozzolans in Concrete, American Concrete Institute, ACI SP 91, Vol. 1, 1986, pp. 1-50.

GIBBON, G.J. and BALLIM, Y. 'Determination of the thermal conductivity of concrete during early stages of hydration'. Magazine of Concrete Research, Vol. 50, No. 3, 1998, pp. 229-235.

GOTO, S. and ROY, D.M. 'The effect of W/C ratio and curing temperature on the permeability of hardened cement paste'. Cement and Concrete Research, Vol. 11, 1987, pp. 575-579.

HANSON, J.A. 'Optimum steam-curing procedures in precasting plants'. ACI Journal, Vol. 60, No. 1, 1963, pp. 75-100.

HIGGINSON, E.C. 'Effect of steam curing on the important properties of concrete'. ACI Journal, Vol. 58, No. 3, 1961, pp. 281-198.

HIGHWAYS AGENCY. 'Manual of contract documents for highway works, Vol. 1, Specification for Highway Works'. Series 1700, 1998, pp. 14-16.

HO, D.W.S. and LEWIS, R.K. 'Carbonation of concrete incorporating fly ash or a chemical admixture', Proceedings of the 1st International Conference on the Use of Fly Ash, Silica Fume, Slag and Other Mineral By-Products in Concrete, Montebello, Canada, ACI Special Publication, SP-79, 1983, pp. 333-346.

HOBBS, D.W. 'Influence of PFA and GGBS upon expansion caused by the alkali-silica reaction'. Magazine of Concrete Research, Vol. 34, 1982, pp. 83-93.

HUTCHINSON, R.G., CHANG, J.T., JENNINGS, H.M. and BRODWIN, M.E. 'Thermal acceleration of Portland cement mortars with microwave energy'. Cement and Concrete Research, Vol. 21, 1991, pp. 795-799.

IDORN, G.M. 'Concrete curing technology'. Concrete and Structures, United States Strategic Highway Research Program, Thomas Telford, 1990, pp. 87-102.

IVANOV, Y. and ZACHARIEVA, S. 'Influence of fly ash on rheology of fresh concrete'. Proceedings of the International Symposium on the Use of PFA in Concrete, Leeds, April 1982, pp. 133-141.

JACKSON, N. and DHIR. R.K. 'Civil engineering materials'. Macmillan Education Ltd, 1988.

JALALI, S. and ABYANEH, M. Y. 'Prediction of final concrete strength in hot climates'. Magazine of Concrete Research, Vol. 47, No. 173, 1995, pp. 291-297.

JAWED, I. and SKALNY, J. 'Hardened mortar and concrete with fly ash'. Fly Ash in Concrete: Properties and Performance, RILEM Report 7, E & FN Spon, 1991, pp. 61-62.

JONASSON, J.E. 'Early strength growth in concrete - preliminary test results concerning hardening at elevated temperatures'. Proceedings 3rd International Rilem

Symposium on Winter Concreting, Espoo, Finland, November 25-27, 1985, pp. 249-254.

KAFRY, I.D. 'Direct electric curing of concrete: basic design'. Whittle Publishing Services, 1993.

KANAZAWA, K., YAMADA, K. and SOGO, S. 'Properties of low-heat generating concrete containing large volumes of blast-furnace slag and fly ash'. Proceedings 4th International Conference on Fly Ash, Silica Fume, Slag and Natural Pozzolans in Concrete, American Concrete Institute, ACI SP 132, Vol. 1, 1992, pp. 97-118.

KHALAF, F.M. and WILSON, J.G. 'Electrical properties of freshly mixed concrete'. Journal of Materials in Civil Engineering, Vol. 11, No. 3, 1999, pp. 242-248.

KIRKBRIDE, T. 'Review of accelerated curing procedures'. Precast Concrete, February, 1971, pp. 93-106.

KJELLSEN, K.O. 'Heat curing and post-heat curing regimes of high-performance concrete: influence on microstructure and C-S-H composition'. Cement and Concrete Research, Vol. 26, No. 2, 1996, pp. 295-307.

KUKKO, H. 'Use of heated fresh concrete'. Proceedings 3rd International Rilem Symposium on Winter Concreting, Espoo, Finland, November 25-27, 1985, pp. 147-159.

LAWRENCE, C.D. 'Laboratory studies of concrete expansion arising from delayed ettringite formation'. British Cement Association, Publication C/16, 1993.

LEUNG, C.K.Y. and PHEERAPHON, T. 'Microwave curing of Portland cement concrete: experimental results and feasibility for practical applications'. Construction and Building Materials, Vol. 9, No. 2, 1995, pp. 67-73.

LEUNG, C.K.Y. and PHEERAPHON, T. 'Very high early strength of microwaved cured concrete'. Cement and Concrete Research, Vol. 25, No. 1, 1994, pp. 136-146.

LEVITT, M. 'Non destructive testing of concrete by initial surface absorption'. Proceedings of the Symposium on Non-Destructive Testing of Concrete and Timber, London, June 1969.

LEVITT, M. 'Precast concrete materials, manufacture, properties and usage'. Applied Science Publishers, 1982.

MAILVAGANAM, N.P., BHAGRATH, R.S. and SHAW, K.L. 'Effect of admixtures on Portland cement incorporating blast-furnace slag and fly ash'. Proceedings 1st International Conference on Fly Ash, Silica Fume, Slag and Natural Pozzolans in Concrete, American Concrete Institute, ACI SP 79, Vol. 1, 1983, pp. 519-535.

MALHOTRA, V.M. 'Supplementary cementing materials for concrete'. CANMET, 1987, pp. 139-142.

MARCIALIS, A., MASSIDDA, L. and SANNA, U. 'Low temperature steam curing hydration of lime-fly-ash compacts'. Cement and Concrete Research, Vol. 13, 1983, pp. 887-894.

MCCARTER, W.J. and. AFSHAR, A.B. 'Diagnostic monitoring of the physio-chemical processes in hydrating cement paste'. Cement, Concrete and Aggregates, Vol. 7, No. 2, 1985, pp. 57-68.

MCCARTER, W.J., CHRISP, T.M. and STARRS, G. 'The early hydration of alkali-activated slag: developments in monitoring techniques'. Cement and Concrete Composites, No. 21, 1999, pp. 277-283.

MCCARTER, W.J. and. CURRAN, P.N. 'The electrical response characteristics of setting cement paste'. Magazine of Concrete Research, Vol. 36, No. 126, March 1984, pp. 42-49.

MEHTA, P.K. 'Pozzolanic and cementitious byproducts as mineral admixtures for concrete - a critical review'. Proceedings of the 1st International Conference on the use of Fly Ash, Silica Fume, Slag and Other Mineral By-products in Concrete, ACI Special Publication SP-79, 1983, pp. 1-46.

MONFORE, G.E. 'Electrical resistivity of concrete'. Journal PCA, Research and Development Laboratories, May 1968, pp. 35-48.

NAIK, T.R. 'Maturity functions for concrete cured during winter conditions'. Temperature Effects of Concrete, ASTM STP 858, 1985, pp. 107-117.

NASSER, K.W. and AL-MANASEER, A. 'Comparison of nondestructive testers of hardened concrete'. ACI Materials Journal, Vol. 84, No. 38, pp. 374-380.

NEVILLE, A.M. 'Properties of concrete'. Longman, 1988.

NIU, Y.Z., TU, C.L. and ZHANG, S.W. 'Modelling of thermomechanical damage of early-age concrete'. Journal of Structural Engineering, Vol. 121, No. 4, 1995, pp. 717-726.

ODLER, I. and CHEN, Y. 'Effect of cement composition on the expansion of heat cured cement pastes'. Cement and Concrete Research, Vol. 25, No. 4, 1995, pp. 853-862.

ORCHARD, D.F. 'Concrete technology'. Applied Science Publishers, 1973.

ORCHARD, D.F. and BARNETT, A.M. 'The electrocuring of concrete test specimens'. JMSLA, Vol. 6, No. 3, 1971, pp. 617-642.

OWENS, P.L. 'Effect of temperature rise and fall on the strength and permeability of concrete made with and without fly ash'. Temperature Effects on Concrete, ASTM STP 858, 1985, pp. 134-149.

PARCEVAUAX, P. 'Pore size distribution of Portland cement slurries at very early stages of hydration (influence of curing temperature and pressure)'. Cement and Concrete Research, Vol. 14, 1984, pp. 419-430.

PARKER JR., F. and SHOEMAKER, W. 'Rapid-setting pavement patching materials'. New Pavement Materials, ASCE, 1987, pp. 81-95

PATEL, H.H., BLAND, C.H. and POOLE, A.B. 'The microstructure of concretes cured at elevated temperatures'. Cement and Concrete Research, Vol. 25, No. 3, 1995, pp. 485-490.

PENTTALA, V. 'Heating of concrete by infra-red radiation'. Proceedings 3rd International Rilem Symposium on Winter Concreting, Espoo, Finland, November 25-27, 1985, pp. 65-82.

PFEIFER, D.W. and LANDGREN, R. 'Energy-efficient accelerated curing of concrete for plant-produced prestressed concrete'. PCI Journal, March 1982, pp. 94-107.

PINK, A. 'Comments on the Rilem recommendations on concreteing in cold weather with particular reference to current practice in the united kingdom'. Proceedings 3rd International Rilem Symposium on Winter Concreting, Espoo, Finland, November 25-27, 1985, pp. 29-39.

PRICE, R.E. 'Recommended practice for atmospheric pressure steam curing of concrete'. ACI Committee 517, ACI Journal, August 1969, pp. 629-646.

RAITT, G. 'Physics in engineering 16 - 19'. Cambridge University Press, 1992.

RAMACHANDRAN, V.S., FELDMAN, R.F. and BEAUDOIN, J.J. 'Concrete science'. Heydon & Son Ltd, 1981.

RICHARDSON, J.G. 'Precast concrete production'. Cement and Concrete Association, 1973.

RIXOM, R.M. 'Concrete admixtures: use and applications'. Construction Press, 1977.

SAUL, A.G.A. 'Principles underlying the steam curing of concrete at atmospheric pressure'. Magazine of concrete research, Vol. 8, No. 6, 1951, pp. 127-140.

SCRIVENER, K.L. 'The effect of heat treatment on inner product C-S-H'. Cement and Concrete Research, Vol. 22, 1992, pp. 1224-1226.

SENBETTA, E. and SCHOLER, C.F. 'A new approach for testing concrete curing efficiency'. ACI Journal, Vol. 81, No. 12, 1984, pp. 82-86.

SHAYAN, A. and IVANUSEC, I. 'An experimental clarification of the association of delayed ettringite formation with alkali-aggregate reaction'. Cement and Concrete Composites, Vol. 18, Issue 3, 1996, pp. 161-170.

SHAYAN, A. and QUICK, G.W. 'Microscopic features of cracked and uncracked railway sleepers'. ACI Materials Journal, Vol. 89, 1992, pp. 348-361.

SKALNY, J., JAWED, I. and TAYLOR, H.F.W. 'Studies on hydration of cement – recent developments'. World Cement Technology, September 1978, pp. 183-195.

SOHN, D. and JOHNSON, D.L. 'Microwave curing effects on the 28-day strength of cementitious materials'. Cement and Concrete Research, Vol. 29, 1999, pp. 241-247.

SRIRAVINDRARAJAH, R. and SWAMY, R.N. 'Development of a conductivity probe to monitor setting time and moisture movement in concrete'. Cement, Concrete and Aggregate, Vol. 4, No. 2, 1982, pp. 73-80.

STANLEY, C. 'Concrete through the ages'. British Cement Association, 1999, pp. 2-15.

TAMAS, D.F. 'Electrical conductivity of cement pastes'. Cement and Concrete Research, Vol. 12, 1982, pp. 115-120.

TURENNE, R.G. 'Curing of concrete in shelters'. Proceedings 3rd International Rilem Symposium on Winter Concreting, Espoo, Finland, November 25-27, 1985, pp. 53-63.

WADHWA, S.S., SRIVASTAVA, L.K., GAUTAM, D.K. and CHANDRA, D. 'Direct electric curing of in situ concrete'. Building Research and Practice, Journal of the CIB, March / April, 1987.

WEAVER, J. and SADGROVE, B.M. 'Striking times of formwork'. Construction Industry Research and Information Association, CIRIA Report 36, October 1971.

WILSON, J.G. and GUPTA, N.K. 'Assessment of concrete by measurement of its electrical resistance'. Building Research and Information, Vol. 24, No. 4, 1996.

XUENQUAN, W., JIANBGO, D. and MINGSHU, T. 'Microwave curing technique in concrete manufacture'. Cement and Concrete Research, Vol. 17, 1987, pp. 205-210.

YANG, R., LAWRENCE, C.D., LYNSDALE, C.J. and SHARP, J.H. 'Delayed ettringite formation in heat-cured Portland cement mortars'. Cement and Concrete Research, Vol. 29, 1999, pp. 17-25.

ZHAO, T.J., ZHOU, Z.H., ZHU, J.Q. AND FENG N.Q. 'An alternating test method for concrete permeability'. Cement and Concrete Research, Vol. 28, 1998, pp. 7-12.

APPENDIX A

Mix Design Sheets

Concrete mix design form

Job title Normal mix

Stage	**Item**		**Reference or calculation**	**Values**
1	1.1	Characteristic strength	Specified	30 N/mm^2 at 28 days Proportion defective 5 %
	1.2	Standard deviation	Fig. 3	____ N/mm^2 or no data 8 N/mm^2
	1.3	Margin	C1 or Specified	(k = 1.64) 1.64 x 8 = 13 N/mm^2 ____ N/mm^2
	1.4	Target mean strength	C2	30 + 13 = 43 N/mm^2
	1.5	Cement type	Specified	OPC ~~/ SRPC / RHPC~~
	1.6	Aggregate type coarse		Crushed ~~/ uncrushed~~
		Aggregate type fine		Crushed ~~/ uncrushed~~
	1.7	Free-water/cement ratio	Table 2, Fig. 4	0.55 } Use the lower value 0.55
	1.8	*Maximum free-water/cement ratio*	*Specified*	0.6 }
2	2.1	Slump or Vebe time	Specified	Slump 10 - 30 mm or Vebe time ____ s
	2.2	Maximum aggregate size	Specified	20 mm
	2.3	Free-water content	Table 3	190 | 190 kg/m^3
3	3.1	Cement content	C3	190 / 0.55 = 345 kg/m^3
	3.2	*Maximum cement content*	*Specified*	____ kg/m^3
	3.3	*Minimum cement content*	*Specified*	300 kg/m^3 use 3.1 if ≤ 3.2 use 3.3 if > 3.1 | 345 kg/m^3
	3.4	Modified free-water/cement ratio		
4	4.1	Relative density of aggregate (SSD)		2.7 known/ ~~assumed~~
	4.2	Concrete density	Fig 5	2440 kg/m^3
	4.3	Total aggregate content	C4	2440 - 345 - 190 = 1905 kg/m^3
5	5.1	Grading of fine aggregate	Percentage passing 0.6 mm sieve	45 %
	5.2	Proportion of fine aggregate	Fig. 6	39 %
	5.3	Fine aggregate content	C5	1905 x 0.39 = 743 kg/m^3
	5.4	Coarse aggregate content	C5	1905 - 743 = 1162 kg/m^3

Quantities	**Cement (kg)**	**Water (kg or L)**	**Fine aggregate (kg)**	**Coarse aggregate (kg) 10 mm**	**20 mm**	**40 mm**
per m^3 (to nearest 5 kg)	345	190	743		1162	
per trial mix of 0.03 m^3	10.35	5.7	22.29		34.86	

Items in italics are optional limiting values that may be specified (see Section 7)

1 N/mm2 = 1 MB/m2 = 1 MPa (see footnote to Section 3).

OPC = ordinary Portland cement. SRPC = sulphate-resisting Portland cement; RHPC = rapid-hardening Portland cement.

Relative density = specific gravity (see footnote to Para 5.4). SSD = based on a saturated surface-dry basis

Concrete mix design form

Job title High strength

Stage	**Item**		**Reference or calculation**	**Values**
1	1.1	Characteristic strength	Specified	50 N/mm^2 at 28 days Proportion defective 5 %
	1.2	Standard deviation	Fig. 3	N/mm^2 or no data 8 N/mm^2
	1.3	Margin	C1 or Specified	(k = 1.64) 1.64 x 8 = 13 N/mm^2 N/mm^2
	1.4	Target mean strength	C2	50 + 13 = 63 N/mm^2
	1.5	Cement type	Specified	OPC ~~/SRPC/RHPC~~
	1.6	Aggregate type: coarse Aggregate type: fine		Crushed ~~/uncrushed~~ Crushed ~~/uncrushed~~
	1.7	Free-water/cement ratio	Table 2, Fig. 4	0.4
	1.8	*Maximum free-water/cement ratio*	*Specified*	0.6 } Use the lower value 0.4
2	2.1	Slump or Vebe time	Specified	Slump 10 - 30 mm or Vebe time s
	2.2	Maximum aggregate size	Specified	20 mm
	2.3	Free-water content	Table 3	190 ☐ 190 kg/m^3
3	3.1	Cement content	C3	190 / 0.4 = 475 kg/m^3
	3.2	*Maximum cement content*	*Specified*	kg/m^3
	3.3	*Minimum cement content*	*Specified*	300 kg/m^3 use 3.1 if £ 3.2 use 3.3 if > 3.1 475 kg/m^3
	3.4	Modified free-water/cement ratio		☐
4	4.1	Relative density of aggregate (SSD)		2.7 known/ ~~assumed~~
	4.2	Concrete density	Fig 5	2440 kg/m^3
	4.3	Total aggregate content	C4	2440 - 475 - 190 = 1775 kg/m^3
5	5.1	Grading of fine aggregate	Percentage passing 0.6 mm sieve	45 %
	5.2	Proportion of fine aggregate	Fig. 6	32 %
	5.3	Fine aggregate content	C5	1775 x 0.32 = 568 kg/m^3
	5.4	Coarse aggregate content	C5	1775 - 568 = 1207 kg/m^3

Quantities	**Cement (kg)**	**Water (kg or L)**	**Fine aggregate (kg)**	**Coarse aggregate (kg) 10 mm**	**Coarse aggregate (kg) 20 mm**	**Coarse aggregate (kg) 40 mm**
per m^3 (to nearest 5 kg)	475	190	568		1207	
per trial mix of 0.03 m^3	14.25	5.7	17.04		36.21	

Items in italics are optional limiting values that may be specified (see Section 7)

1 N/mm2 = 1 MB/m2 = 1 MPa (see footnote to Section 3)

OPC = ordinary Portland cement. SRPC = sulphate-resisting Portland cement; RHPC = rapid-hardening Portland cement.

Relative density = specific gravity (see footnote to Para 5.4) SSD = based on a saturated surface-dry basis

Concrete mix design form

Job title High slump

Stage	**Item**		**Reference or calculation**	**Values**
1	1.1	Characteristic strength	Specified	30 N/mm^2 at 28 days Proportion defective 5 %
	1.2	Standard deviation	Fig 3	____ N/mm^2 or no data 8 N/mm^2
	1.3	Margin	C1 or Specified	(k = 1.64) 1.64 x 8 = 13 N/mm^2 ____ N/mm^2
	1.4	Target mean strength	C2	30 + 13 = 43 N/mm^2
	1.5	Cement type	Specified	OPC ~~/ SRPC / RHPC~~
	1.6	Aggregate type coarse Aggregate type fine		Crushed ~~/ uncrushed~~ Crushed ~~/ uncrushed~~
	1.7	Free-water/cement ratio	Table 2, Fig 4	0.55 } Use the lower value 0.55
	1.8	*Maximum free-water cement ratio*	*Specified*	0.6
2	2.1	Slump or Vebe time	Specified	Slump 60 - 180 mm or Vebe time ____ s
	2.2	Maximum aggregate size	Specified	20 mm
	2.3	Free-water content	Table 3	225 | 225 kg/m^3
3	3.1	Cement content	C3	225 / 0.55 = 409 kg/m^3
	3.2	*Maximum cement content*	*Specified*	____ kg/m^3
	3.3	*Minimum cement content*	*Specified*	300 kg/m^3 use 3.1 if £ 3.2 use 3.3 if > 3.1 | 409 kg/m^3
	3.4	Modified free-water/cement ratio		
4	4.1	Relative density of aggregate (SSD)		2.7 known/ ~~assumed~~
	4.2	Concrete density	Fig 5	2380 kg/m^3
	4.3	Total aggregate content	C4	2380 - 409 - 225 = 1746 kg/m^3
5	5.1	Grading of fine aggregate	Percentage passing 0.6 mm sieve	45 %
	5.2	Proportion of fine aggregate	Fig 6	43 %
	5.3	Fine aggregate content	C5	1746 x 0.43 = 751 kg/m^3
	5.4	Coarse aggregate content	C5	1746 - 751 = 995 kg/m^3

Quantities	**Cement (kg)**	**Water (kg or L)**	**Fine aggregate (kg)**	**Coarse aggregate (kg) 10 mm**	**20 mm**	**40 mm**
per m^3 (to nearest 5 kg)	409	225	751		995	
per trial mix of 0.03 m^3	12.27	6.75	22.53		29.85	

Items in italics are optional limiting values that may be specified (see Section 7)

1 N/mm2 = 1 MB/m2 = 1 MPa (see footnote to Section 3).

OPC = ordinary Portland cement, SRPC = sulphate-resisting Portland cement, RHPC = rapid-hardening Portland cement.

Relative density = specific gravity (see footnote to Para 5.4). SSD = based on a saturated surface-dry basis

Concrete mix design form **Job title** Air entrained (2%)

Stage	Item		Reference or calculation	Values
1	1.1	Characteristic strength	Specified	30 N/mm² at 28 days Proportion defective 5 %
	1.2	Standard deviation	Fig 3	N/mm² or no data 8 N/mm²
	1.3	Margin	C1 or Specified	(k = 1.64) 1.64 x 8 = 13 N/mm² N/mm²
	1.4	Target mean strength	C2	30 + 13 = 43 N/mm²
	1.4.1	Air content		2 %
	1.4.2	Modified target mean strength		43 / (1-0.055 x 2) = 48 N/mm²
	1.5	Cement type	Specified	OPC ~~/SRPC / RHPC~~
	1.6	Aggregate type coarse Aggregate type fine		Crushed ~~/uncrushed~~ Crushed ~~/uncrushed~~
	1.7	Free-water/cement ratio	Table 2, Fig 4	0.43 } Use the lower value 0.43
	1.8	*Maximum free-water/cement ratio*	*Specified*	0.6
2	2.1	Slump or Vebe time	Specified	Slump 10 - 30 mm or Vebe time s
	2.2	Maximum aggregate size	Specified	20 mm
	2.3	Free-water content	Table 3	190 | 190 kg/m³
3	3.1	Cement content	C3	190 / 0.43 = 442 kg/m³
	3.2	*Maximum cement content*	*Specified*	kg/m³
	3.3	*Minimum cement content*	*Specified*	300 kg/m³ use 3.1 if £ 3.2 use 3.3 if > 3.1 | 442 kg/m³
	3.4	Modified free-water/cement ratio		
4	4.1	Relative density of aggregate (SSD)		2.7 known/ ~~assumed~~
	4.2	Concrete density	Fig 5	2440 - (10 x 2 x 2.7) 2386 kg/m³
	4.3	Total aggregate content	C4	2386 - 442 - 190 = 1754 kg/m³
5	5.1	Grading of fine aggregate	Percentage passing 0.6 mm sieve	45 %
	5.2	Proportion of fine aggregate	Fig 6	39 %
	5.3	Fine aggregate content	C5	1754 x 0.39 = 684 kg/m³
	5.4	Coarse aggregate content	C5	1754 - 684 = 1070 kg/m³

Quantities		Cement (kg)	Water (kg or L)	Fine aggregate (kg)	Coarse aggregate (kg) 10 mm	20 mm	40 mm
per m³ (to nearest 5 kg)		442	190	684		1070	
per trial mix of	0.03 m³	13.26	5.7	20.52		32.1	

Items in italics are optional limiting values that may be specified (see Section 7)

1 N/mm2 = 1 MB/m2 = 1 MPa (see footnote to Section 3)

OPC = ordinary Portland cement; SRPC = sulphate-resisting Portland cement, RHPC = rapid-hardening Portland cement.

Relative density = specific gravity (see footnote to Para 5.4) SSD = based on a saturated surface-dry basis

Concrete mix design form

Job title Air entrained (5%)

Stage	**Item**		**Reference or calculation**	**Values**
1	1.1	Characteristic strength	Specified	30 N/mm^2 at 28 days Proportion defective 5 %
	1.2	Standard deviation	Fig. 3	N/mm^2 or no data 8 N/mm^2
	1.3	Margin	C1 or Specified	(k = 1.64) 1.64 x 8 = 13 N/mm^2 N/mm^2
	1.4	Target mean strength	C2	30 + 13 = 43 N/mm^2
	1.4.1	Air content		5 %
	1.4.2	Modified target mean strength		43 / (1-0.055 x 5) = 59 N/mm^2
	1.5	Cement type	Specified	OPC ~~/SRPC/ RHPC~~
	1.6	Aggregate type coarse		Crushed ~~/uncrushed~~
		Aggregate type fine		Crushed ~~/uncrushed~~
	1.7	Free-water/cement ratio	Table 2, Fig. 4	0.43 } Use the lower value 0.43
	1.8	*Maximum free-water/cement ratio*	*Specified*	0.6 }
2	2.1	Slump or Vebe time	Specified	Slump 10 - 30 mm or Vebe time s
	2.2	Maximum aggregate size	Specified	20 mm
	2.3	Free-water content	Table 3	190 | 190 kg/m^3
3	3.1	Cement content	C3	190 / 0.43 = 442 kg/m^3
	3.2	*Maximum cement content*	*Specified*	kg/m^3
	3.3	*Minimum cement content*	*Specified*	300 kg/m^3 use 3.1 if £ 3.2 use 3.3 if > 3.1 | 442 kg/m^3
	3.4	Modified free-water/cement ratio		
4	4.1	Relative density of aggregate (SSD)		2.7 known/ ~~assumed~~
	4.2	Concrete density	Fig. 5	2440 - (10 x 5 x 2.7) 2305 kg/m^3
	4.3	Total aggregate content	C4	2305 - 442 - 190 = 1673 kg/m^3
5	5.1	Grading of fine aggregate	Percentage passing 0.6 mm sieve	45 %
	5.2	Proportion of fine aggregate	Fig. 6	39 %
	5.3	Fine aggregate content	C5	1673 x 0.39 = 652 kg/m^3
	5.4	Coarse aggregate content	C5	1673 - 652 = 1021 kg/m^3

Quantities	**Cement (kg)**	**Water (kg or L)**	**Fine aggregate (kg)**	**Coarse aggregate (kg) 10 mm**	**20 mm**	**40 mm**
per m^3 (to nearest 5 kg)	442	190	652		1021	
per trial mix of 0.03 m^3	13.26	5.7	19.56		30.63	

Items in italics are optional limiting values that may be specified (see Section 7)

1 N/mm2 = 1 MB/m2 = 1 MPa (see footnote to Section 3)

OPC = ordinary Portland cement, SRPC = sulphate-resisting Portland cement, RHPC = rapid-hardening Portland cement

Relative density = specific gravity (see footnote to Para 5.4) SSD = based on a saturated surface-dry basis